

THE UNIVERSITY OF HULL

**Fabrication, functionalization and characterization of silica
monolith for forensic chemistry applications**

a thesis submitted for the Degree of
Doctor of Philosophy
at the University of Hull

by

Amin Khalid Khattab

**BSc (King Abdul-Aziz University, Saudi Arabia)
MSc (University of Hull, UK)**

May 2014

Abstract

The physiochemical properties of silica monolith make it an ideal base material for drugs extracting, pre-concentrating and separation from biological samples which can interact not only with molecules but also with ions and atoms. However, the fabrication of silica monoliths still has some problems, such as cost, limited capacity and fabrication and modification methodology, which can be time consuming and labour intensive. Structure evolution of silica monolith was studied in microwave and conventionally processed samples over the temperature range from 25 to 70 °C. The samples were produced using sol-gel processing. The microwave process was performed using a single mode cavity at 2.45GHz. Characterization of produced silica monoliths were carried out using a variety of techniques, including Scanning Electron Microscopy (SEM) analysis, EDX analysis, BET and BJH analysis. The data obtained showed that structural differences do exist between conventional and microwave processed samples. It was found however, that microwave based fabrication offered a significantly quicker (11 min) gelation process, compared to those obtained using the thermal heated oven methodology (4,320 min).

The silica monolithic surfaces were modified with three different phases C₁₈, gold nanoparticles and graphene which received a thermal treatment at different programmed powers in two different ovens, conventional and microwave. Three substantial variance were also identified from the structural characterization of modified silica surfaces processed using microwave heating and conventional heating methods:

- 1- The use of microwave heating during C₁₈ surface modification improved not only the attachment of C₁₈ groups to the silica surface but also increased the extraction efficiency of caffeine and eserine from standard solutions (102 % and 97 %, respectively).

2- The fabrication of gold nanoparticles-NH₂-silica monolith using microwave heating was found to improve the sensitivity and selectivity of modified silica surface and make possible to extract, detect and quantify more than one type of drugs of abuse at the same time within few minutes.

3- Using graphene-silica monolith makes the extraction of non-polar, polar, very polar and water-soluble analytes, based on both hydrophobic and electronic interactions, easy and simple.

Fabrication and modification of silica monoliths using microwave heating make the sol-gel procedure much faster and easier and allow for non-polar, polar, very polar and water-soluble analytes to be extracted more efficiently to produce accurate and precise results compared to the conventional method for fabrication and modification of silica monoliths using three phases (C₁₈, gold nanoparticles and graphene).

Finally, this technique make the modified silica monolithic column capable to extract selected drugs of abuse from biological samples and produce qualitative and quantitative results at the same time using chemiluminescence based immunoassays or HPLC-UV.

Acknowledgements

I would like to express unlimited thanks to my first supervisor **Prof. S. J. Haswell** for providing guidance and for keeping me motivated. For his support and advice I would like to express my appreciation to my second supervisor, **Dr. Thomas McCreedy**.

I also wish to thank my friends and colleagues for their help, support and technical assistance.

Finally I would like to thank my **family** (brothers and sisters), especially **Mama** and **Baba** for their constant love, support and encouragement.

Special love and thanks to my wife **Baraah** and my children **Alzahraa** and **Khalid**.

This work was funded by the Saudi Arabian Government.

Abbreviations

A	
A	Amber
AMP	Amphetamine
APTES	3-aminopropyl triethoxysilane
B	
BET	Brunauer-Emmett-Teller
BJH	Barett-Joyner-Halenda
BuMA	Butyl methacrylate
BP	Benzoyl peroxide
BZE	Benzoylcegonine
C	
CDMOS	Chlorodimethyl octadecyl silane
COD	Codeine
CTAB	Cetyltrimethyl ammonium bromide
CE	Capillary electrophoresis
D	
Da	Dalton
DAP	2, 2-Dimethoxy-2-phenylacetophenone
DVB	Divinylbenzene
DNA	Deoxyribonucleic acid
DXM	Dextromethorphan
E	
EDC	N-(3-dimethylaminopropyl)-N-ethylcarbodiimide hydrochloride
EDX	Energy dispersive X-ray spectroscopy
EOF	Electroosmotic flow
EM	Electromagnetic
ESI	Electrospray ionization
F	
F. r	Flow rate
FIA	Flow-injection analysis
G	
g	Gram

GC	Gas Chromatography
GCB	Graphitized carbon black
GHB	γ -Hydroxybutyric acid
GO	Graphene oxide
GNP	Gold nanoparticles
H	
HETP	Height of theoretical plate
HIC	Hydrophobic Interaction Chromatography
HILIC	Hydrophilic Interaction Liquid Chromatography
HPLC	High Performance Liquid Chromatography
HMDS	Hexamethyldisilazane
I	
I. D.	Internal diameter
IR	Infra-red
K	
k	kilo
kDa	kilo Dalton
L	
L	Length
LC	Liquid chromatography
LLE	Liquid-liquid extraction
LSD	Lysergic acid diethylamide
M	
μ	Micro
m	Meter
M	Molar
MO	Morphine
min	Minute
mL	millilitre
MM	Molecular Mass
MS	Mass Spectrometry
MSDS	Material Safety Data Sheet
MTMS	Methyltrimethoxysilane

MDE	Methylenedioxyethylamphetamine
MDMA	Methylenedioxymethamphetamine
N	
N	Theoretical Plates
NARP	Non-Aqueous Reverse Phase
NHS	N-Hydroxysulfosuccinimide
nm	Nano meter
O	
ODS	Chloro(dimethyl)octadecylsilane
O. D.	Outer diameter
P	
P	Pico
PCP	Phencyclidine
PEO	Polyethylene oxide
PEEK	Polyaryletheretherketone
PEG	Polyethylene glycol
PDA	Photodiode array
PGC	Porous graphitic carbon
PTFE	Poly (tetrafluoroethylene)
R	
RP	Reversed phase
R-MTPCl	R-alpha-methoxy-alpha-(trifluoromethyl)phenylacetyl chloride
RSD	Relative standard deviation
S	
SCSE	Stir-Cake-Sorptive Extraction
SEM	Scanning Electron Microscope
SIM	Selective Ion Monitoring
SPE	Solid-Phase Extraction
SPME	Solid Phase Microextraction
SWNT	Single-Walled Nanotubes
T	
TEOS	Tetraethyl orthosilicate
TLC	Thin Layer Chromatography
TMOS	Tetramethylorthosilicate

TFA	Trifloro acetic acid
TMCS	Trimethylchlorosilane
U	
UV	Ultra Violet
V	
V	Volume
W	
t_r	Retention time
Wt	Weight
λ	Wavelength
°C	Degree Celsius
3D	Three-dimensional
6-MAM	6-monoacetylmorphine

Contents

1	Introduction	1
1.1	<i>Forensic science</i>	2
1.2	<i>Drugs of abuse</i>	2
1.2.1	Drugs of abuse analysis	3
1.3	<i>Sample preparation techniques</i>	4
1.3.1	Liquid-liquid extraction	4
1.3.2	Solid phase extraction	6
1.3.3	Materials used on SPE sorbent	8
1.3.4	Solid phase extraction procedure	9
1.4	<i>Particulate stationary phases</i>	10
1.5	<i>Monolithic stationary phases</i>	13
1.5.1	Silica monoliths fabrication	16
	<i>Precursor materials</i>	17
	<i>Mixing</i>	17
	<i>Casting</i>	17
	<i>Gelation</i>	18
	<i>Aging</i>	19
	<i>Drying</i>	19
	<i>Stabilization</i>	21
	<i>Calcination</i>	21
1.5.2	Polymer monoliths fabrication	22
1.6	<i>Advantages of monoliths over particles</i>	23
1.7	<i>Comparison between silica monolith and polymeric monolith</i>	25

1.8	<i>Modification of silica surfaces</i>	28
1.8.1	C ₁₈ phase.....	30
1.8.2	Graphene	34
1.8.2.1	Retention studies on PGC	36
1.8.2.2	Application of graphene silica monoliths	38
1.8.3	Gold Nano Particles (GNP).....	40
1.9	<i>Characterisation of modified stationary phases</i>	43
1.9.1	Scanning electron microscopy - Energy dispersive X-ray spectroscopy (SEM-EDX)	43
1.9.2	Extraction performance	44
1.9.3	Nitrogen physisorption method.....	45
1.10	<i>Microwaves</i>	47
1.10.1	Microwave energy.....	47
1.10.2	Conventional and microwave heating	48
1.10.3	Microwave interactions with materials	49
1.10.4	Dielectric materials	50
1.10.5	Types of polarization.....	50
1.10.6	Dielectric constant and dielectric loss.....	53
1.10.7	Microwave power dissipation	54
1.10.8	Microwave hybrid heating	55
1.10.9	Microwave cavities	55
1.11	<i>Aims of the project</i>	56
2	Experimental	58
2.1	<i>Fabrication of monolithic materials</i>	59
2.1.1	Fabrication of silica monoliths using a conventional heating method.....	59

2.1.2	Fabrication of silica monolith using a microwave heating method	61
2.1.3	Connecting the silica monolith with the borosilicate tube using the heat shrinkable sleeving polytetrafluoroethylene (PTFE) tube	64
2.2	<i>Derivatisation of the silica based monoliths with C₁₈ phase</i>	65
2.2.1	C ₁₈ phase modified silica monolith using conventional heating method	65
2.2.2	C ₁₈ phase modified silica monolith using microwave heating method	65
2.3	<i>Extraction</i>	66
2.3.1	Materials.....	66
2.3.2	Preparation of standard solutions	66
2.3.3	HPLC conditions	66
2.4	<i>Fabrication of silica based monoliths with gold nanoparticles</i>	67
2.4.1	Fabrication of silica monolith embedded by gold nanoparticles	67
2.4.2	Physical modification of silica based monolith with gold nanoparticles labelled with NH ₂ groups	68
2.4.3	Connecting silica monoliths with borosilicate tubes using heat shrinkable sleeving polytetrafluoroethylene (PTFE) tube and heat gun	69
2.4.4	Oxazepam detection (antigen-antibody reaction)	69
2.4.5	CCD camera	70
2.5	<i>Graphene monoliths</i>	71
2.5.1	Fabrication of graphene monoliths using microwave heating	71
2.5.2	Modification of silica based monolith with graphene using microwave heating	71
2.5.3	Amphetamine extraction	72
2.6	<i>Characterisation of monolithic materials</i>	73
2.6.1	SEM analysis.....	73

2.6.2	BET and BJH analysis	73
2.6.3	EDX analysis.....	74
3	Fabrication of silica monoliths based on microwave heating.....	75
3.1	<i>Introduction</i>	76
3.2	<i>Experimental</i>	77
3.3	<i>Results and discussion</i>	78
3.3.1	Silica monoliths fabrication using conventional thermal heating	78
3.3.2	Silica monolith fabrication using microwave heating.....	80
3.3.3	Effects of the concentration and molecular weight of polymer in the internal structure of the silica monoliths.....	88
3.3.4	Comparison between the weights of silica monoliths obtained by microwave heating and similar monoliths obtained by thermal heating.....	91
3.3.5	Effect of use F127 on the internal structures of silica monolith	92
3.4	<i>Summary</i>	93
4	Modification of silica based monoliths with C₁₈ phase using microwave heating.....	95
4.1	<i>Introduction</i>	96
4.2	<i>Experiment</i>	97
4.2.1	C ₁₈ phase modification.....	97
4.3	<i>Results and discussion</i>	98
4.3.1	Optimisations of silica monoliths modification with C ₁₈ phase.....	101
4.3.2	Calibration curve.....	102
4.3.3	Characterisations of silica monoliths before and after silica surface modification with C ₁₈ phase	111

4.3.4	Physical properties of C ₁₈ silica monoliths	112
4.3.5	Performance of C ₁₈ silica monoliths.....	114
4.3.5.1	Extraction procedure	114
4.3.5.2	Breakthrough curve.....	114
4.3.5.3	Capacity of C ₁₈ phase.....	115
4.3.5.4	Evaluation of recovery	116
4.3.5.5	Method Validation	117
4.4	<i>Summary</i>	119
5	Using gold nanoparticles within silica monoliths structure and for surface modification	121
5.1	<i>Introduction</i>	122
5.2	<i>Experimental</i>	123
5.2.1	Fabrication of silica monoliths embedded by gold nanoparticles using microwave heating during gel formation process	123
5.3	<i>Results and discussions</i>	123
5.3.1	Characterization	123
5.3.1.1	External morphology.....	124
5.3.1.2	SEM analysis.....	125
5.3.1.3	Physical properties of GNP silica monoliths.....	126
5.3.2	Assay condition optimization.....	129
5.3.3	Calibration Curve	131
5.3.4	Coating the surface of silica based monolith with GNP-NH ₂	133
5.3.5	Immobilisation of anti-oxazepam on the top surface of silica monolithic column coated by GNP-NH ₂	134
5.4	<i>Summary</i>	144

6	Using microwave heating for fabrication graphene monoliths and graphene silica monoliths	145
6.1	<i>Introduction.....</i>	146
6.2	<i>Experiment</i>	147
6.2.1	Graphene monoliths	147
6.2.1.1	A typical procedure for graphene oxide (GO) reduction	147
6.2.1.2	Characterization of graphene monoliths	147
6.2.2	Silica monoliths.....	148
6.2.3	Fabrication of silica monolith	148
6.2.4	Modification of silica monoliths with graphene phase	148
6.2.5	Characterization of modified silica monoliths with graphene phase	148
6.3	<i>Result and discussion</i>	148
6.3.1	Graphene monoliths	148
6.3.2	Graphene-silica monoliths	152
6.3.3	Optimization of amphetamine extraction using graphene silica monolithic column.....	157
6.3.4	Calibration curve.....	161
6.4	<i>Summary.....</i>	167
7	Conclusion and future work.....	169
7.1	<i>Fabrication of silica monoliths using microwave heating (chapter 3).....</i>	169
7.2	<i>C₁₈ modification of silica monoliths using microwave heating (chapter 4).....</i>	170
7.3	<i>Modification of silica monolithic column with gold nanoparticles using microwave heating (chapter 5)</i>	171

7.4	<i>Modification of silica monolithic column with graphene phase using microwave heating (chapter 6)</i>	172
8	References	173
9	Presentations	197
9.1	<i>Poster presentations</i>	197
9.2	<i>Oral presentations</i>	197

List of figures

FIGURE 1-1 LIQUID–LIQUID EXTRACTION (LLE) TECHNIQUE. THE PROCESS OF LIQUID- LIQUID EXTRACTION INVOLVES THE DISTRIBUTION OF A COMPOUND BETWEEN TWO SOLVENTS THAT ARE INSOLUBLE IN EACH OTHER. BY TAKING ADVANTAGE OF THE DIFFERING SOLUBILITIES OF A SOLUTE IN A PAIR OF SOLVENTS, COMPOUNDS CAN BE SELECTIVELY TRANSPORTED FROM ONE LIQUID PHASE TO THE OTHER. [24]	5
FIGURE 1-2 THE SOLID PHASE EXTRACTION PROCESS BASICALLY CONSISTS IN FOUR DIFFERENT STEPS: CONDITIONING, SAMPLE ADDITION, WASHING AND ELUTION. DURING THE CONDITIONING THE FUNCTIONAL GROUPS OF THE SORBENT BED ARE SOLVATED IN ORDER TO MAKE THEM ABLE TO INTERACT WITH THE SAMPLE. THE ANALYTES AS WELL AS SOME MATRIX COMPONENTS ARE RETAINED ON THE SPE PACKING MATERIAL DURING THE LOADING OR SAMPLE ADDITION PROCESS. AFTER THAT THE IMPURITIES WILL BE RINSED THROUGH WITH WASH SOLUTIONS. FINALLY, THE ADSORBED COMPOUNDS WILL BE ELUTED USING A PROPER SOLVENT. [49]	10
FIGURE 1-3 KNOX PLOT (REDUCED PLATE HEIGHT VS. REDUCED LINEAR VELOCITY) SHOWING THE EFFECT OF REDUCING PARTICLE DIAMETER ON PLATE HEIGHT. [50]	11
FIGURE 1-4 SCHEMATIC DEPICTING TWO POSSIBLE PATHS WITHIN A PACKED COLUMN FROM POINT (A) TO POINT (B). [51]	12
FIGURE 1-5 PHOTOGRAPH OF THE POROUS MONOLITH ERECTED AT THE ENTRANCE OF THE SUMMER PALACE PARK, BEIJING, CHINA. [57]	13
FIGURE 1-6 GENERAL STEPS INVOLVED IN THE PRODUCTION OF SILICA MONOLITH.....	16
FIGURE 1-7 STRESSES IN A MONOLITHIC SILICA GEL BODY: (A) EVALUATION OF FORCES IN PORE I; (B) HORIZONTAL STRESSES IN DIFFERENT PORE SIZE. [90]	21
FIGURE 1-8 SCHEMATIC FOR THE PREPARATION OF RIGID MACRO POROUS POLYMER MONOLITHS. [63]	22

FIGURE 1-9 PLOTS OF PLATE HEIGHT VALUES FOR URACIL AGAINST LINEAR VELOCITY OF MOBILE PHASE: CONVENTIONAL SIZE COLUMNS; MIGHTYSIL () AND CHROMOLITH (O). ^[106]	24
FIGURE 1-10 SEM IMAGES OF A SILICA MONOLITH SHOWING (A) THE MACRO-PORES OR THROUGH-PORES AND (B) THE MESO-POROUS STRUCTURE OF THE SILICA SKELETON. ^[70]	25
FIGURE 1-11 SEM OF POLYMERIC (METHACRYLATE) MONOLITH SHOWING MACRO- POROUS. ^[110]	26
FIGURE 1-12 SCHEMATIC DIAGRAM SHOWS THE POROUS SILICA-BASED SURFACE, SHOWING THE INACCESSIBILITY OF SOME MICROPOROUS. ^[43]	31
FIGURE 1-13 C18 MONOLITHIC COLUMN ENDCAPPED WITH TWO DIFUNCTIONAL DIALKYLSILANE REAGENTS TO DECREASE THE NUMBER OF FREE SILANOL GROUPS ON THE SURFACE, WHICH MAY CAUSE POLAR-POLAR INTERACTION WITH A POLAR FUNCTIONAL GROUPS IN THE SAMPLE MATRIX. ^[222]	32
FIGURE 1-14 SCHEMATIC DIAGRAM SHOWING THE EFFECT OF CONDITIONING STEP ON OCTADECYL BONDED SILICA: (A) WITHOUT CONDITIONING. (B) PARTIALLY CONDITIONED. (C) FULLY CONDITIONED. ^[43]	33
FIGURE 1-15 SURFACE COMPARISON BETWEEN C18 BONDED SILICA AND POROUS GRAPHITIC CARBON. ^[161]	37
FIGURE 1-16 (A) PHOTOGRAPHS OF POLY(EDMA) MONOLITH AND POLY(EDMA/GO) MONOLITH, (B) TEM IMAGE OF POLY(EDMA/GO) MONOLITH, (C) SEM OF POLY(EDMA/GO) MONOLITH AT 5000 × MAGNIFICATION. ^[175]	39
FIGURE 1-17 SCHEMATICS OF TWO-PHASE (A) AND THREE-PHASE (B) COASSEMBLY METHODS. WHITE ARROWS POINT TO THE BRIGHTER CONTRAST GOLD NANOPARTICLES IN THE SEM IMAGE (C). THE GOLD NANOPARTICLES IN THE TEM IMAGE APPEAR AS DARK SPOTS (C). ^[180]	41

FIGURE 1-18 THE IUPAC CLASSIFICATION OF THE SORPTION ISOTHERMS. THE ADSORPTION AND DESORPTION ISOTHERMS CAN BE FOUND IN SIX SHAPES (I-VI). ^[189]	46
FIGURE 1-19 SHOWS THE MICROWAVE RANGE WITH SOME OF THE MAJOR APPLICATIONS EXISTING AT VARIOUS FREQUENCIES. IT ALSO SHOWS SOME OF THE FREQUENCIES USED FOR MICROWAVE PROCESSING OF MATERIALS. ^[90]	47
FIGURE 1-20 MATERIAL CLASSIFICATION BASED ON MICROWAVE INTERACTION: A) TRANSPARENT, B) OPAQUE, C) ABSORBER, D) PARTIAL ABSORBER. SILICA GEL IS COMPOSED OF A TRANSPARENT MATRIX AND ABSORBING PHASE AND IS THUS A PARTIAL ABSORBER. ^[90, 195]	49
FIGURE 1-21 POLARIZATION TYPES WITH AND WITHOUT AN ELECTRIC FIELD APPLIED: A) ELECTRONIC, B) ATOMIC, C) DIPOLE, AND D) INTERFACIAL SPACE CHARGE POLARIZATION. ^[90, 198]	51
FIGURE 2-1 EXPERIMENTAL SETUP FOR SILICA MONOLITH FABRICATION. THE STARTER MIXTURE CONTAINS POLYMER, ACID CATALYST AND METAL ALKOXIDE. ICE BATH AND STIRRER PLATE ARE USED FOR DISSOLVING STARTER MIXTURE COMPONENT. MICROPIPETTES ARE USED TO MEASURE AND TRANSFER SMALL VOLUMES OF LIQUIDS. FALCON TUBE IS USED FOR MIXING THE CHEMICAL COMPOSITION.	60
FIGURE 2-2 SET UP FOR AMMONIA TREATMENT PROCESS. AQUEOUS AMMONIUM HYDROXIDE WAS USED AS A POROGEN FOR FORMING MESOPOROUS. THE MESOPOROUS IN THE WET GEL SKELETON WAS MADE BY ALTERNATING THE FLUID PHASE WITH AN EXTERNAL SOLUTION (AMMONIUM HYDROXIDE SOLUTION).	61
FIGURE 2-3 SET UP FOR SILICA MONOLITH FABRICATION AND MODIFICATION USING SINGLE MODE CAVITY MICROWAVE. THE FIBRE OPTIC TEMPERATURE MEASUREMENT WAS USED TO MONITOR THE TEMPERATURE OF THE EXTERNAL SURFACE OF THE SILICA	

MONOLITH DURING THE FABRICATION AND MODIFICATION PROCESSES IN ADDITION TO THE INFRARED SENSOR FITTED IN THE MICROWAVE CAVITY.....	63
FIGURE 2-4 SINGLE CAVITY MICROWAVE THAT FOCUSES THE MICROWAVES (2.45 GHz) AROUND THE SAMPLE WITH MAXIMUM EFFICIENCY AND OFFERS RAPID, RELIABLE AND REPRODUCIBLE MICROWAVE-ASSISTED FABRICATION AND MODIFICATION OF SILICA MONOLITHS.	63
FIGURE 2-5 PHOTOGRAPH OF SILICA MONOLITHIC RODS OBTAINED USING MICROWAVE HEATING CUT TO 1 CM.	64
FIGURE 2-6 SILICA-BASED MONOLITH THAT WAS CONNECTED TO THE BOROSILICATE TUBE USING PTFE SHRINKABLE TUBE.	65
FIGURE 2-7 MODIFIED SILICA BASED MONOLITHS WITH GOLD NANOPARTICLES.....	68
FIGURE 2-8 THE PROCEDURE FOR IMMOBILIZATION OF ANTI-OXAZEPAM ON THE SURFACE OF GNP COATED SILICA MONOLITHIC RODS AND DETECTION OF OXAZEPAM-HRP...	70
FIGURE 2-9 SILICA BASED MONOLITHS BEFORE AND AFTER GRAPHENE MODIFICATION....	72
FIGURE 3-1 PHOTOGRAPH OF WHITE AND CRACK-FREE SILICA MONOLITHIC RODS USING THERMAL HEATING FOR PREPARATION.	78
FIGURE 3-2 PHOTOGRAPHS FOR SILICA MONOLITH CONSIST OF TMOS + PEO + 1 M NITRIC ACID (A) BEFORE 1 M NH ₄ OH TREATMENT (B) AFTER 1 M NH ₄ OH TREATMENT (C) AFTER 1 M NH ₄ OH TREATMENT BUT BEFORE CALCINATION (D) AFTER 1 M NH ₄ OH TREATMENT AND CALCINATION.	79
FIGURE 3-3 PHOTOGRAPH OF SILICA MONOLITH PREPARED FROM TMOS + 1 M NITRIC ACID + PEO USING MICROWAVE HEATING AT 180-260 °C FOR 10 MIN AND 300 W..	81
FIGURE 3-4 PHOTOGRAPH OF SILICA MONOLITH PREPARED FROM TMOS + 1 M NITRIC ACID + PEO USING MICROWAVE HEATING AT 100 °C FOR 10 MIN AND 150 W.	81
FIGURE 3-5 PHOTOGRAPH OF SILICA MONOLITH PREPARED FROM TMOS + 1 M NITRIC ACID + PEO USING MICROWAVE HEATING AT 40 °C FOR 30 MIN AND 50 W.	82

FIGURE 3-6 PHOTOGRAPH OF SILICA MONOLITH PREPARED FROM TMOS + 1M NITRIC ACID + PEO USING MICROWAVE HEATING WITH THIS CONDITION 1 MIN AT 10 W THEN 1 MIN AT 20 W THEN 1 MIN AT 40 W THEN 1 MIN AT 80 W THEN 1 MIN AT 160 W.....	83
FIGURE 3-7 PHOTOGRAPH OF SILICA MONOLITH PREPARED FROM TMOS + 0.02 M ACETIC ACID + PEO USING MICROWAVE HEATING WITH THIS CONDITION 1 MIN AT 10 W THEN 1 MIN AT 20 W THEN 1 MIN AT 40 W THEN 1 MIN AT 80 W THEN 1 MIN AT 160 W.....	83
FIGURE 3-8 SCANNING ELECTRON MICROGRAPHS FOR SILICA MONOLITH PREPARED FROM TMOS + 0.02 M ACETIC ACID + PEO USING MICROWAVE HEATING AT THIS CONDITION 1 MIN AT 10 W THEN 1 MIN AT 20 W THEN 1 MIN AT 40 W THEN 1 MIN AT 80 W THEN 1 MIN AT 160 W.....	84
FIGURE 3-9 THE RELATION BETWEEN APPLIED POWER (W) BY SINGLE CAVITY MICROWAVE AND TEMPERATURE (°C) OF THE EXTERNAL SURFACE OF THE SILICA MONOLITH MEASURED USING THE FIBRE OPTIC TEMPERATURE SENSOR. THE ERROR BARS REPRESENT THE STANDARD DEVIATION OF 5 REPEAT EXPERIMENTS.....	85
FIGURE 3-10 PHOTOGRAPH OF (TMOS + PEO + 0.02 M ACETIC ACID) MONOLITH OBTAINED USING MICROWAVE HEATING AT THIS CONDITION 2 MIN AT 10 W THEN 2 MIN AT 20 W THEN 2 MIN AT 40 W THEN 2MIN AT 80 W THEN 2 MIN AT 160 W THEN 1 MIN AT 300 W.	86
FIGURE 3-11 SCANNING ELECTRON MICROGRAPHS FOR SILICA MONOLITH PREPARED FROM TMOS + 0.02 M ACETIC ACID + PEO USING MICROWAVE HEATING AT THIS CONDITION 2 MIN AT 10 W THEN 2 MIN AT 20 W THEN 2 MIN AT 40 W THEN 2MIN AT 80 W THEN 2 MIN AT 160 W THEN 1 MIN AT 300 W.	86
FIGURE 3-12 METHODS FOR SILICA MONOLITH PREPARATION BASED ON MICROWAVE HEATING AND CONVENTIONAL THERMAL HEATING.	87

FIGURE 3-13 SCANNING ELECTRON MICROGRAPHS OF SILICA MONOLITHS PREPARED FROM TETRAMETHOXYSILANE, (0.02 M) ACETIC ACID AND POLYETHYLENE OXIDE PEO 0.282 G (A) MW HEATED, (B) OVEN HEATED; OR 0.305G PEO (C) MW HEATED, (D) OVEN HEATED.	88
FIGURE 3-14 SCANNING ELECTRON MICROGRAPHS OF SILICA MONOLITHS PREPARED FROM TETRAMETHOXYSILANE, 0.02 M ACETIC ACID AND POLYETHYLENE OXIDE PEO 0.282 G (A) MW HEATED AND (B) OVEN HEATED.	89
FIGURE 3-15 SCANNING ELECTRON MICROGRAPHS OF SILICA MONOLITHS PREPARED FROM TETRAMETHOXYSILANE, (0.02 M) ACETIC ACID AND F127 (A) OVEN HEATED AND (B) MW HEATED.	92
FIGURE 3-16 SURFACE AREAS OF MONOLITHIC SILICA COLUMNS 1-10 USING MICROWAVE HEATING AND OVEN HEATING METHODOLOGY DURING GEL FORMATION PROCESS. ...	93
FIGURE 4-1 EFFECT OF USING HIGH TEMPERATURE (330 °C FOR 2 HOURS) DURING SEALING PROCESS ON THE APPEARANCE OF THE OCTADECYLATED SILICA MONOLITHIC COLUMNS.	97
FIGURE 4-2 SHOWS THE REACTION OF THE SILANOL GROUPS OF THE MONOLITHIC SILICA SURFACE WITH OCTADECYL GROUPS IN THE CHLORODIMETHYLOCTADECYLSILANE SOLUTION. ^[66]	98
FIGURE 4-3 EDX SPECTRA OF NON-MODIFIED SILICA-BASED MONOLITH.	99
FIGURE 4-4 EDX SPECTRA OF SILICA-BASED MONOLITH MODIFIED WITH C ₁₈ PHASE USING THERMAL HEATING METHOD.	100
FIGURE 4-5 CHART OF PERCENTAGES OF EXTRACTED CAFFEINE (100 µG/ML) AT THREE DIFFERENT FLOW RATES 50, 100 AND 200 mL/MIN USING C ₁₈ SILICA MONOLITHIC COLUMN PREPARED USING CONVENTIONAL THERMAL HEATING. THE ERROR BARS REPRESENT THE STANDARD DEVIATION OF 3 REPEAT EXPERIMENTS.	101

FIGURE 4-6 CALIBRATION CURVE FOR CAFFEINE WAS OBTAINED USING A WIDE RANGE OF CONCENTRATIONS: 10, 50, 100, 200, 300 AND 400 $\mu\text{G}/\text{mL}$ IN ORDER TO CHECK THE ABILITY OF COLUMN TO EXTRACTE LOW AND HIGH CONCENTREATION SAMPLE. THE ERROR BARS REPRESENT THE STANDARD DEVIATION OF 3 REPEAT EXPERIMENTS. .	102
FIGURE 4-7 UV ABSORBANCE WAVELENGTH FOR CAFFEINE STANDARD (100 $\mu\text{G}/\text{mL}$). ..	103
FIGURE 4-8 THE UV CHROMATOGRAMS OF CAFFEINE STANDARD (100 $\mu\text{G}/\text{mL}$). EXPERIMENTAL CONDITIONS: THE MOBILE PHASE WAS METHANOL / 0.01 ACETIC ACID (30:70) (V/V) RUN UNDER ISOCRATIC CONDITIONS AT FLOW RATE 1 mL/min AND THE DETECTION WAVELENGTH WAS ADJUSTED TO 205 nm , INJECTION VOLUME WAS 20 μL . THE SEPARATION COLUMN WAS SYMMETRY C_{18} , 4.6 $\text{mm} \times 250 \text{ mm}$ PACKED WITH SILICA PARTICLES SIZE 5 μm . ALL EXPERIMENTS WERE PERFORMED AT AMBIENT TEMPERATURE AROUND 25 $^{\circ}\text{C}$	104
FIGURE 4-9 EDX SPECTRA OF SILICA-BASED MONOLITH MODIFIED WITH C_{18} PHASE USING MICROWAVE HEATING FOR 10 min AT 80 $^{\circ}\text{C}$ AND 120 W	106
FIGURE 4-10 EDX SPECTRA OF SILICA-BASED MONOLITH MODIFIED WITH C_{18} PHASE USING MICROWAVE HEATING FOR 20 min AT 80 $^{\circ}\text{C}$ AND 120 W	107
FIGURE 4-11 EDX SPECTRA OF SILICA-BASED MONOLITH MODIFIED WITH C_{18} PHASE USING MICROWAVE HEATING AT 80 $^{\circ}\text{C}$ AND 120 W FOR 30 min	108
FIGURE 4-12 EDX SPECTRA OF SILICA-BASED MONOLITH MODIFIED WITH C_{18} PHASE USING MICROWAVE HEATING AT 80 $^{\circ}\text{C}$ FOR 40 min AND 120 W	109
FIGURE 4-13 SILICA MONOLITHIC COLUMN USING MICROWAVE HEATING FOR 50 min AT 80 $^{\circ}\text{C}$ DURING C_{18} SURFACE MODIFICATION.	110
FIGURE 4-14 SEM IMAGES OF THE SILICA-BASED MONOLITH BEFORE C_{18} SURFACE MODIFICATION (A AND D), AND AFTER SURFACE MODIFICATION WITH C_{18} PHASE (B AND C) USING THERMAL HEATING, (F AND G) USING MICROWAVE HEATING.	111



FIGURE 4-15 BREAKTHROUGH CURVES FOR CAFFEINE STANDARD (100 $\mu\text{g}/\text{mL}$), EACH POINT REPRESENTS ONE FRACTION OF SOLUTION (350 μL) CONTAIN (35 μg) OF CAFFEINE ADSORBED ON () MICROWAVE C_{18} SILICA MONOLITH AND () ON THERMAL C_{18} SILICA MONOLITH.....	115
FIGURE 4-16 PHOTOGRAPH OF SILICA MONOLITHIC ROD CONNECTED TO THE BOROSILICATE TUBE (O.D. 3.90 MM) WITHIN THE POLY (TETRAFLUOROETHYLENE) (PTFE) SHRINKABLE TUBE TO BE SUITABLE FOR DRUG EXTRACTION.	116
FIGURE 4-17 THE UV CHROMATOGRAMS OF CAFFEINE AND ESERINE STANDARDS (100 $\mu\text{g}/\text{mL}$). THE SEPARATION COLUMN WAS SYMMETRY C_{18} , 4.6 MM \times 250 MM PACKED WITH SILICA PARTICLES SIZE 5 MM. ALL EXPERIMENTS WERE PERFORMED AT AMBIENT TEMPERATURE AROUND 25 $^{\circ}\text{C}$ ACCORDING TO THE HPLC CONDITIONS IN SECTION 2.3.3.....	117
FIGURE 4-18 RECOVERIES (%) OF CAFFEINE (100 $\mu\text{g}/\text{mL}$) EXTRACTED BY FOUR C_{18} -TMOS COLUMNS USING MICROWAVE HEATING DURING C_{18} MODIFICATION FOR 10, 20, 30 AND 40 MIN RESPECTIVELY AT 80 $^{\circ}\text{C}$	120
FIGURE 5-1 IMAGES OF TMOS SILICA MONOLITHS: (GNP-MONOLITH) EMBEDDED BY GOLD NANOPARTICLES 5 μL USING MICROWAVE HEATING FOR 5 MIN AT 300 W DURING GELATION TIME AND (NORMAL-MONOLITH) FABRICATED WITHOUT GOLD NANOPARTICLES USING MICROWAVE HEATING DURING GELATION TIME FOR 11 MIN AT 10-300 W.....	124
FIGURE 5-2 IMAGES OF TMOS SILICA MONOLITHS: (GNP 5-MONOLITH) EMBEDDED BY GOLD NANOPARTICLES 5 μL USING MICROWAVE HEATING FOR 5 MIN AT 300 W DURING GELATION TIME AND (GNP 10-MONOLITH) EMBEDDED BY GOLD NANOPARTICLES 10 μL USING MICROWAVE HEATING FOR 5 MIN AT 300 W DURING GELATION TIME.	124

FIGURE 5-3 SCANNING ELECTRON MICROGRAPHS OF TMOS SILICA MONOLITH EMBEDDED BY GOLD NANOPARTICLES 5 μ L, USING MICROWAVE HEATING DURING GELATION TIME (5 MIN AT 300 W).	125
FIGURE 5-4 SCANNING ELECTRON MICROGRAPHS OF TMOS SILICA MONOLITH EMBEDDED BY GOLD NANOPARTICLES 10 μ L, USING MICROWAVE HEATING DURING GELATION TIME (5 MIN AT 300 W).	125
FIGURE 5-5 SCANNING ELECTRON MICROGRAPHS OF TMOS SILICA MONOLITH WITHOUT GOLD NANOPARTICLES, USING MICROWAVE HEATING DURING GELATION TIME (11 MIN).	126
FIGURE 5-6 IMAGE OF ANTIGEN ANTIBODY REACTION TOOK PLACE IN THREE GLASS TUBES CONTAIN 1 mL OF PURIFIED WATER AND 5 mL OF GNP-NH ₂ IN TUBE (A) PLUS 5 mL ANTI-OXAZEPAM IN TUBE (B) AND 5 mL ANTI-OXAZEPAM AND THEIR ANTIGEN-HRP IN TUBE (C) (AFTER 5 MIN).....	128
FIGURE 5-7 IMAGE OF ANTIGEN ANTIBODY REACTION TOOK PLACE IN THREE GLASS TUBES CONTAIN 1 mL OF PURIFIED WATER AND 5 mL OF GNP-NH ₂ IN TUBE (A) PLUS 5 mL ANTI-OXAZEPAM IN TUBE (B) AND 5 mL ANTI-OXAZEPAM AND THEIR ANTIGEN-HRP IN TUBE (C) (AFTER 10 MIN).	129
FIGURE 5-8 IMAGE OF ANTIGEN ANTIBODY REACTION TOOK PLACE IN THREE GLASS TUBES CONTAIN 1 mL OF PURIFIED WATER AND 5 mL OF GNP-NH ₂ IN TUBE (A) PLUS 5 mL ANTI-OXAZEPAM IN TUBE (B) AND 5 mL ANTI-OXAZEPAM AND THEIR ANTIGEN-HRP IN TUBE (C) (AFTER 3 MONTHS).	129
FIGURE 5-9 PARAMETER OPTIMIZATION FOR CHEMILUMINESCENCE-BASED IMMUNOASSAY. EACH DATUM REPRESENTS THE AVERAGE OF THREE REPEAT EXPERIMENTS, WHILE THE ERROR BARS INDICATE ONE STANDARD DEVIATION. (◆) EFFECTS OF THE LUMINOL CONCENTRATION ON THE SIGNAL / NOISE RATIO OF CHEMILUMINESCENCE DETECTION. (■) EFFECTS OF THE HYDROGEN PEROXIDE (H ₂ O ₂)	

CONCENTRATION ON THE SIGNAL / NOISE RATIO OF CHEMILUMINESCENCE DETECTION.	130
FIGURE 5-10 PARAMETER OPTIMIZATION FOR CHEMILUMINESCENCE-BASED IMMUNOASSAY. EFFECTS OF THE LUMINOL AND H ₂ O ₂ CONCENTRATIONS ON THE EXPOSURE TIME OF CHEMILUMINESCENCE SIGNAL.	130
FIGURE 5-11 CALIBRATION CURVE FOR OXAZEPAM-HRP ANALYSIS BASED IMMUNOASSAYS. EACH DATA POINT REPRESENTS AN AVERAGE FROM THREE REPEAT EXPERIMENTS USING CHEMILUMINESCENCE, AND THE ERROR BARS INDICATE ONE STANDARD DEVIATION.	131
FIGURE 5-12 IMAGES OF THE ANTIGEN-ANTIBODY REACTION BASED ON CHEMILUMINESCENCE RESPONSE UPON ADDITION OF LUMINOL AND HYDROGEN PEROXIDE (A) NEGATIVE SAMPLE (B) WASHING FRACTION AND (C) POSITIVE SAMPLE.	132
FIGURE 5-13 IMAGE OF SILICA MONOLITHIC COLUMN COATED BY GNP-NH ₂	133
FIGURE 5-14 MECHANISM OF REACTION OF THE ANTIBODY WITH THE SURFACE OF GNP- NH ₂	134
FIGURE 5-15 DIFFERENT IMAGES FOR SILICA MONOLITHS COATED BY GOLD NANOPARTICLES (GNP 10 μL + ANTI-OXAZEPAM 5 μL) REACTED WITH A SAME CONCENTRATIONS OF OXAZEPAM-HRP (1000 μL). (A) NEGATIVE SAMPLE (B, C AND D) 0.5 μG/ML OF OXAZEPAM-HRP.....	135
FIGURE 5-16 DIFFERENT IMAGES FOR SILICA MONOLITHS COATED BY GOLD NANOPARTICLES (GNP 10 μL + ANTI-OXAZEPAM 5 μL) REACTED WITH THREE DIFFERENT CONCENTRATIONS OF OXAZEPAM-HRP (1000 μL). (A) NEGATIVE SAMPLE (B) 0.5 μG/ML OF OXAZEPAM-HRP (C) 1 μG/ML OF OXAZEPAM-HRP (D) 1.5 μG/ML OF OXAZEPAM-HRP.	136

FIGURE 5-17 IMAGES OF CONE SHAPE TMOS SILICA MONOLITHS COATED BY GNP-NH ₂	
USING MICROWAVE HEATING DURING GEL FORMATION STEP FOR 11 MIN.	138
FIGURE 5-18 DIFFERENT IMAGES FOR CONE SHAPED SILICA MONOLITHS COATED BY GOLD	
NANOPARTICLES (GNP 5 μL + ANTI-OXAZEPAM 5 μL) REACTED WITH THREE	
DIFFERENT CONCENTRATIONS OF OXAZEPAM-HRP (1000 μL). (A) 0.5 μG/ML OF	
OXAZEPAM-HRP (B) 1 μG/ML OF OXAZEPAM-HRP (C) 1.5 μG/ML OF OXAZEPAM-	
HRP.....	138
FIGURE 5-19 SQUARE SURFACE OF SILICA MONOLITHIC COLUMN COATED WITH GOLD	
NANOPARTICLES.....	140
FIGURE 5-20 IMAGES FOR THE TOP SQUARE SURFACE OF THE SILICA MONOLITHIC COLUMN	
COATED BY (GNP-NH ₂ 50 μL + ANTI-OXAZEPAM 5 μL) REACTED WITH A-) NEGATIVE	
SAMPLE B-) OXAZEPAM-HRP 0.5 μG/ML.	140
FIGURE 5-21 IMAGES FOR THE DIVIDED SQUARE SURFACE OF THE SILICA MONOLITHIC	
COLUMN COATED BY GNP-NH ₂ 50 μL + ANTI-AMPHETAMINE 5 μL IN SIDE (A) AND	
ANTI-METHAMPHETAMINE 5 μL IN SIDE (B) REACTED WITH A) NIGATIVE SAMPLE B)	
AMPHETAMINE-HRP 0.5 μG/ML IN SIDE (I) AND METHAMPHETAMINE-HRP 0.5 μG/ML	
IN SIDE (II).	141
FIGURE 5-22 IMAGES FOR THE DIVIDED SQUARE SURFACE OF THE SILICA MONOLITHIC	
COLUMN COATED BY GNP-NH ₂ 50 μL + ANTI-AMPHETAMINE 5 μL IN SIDE (I) AND	
ANTI-METHAMPHETAMINE 5 μL IN SIDE (II) REACTED WITH A) NEGATIVE SAMPLE B)	
AMPHETAMINE-HRP 0.5 μG/ML IN SIDE (I) AND METHAMPHETAMINE-HRP 1 μG/ML	
IN SIDE (II).	143
FIGURE 6-1 IMAGES OF GRAPHENE MONOLITHS A) USING MICROWAVE HEATING DURING	
REDUCTION OF GO B) USING CONVENTIONAL THERMAL HEATING FOR REDUCING	
GO. ^[203]	149

FIGURE 6-2 SCANNING ELECTRON MICROGRAPH FOR INTERNAL STRUCTURE OF GRAPHENE MONOLITH USED CONVENTIONAL THERMAL HEATING FOR GO REDUCTION. ^[203]	149
FIGURE 6-3 SCANNING ELECTRON MICROGRAPH (A AND B) FOR INTERNAL STRUCTURE OF GRAPHENE MONOLITH USED MICROWAVE HEATING FOR GO REDUCTION.	150
FIGURE 6-4 SCANNING ELECTRON MICROGRAPHS OF THE GRAPHENE MONOLITHS USING MICROWAVE HEATING DURING GO REDUCTION.	151
FIGURE 6-5 IMAGES OF SILICA MONOLITHS A) NON-MODIFIED SILICA ROD B) MODIFIED SILICA ROD WITH GRAPHENE PHASE (GO 1 MG/ML).	153
FIGURE 6-6 SCANNING ELECTRON MICROGRAPH (A AND B) FOR MODIFIED SILICA MONOLITHS WITH GRAPHENE PHASE (GO 1 MG/ML).	153
FIGURE 6-7 EDX SPECTRA OF SILICA-BASED MONOLITH MODIFIED WITH GRAPHENE PHASE USING MICROWAVE HEATING FOR 10 SECONDS AT 90 °C AND 130 W.	154
FIGURE 6-8 EDX SPECTRA OF SILICA-BASED MONOLITH MODIFIED WITH GRAPHENE PHASE USING MICROWAVE HEATING FOR 60 SECONDS AT 90 °C AND 130 W.	155
FIGURE 6-9 SCANNING ELECTRON MICROGRAPH (A AND B) FOR MODIFIED SILICA MONOLITH WITH GRAPHEME PHASE (GO 0.5 MG/ML).	156
FIGURE 6-10 CHROMATOGRAMS OF AMPHETAMINE AND THOSE SAMPLES WERE COLLECTED DURING LOADING, WASHING AND ELUTION STEPS; THE CONCENTRATION OF AMPHETAMINE WAS 20 µG/ML. ALL RESULTS WERE OBTAINED FROM HPLC-UV SYSTEM UNDER THAT HPLC CONDITIONS DESCRIBED IN SECTION 2.5.3.	158
FIGURE 6-11 PERCENTAGE OF AMPHETAMINE STANDARD (100 µG/ML) EXTRACTED USING GRAPHENE-SILICA MONOLITHIC COLUMN (GO 0.5 MG/ML) AT FLOW RATE 50 ML/MIN COMPARED TO DIRECT INJECTION OF THE SAME AMPHETAMINE STANDARD. THE ERROR BARS REPRESENT THE STANDARD DEVIATION OF 3 REPEAT EXPERIMENTS. .	159
FIGURE 6-12 PERCENTAGE OF AMPHETAMINE STANDARD (100 µG/ML) EXTRACTED USING GRAPHENE-SILICA MONOLITHIC COLUMN (GO 0.5 MG/ML) AT FLOW RATE 100	

Ml/min compared to direct injection of the same amphetamine standard.

The error bars represent the standard deviation of 3 repeat experiments.

..... 160

FIGURE 6-13 PERCENTAGE OF AMPHETAMINE STANDARD (100 µg/mL) EXTRACTED USING GRAPHENE-SILICA MONOLITHIC COLUMN (GO 0.5 mg/mL) AT FLOW RATE 200

ml/min compared to direct injection of the same amphetamine standard.

The error bars represent the standard deviation of 3 repeat experiments.

..... 160

FIGURE 6-14 CALIBRATION CURVE FOR WIDE RANGE CONCENTRATIONS OF AMPHETAMINE (40, 20, 10, 5, 2 AND 1 µg/mL). (W.L. 254 nm). THE ERROR BARS REPRESENT THE

STANDARD DEVIATION OF 3 REPEAT EXPERIMENTS. 162

FIGURE 6-15 PERCENTAGE OF AMPHETAMINE STANDARD (40 µg/mL) EXTRACTED USING

GRAPHENE-SILICA MONOLITHIC COLUMN (GO 0.5 mg/mL) AT FLOW RATE 50 ml/min

compared to direct injection of the same amphetamine standard. The

error bars represent the standard deviation of 3 repeat experiments. . 163

FIGURE 6-16 PERCENTAGE OF AMPHETAMINE STANDARD (20 µg/mL) EXTRACTED USING

GRAPHENE-SILICA MONOLITHIC COLUMN (GO 0.5 mg/mL) AT FLOW RATE 50 ml/min

compared to direct injection of the same amphetamine standard. The

error bars represent the standard deviation of 3 repeat experiments. . 163

FIGURE 6-17 PERCENTAGE OF AMPHETAMINE STANDARD (2 µg/mL) EXTRACTED USING

GRAPHENE-SILICA MONOLITHIC COLUMN (GO 0.5 mg/mL) AT FLOW RATE 50 ml/min

compared to direct injection of the same amphetamine standard. The

error bars represent the standard deviation of 3 repeat experiments. . 164

FIGURE 6-18 PERCENTAGE OF AMPHETAMINE STANDARD (2 µg/mL) EXTRACTED USING

GRAPHENE-SILICA MONOLITHIC COLUMN (GO 0.25 mg/mL) AT FLOW RATE 50

ml/min compared to direct injection of the same amphetamine standard.

THE ERROR BARS REPRESENT THE STANDARD DEVIATION OF 3 REPEAT EXPERIMENTS.

..... 165

FIGURE 6-19 PERCENTAGE OF AMPHETAMINE STANDARD (20 $\mu\text{g/mL}$) EXTRACTED USING GRAPHENE-SILICA MONOLITHIC COLUMN (GO 0.25 mg/mL) AT FLOW RATE 50 mL/min COMPARED TO DIRECT INJECTION OF THE SAME AMPHETAMINE STANDARD.

THE ERROR BARS REPRESENT THE STANDARD DEVIATION OF 3 REPEAT EXPERIMENTS.

..... 165

FIGURE 6-20 PERCENTAGE OF AMPHETAMINE STANDARD (40 $\mu\text{g/mL}$) EXTRACTED USING GRAPHENE-SILICA MONOLITHIC COLUMN (GO 0.25 mg/mL) AT FLOW RATE 50 mL/min COMPARED TO DIRECT INJECTION OF THE SAME AMPHETAMINE STANDARD.

THE ERROR BARS REPRESENT THE STANDARD DEVIATION OF 3 REPEAT EXPERIMENTS.

..... 166

List of tables

TABLE 1-1 LIST OF ABUSED DRUGS ACCORDING TO NATIONAL INSTITUTES ON DRUG ABUSE ^[5]	3
TABLE 1-2 SUMMARY OF THE ADVANTAGES AND DISADVANTAGES OF ORGANIC AND INORGANIC MONOLITHS BASED ON LITERATURE REVIEW.....	27
TABLE 1-3 CHEMICAL MODIFICATION REACTIONS OF SILICA MONOLITHS.	29
TABLE 3-1 COMPOSITION AND REACTION CONDITIONS FOR THE PREPARATION OF MONOLITHIC SILICA COLUMNS.	77
TABLE 3-2 CHEMICAL COMPOSITION FOR PREPARATION SILICA MONOLITHIC COLUMNS USING MICROWAVE HEATING.....	80
TABLE 3-3 CHEMICAL COMPOSITION AND CONDITIONS FOR SILICA MONOLITH FABRICATION USING MICROWAVE HEATING.	85
TABLE 3-4 PHYSICAL PROPERTIES OF SILICA MONOLITHS 1-8 USING MICROWAVE HEATING AND OVEN HEATING METHODOLOGY DURING GEL FORMATION PROCESS.....	90
TABLE 3-5 COMPOSITION AND WEIGHTS OF MONOLITHIC SILICA COLUMNS 1-8 USING MICROWAVE HEATING AND OVEN HEATING METHODOLOGY DURING GEL FORMATION PROCESS.	91
TABLE 3-6 PHYSICAL PROPERTIES OF MONOLITHS 9 AND 10 USING MICROWAVE HEATING AND OVEN HEATING METHODOLOGY DURING GEL FORMATION PROCESS.....	92
TABLE 4-1 CHEMICAL COMPOSITION AND REACTION CONDITIONS FOR C ₁₈ PHASE MODIFICATION	98
TABLE 4-2 QUANTITATIVE EDX ANALYSIS FOR ALL ELEMENTS IN NON-MODIFIED SILICA-BASED MONOLITH USING QUANTITATIVE EDX ANALYSIS.	99
TABLE 4-3 QUANTITATIVE EDX ANALYSIS FOR ALL ELEMENTS IN SILICA-BASED MONOLITH MODIFIED WITH C ₁₈ PHASE USING THERMAL HEATING METHOD.....	100

TABLE 4-4 QUANTITATIVE EDX ANALYSIS FOR ALL ELEMENTS IN THREE SILICA- MONOLITHIC COLUMNS MODIFIED WITH C ₁₈ PHASE USING MICROWAVE HEATING AT 80 °C, 100 °C AND 110 °C FOR 10 MIN.....	105
TABLE 4-5 SEQUENCE OF EXTRACTION PROCEDURE OF CAFFEINE STANDARD USING THE C ₁₈ SILICA MONOLITHIC COLUMN.	105
TABLE 4-6 QUANTITATIVE EDX ANALYSIS FOR ALL ELEMENTS IN SILICA-BASED MONOLITH MODIFIED WITH C ₁₈ PHASE USING MICROWAVE HEATING FOR 10 MIN AT 80 °C AND 120 W.	106
TABLE 4-7 QUANTITATIVE EDX ANALYSIS FOR ALL ELEMENTS IN SILICA-BASED MONOLITH MODIFIED WITH C ₁₈ PHASE USING MICROWAVE HEATING FOR 20 MIN AT 80 °C AND AT 120 W.	107
TABLE 4-8 QUANTITATIVE EDX ANALYSIS FOR ALL ELEMENTS IN SILICA-BASED MONOLITH MODIFIED WITH C ₁₈ PHASE USING MICROWAVE HEATING FOR 30 MIN AT 80 °C AND 120 W.	108
TABLE 4-9 QUANTITATIVE EDX ANALYSIS FOR ALL ELEMENTS IN SILICA-BASED MONOLITH MODIFIED WITH C ₁₈ PHASE USING MICROWAVE HEATING FOR 40 MIN AT 80 °C AND 120 W.	109
TABLE 4-10 PHYSICAL PARAMETERS OF SILICA MONOLITHS BEFORE AND AFTER C ₁₈ SURFACE MODIFICATION USING MICROWAVE HEATING AND THERMAL HEATING METHODOLOGY.	112
TABLE 4-11 QUANTITATIVE EDX ANALYSIS FOR ALL ELEMENTS IN ALL CROSS SECTIONS OF SILICA- MONOLITHS MODIFIED WITH C ₁₈ PHASE USING MICROWAVE HEATING FOR 40 MIN AT 80 °C.....	113
TABLE 4-12 COMPOSITION AND CAPACITY OF MICROWAVE C ₁₈ -TMOS COLUMN (C ₁₈ AT 80 °C FOR 40 MIN AND 120 W) AND THERMAL C ₁₈ -TMOS COLUMN.....	116

TABLE 4-13 PERCENTAGES OF RECOVERIES OF CAFFEINE AND ESERINE FROM STANDARD SOLUTIONS (100 MG/ML) USING MICROWAVE C ₁₈ -TMOS COLUMN (C ₁₈ AT 80 °C FOR 40 MIN AND 120 W) AND THERMAL C ₁₈ -TMOS COLUMN.....	118
TABLE 4-14 PRECISION OF EXTRACTION CAFFEINE FROM STANDARD SOLUTIONS SAMPLES.	119
TABLE 5-1 COMPOSITION AND REACTION CONDITIONS FOR PREPARATION OF SILICA MONOLITHIC COLUMNS EMBEDDED BY GOLD NANOPARTICLES.	123
TABLE 5-2 PHYSICAL PROPERTIES OF SILICA MONOLITHS WITHOUT AND WITH GNP-NH ₂	127
TABLE 5-3 PHYSICAL PROPERTIES OF SILICA MONOLITHS WITHOUT AND AFTER COATING BY GNP-NH ₂	133
TABLE 5-4 RLU-VALUES FOR THREE SILICA MONOLITHIC COLUMNS COATED BY GNP-NH ₂ -ANTI OXAZEPAM REACTED WITH SAME CONCENTRATION OF OXAZEPAM-HRP.	136
TABLE 5-5 RLU-VALUES FOR THREE SILICA MONOLITHIC COLUMNS COATED BY GNP-NH ₂ -ANTI OXAZEPAM REACTED WITH THREE DIFFERENT CONCENTRATIONS OF OXAZEPAM-HRP.....	137
TABLE 5-6 RLU-VALUES FOR THREE CONE SHAPED SILICA MONOLITHIC COLUMNS COATED BY GNP-NH ₂ -ANTI OXAZEPAM REACTED WITH THREE DIFFERENT CONCENTRATIONS OF OXAZEPAM-HRP.	139
TABLE 5-7 RLU-VALUES FOR THREE DIVIDED SQUARE SHAPE SILICA MONOLITHIC COLUMNS COATED BY GNP-NH ₂ + ANTI-AMPHETAMINE AND ANTI-METHAMPHETAMINE AND DETECTED SAME CONCENTRATION FROM AMPHETAMINE-HRP AND METHAMPHETAMINE-HRP.	142
TABLE 5-8 RLU-VALUES FOR THREE DIVIDED SQUARE SHAPE SILICA MONOLITHIC COLUMNS COATED BY GNP-NH ₂ + ANTI-AMPHETAMINE AND ANTI-	

METHAMPHETAMINE AND DETECTED DIFFERENT CONCENTRATIONS FROM AMPHETAMINE-HRP AND METHAMPHETAMINE-HRP.	143
TABLE 6-1 PHYSICAL PROPERTIES OF THE GRAPHENE MONOLITHS USING MICROWAVE AND THERMAL HEATING METHODS FOR GO REDUCTION.	151
TABLE 6-2 QUANTITATIVE EDX ANALYSIS FOR ALL ELEMENTS IN GRAPHENE MONOLITH USING MICROWAVE HEATING DURING REDUCING OF GO.	152
TABLE 6-3 PHYSICAL PROPERTIES OF THE GRAPHENE MONOLITHS USING MICROWAVE HEATING METHODS BEFORE AND AFTER GO REDUCTION.	157
TABLE 6-4 RECOVERIES OF THREE AMPHETAMINE STANDARDS (LOW, MID AND HIGH) USING GRAPHENE SILICA MONOLITH AND C ₁₈ SILICA MONOLITH DURING EXTRACTION PROCESSES.	167

1 Introduction

(Chapter 1)

1.1 Forensic science

The term forensic science is very broad because there are a very large number of forensic traces or sample types that can be found at the scene of a crime. Accordingly, forensic investigations are typically divided into several areas, for example blood spatter analysis, DNA profiling, illicit drugs and explosives.^[1] To aid investigation, analytical screening at a crime scene should be fast, simple, cheap and robust, whilst offering high sensitivity and selectivity. This approach to direct analysis of forensic traces can provide immediate results that help to identify and classify the evidence. This research project is focused on the analysis of drugs of abuse, with the main sample types including blood, plasma, urine and saliva. However, it can be difficult to test these matrices without preparation. Therefore, the sample preparation process is very necessary in procedures of drugs testing.^[2]

1.2 Drugs of abuse

Drugs of abuse can be divided into a number of classes and their potential dangers to health and life. The first group of drugs of abuse have sedative effects (such as heroin, alcohol, benzodiazepines and tranquillisers), which slow down the function of the body and brain.^[3] The second group include cocaine, amphetamine, crack, ecstasy and other drugs, which have a stimulant effect that make people more energetic, active and alert.^[4] The third group of drugs has a hallucinogenic effect (such as LSD, magic mushrooms and cannabis) which changes the way the user feels, hears, sees and smells.^[2] Recently, other groups of drugs have been added to the list of abused drugs (see Table **1-1**).

Table 1-1 List of abused drugs according to National Institutes on Drug Abuse ^[5]

Substances	Examples
Tobacco	Nicotine
Alcohol	Alcohol (ethyl alcohol)
Cannabinoids	Marijuana and Hashish
Opioids	Heroin and Opium
Stimulants	Cocaine, Amphetamine and Methamphetamine
Club Drugs	MDMA (methylenedioxymethamphetamine), Flunitrazepam and GHB
Dissociative Drugs	Ketamine, PCP and analogs, Salvia divinorum, Dextromethorphan (DXM)
Hallucinogens	LSD, Mescaline and Psilocybin
Other Compounds	Anabolic steroids and Inhalants

1.2.1 Drugs of abuse analysis

In 1923 the U.S. Federal Rules of Evidence accepted the first scientific methodology for forensic drug analysis.^[6] The analysis of forensic drugs can be performed by various tests, such as spot tests, thin layer chromatography (TLC), infrared spectroscopy (IR), immunoassay, capillary electrophoresis (CE), fluorimetry, high performance liquid chromatography (HPLC) and gas chromatography (GC).^[7, 8]

This wide range of analytical methodology prompted Manfred R. Möller to say “it would be easier to get two forensic drug analysts to share the same toothbrush than to share the same method of analysis”.^[2] For that reason, recently, a combination of techniques have been used to analyse samples of drugs of abuse, such as gas chromatography-mass spectrometry (GC/MS) ^[9, 10] and liquid chromatography tandem mass spectrometric analysis (LC-MS-MS).^[10-12] GCMS is emerging high-resolution technology which uses long GC columns to achieve separations with MS for detection.

The detection of drugs of abuse in biological samples is usually difficult due to the complexity of the samples, which contain different types of proteins and contaminants such as salts, lipids, nucleic acids, buffers and detergents that can interfere with target drugs analysis.^[1, 13] These challenges make the extraction of drugs of abuse one of the

most critical steps in the analytical process.^[14] Conventional techniques for analysing drugs of abuse require multiple tests and relatively large amount of samples, which can be both time-consuming and expensive.^[15] Recently, new techniques used in forensic toxicology, such as HPLC, GC-MS and LC-MS-MS, have provided an easy and rapid way for detecting and quantifying multi-drugs of abuse from different matrices (such as urine, saliva and serum).^[16, 17] However, these methods cannot handle the target analytes directly from the sample without preparation.^[18] Therefore, sample preparation plays a very important role in the analytical methodology of drugs of abuse in cleaning-up, removing interfering materials, and preconcentrate the target drugs for easy detection.^[10, 19] Finding an appropriate sample preparation method is a key factor in the success of drugs of abuse analysis. Generally, the extraction and preconcentration of drugs of abuse from biological samples can be time consuming, labour-intensive, complex and prone to contamination. The best sample preparation technique should be fast, as simple as possible, reproducible and provide high extraction recovery for the target analytes. In addition, it should be environmentally friendly, have potential to improve detection limits and be suitable for use in off-line and on-line methods of detection.^[20]

1.3 Sample preparation techniques

1.3.1 Liquid-liquid extraction

Traditionally, the oldest and standard method of sample preparation for drugs analysis has been based on liquid–liquid extraction (LLE).^[21] The application of this procedure depends on the separation of liquid phases from each other by mixing an immiscible organic solvent with an aqueous solvent. The target analytes in this process move from the biological matrix in the aqueous phase to the organic layer. The organic layer is then used for further manipulation or analysis (see Figure **1-1**).^[22, 23]

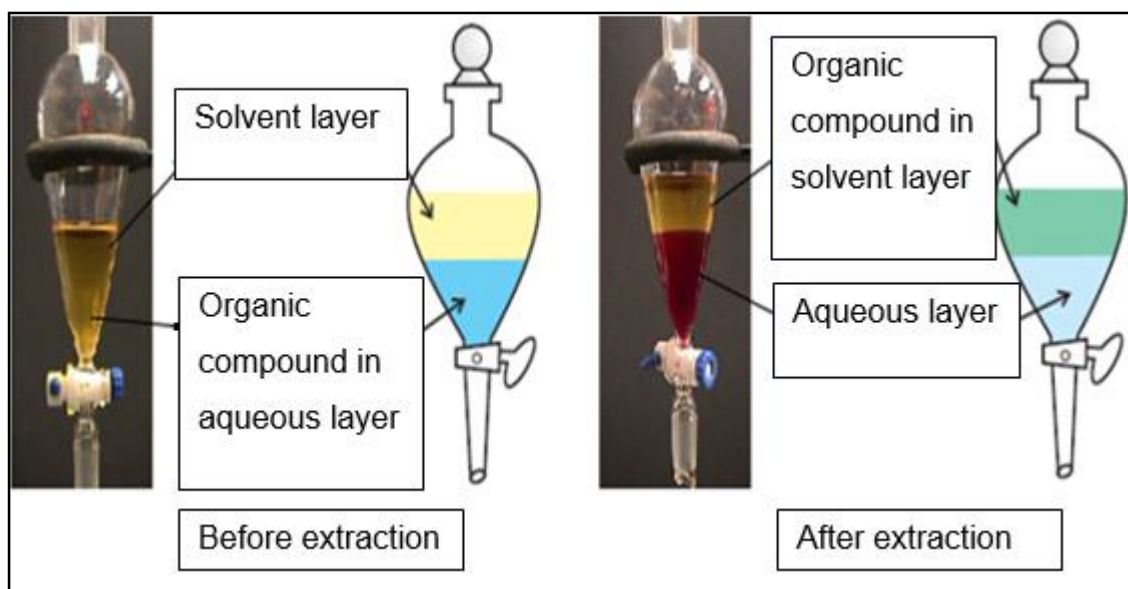


Figure 1-1 Liquid–liquid extraction (LLE) technique. The process of liquid-liquid extraction involves the distribution of a compound between two solvents that are insoluble in each other. By taking advantage of the differing solubilities of a solute in a pair of solvents, compounds can be selectively transported from one liquid phase to the other. [24]

In 2003 Kronstrand and a co-worker [25] used the LLE technique to extract the selegiline metabolites methamphetamine and amphetamine from hair samples. Analyses were performed on both the pigmented and non-pigmented whole hairs, and metabolites were analysed quantitatively using GC/MS. They found significant variation in the concentrations of both methamphetamine ($p < 0.01$) and amphetamine ($p < 0.02$) in pigmented and non-pigmented hairs, with mean concentration ratios of 2.95 ± 1.16 ng/mL and 3.69 ± 1.88 ng/mL for amphetamine and methamphetamine, respectively.

Rasmussen LB *et al.* [26] in 2006 extracted the amphetamines from 0.5 g of whole blood using liquid-liquid extraction. These analytes were derivatized with R-MTPCl, in order to change their chemical properties to be more suitable for separation by GC and finally detected by SIM-MS. The method was validated and found to be linear from 0.004 to 3 μ g/g. The method was applied to the analysis of whole blood samples originating from traffic, criminal and post mortem cases. The accuracy was found to be between 91 and 115 %, while the repeatability and reproducibility were less than or equal to 15 % R.S.D.

As can be seen LLE can offer several advantages of the technique, such as large sample capacity, good extraction recovery, provision of some clean-up and removal of protein. However, there are some drawbacks to this procedure such as use of hazardous organic solvents and it requires labour-intensive transfer steps. Furthermore, the formation of emulsions in the process of LLE can make the identification of the desired organic layer very difficult and lead to loss of the analytes due to incomplete extraction.^[27] To overcome these problems other kinds of extraction have been considered.

1.3.2 Solid phase extraction

Drugs of abuse can be readily extracted from the biological samples using solid phase extraction (SPE).^[28] SPE is an increasingly useful technique for sample preparation that can be used in different applications such as the forensic which provides reproducible protocols designed to prepare different biological samples for injection onto HPLC or LC/MS ^[29], pharmaceutical ^[30], clinical ^[29], environmental ^[31] and industrial field.^[32] SPE was introduced in the 1970s as a new method for sample preparation that has ability to concentrate and purifies the target analytes from an original solution by adsorbing them onto a disposable solid-phase cartridge. The target analytes could then eluted with an appropriate solvent for further analysis.^[33] In addition, the SPE can also remove the interfering compounds from the complex matrices to produce a cleaner extract.^[34] In 1998 Wolfgang Weinman and Michal Svoboda ^[35] used a rapid analytical methodology based on biological samples (serum and urine) for the simultaneous quantitative screening of drugs of abuse. They combined solid-phase extraction (SPE) followed by flow-injection analysis (FIA) with ionspray-ionization and tandem mass spectrometry (MS-MS). Analysis was performed for morphine (MO), codeine (COD), amphetamine (AMP), and benzoylecgonine (BZE). Quantitative results were obtained and no interferences with metabolites or other compounds were found. As demand grew

Girod C and Staub C ^[36] developed an automatic solid-phase extraction method in 2000. They used a robot ASPEC to treat a large number of samples at the same time. This method was performed for codeine, 6-monoacetylmorphine (6-MAM), morphine, cocaine, methadone, ecstasy (MDMA) and Eve (MDE). Analysis of these drugs was achieved by a gas-chromatography-mass spectrometry (GC/MS). Different validation parameters, linearity, recovery, repeatability and detection limits were obtained, as well as the application of this method to some real cases. The results demonstrated the usefulness of this technique for routine analysis.

Actually, SPE makes sample preparation much faster, more reproducible, more accurate and precise. Furthermore, it improves the efficiency of the extraction by increasing recovery and minimising solvent consumption, waste produced and sample required, compared to the LLE.^[37] However, the SPE technique still has some drawbacks such as cost, blockage of the cartridge by solid particles, limited capacity, back pressure, contamination through manufacturing and a time consuming sorbent fabrication process.^[38] These limitations on this method do not prevent SPE being the most widely used technique of sample preparation.^[39]

The SPE can be coupled with different chromatographic systems such as HPLC, GC, GC-MS and LC-MS-MS.^[16] Integration of SPE with HPLC is very useful since both techniques are based on aqueous mobile phase.^[40, 41]

Off-line sample preparation is the most popular type of SPE that can be used to optimise the extraction and separation independently, despite the on-line procedure offering many advantages, such as reducing the risk of sample contamination and loss of the sample by evaporation, in addition to reducing the time taken for analysis.^[42]

1.3.3 Materials used on SPE sorbent

Several types of materials can be used for solid phase fabrication. Selection of the extraction media usually depends on the physiochemical properties of the sample matrix, in particular the nature of any potential interfering compounds and the target analytes that need to be retained. The sorbent used in SPE should be: i) chemically stable and unreactive with the cleaning, conditioning, washing and eluting solvents; ii) physically stable not damaged by micro-organisms when using a biological sample; and iii) thermally stable so it can be used at high temperatures if required. The SPE should also have a high surface area and good permeability to enable the extraction of target analytes from a large sample at a high flow rate with a low back pressure.^[43] In 1999 Marie-Claire Hennion^[44] outlined the most important features of the new solid-phase extraction (SPE) materials. These include polymeric sorbents and silica sorbents; one limitation of both sorbents is that they need to be conditioned with a wetting solvent before the extraction process and not allowed to dry before the loading of an aqueous solvent. The surface functionalization of polymeric sorbents will increase the extraction recoveries of polar compounds and provided a better wettability.^[45] The new generation of polymeric sorbents (Oasis from waters, Absolut from Varian) are designed to be suitable for the extraction of a wide range of analytes such as, lipophilic, hydrophobic, basic, acidic and neutral, with a simplified procedure that needs no conditioning step.^[46] However, the limitation in this procedure is the handling of biological samples, as the recommended sample volume is 1 mL.^[44] The problem of the extraction of target analytes from biological samples has been solved by the introduction of silica sorbents (non-encapped C₁₈ silicas and monofunctional C₁₈ silicas) that have high specific surface areas of up to 1000 m²/g and a high degree of purity.^[47, 48]

The development of SPE based on 3D monolithic structure allowed for extraction and clean-up of samples at the same time. Furthermore, they are suitable for the handling of

biological samples, which can prevent the access of matrix components such as proteins, while retaining the target analytes in the internal structure.^[43]

1.3.4 Solid phase extraction procedure

Typically, there are five steps (see Figure 1-2) in processing a sample based on solid phase extraction: i) activation of the sorbent by an appropriate solvent; ii) removal of impurities by equilibration of the sorbent bed; iii) loading the sample solution into the SPE media, where the analytes of interest are retained by the specific selected chemistry and the unwanted components are allowed to flow through the sorbent to waste; iv) washing of SPE media with a solvent to remove any interfering matrix; and finally, v) elution of the target compounds from the sorbent and collection in a clean tube for further analysis.^[43, 49]

The activation, loading and elution of a sample can be achieved by gravity or pumping, but it is very important to make sure that the flow rate during loading, washing and eluting is adjusted to enable efficient retention of the analytes.^[33]

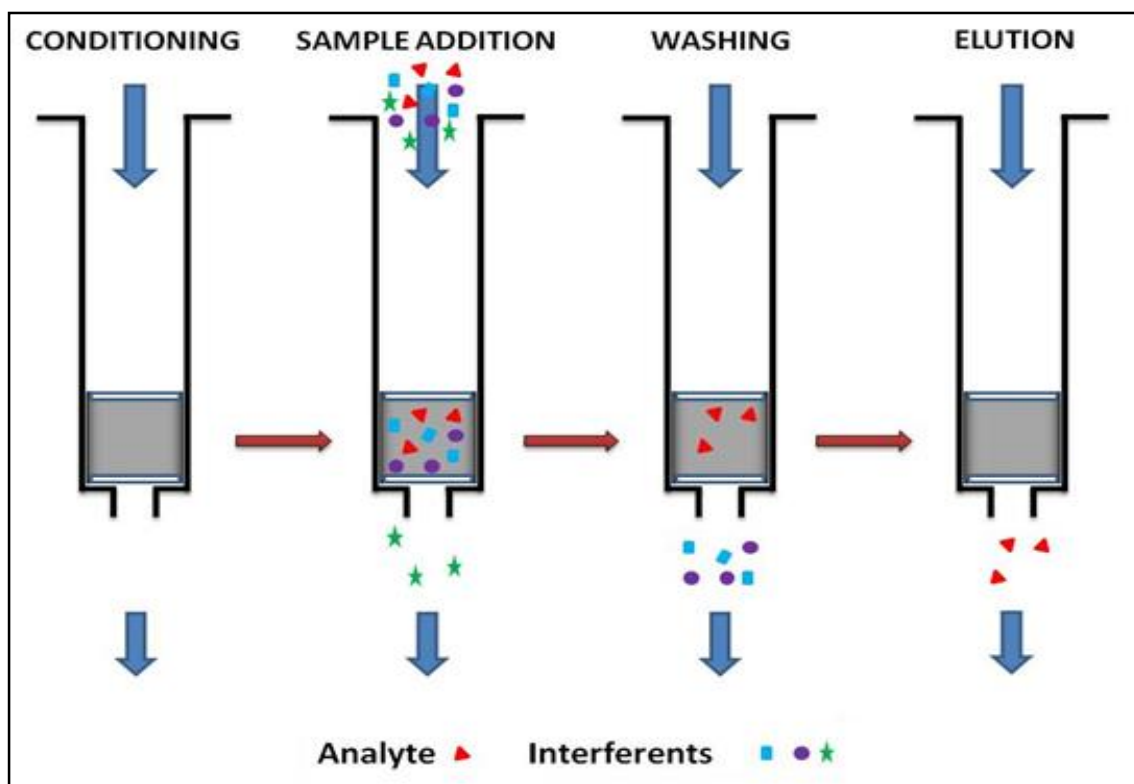


Figure 1-2 The solid phase extraction process basically consists in four different steps: conditioning, sample addition, washing and elution. During the conditioning the functional groups of the sorbent bed are solvated in order to make them able to interact with the sample. The analytes as well as some matrix components are retained on the SPE packing material during the loading or sample addition process. After that the impurities will be rinsed through with wash solutions. Finally, the adsorbed compounds will be eluted using a proper solvent. ^[49]

1.4 Particulate stationary phases

The most important part of a solid phase extraction is the stationary phase component. The performance of the solid phase extraction is significantly influenced by the efficiency and selectivity of the stationary phase. Commonly, two types of particles have been used as stationary phase for solid phase extraction: silica and polymeric beads. Recently, the size of the particles has decreased, to be in the range of 3 to 10 μm diameter.^[50] It is notable that between the 1950s and 2000 the size of the particles dropped from 100 μm to 3 μm and their efficiencies increased from $\sim 1,300$ to $\sim 160,000 \text{ Nm}^{-1}$, respectively.^[50] The efficiency of small particles has also reduced the plate height (see Figure 1-3).

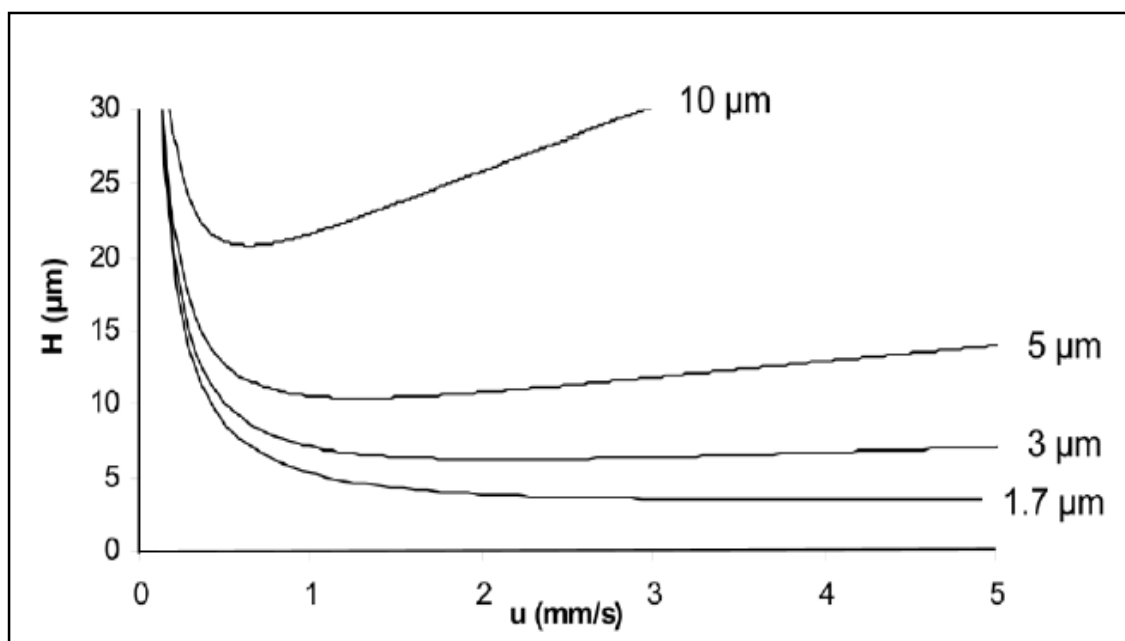


Figure 1-3 Knox plot (reduced plate height vs. reduced linear velocity) showing the effect of reducing particle diameter on plate height.^[50]

In 1956 J. J. Van Deemter ^[50] described the main factors contributing to the height of theoretical plate (HETP) of a column: $HETP = A + B/u + Cu$ Eq. 1

Where A = Eddy diffusion, B = axial diffusion, C= mass transfer and u = linear velocity of the mobile phase.

A) Eddy diffusion: represents the movement of the analytes in the mobile phase through the column using multiple paths to reach the same point (see Figure 1-4). The interparticulate voids inside the packed columns, and through-pores structures in the monolithic column, generate the possible paths for the analytes into the column. Some molecules can move on the easiest path compared the majority of molecules, and they will elute from the column in a shorter time. Conversely, those molecules which move through the column on a more circuitous path usually take longer to leave.^[51]

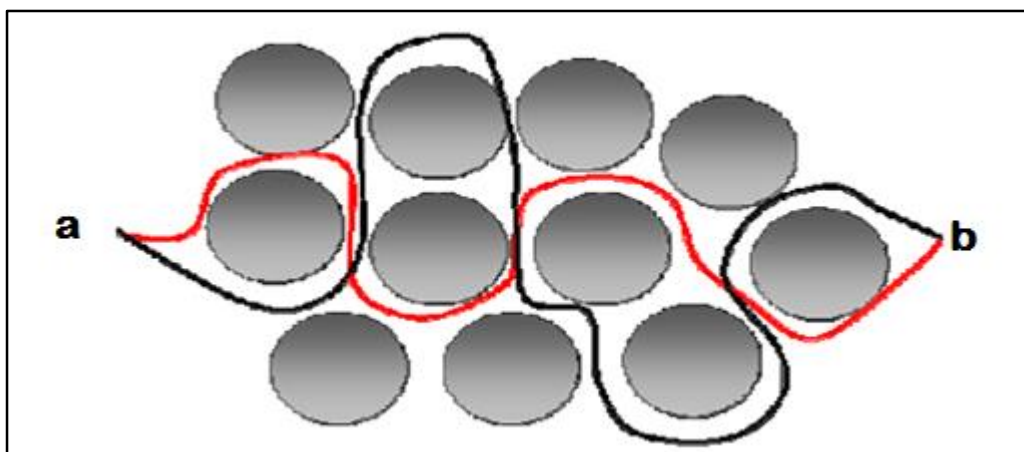


Figure 1-4 Schematic depicting two possible paths within a packed column from point (a) to point (b).^[51]

B) Longitudinal diffusion: when the sample analyte is introduced and flows through the column it will undergo diffusion symmetrically around its centre of mass, however in the SPE the contribution of longitudinal diffusion is small.^[51]

C) Mass transfer: During movement of the analytes inside the column between the stationary phase and mobile phase or elution phase partition will occur. Therefore, the time spent in the stationary phase will determine which analyte is retarded compared to the centre of mass. The time will be short when the difference between the analyte in the stationary phase and the centre of mass is low (i.e. fast transfer kinetics), whereas the time will be long when the difference between them is high (i.e. slow transfer kinetics).^[51]

The use of packed particles is advantageous for both efficiency and selectivity of SPE, because their surface area is high and easily modified or functionalized.^[52] However, the preparation of the particle requires special equipment and skilled technicians. Moreover, this type of technique needs highly porous and rigid frits to keep the particles in place, which is often difficult to achieve.^[53] Reducing the particle size resulted in an increase in the surface area and improved the efficiency of extraction; however, that led to an increase in the back pressure.^[52]

Increase of the back pressure is directly proportional with the cube of the particle diameter. In order to decrease the back pressure, the length of the bed should be reduced,

however, decreasing the bed length can reduce the capacity of the sorbent, the number of interaction sites and the efficiency of extraction. Another way to solve this problem is the use of “monolithic” stationary phases, where the surface area is also high but the back pressure is relatively low due to porous nature of the structure.^[54]

1.5 *Monolithic stationary phases*

“The term monolith comes from Greek for one stone or in this case one piece”.^[55]

A monolithic stationary phase is a single piece of material that includes through pores, which the mobile phase can flow with minimal resistance.^[56]



Figure 1-5 Photograph of the porous monolith erected at the entrance of the Summer Palace Park, Beijing, China.^[57]

The monolithic structures can be defined as rigid macro-porous stationary phases, constructed from either silica or polymer.^[58] In the last few decades, the fabrication of macroporous materials has been extensively studied. The formation of the silica network can be achieved by templating close-packed colloidal crystals infiltrated by gas or liquid-

phase precursors in order to enclose and freeze the structure of the template.^[59] Then, removal of the frame can be carried out by either thermal treatment or chemical etching.^[60] However, in this case the main drawback of the purely macroporous network is that the low surface areas and a low loading of potential substitution sites for functional groups on the surface.^[59] To improve the surface area, new methods for formation of macroporous silica monoliths have been developed. Galarneau and co-workers^[61] reported that a pseudomorphic transformation is conducted at the surface of the macroporous, while the size of pores and the particle is preserved. This methodology generated silica materials, which have a high loading of functional organic moieties and a high mechanical stability; however, the surface area was quite low. Brook and Brennan prepared macroporous silica monoliths based on sol gel process where allyl- and silyl-modified poly (ethylene glycol) (PEG) polymers are used to induce aggregation of the particles process and obtained the macroporous network structure. Macroporous materials provide high permeability for large molecules, such as proteins and DNA^[62], however, the high throughput and low specific surface areas, do not make them ideal candidates for extraction of small organic molecules.^[63, 64]

The combination of mesoporous and macroporous in the silica monolithic structure can, however, provide the necessary amount of active sites and high surface areas, in addition to a high diffusion rate for separation, extraction and catalysis applications.^[65] A number of approaches towards sponge architecture materials have been developed where the interconnected framework consisting of macropores structure allows for a high solvent diffusion rate and mass transfer, while the smaller pores (mesoporous) in the skeleton structure increases the surface area and makes the adsorption of small molecules much better.^[54, 66]

In 1992 Nakanishi and co-workers^[67] presented one of the most important sol-gel procedures. They prepared a silica-based monolith with bipores structure, combining two

processes: phase separation and sol–gel transition. A gel is a state where both solid and liquid are dispersed in each other.^[68] The silica monoliths generated were highly porous and offered the potential to be used in different fields of technology, such as electronic, chemical separation, extraction and fabrication, optical, bio-analysis and energy storage.^[69-71] The properties of silica monoliths are influenced by several factors, including physical parameters, chemical composition and the thermal process that can be used during the fabrication process.^[53, 72] In general, the structure of silica monoliths contain, large (micron) flow-through pores, with up to 99 % porosity,^[73] which can give a high permeability and small (Nano) diffusion pores that can generate high surface areas of up to 1,000 m²/g.^[74] In addition, silica monoliths have good optical transmission (~90 %) ^[75], low density (~ 50 g cm⁻³) ^[76], dielectric constant (~ 2) ^[77] and thermal conductivity (~ 0.05 W/mK) ^[78]. A number of chemical, catalytic, optical, and thermal applications have been reported based on silica monoliths.^[79] In 2006 Randon *et al.* used inorganic monolithic column for the separation of a mixture of alkoxybenzene (consisting of thiourea, toluene, ethylbenzene, propylbenzene) and amines (consisting of naphthalene, orthotoluidine and aniline).^[80] In 2006 the same group also applied a similar technique for the separation of caffeine, naphthalene, theophylline and 7-(β-hydroxyethyl) theophylline in hydrophilic interaction liquid chromatography (HILIC).^[81]

The advantage of monolithic shape make it possible to use luminescence therefore, maintaining quantum confinement effects in sol-gel can be achieved by either limiting the dimensionality (density) of the network or by introducing spacers between particles to limit interactions. ^[82, 83] Furthermore, modification of inorganic surface with potassium and platinum made it suitable to be used as catalysts and it shows spurious support properties^[84]. In addition, the laser action was also obtained by the interference of multiple scattered light from organic dyes incorporated in the pores of inorganic monoliths.^[85]

1.5.1 Silica monoliths fabrication

In 1996 Fields ^[86] filled an empty fused silica column with potassium silicate solution and heated it for 1 hour at 100 °C, and dried it by helium at 120 °C for 24 hours.^[86, 87]

The resulted column was then modified using dimethyloctadecylchlorosilane at 70 °C for 5 hours. The method formed a continuous silica monolith; however, the internal morphology of the monolith was not homogeneous. The second method for fabrication was based on the sol-gel process. Minakuchi *et al.* introduced this procedure, which generated a silica monolith that was uniform, high purity and good homogeneity.^[53]

For that reason, it was decided to use the second sol-gel method for silica monolith fabrication in this work. The general sequence of steps involved in the sol-gel process are shown in (Figure 1-6).^[68]

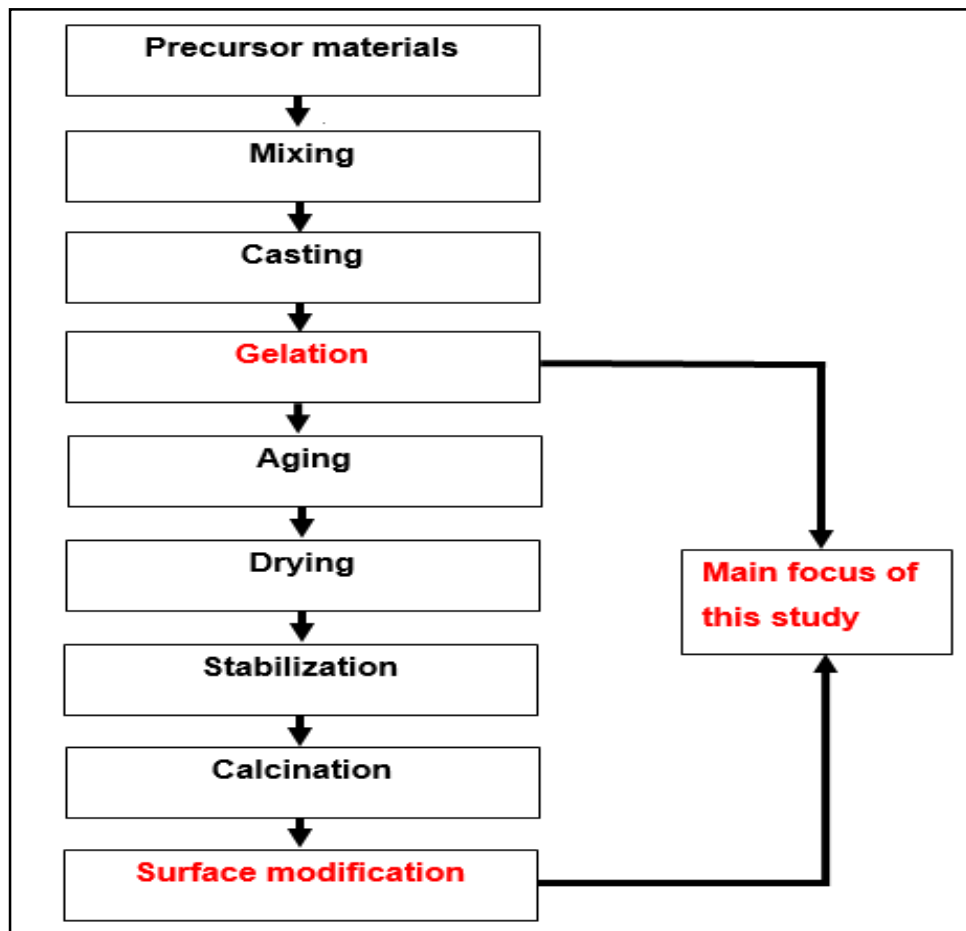


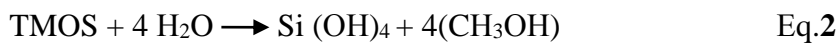
Figure 1-6 General steps involved in the production of silica monolith.

Precursor materials

Different types of precursors can be used to form a silica monolithic structure. The most common precursors used in the sol-gel process are metal alkoxides (such as tetramethylorthosilicate/TMOS and tetraethylorthosilicate/TEOS). These precursors have an organic group attached to a negatively charged oxygen linked to a metal atom.^[88, 89]

Mixing

In this step a liquid alkoxide is hydrolyzed with water to form a homogeneous solution. The hydrolysis reaction using TMOS is illustrated in Eq.2. The TMOS is a type of metal alkoxide used in this research.



The hydrolysis reaction resulted in the formation of silicon hydroxyl groups. The interaction of these silicon hydroxyl groups (Si—OH) with each other is known as condensation and this produces siloxane species ($\equiv\text{O—Si—O}\equiv$) and H₂O (see Eq.3).



The condensation reaction continues and a three-dimensional network is formed according to polycondensation behaviour.^[90, 91]

Casting

The casting process consists of pouring a partially polymerized solution into a mould before its viscosity becomes too high. The casting process can be influenced by several factors such as:

1. The shape of the container that can determine the shape of the final product.
2. The quality of the surface of the container that can affect the surface of the product.
3. The type of the mould to eliminate any reaction between the mould and solution.
4. Cleanliness of the container to prevent any contamination.^[90, 92]

In the current work the barrel of a plastic syringe (BD – 1 mL) is used as mould for the fabrication of silica monoliths.

Gelation

During the gelation process the condensation reactions produce particles that subsequently form clusters and increase the viscosity of the solution. A three-dimensional network is created by linking these clusters together to produce a semi solid wet gel material. This process is known as gelation, and the time it takes is defined as the gelation time.^[93]

The hydrolysis and condensation reactions can be affected by any variation on the processing parameters. Many researchers have investigated the effects of using different chemical composition and physical parameters during gel formation process on the internal structure of silica monoliths.^[94]

In 2002 Masanori Motokawa *et al.*^[95] fabricated monolithic silica columns from 18 mixtures of methyltrimethoxysilane and tetramethoxysilane. The prepared silica monoliths showed range of through-pores size from 2 to 8 mm, and skeleton sizes from 1 to 2 mm. As a result, a silica monolithic column with smaller domain size provided higher pressure drop and greater column efficiency.

In 2004, Wenhui and a co-worker^[96] prepared biporous silica monolith with both through-pores (μm) and mesopores (nm) in the skeleton's structure. A high concentration of ammonium hydroxide solution was used (e.g., 2 mol/L) in order to increase the size of mesopores. The effect of concentration of polyethylene glycol in the starting mixture was also investigated. They found that decreasing PEG concentration was also suitable for forming the network monolithic structure, but the mechanism of the phase separation and experimental results were different at low concentration.

In 2002 Gisele M. Neves *et al.*^[97] reported the effect of microwaves in the internal structure of silica monolith obtained through sol-gel process. X-ray diffraction confirmed

that the amorphous structure of silica monolith was prepared via microwave heating. Physical parameters of microwave silica monolith were measured. The results showed that the average pore size was 1.2 nm, specific surface area was 112 m²/g and specific volume of pores was 0.06 cm³/g.

This means that the silica monolithic structure can be formed using microwave radiation during sol-gel process; however, the created surface area was very low. Therefore, in the current work it was proposed to fabricate silica monoliths based on microwave heating during gelation process and evaluate the internal structure of produced silica monoliths.

Aging

In the aging step the structure of the gel can be changed according to pH, solvent, temperature and time of aging process. Flexibility in the formation of the gel, make it more viscous and condense, which releases the liquid from the interior phase and shrinkage of the wet gel structure.

There are three possible explanations for this contraction:

- i. Increased bridging bonds due to continuing condensation reactions.
- ii. Dissolution and reprecipitation of the silica primary particulates on the surface of the network structure.
- iii. Addition of new monomers or linkage of un-reacted oligomers after the gelation process.

During the aging process the thickness and strength of the skeleton structure increased and porosity of the monolith decreased.^[93]

Drying

A relatively large amount of liquid is removed from the wet gel monolith during the drying process, which leads to extra shrinkage in the internal structure.^[98] Evaporation of liquid from the pores' structure can create a concave liquid/vapor meniscus inside the

pores, which generates capillary pressures.^[99] The amount of shrinkage is governed by a balance between capillary pressure P_c , and modulus of the solid matrix as described by Laplace's equation (Eq.4).^[100]

$$P_c = \frac{2\gamma(\cos\theta)}{r} \quad \text{Eq.4}$$

Where,

P_c capillary pressure

γ specific surface energy of the vapor-liquid interface

θ contact angle

r = pore radius

This capillary pressure generates tension into the liquid (L, Figure 1-7). It is important to maintain horizontal and vertical forces with the same magnitude but at an opposite direction to keep Pore I in equilibrium, (L_x and L_y). The weight of the liquid (WL) equilibrates with L_y , and L_x is equilibrated with the S_x force produced by the solid phase. Equilibrium also should be maintained between different pores (Pore I, Pore II, Figure 1-7), but because there are variations in pore size, differences in capillary pressure are induced that produce stresses ($\Delta\sigma = \sigma_2 - \sigma_1 \neq 0$).

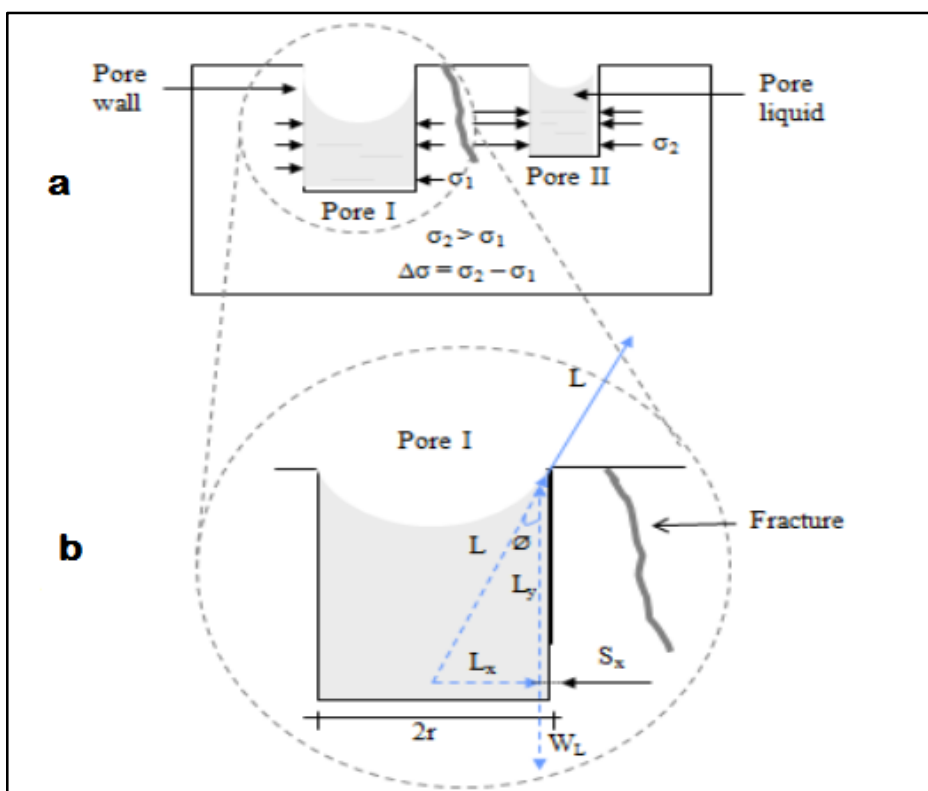


Figure 1-7 Stresses in a monolithic silica gel body: (a) evaluation of forces in Pore I; (b) horizontal stresses in different pore size.^[90]

Stabilization

There are a huge number of silanol groups (Si—OH) on the surface area of the monolithic structure. An increase in the number of OH groups on the internal surface of the silica monoliths can reduce their transparency. Furthermore, these free negative groups can cause an interaction with the analytes group during the separation and extraction processes. Removing the OH groups from the internal surface of the silica monolith requires a thermal or chemical treatment to take place.^[68]

Calcination

After drying and stabilization of the silica monolith, subsequent heat treatment is carried out to decompose the organic residues without serious deformation on the monolithic structure.^[66]

1.5.2 Polymer monoliths fabrication

Several organic polymers have been used for monolithic fabrication such as methacrylate, polystyrene and acrylamide.^[57] The synthesis of polymeric monoliths requires monomers to form the monolithic structure, a porogen system that contains one or more solvents, and a free radical initiator to start the polymerisation. Decomposition of the initiator and forming a free radical starts the polymerisation process. The solubility of the polymer decreases with growing the length of the polymer chains. These chains then precipitate as nuclei and the ability of the nuclei to solve in the un-polymerised monomers creates polymerisation within the nuclei and forming micro-globules as a polymerisation progress. Finally this technique forms the network structure where the macro-pores of the monolith are occupied by the porogen system.^[101]

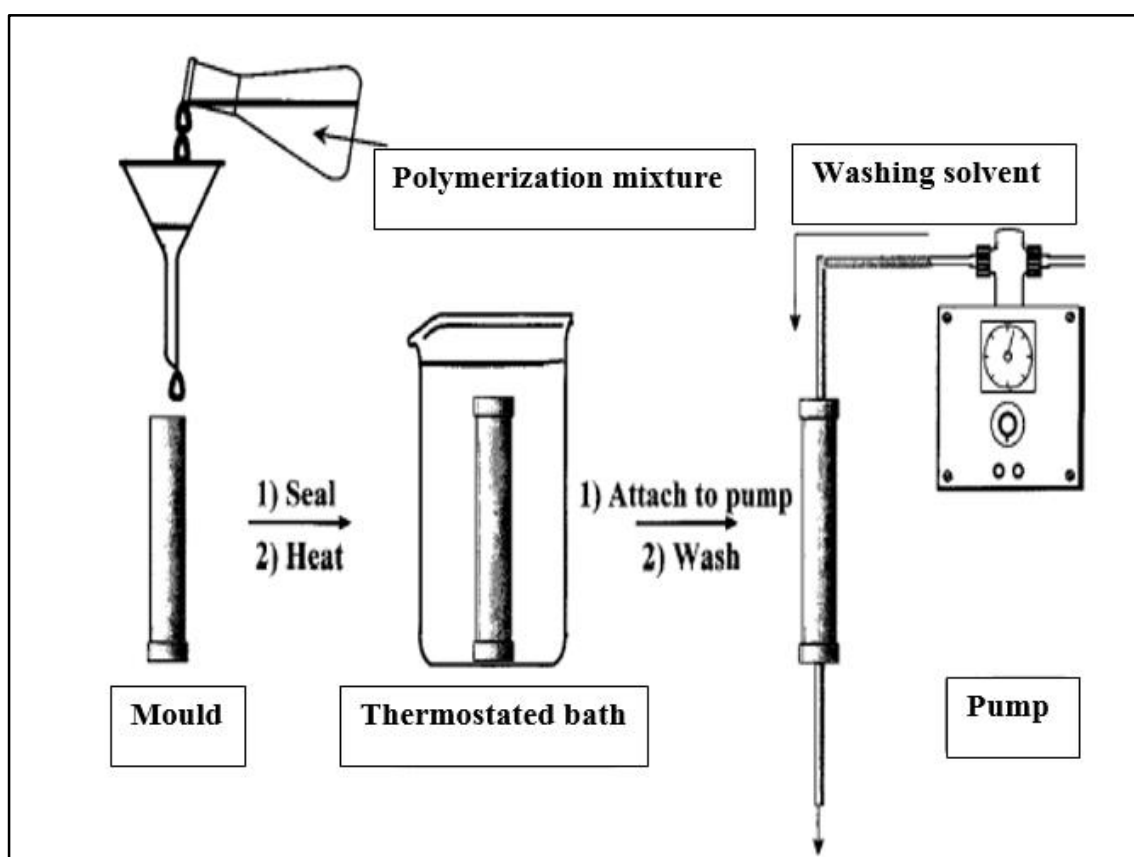


Figure 1-8 Schematic for the preparation of rigid macro porous polymer monoliths.^[63]

In 1998 Xie *et al.*^[102] introduced the use of a porous polymeric monolith for solid phase extraction. The polymeric monolith was fabricated inside a threaded (PEEK) polyetheretherketone tube (20 mm × 1 mm i.d.) using 20 % ethylstyrene, 80 % divinylbenzene and dodecanol with toluene as a porogenic solvent. This column was produced through thermal initiation at a temperature of 70 °C for 24 hours. The resultant monolith showed good properties since it had excellent hydrodynamic properties and was characterized by evaluating its preconcentration efficiency for polar organic compounds. Quite high recoveries of about 85 % were achieved. Later Lee *et al.*^[103] prepared a poly (butyl methacrylate-*co*-ethylene dimethacrylate) (BuMA-*co*-EDMA) monolith for extraction of standard proteins (lysozyme, cytochrome C, and trypsinogen A). Schley *et al.*^[104] also fabricated a poly (styrene-*co*-divinylbenzene) (PS-*co*-DVB) monolith for preconcentration and separating seven standard proteins including, ribonuclease A, cytochrome C, lysozyme, transferrin, myoglobin, α -lactoglobulin B, and carbonic anhydrase.

Although polymeric monoliths are becoming increasingly popular as sorbents, especially for the extraction of large molecules such as proteins, few papers describe their use as a material for extracting small organic molecules (such as drugs of abuse); therefore, the advantages and disadvantages of particulate and monolithic stationary phases will be discussed in section (1-6). In addition, the comparison between polymeric monoliths and silica monoliths will be reviewed in section (1-7).

1.6 Advantages of monoliths over particles

When van Deemter plots (see Figure 1-9) of particulate and monolithic columns are compared one major difference is apparent: the contribution of the *C* term (mass transfer). The *C* term contribution in monolithic columns is much lower than that of particulate columns (see Eq.1).^[105]

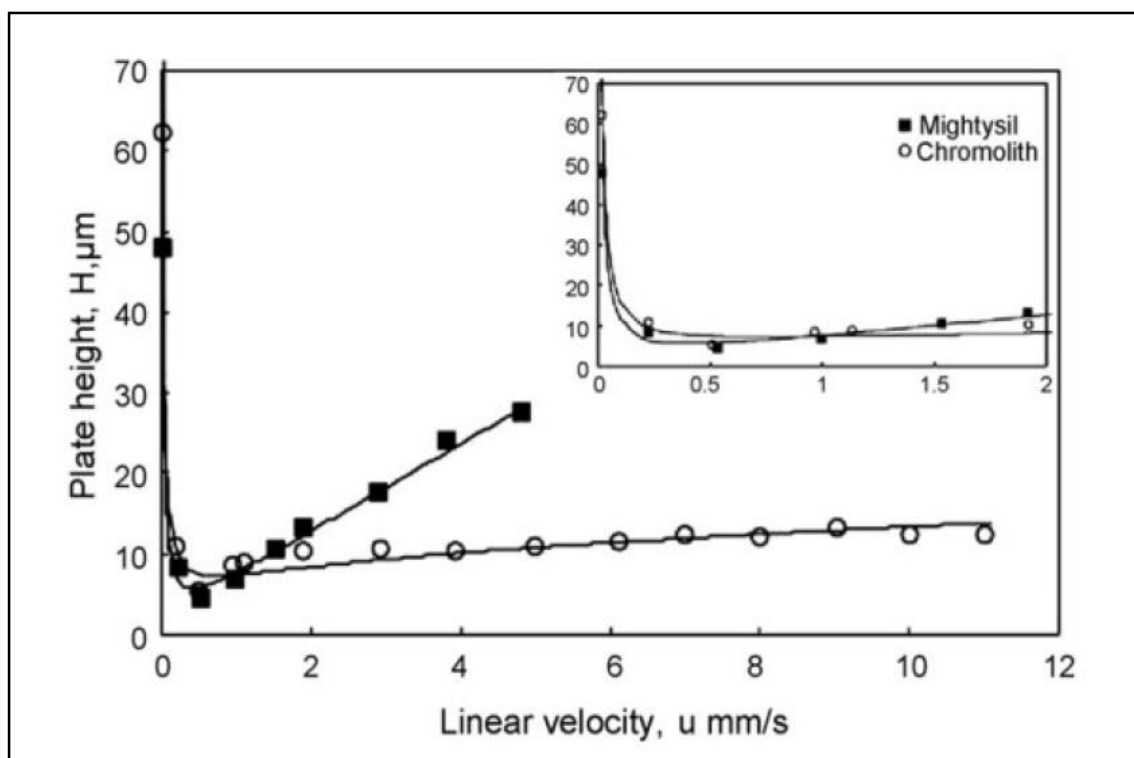


Figure 1-9 Plots of plate height values for uracil against linear velocity of mobile phase: conventional size columns; Mightysil (■) and Chromolith (o).^[106]

The low value for C with monolithic columns results in a faster partitioning of analytes between the mobile or elution phase and stationary phase, in comparison with particle packed columns. The mass transfer of monolithic columns is usually high. From Figure 1-9 it is clear that the ability of monolithic column to be used high flow rates without a significant loss in efficiency. The mass transfer of monolithic stationary phases is attributed to convection rather than diffusion. For that reason the mobile or elution phase in a monolithic column flows through the pores, whereas the majority of the mobile or elution phase, in a packed column, flows between the particles.^[106] Other advantages of monolithic stationary phases over particle packed phases include lower back pressures due to their higher permeability, no need frits to retain the phase; ease of modification, and their ability to be produced in different formats (e.g. rod, disks, capillary).^[107, 108]

1.7 Comparison between silica monolith and polymeric monolith

The major difference between a polymeric and silica monolith is in their internal structures.^[70, 109] Bimodal pore structure of silica monoliths includes two types of pores (see Figure 1-10): macro-pores (or through-pores) where the mobile phase passes through the column, and meso-pores on the surface of the through-pores' structure, which increases the surface area. The bimodal pores structure of the silica monolith allows for small molecules to interact with the internal surface of silica monoliths, and makes the diffusion rates of small molecules within silica column higher than macromolecules. Those pores structures of silica monoliths not only increased the surface area but also improved the efficiency of extraction and separation of small and large molecules.^[70]

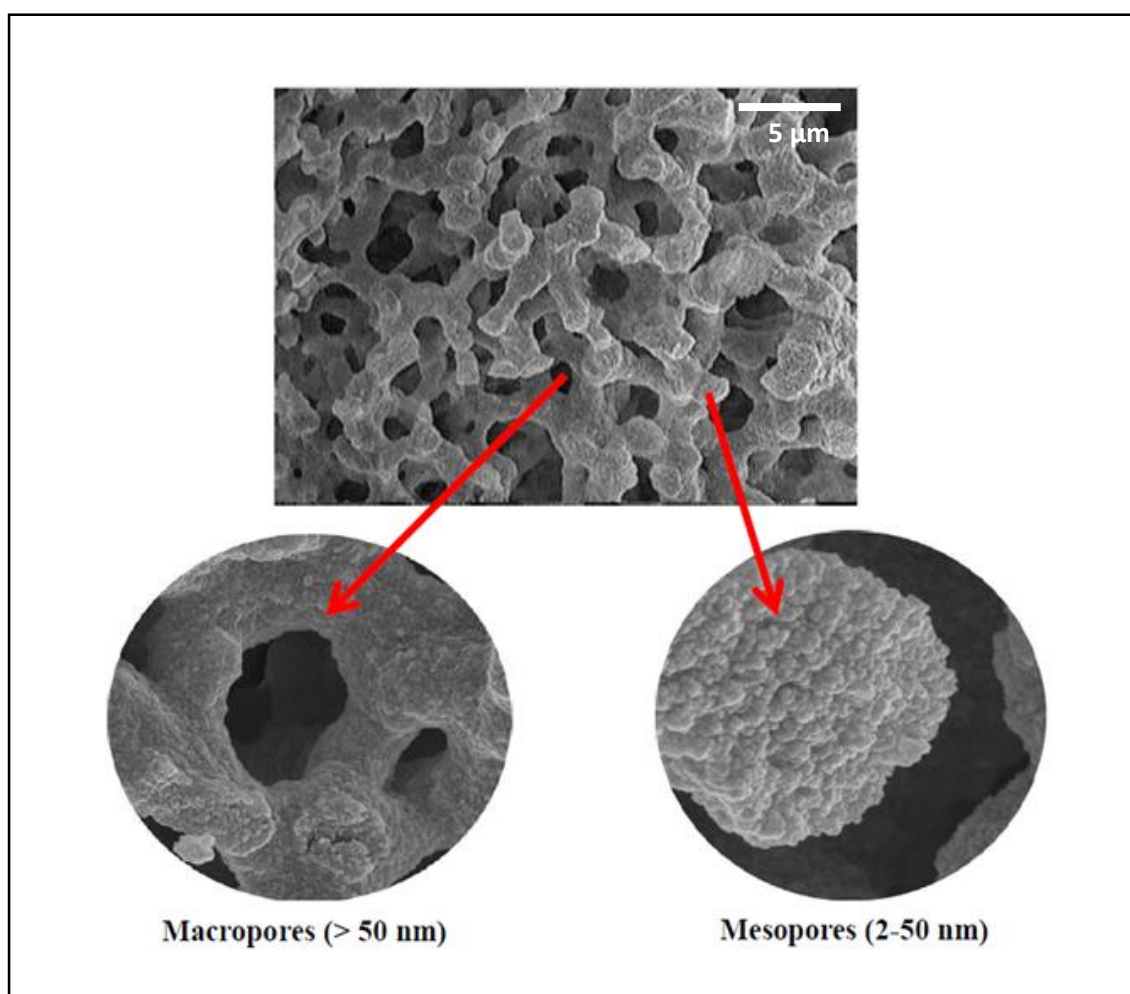


Figure 1-10 SEM images of a silica monolith showing (a) the macro-pores or through-pores and (b) the meso-porous structure of the silica skeleton.^[70]

In contrast, the internal structure of polymeric monoliths contains only macro-porous (see Figure 1-11), where the extraction and separation of small molecules are very difficult and not recommended. Furthermore, the existence of an only macro-porous structure in a polymeric monolith results in a low surface area compared to the silica monoliths.^[57]

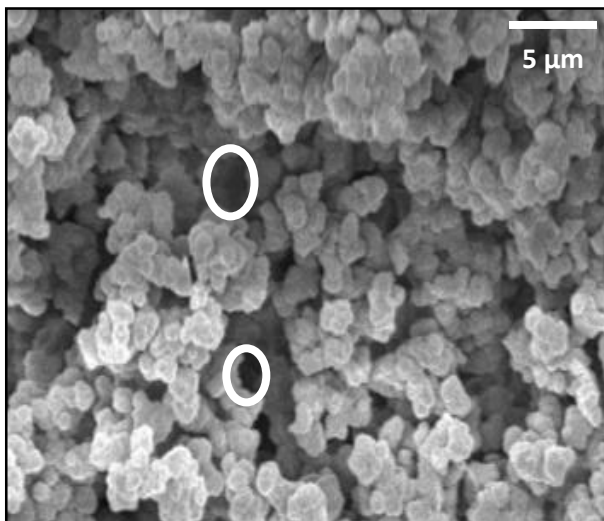


Figure 1-11 SEM of polymeric (methacrylate) monolith showing macro-porous.^[110]

A comparison between silica and polymeric monoliths is in Table 1-2.

Table 1-2 Summary of the advantages and disadvantages of organic and inorganic monoliths based on literature review.

Comparison	Inorganic monoliths	Organic monoliths
Simple preparation method	Yes	Yes
Preparation time	Long, since they should be prepared and chemically modified independently. ^[112]	Short, since the fabrication of the organic monolith is a single-step process. ^[113, 114]
Surface area	High. ^[44, 115, 116]	Although some attempts have been made to increase the surface area of organic monoliths, the fabricated monoliths in previous reports showed relatively low surface areas. ^[63, 102]
Permeability	High. ^[44, 115, 116]	Moderate. ^[117, 118]
Affected by temperature and/or solvents	They have high mechanical strength, and relatively high thermal stability. ^[57]	They are affected by temperature and/or organic solvents causing shrinking or swelling. ^[117, 118]
Stable over the whole pH range	They are not stable at high pH values. ^[119]	They are stable over a wide range of pH values. ^[120]
Option for stationary phase	They can be fabricated by using different chemical composition. ^[94]	They can be fabricated by using a wide range of monomers and crosslinking agents enabling the porous properties of the monolith to be controlled. ^[121]
Surface modification of the monolith	They can be easily derivatised with many functional moieties leading to additional efficiency and selectivity. ^[43, 122]	They have a high number of crosslinking bonds, which require hours to reach equilibrium for surface activation. ^[122]
Fabrication inside microchip	Difficult, since the location of the monolith inside the microchip cannot be defined because their fabrication depends on using thermal initiation. ^[123, 124]	Easy, since the initiation of a polymerisation reaction can be performed by photoinitiation (light). ^[125, 126]
Use for drugs of abuse extraction	Many papers describe their use as materials for extraction with high efficiency. ^[127]	Many papers describe their use as materials for extraction with relatively good efficiency. ^[111]
Swelling	Non-swelling property. ^[221]	The swelling would affect the reproducibility in some cases and the deficiency in mechanical stability would result in the short service life. ^[221]

Monolithic materials have been developed for use as SPE sorbents and their application has also increased, especially in the field of extraction. The structure of silica monoliths make them ideal for the extraction of small organic molecules in comparison with other types of columns (particulate and polymers monolithic columns), where the porosity is over 80 %, the surface area is too high and the back pressure is very low. In addition, silica monolithic columns have the potential to elute adsorbed analytes with a very small volume due to their high surface area for each unit volume compared to silica particle packed columns or polymers columns. Furthermore, the required volume of the silica monolithic column to extract the target analytes is also smaller than other conventional techniques.^[128, 129]

In terms of the surface area, the recovery of the porous polymer monolith is theoretically much lower than bi-pores silica monoliths, where the number of theoretical plates within the silica monolith is much higher than in polymer monoliths.^[130] Published reports suggest that extraction of low molecular weight compounds (such as drugs or medication) are with silica monoliths, whereas the extraction of biomolecules that have high molecular weight (such as peptides or proteins) are by porous polymer monolith.^[129]

From this review it has been concluded that the applications of silica monolithic columns for the extraction of drugs are strongly recommended. Nevertheless, the fabrication of silica monoliths is still time-consuming and laborious. For that reason, in this research methodology microwave heating will be introduced to reduce fabrication time of the silica monolith, rather than using conventional oven heating method.

1.8 Modification of silica surfaces

The normal phase of silica monolith is polar, due to the presence of uncondensed hydroxyl groups on the surface of each molecule.^[23] Since silanols are quite weak acids their ionization can be easily suppressed and their ability as ion-exchanger is quenched.^[131] Furthermore, the concentration and activity of silanols can vary from batch to batch.^[132]

The surface of silica monoliths can however be modified using different techniques and various functional moieties. Modification of the silica monolith results in a wide range of chemical selectivity that can be used to retain target analytes. The first modification method is known as a surfactant coating, where a surfactant molecule possesses both hydrophilic and hydrophobic characteristics. The hydrophilic nature of ionic surfactants is due to an ionic group (e.g. SO_3^-) and hydrophobic nature is generally due to alkyl chain (e.g. $\text{C}_{18}\text{H}_{37}$).^[23, 133, 134]

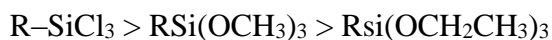
This modification method has improved the potential of both particulate and monolithic columns in order to make it suitable for extraction of small molecules and inorganic ions. In addition, using this procedure with a reversed-phase monolithic column allowed higher flow rates and greater efficiencies of these stationary phases. However, this method of modification is not permanent, because the coating layer can be removed during washing of the sorbent with organic solvents, or leach in an aqueous eluent.^[134-138]

For permanent modification of silica surface the formation of chemical bonds are necessary. Therefore, this modification method is known as a chemical modification. In this case, the modification process can be carried out through chemical reactions.^[23] The most common reactions for chemical modification of silica surface are shown in Table 1-3.^[43]

Table 1-3 Chemical modification reactions of silica monoliths.

Type of reaction	Surface linkage
1) Organosilanization	Si-O-Si-C
2) Esterification	Si-O-C
3) Chlorination	Si-Cl

On the silica surface silanes allow the formation of a Si–O–Si bond. These bonds are stable across a wider pH range compared to Si–O–C bonds. In general, the modification of silica monoliths can be achieved by two mechanisms based on alkoxy silanes and chlorosilanes. The types and rates of reaction are different in both of them.^[23]



Trichlorosilane > Trimethoxysilane > Triethoxysilane

The reactivity of chlorosilanes is much higher than alkoxy silanes. Chlorosilanes can be reacted immediately on contact with reactive groups. The generated bonded phase is significantly affected by the type of substitution on the silane.^[44]

Monochlorosilanes are traditionally used for modification of silica surface with C₈ and C₁₈ phases, or for endcapping active sites. Dichlorosilanes and trichlorosilanes can be used for modification as well. However, the presence of water in these types of reaction can result in cross-linking and decrease the permeability of the silica monolith. Furthermore, linear polymers and three-dimensional polymers are difficult to manufacture and produce. Therefore, in this work the surface modification of silica monoliths was carried out by using monochlorosilanes.^[23]

1.8.1 C₁₈ phase

Applications of reversed-phase silica monolith as SPE are found in the forensic science, pharmaceutical, environmental industries and food analysis. The most common phase used for extraction of drugs of abuse is octadecylated phase (C₁₈ phase), where the octadecyl groups attached to the silica surface and the retention depend on the hydrophobicity.^[44]

The surface silanol groups in the mesoporous structures (2-50 nm) offer good access to the surface for modification, whereas the microporous structures (less than 2 nm) can become inaccessible for modification because they are blocked by the bonded moieties in the mesoporous, as can be seen in Figure 1-12.^[43]

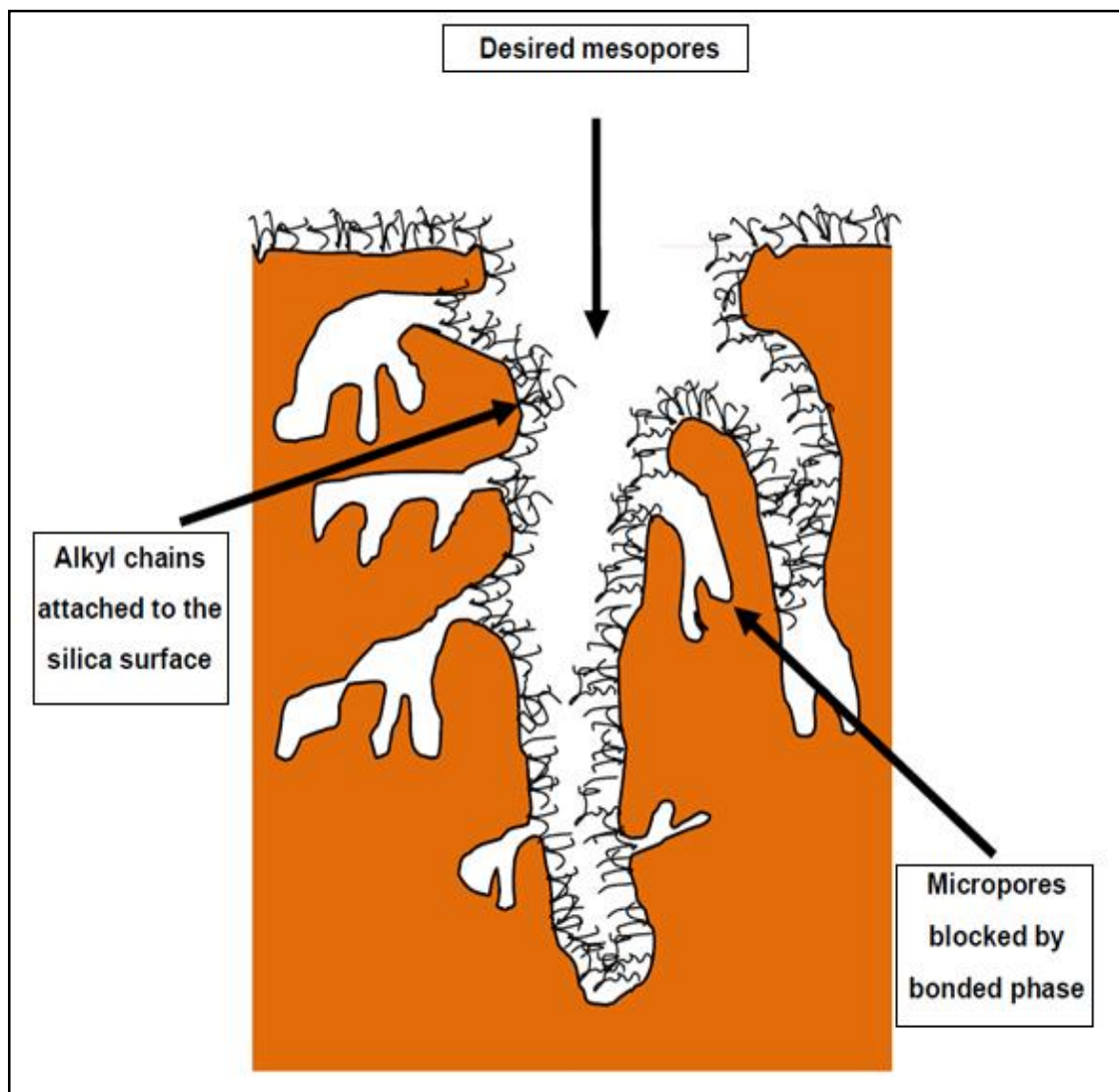


Figure 1-12 Schematic diagram shows the porous silica-based surface, showing the inaccessibility of some microporous.^[43]

Since the size of the organic moieties used for modification of silica surface is large (such as octadecyl groups), attached silanol groups act as a barrier for free neighbouring silanol groups to be modified by other organic moieties. Therefore, using the small organic group during surface modification results in decreasing the free silanol groups on the silica surface.

The performance of modified silica monolith can be affected by the number of free silanol groups on the surface, which may cause secondary interaction with polar functional groups in the sample matrix and decrease the resolution in the case of separation.^[43]

Decreasing the number of free silanol groups on the silica surface can be performed by a second reaction called “end capping” (see Figure 1-13), in which the free silanol groups are coated by small silane-type molecules such as trimethylchlorosilane (TMCS) or hexamethyldisilazane (HMDS).^[139]

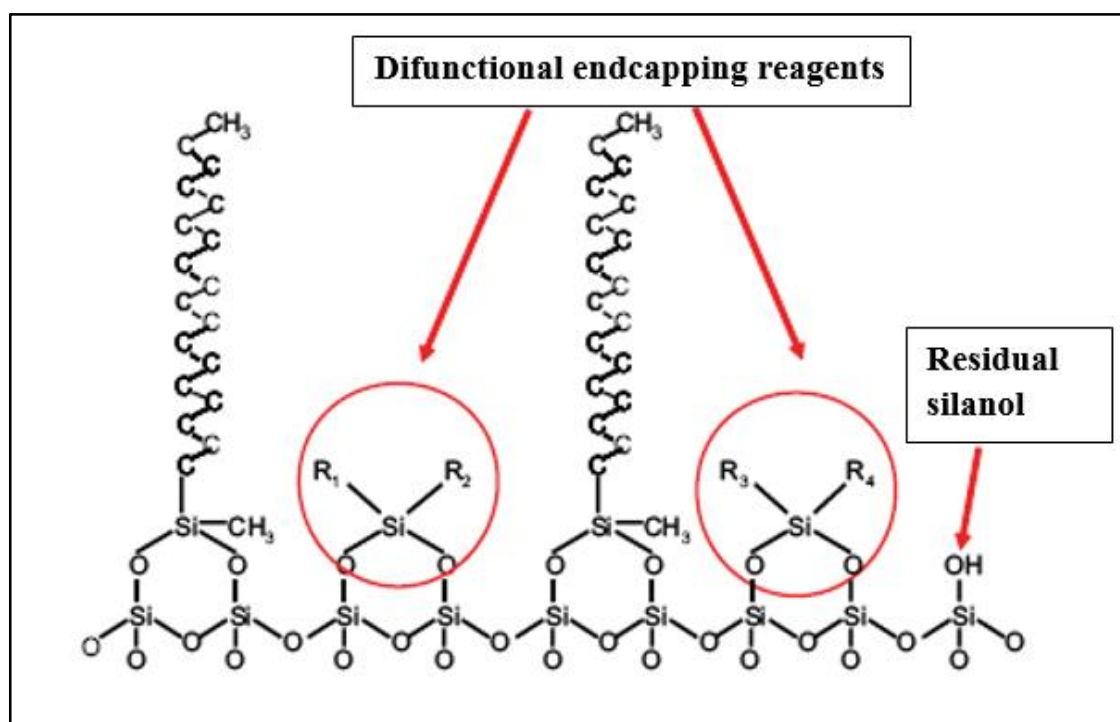


Figure 1-13 C18 monolithic column endcapped with two difunctional dialkylsilane reagents to decrease the number of free silanol groups on the surface, which may cause polar-polar interaction with a polar functional groups in the sample matrix.^[222, 223]

The orientation of octadecyl groups on the silica surface is random, therefore, conditioning the reverse phase silica surface before loading the sample solution is very important, in order to decrease the aggregation of the octadecyl bonded phase and make ready for interaction with the sample analytes, as can be seen in Figure 1-14.^[43] Also, it can improve the efficiency of the modified silica surface and increase the extraction recovery of the target analytes. Several types of solvents can be used for conditioning the octadecyl group's bonded silica surface such as acetonitrile, tetrahydrofuran and

methanol. Commonly, the selection of the conditioning solvent is influenced by the type of the bonded organic moiety.^[140]

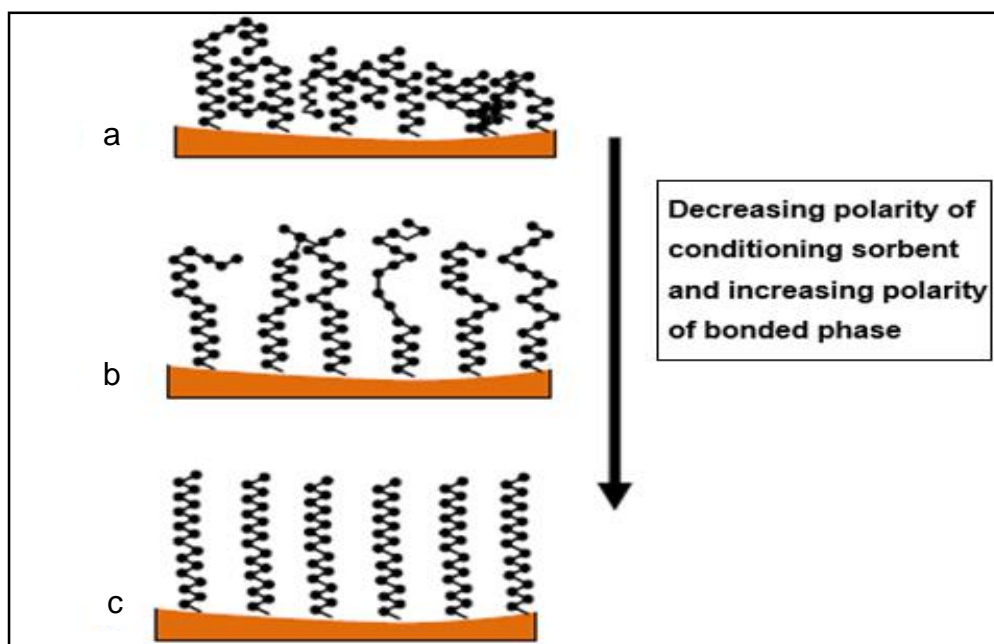


Figure 1-14 Schematic diagram showing the effect of conditioning step on octadecyl bonded silica: (a) without conditioning. (b) Partially conditioned. (c) Fully conditioned.^[43]

The limitations of extracting small molecules by polymeric monoliths can be overcome by using the silica based monoliths, where the mesoporous structure creates high surface area coupled with an increase in the load capacity of the sorbent.^[115, 116] In addition, the surface silanol groups (Si-OH) on the silica structure make the modification process much easier compared to the organic monoliths, where the number of crosslinking bonds is huge and the time to reach equilibrium is too long.^[122]

However, several problems may be encountered when using the C₁₈ solid phase for extracting the analytes from biological matrices. Martin *et al.*^[44] investigated the influence of carbon loading on the silica surface during the extraction of basic and acidic analytes. A wide range of silica sorbents containing from 5 to 22 % of carbon, fabricated without or with endcapping, was evaluated for the two model acidic and basic analytes (anisidic acid and propanolol) from 1 mL of buffered plasma. Recovery of analytes with

high carbon loadings was found to be poor, with the loss of some analytes during loading and washing. The best SPE phases for two analytes were found with those of intermediate carbon loading.

In a further study, recoveries obtained for polar priority phenols using two C₁₈ silica monoliths were compared and found to be lower with a C₁₈ silica monolith modified by trifunctional silane than the C₁₈ silica modified by monofunctional silane. Recoveries were 25 % for 4-methylphenol and 33 % for 4-nitrophenol with trifunctional C₁₈ and 54 % and 56 % with monofunctional C₁₈.

In this work microwave methodology was used for C₁₈ modification in order to control the loading of carbon during the modification process, which generates cleaner, faster, selective and efficient heating, in comparison with the conventional heating methodology.

1.8.2 Graphene

Although there is a potential for C₁₈ SPE sorbents to extract weakly acidic, weakly basic and neutral compounds from complex mixtures, they still have difficulty in extracting polar and very-polar compounds from large sample volumes. In addition, they also have low extraction efficiency for the trace level of non-polar analytes.^[44]

To solve these problems, Knox and Gilbert^[141] introduced the first carbon-based solid phase matrix in 1978. The oldest method for fabrication of carbon-based SPE is water graphitized carbon blacks (GCBs) that can be obtained at very high temperature (2700–3000 °C). The specific surface area for first GCBs was very low and non-porous (Carbopack B or ENVI-Carb SPE from Supelco, Carbograph from Alltech).^[142] However, their extraction efficiency for polar pesticides was higher than C₁₈ silica monoliths.^[143] To improve the physical features of carbon-based SPE, Carbograph 4 was introduced with a surface area of 210 m²/g.^[144] Several methods for extraction and preconcentration of

pesticides have employed carbon-based SPE.^[143, 145, 146] One group of researchers used Carboglyph 4 for the extraction and preconcentration of 15 post-emergence herbicides from drinking water. The detection limits for these herbicides were reported to be 5 ng/L.^[147] The same property was also applied to extract of naphthalene sulfonate and benzene, as it appeared to be more efficient than conventional C₁₈ silicas or ion-pair extraction.^[148] A further group also used Carboglyph 4 for the extraction of alcohol ethoxylate surfactants and for determination of N-nitro sodimethylamine at the ng/L level in ground water.^[149]

At the end of the 1980s, porous graphitic carbon (PGC) had clearly been demonstrated to be a new sorbent for SPE.^[141] Graphite is a crystalline material with no functional groups on the surface. Therefore, graphite structures may be able to overcome many disadvantages associated with silica based materials, where the aromatic carbons have all their valencies satisfied.^[150] Furthermore, graphite material is more tolerant with high pH solutions (> 9) than silica-based materials.^[151] Graphitic sheets are held together by weak Van der Waals forces; however, the retention mechanism was found to be different to that of other reversed-phase sorbents such as C₁₈ silicas.^[152, 153] In the porous graphitic carbon, non-polar, very polar and water-soluble analytes can be retained based on both hydrophobic and electronic interactions.^[154-156] Manufactured PGC is characterized by an ordered homogeneous structure with a surface area of 120 m²/g and a porosity of approximately 70 %.^[154]

Recently, the retention of morphine and its metabolites in the porous graphitic carbon was found to be very strong.^[156] High retention in the porous graphitic carbon for planar molecules containing several polar groups with delocalized electronic charges via ρ -bonds and lone pairs of electrons can solve the problems associated with extraction of very polar compounds using C₁₈ phase.^[44]

This development in the graphitisation process resulted in more efficiencies in comparison with other bonded phase silicas.^[154]

1.8.2.1 Retention studies on PGC

Initially, it was assumed that the retention behaviour of graphite surface with analytes would be similar to that of C₁₈ phase, and the main difference was that of extended pH ranges to high pHs. Many researchers supported this view such as Kaur^[157], however, Knox and Ross^[158] compared the retention on graphite surface and other stationary phases^[159] (see Figure 1-15).

They highlighted observations regarding interactions such as:

- a) An increase in the retention of non-polar analytes compared to other reversed phase silica monoliths.
- b) An improvement in the selectivity to similar structural analytes such as isomers.
- c) Greater retention of polar analytes to the graphite surface compared to other reversed phase silica monoliths. These observations were unexpected and due to the graphite surface, which has no functional polar groups.^[160]

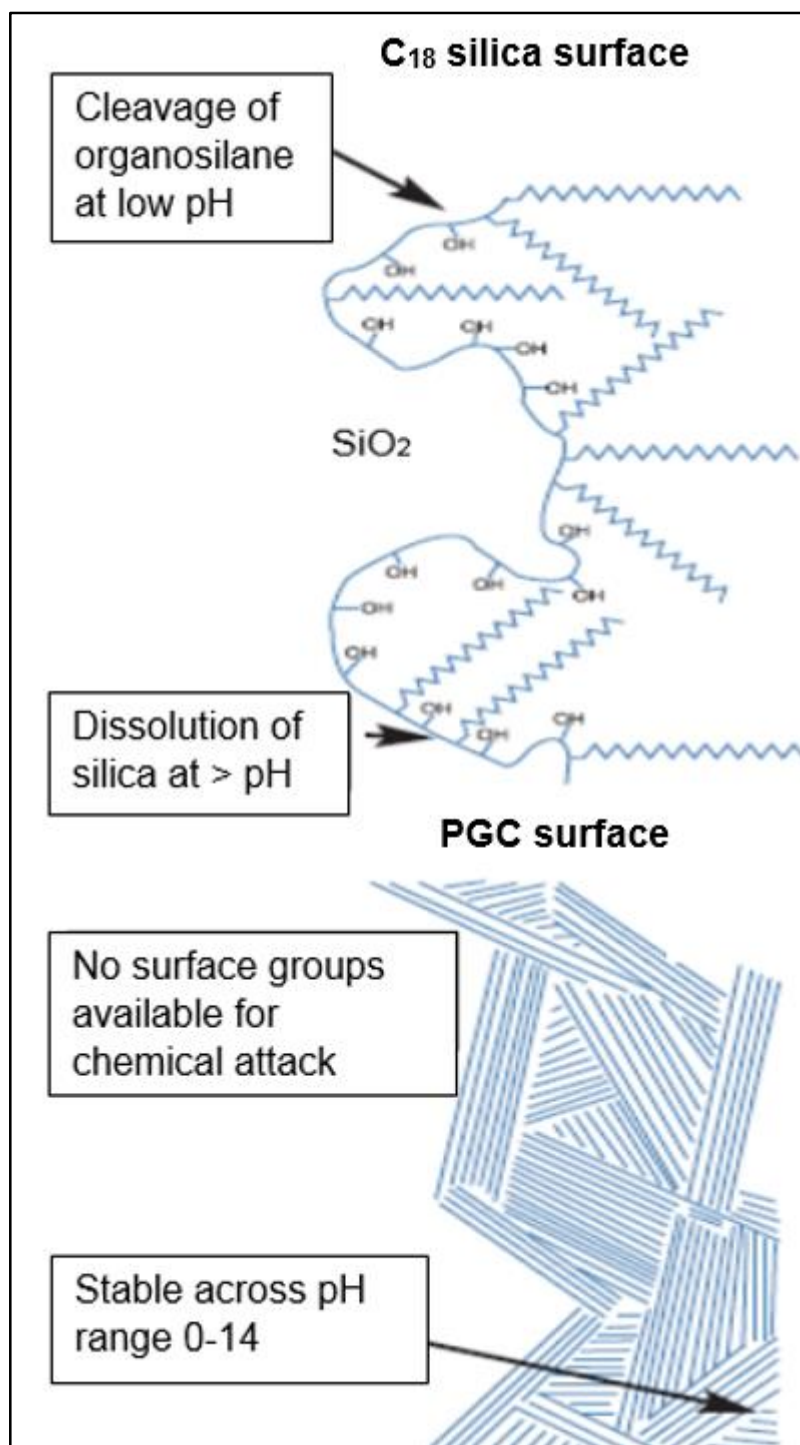


Figure 1-15 Surface comparison between C₁₈ bonded silica and porous graphitic carbon.^[161]

Tanaka *et al.*^[162] investigated the reduction in retention for a series of alkanols on ODS while the retention increased on PGC. Kaliszan and co-workers^[163] also observed retention differences of polar analytes on PGC, which was stronger than on ODS phase. In a further study Coquart and Hennion^[154, 164] reported an increase in the retention of small aromatic compounds on PGC by increasing the number of polar functionalities.

In contrast, the retention of the benzene ring on the ODS was significantly decreased by increasing the number of polar groups.

Despite the potential of PGC to be used as sorbents for extracting non-polar, polar and very polar compounds, there remains a problem in the elution of several analytes, which are strongly retained on the graphite surface, and using acetonitrile and methanol it could be inefficient to remove them.^[164]

To overcome this, it was decided to use a single layer of graphite, which is known as graphene, and hold the advantageous properties of carbon-based materials. Graphene is a two dimensional material consisting of a single layer of carbon atoms arranged in a honeycomb or chicken wire structure.^[165] Graphene, in particular, has superior physiochemical properties such as the thinnest and strongest material known to date. Furthermore, it can also be employed as a conductor of electricity and heat. However, the permeability of graphene structure is too low compared to 3D silica monoliths.^[165]

For that reason, this work investigated the ability of graphene phase by modifying a silica monolithic structure and evaluated the extraction efficiency of amphetamine compound by graphene-silica monoliths.

1.8.2.2 Application of graphene silica monoliths

Recently, many applications have been developed using graphene silica materials, such as energy storage and conversion ^[166-168], catalysis ^[169], water purification ^[170, 171] and oil absorption ^[172].

Chen *et al.*^[173] proposed, for the first time in 2010, the use of graphene as coating in SPME. The fibre coating was prepared by dipping a stainless steel wire (support) into an ethanolic dispersion of graphene. The fibre was reinforced by curing at high temperature and the coating presented a wrinkled and porous surface. Enhanced extraction of six pyrethroid pesticides was reported with the fibre coating, which was also thermally stable and offered good fibre-to-fibre and batch-to-batch reproducibility.

Following a similar process, Zhang and Lee ^[174] applied this strategy to prepare a graphene-based coating for extraction of polybrominated diphenyl ethers. Novel monolithic columns with embedded graphene were developed and coupled to LC-MS analysis. The extraction performance of the graphene-monolithic column was evaluated using glucocorticoids and recoveries for spiked samples were 83.7 % to 103.8 %.

More recently, in 2014 Xiaojia Huang and co-worker ^[175] prepared poly(ethylene glycol dimethacrylate/graphene oxide) (EDMA/GO) monolith as the sorbent of stir cake sorptive extraction (SCSE) for preconcentration of strongly polar aromatic amines from water samples (see Figure 1-16). Analysis of polar compounds was achieved by combining SCSE and HPLC with diode-array detection system. Good reproducibility of the method was obtained as intra- and inter-day precisions, the relative standard deviations (RSDs) were less than 4.0 %. Finally, the proposed method was successfully applied to the determination of trace aromatic amines in environmental water samples. The recoveries of aromatic amines spiked in different matrices ranged from 74.2 % to 105 %, and RSDs of repeatability ranged from 1.6 % to 9.6 %.

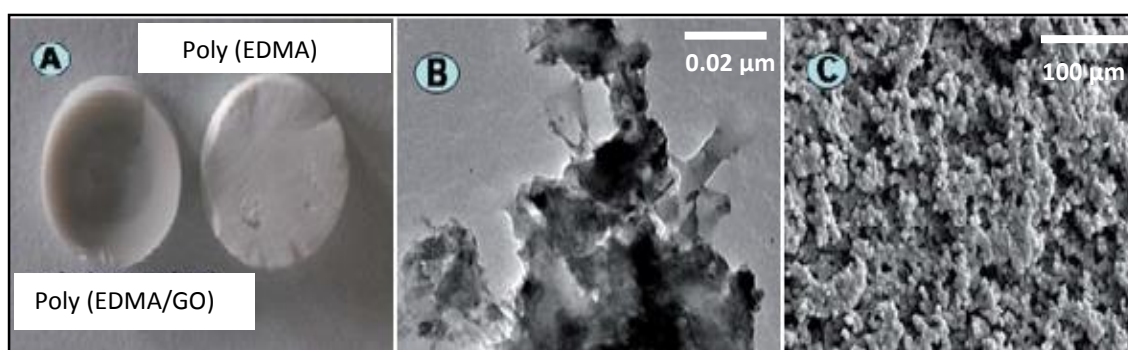


Figure 1-16 (A) Photographs of poly(EDMA) monolith and poly(EDMA/GO) monolith, (B) TEM image of poly(EDMA/GO) monolith, (c) SEM of poly(EDMA/GO) monolith at 5000 × magnification. ^[175]

The present work will investigate the ability of graphene-silica-monolithic column to extract polar compounds such as amphetamine or methamphetamine (as an example for drugs of abuse). In addition, the recoveries of selected polar compound from graphene silica monolith and C₁₈ silica monolith will be compared.

1.8.3 Gold Nano Particles (GNP)

Despite silicon being the material of choice for monolithic fabrication of SPE, the limited active optical properties of silica structures slows down their progress in photonics' applications. Nanoparticles have the potential to remove this bottleneck by exploiting their optical and electrical properties whilst integrated into silica monolithic structures to make them ideal for *in situ* optical detection.

In 2001 Khushalani D *et al.*^[176, 177] dispersed gold nanoparticles in mesostructured silica monolith. The starter mixture involved SiCl_4 and Pluronic triblock copolymer template in ethanolic reaction condition. The resulted monolithic column consisted of distributed gold nanoparticles within a mesostructured silica matrix. This combination between the silica frameworks, with the chemical properties of the embedded nanoparticles, can produce multifunctional solid phase matrixes. However, the fabrication of silica monolith by conventional sol gel process is still time consuming and quite complicated. The dispersion of gold nanoparticles within solid matrices was developed by M. T. Laranjo and his group in 2011.^[178] They successfully trapped GNPs in the silica monolith using high-pressure process at 7.7 GPa and at 25° C. Nevertheless, the generated physical parameters of the silica monoliths confirmed reduced values for specific surface areas due to closed pores.

To solve this problem, in 2012 Mohamed Guerrouache *et al.*^[179] developed a new method for the surface functionalisation of the porous monoliths based on gold nanoparticles. The modification process was established by attaching primary amino groups to the functionalized monolith surface via thiolyne radical addition reaction. After that, the surface of skeleton structure was immobilised with gold nanoparticles. This technique offers great potential for Lab-on-a chip technology.

In 2013 Yolanda Vasquez group *et al.* recently presented ^[180], a reproducible method for the fabrication of highly-ordered porous silica films embedded with gold nanoparticles. The gold nanoparticles were uniformly distributed in the silica matrix. They used co-assembly methods with two-phase (a) and three-phase (b) to format a composite thin film (see Figure 1-17 a and b). The opal structure in the silica film was then created by removing the organic colloidal template through calcination. In the case of three-phase co-assembly, gold nanoparticles were embedded in the walls of the opal structure (“gold-loaded” opals). TEM and SEM images showed ordered, crack-free, thin films and opals structures loaded with gold nanoparticles. The optical properties of these films can be utilized in different photonics’ applications. In addition, functionalization of gold nanoparticles can improve the selectivity of this technique.

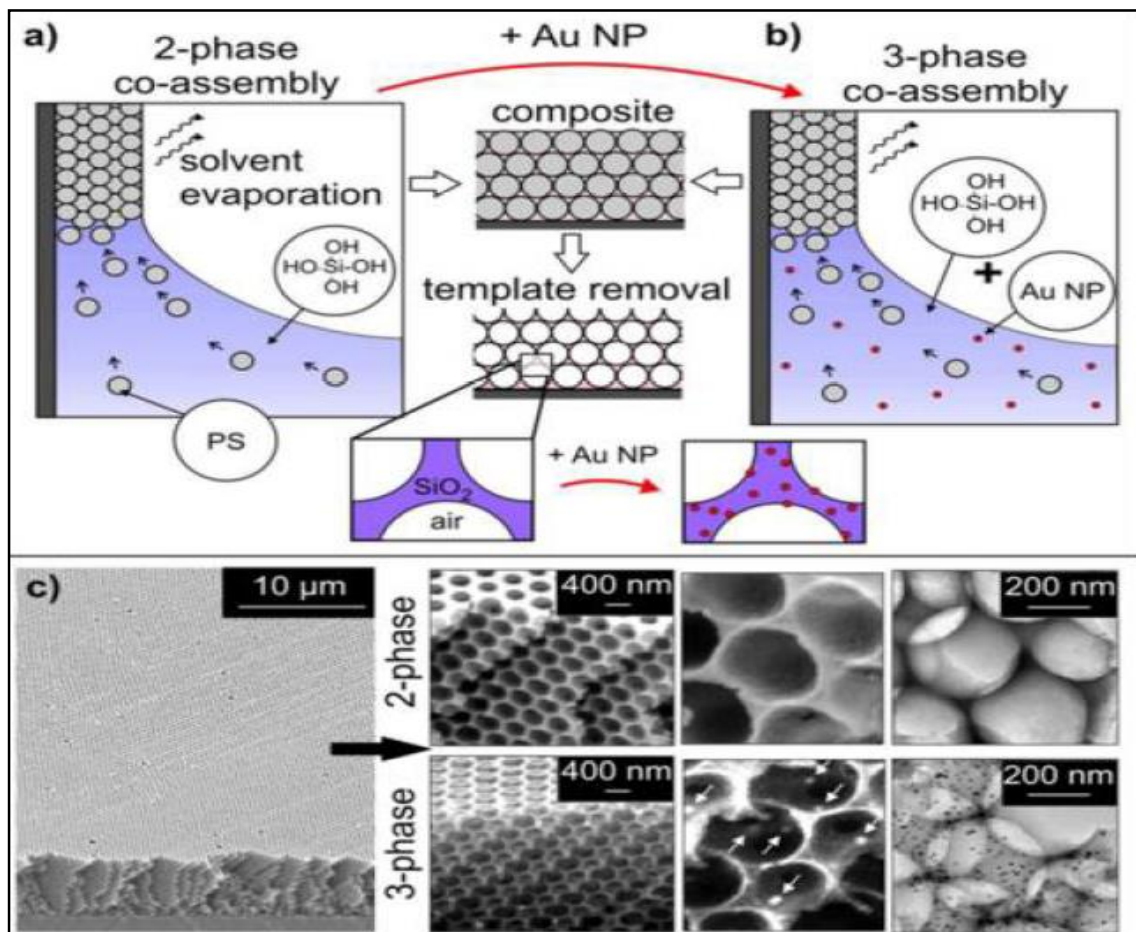


Figure 1-17 Schematics of two-phase (a) and three-phase (b) coassembly methods. White arrows point to the brighter contrast gold nanoparticles in the SEM image (c). The gold nanoparticles in the TEM image appear as dark spots (c). ^[180]

SPE is a very robust approach; however, attachment of any biological substrate such as antibodies, enzymes or proteins can improve the selectivity of the silica surface to be collected just the target analytes. The attachment of amine groups to any surface allowed biomolecules to be immobilized on the surface. This technique was introduced a few years ago and its application in the extraction of drugs of abuse investigated by many researchers.

In 2013 Hideharu Shintani^[181] used this procedure in solid phase extraction, such that the surface of the column was immobilized with anti-benzodiazepines. Most benzodiazepines were collected based on immunoaffinity. The major problem with this technique was the covalent linkage, which can be hydrolysed during the sol gel process.

More recently, Shao-Hsuan Chuag and co-worker^[182] designed a new platform that can be used in colorimetric immunoassay tests. They fabricated a porous monolith–AuNP complex to be used as solid support for high-mass transport and antigen–antibody interactions. Modified gold nanoparticles with detection antibodies were utilized as signals for colorimetric immunoassays, speeding up the analysis and decreasing reagent consumption. This technique improved the binding efficiency between antibodies and the mobile analytes and resulted in a decrease in the incubation times for antibody–antigen binding. Upon formation of the antigen–antibody complex, the colour of the monolith turned dark red. The limit of detection for this platform, which used HIgG, was 0.1 ng/mL with a linear correlation over a range of 0.1 ng/mL – 10 µg/mL. The time of analysis in this platform was very short (1 h) and efficient (0.1 ng/mL) compared to typical sandwich assays that usually require six hours. This colorimetric assay could be performed using visual inspection such as a desktop scanner or smart phones, and can be used in different applications such as drugs of abuse detection. Moreover, it can also be combined with a high sensitivity, low sample consumption and high throughput diagnostic system such as

chemiluminescence. Therefore, in this research, it was decided to explore this idea in order to investigate the effect of using microwaves on the internal structure of gold nanoparticles-silica monoliths. In addition, evaluation of the extraction efficiency for selected drugs of abuse by GNP-silica monolith using chemiluminescence as detection system was carried out.

1.9 Characterisation of modified stationary phases

Several methods that can be used to characterize stationary phases. The most common method is evaluation of chromatographic performance (such as retention time) or extraction efficiency (such as recovery of target analytes). However, analysis at the morphological, chemical and physical levels usually requires destructive methods (such as SEM-EDX, BET and BJH).

1.9.1 Scanning electron microscopy - Energy dispersive X-ray spectroscopy (SEM-EDX)

One of the most important methods for the analysis of modified stationary phase is scanning electron microscopy (SEM), which can be coupled with energy dispersive X-ray spectroscopy (EDX).

SEM analysis allows the analyst to investigate the morphological structure of silica monoliths, which can image each single point within the silica surface at the micrometre down to the nanometre level. Moreover, combined SEM and EDX analysis allows for each element with an atomic weight greater than 10 in the silica surface to be identified. SEM-EDX is a valuable tool, especially when comparing the morphological features of two products and monitoring product quality. However, preparation of the sample for SEM-EDX analysis requires the destruction of the column or solid sample.^[183]

1.9.2 Extraction performance

The easiest way to investigate the effect of modification phase chemistry without the need to destroy the material structure is monitoring changes in the extraction efficiency of the monolithic column. Modification of the silica surface with a new phase chemistry can change the selectivity and the extraction behaviour of modified silica monolith. For example, the coating of silanol groups on the silica monolith with a C₁₈ phase changes its selectivity from normal phase to reversed-phase and creates hydrophobic interaction with analytes.^[184]

In 2003 Zhao et al.^[185] determined eserine and its major metabolite eseroline in rat plasma using a one-step SPE procedure and photodiode array (PDA) detection. Different chemistry phases of SPE were applied. The best result was obtained using a Bond Elut C₁₈ column with a recovery of 88 ± 3 % at a concentration of 0.25 µg/mL. In 2007 Takeshi Kumazawa and co-worker^[186] used the C₁₈ phase column for the extraction of methamphetamine and amphetamine from human urine samples. Recoveries of amphetamine and methamphetamine into urine were more than 82.2 % and 82.9 %, respectively.

Maria E. Salinas-Vargas and Maria P. Cañizares-Macías^[187] extracted caffeine from coffee beans using C₁₈ reverse-phase mini-column. Recoveries of caffeine into green coffee and roasted coffee beans were in range between 99 % and 105 %.

Recently, the production of monolithic columns with modified phases is becoming more popular in the SPE. The performance of these phases is considered one of the most important factors for evaluating the modification process and investigating the efficiency of modified surfaces. Furthermore, this procedure is non-destructive and can give an overall picture of the column. However, such methodology does not allow for investigations in the longitudinal distribution of functional groups along the column length.^[43]

1.9.3 Nitrogen physisorption method

The physical properties of silica monoliths such as surface area, mesoporous size and mesoporous volume can be measured through a physisorption technique. In the physisorption method, the nitrogen gas adsorb in the silica monolith structure at constant temperature. The amount of adsorbed gas in a sol-gel material depends on the applied pressure. This adsorption process due to van der Waals force usually produces reversible change. At the equilibrium pressure (P) the progress of gas adsorption stops and the number of adsorption molecules equals the number of desorption molecules. P_o is the saturation pressure of pure adsorptive at a measurement temperature. Often, “Equilibrium relative pressure (P/P_o)” is used for physisorption measurement.^[188] The isotherm curve represents the amount of adsorptive (y-axis) against the relative pressure (P/P_o) (x-axis). The types of isotherm curves are classified by the International Union of Pure and Applied Chemistry (IUPAC), as shown in Figure 1-18.^[189]

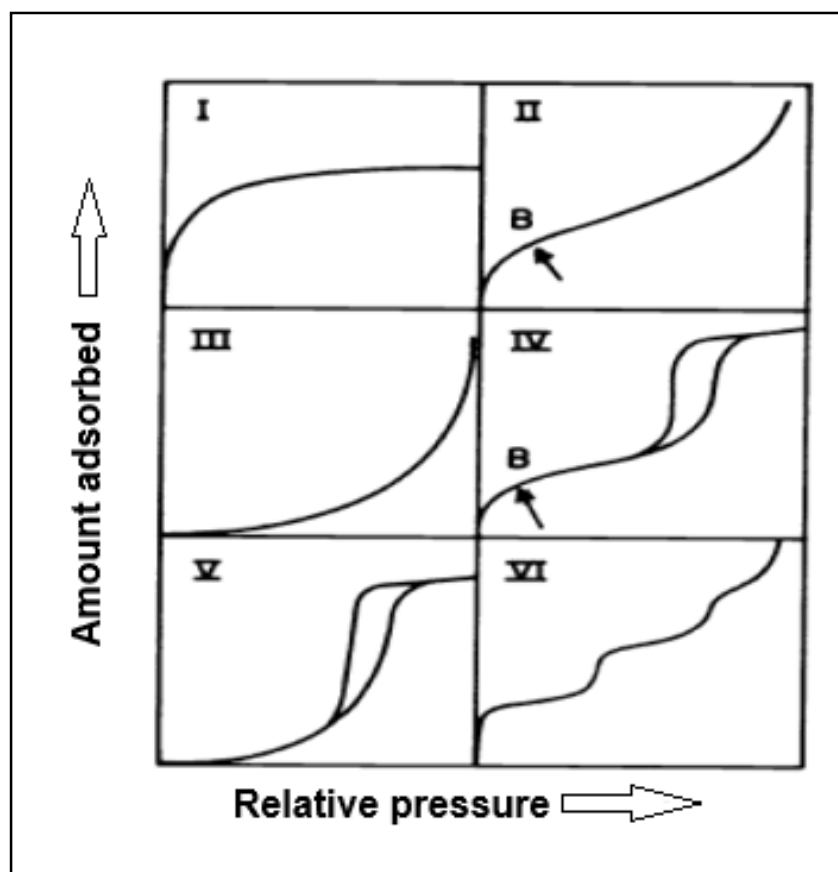


Figure 1-18 the IUPAC classification of the sorption isotherms. The adsorption and desorption isotherms can be found in six shapes (I-VI).^[189]

Type IV isotherm is usually associated with mesoporous materials ($2 \text{ nm} < \text{pore size} < 50 \text{ nm}$). Its hysteresis loop is related with condensation of mesoporous structure, and the limiting uptake over a range of high relative pressure (P/P_o).^[189]

In this work, the nitrogen physisorption measurements were performed for silica monolithic rods using the instrument software Brunauer-Emmett-Teller (BET) and Barrett-Joyner-Halenda (BJH). The ability of nitrogen physisorption method to measure the physical parameters of silica monoliths and characterise the whole structure is an advantage compared to the remaining characterisation methods.

1.10 Microwaves

1.10.1 Microwave energy

The region of the electromagnetic spectrum with wavelengths between 1m and 1mm and frequency between 300MHz and 300GHz is known as microwave range (see Figure 1-19). Since the Second World War, microwave technology has been used extensively in communication (radar and radio) and in many different applications, including diagnostics/analysis, manufacturing, weapons and medical treatment.^[190]

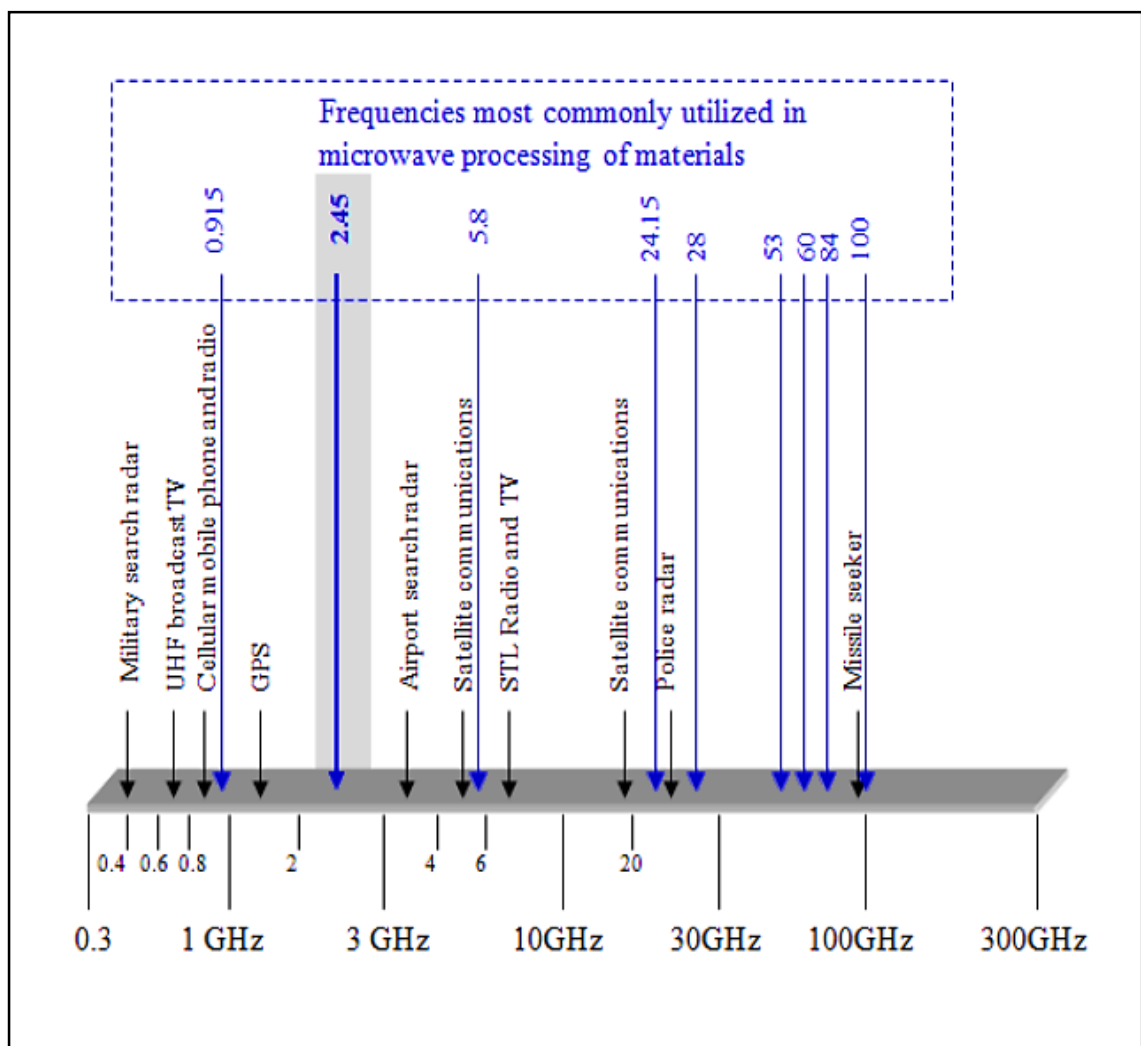


Figure 1-19 shows the microwave range with some of the major applications existing at various frequencies. It also shows some of the frequencies used for microwave processing of materials.^[90]

In the 1950s processing and manufacturing became one of the most important areas of microwave applications due to the appearance of home and industrial microwave

ovens^[191]. The radiation produced by microwave ovens (2.45 GHz) is usually absorbed by water molecules, which are the major ingredient in food. While drying alumina in the 1970s, Sutton^[192] observed that microwaves not only removed water from raw materials, but also heated the ceramic. In the following years, many researchers worked in different fields to explain the effects of using microwave radiations on different applications in order to improve our understanding of microwave radiation, such as generation, transmission, detection and control.^[193]

1.10.2 Conventional and microwave heating

Microwave heating is fundamentally different from conventional heating.^[194] With conventional radioactive or conductive heating energy is delivered from the surface to the interior of a container, whereas the energy in microwave heating is transferred directly to the material.^[90] This occurs because in microwave heating the electromagnetic energy is converted to thermal energy due to the molecular interaction of the material with the electromagnetic field.^[190] Therefore, microwave heating is defined as energy conversion rather than a heat transfer. Heat transfer in monoliths and polymers during conventional heating methods is very slow compared to microwave heating where the processing time can be short. In addition, localized thermal effects may offer a number of advantages over conventional heating methods. In this project a study into the influence of microwave heating during gel formation and surface modification of silica monoliths will be carried out to evaluate the chemical and physical properties of functionalized silica monoliths.

1.10.3 Microwave interactions with materials

Materials can be classified into four categories according to their interaction with microwaves (see Figure 1-20):

- 1- Transparent materials: the microwaves can pass through this type of material without losing any significant amount of energy (e.g. pure silica).
- 2- Opaque materials: do not allow for microwaves to penetrate and reflects them (e.g. metals).
- 3- Absorbing materials: allow for microwaves to penetrate and absorbs them (e.g. water).
- 4- Partial absorbing materials: combination of two or more previous materials (e.g. silica gel).^[90, 195]

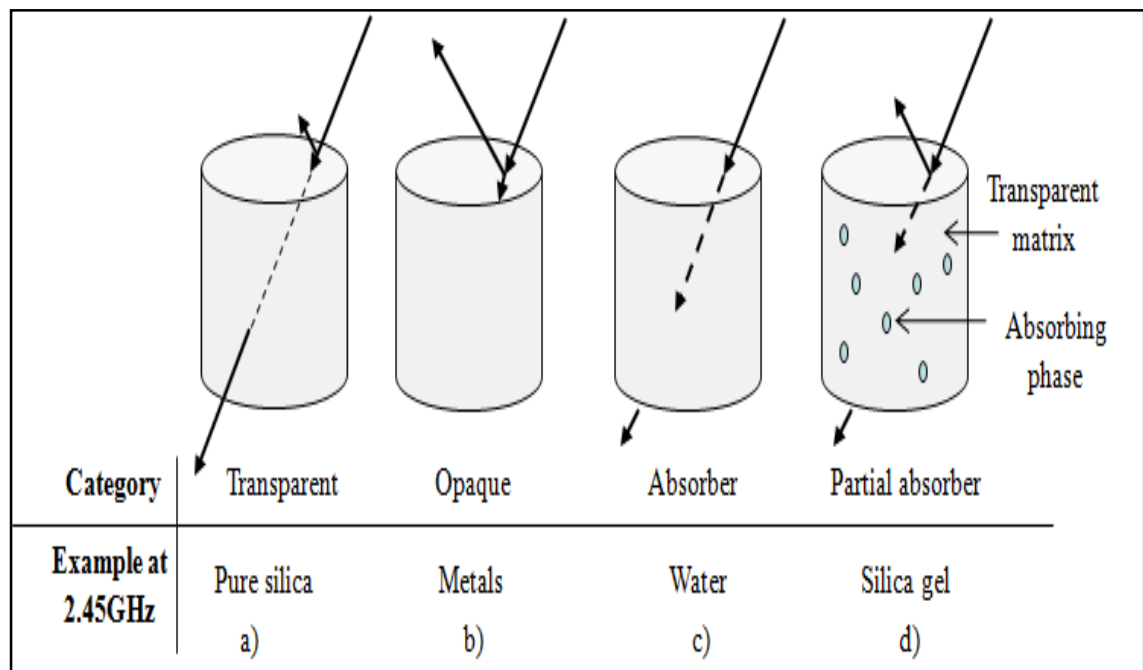


Figure 1-20 Material classification based on microwave interaction: a) transparent, b) opaque, c) absorber, d) partial absorber. Silica gel is composed of a transparent matrix and absorbing phase and is thus a partial absorber.^[90, 195]

When microwaves are absorbed, the charged particles (e.g. electrons, ions or dipoles) within the materials polarize or rotate in response to the applied electric field (E).

Losing and attenuating of the electromagnetic field due to elastic, frictional or inertial forces, results in internal heating.^[196]

1.10.4 Dielectric materials

Two mechanisms can produce losses when materials interact with microwaves. First is conduction, which includes the long-range motion of charged particles (electrons or ions) when an electric field E is applied.^[68] In electronic conduction (EC), the electrical charge is transported in metals and semiconductors through the electrons. In this case losses of EC occur due to resistance in the material. In contrast, conduction in the ionic materials is achieved by displacement of the charge with ions. The collision of charged particles with other particle species, when moving within the material, leads to generating losses in i . The losses in conduction are often observed at low frequency range. Increases in the frequency result in a decrease in the time of displacement of the charged particle and, as a result, the charged particles cannot be transported in the direction of the field.^[197]

Another mechanism for the interaction of E with a dielectric material is known as polarization or short-range motion of the charge. The charge in this case is transported via orientation or oscillation of electric dipoles. Several types of polarizations can generate losses due to the resistance of the dipoles to movement under an alternating field. These losses are usually show at high frequencies.^[90]

1.10.5 Types of polarization

There are four types of polarization in sol-gel materials and are the result of the displacement of the charged particles from their equilibrium position, forming dipoles that try to follow the direction of the electric field (see Figure 1-21).

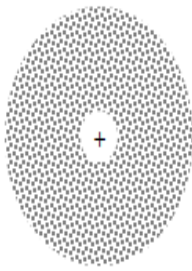
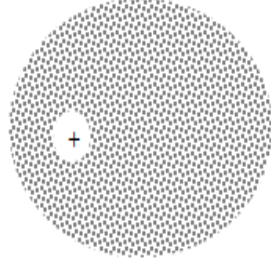



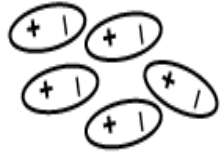
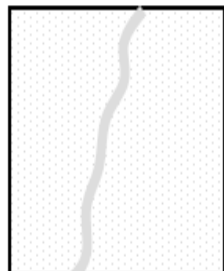
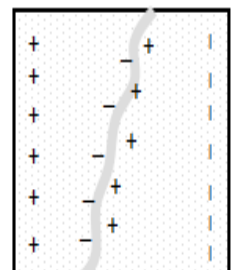
Electromagnetic spectrum where interaction occurs	Frequency (Hz)	Polarization Mechanism	No field	Field applied - ← + E
a) Visible Ultraviolet	10^{15}	Electronic polarization		
b) Infrared	$10^{12} - 10^{13}$	Atomic or Ionic Polarization		
c) Radio Frequency Microwaves Near Infrared	$10^3 - 10^6$ $10^{10} - 10^{12}$	Dipole Polarization		
d) Long Waves Microwaves	$10^{-3} - 10^3$ $10^6 - 10^{10}$	Interfacial Polarization		

Figure 1-21 Polarization types with and without an electric field applied: a) electronic, b) atomic, c) dipole, and d) interfacial space charge polarization.^[90, 198]

Each type of polarization is described in more detail below:

1. Electronic polarization is the effect of the electrons' displacement in the atoms relative to the positive atom nucleus in an electrical field (see Figure 1-21 a). This process takes around 10^{-15} sec and corresponds approximately to the frequency of ultraviolet light.
2. Atomic or ionic polarization is the result of the movement of the ions relative to one another inside the molecule, as shown in Figure 1-21 b. This process requires from

10^{-12} to 10^{-13} sec and corresponds to the frequency of infrared radiation. A similar polarization in ionic crystals arises with the displacements of oppositely charged ions requiring 10^{-12} sec, which corresponds to the far infrared frequency. Ionic polarization gives rise to resonance absorption at a narrow frequency range, characteristic of the bond strength between the ions.

3. Dipolar polarization is the perturbation of the thermal motion of ionic or molecular dipoles, producing a net dipolar orientation in the direction of an applied field (see Figure **1-21** c).

Due to this behaviour, this polarization is also known as orientation polarization and is probably one of the most important in the microwave range. There are two primary mechanisms that take effect in orientation polarization. The first is the rotation of the permanent dipoles against the elastic restoring forces to the equilibrium position. This process also is referred to as deformation polarization and takes 10^{-10} - 10^{-12} sec at room temperature. This mechanism is not common in sol-gel materials, but is important for a diversity of liquids, gasses and polar solids. The second mechanism is the rotation of dipoles between two equilibrium positions. It involves a spontaneous alignment of the dipoles in one of the equilibrium positions when an electrical field is applied. As the frequency of the electric field increases, the dipoles cannot follow the direction of the field. This type of polarization requires between 10^{-9} - 10^{-12} sec and 10^{-3} - 10^{-6} sec.

4. Interfacial polarization results from the accumulation of charges at the interfaces between phases that have differences in dielectric constant and conductivity. The interfaces between phases, impurities or second phases act as physical barriers that reduce charge displacement (see Figure **1-21** d). This polarization is observed over two ranges of frequencies. One range is between 10^{-3} and 10^3 Hz and is due to an accumulation of charge (localized polarization) on the barriers. The other range is between 10^6 and 10^{10}

Hz and occurs when one of the phases is highly conductive and dominates the total loss in the dielectric.

The important mechanisms resulting in microwave heating for most sol-gel materials are dipole and interfacial polarizations because they are active in the microwave frequency range. The electromagnetic spectrum, including the frequency range where each polarization mechanism occurs, is shown in Figure 1-21. [90, 198]

1.10.6 Dielectric constant and dielectric loss

In a dielectric the stored charge (q) is expressed as a function of the applied voltage (V) and the capacitance (C):

$$q = V/C \quad \text{Eq.5}$$

$$k = C/C_0 - [i(G_{dc} + G_{ac})]/\omega C_0 \quad \text{Eq.6}$$

The loss current in a real dielectric can be expressed as a function of one complex parameter, k . This parameter will be called the complex dielectric constant (k^*).

The real part of k^* is

$$k' = C/C_0 \quad \text{Eq.7}$$

The imaginary part of k^* is

$$k'' = (G_{dc} + G_{ac})/\omega C_0 \quad \text{Eq.8}$$

Also expressed as

$$k^* = k' - ik'' \quad \text{Eq.9}$$

The ability of the material to store charges under an E is known as the dielectric constant (k'). The value of loss can be occurred by the material under an E is known as dielectric loss factor (k''). The ratio of the dielectric loss factor to the dielectric constant (k''/k') is equal to the ratio of the loss current to the charging current (I_L/I_C) and is called the loss angle, dissipation factor or $\tan\delta$. Type equation here.

All types of losses that can occur during long-range motion (conduction) and short-range motion (polarization) have been designated with one term, the effective loss factor, ϵ''_{eff} , given by

$$\epsilon''_{\text{eff}} = \epsilon''(\omega) + \sigma_{\text{dc}}/(\epsilon_0\omega) = \epsilon''_{\text{sc}}(\omega) + \epsilon''_{\text{o}}(\omega) + \epsilon''_{\text{a}}(\omega) + \epsilon''_{\text{e}}(\omega) + \sigma_{\text{dc}}/(\epsilon_0\omega) \quad \text{Eq.10}$$

Where $\epsilon''(\omega)$ represents the losses related with polarization (frequency dependent), and the $\sigma_{\text{dc}}/(\epsilon_0\omega)$ is associated with the losses from dc conductivity. The subscripts of the different components refer to the diverse polarization mechanisms: space charge or interfacial (sc), orientation (o), atomic (a), and electronic (e).

One group of research states that sol-gel materials with ϵ''_{eff} between 10^{-2} and 5 are good for microwave heating, whereas sol-gel materials with $\epsilon''_{\text{eff}} < 10^{-2}$ are difficult to heat by microwave. Silica gel has a dielectric loss at room temperature of 0.27 (2.45 GHz). Therefore, it is not possible to heat this material inside a multimode cavity applying 1200W; however, the heating of this material can be achieved by a single mode cavity under a higher electrical field and at much lower input power.^[90, 198, 199]

1.10.7 Microwave power dissipation

The application of an electromagnetic (EM) wave to a material leads to the transport of energy. When this energy flows through a closed surface, dissipation of the energy volumetrically inside the material can occur and results in a form of heat which can be calculated from the integration of the Poynting vector P :

$$P = E \times H = (V/m) \times (A/m) = (\text{Watts} / \text{m}^2) \quad \text{Eq.11}$$

Where: V = volts and A = amps

Here, E and H are the electric and magnetic components of the electromagnetic field, respectively.^[90, 198]

1.10.8 Microwave hybrid heating

Microwave hybrid heating can be performed by two different techniques:

1. Heating the sample outside the microwave cavity using an external heat source then introducing it into the cavity.
2. Heating the sample inside the microwave cavity after adding microwave absorbing material with the original sample. The microwave energy is applied to both materials at the same time. This is the technique used in the present study for fabricating the silica monolith (using gold nanoparticles). These techniques can make the sample a more efficient microwave absorber. It also can produce different results depending on what type of microwave cavity is used. The EM field on the sample has characteristics that are influenced by the cavity design; thus, a given material will respond to the field differently in a different microwave cavity.^[90, 201]

1.10.9 Microwave cavities

The microwave cavity is a metallic enclosure device where the microwave undergoes multiple reflections whilst transferring energy to the sample. The size and shape of the cavity and microwave frequency must be optimized to ensure a high conversion efficiency of the microwave energy to the sample. There are two types of cavities: the multimode and the single mode. A multimode is a type of cavity in which different patterns of electromagnetic waves are present, and the total field is the summation of all excited modes. The multiple modes result in multiple reflections in a cavity, which produce uniform heating. More uniform radiation of the sample can be obtained using mode stirrers inside the microwave field. However, a non-continuous distribution of low and high field intensities can occur due to using multimode cavities. Furthermore, the position of the sample in the cavity is critical. To solve this problem a single mode cavity can be used, where the field distribution and the position of the sample can be precisely

determined in order to optimize and reproduce the thermal process. The main drawback in these type of cavities is the restricted size of the sample due to a small cavity.^[202]

1.11 Aims of the project

According to the literature it is clear that the structure of the silica monoliths can be changed when different chemical compositions, physical parameters and heating methods are used. However, the fabrication of silica monoliths remains time-consuming and laborious.

Recently, microwave energy has been used to calcinate and crystallize different materials that reduce the time of these processes compared to conventional thermal heating methodology.

The main goal of this research was to explore the effect of using microwave heating during the gel formation process in the internal structure of the silica monolith, and compare the meso and macro porous structure of the prepared silica monolith using conventional heating and microwave heating methodology. In addition, to evaluate the efficiency of using microwave heating during the modification of silica surface with C₁₈ phase, gold nanoparticles and graphene phase.

In order to reach this goal, five objectives were proposed

1. Developed a method for the reliable and consistent production of silica monolith using microwave heating during gelation process. (See **chapter 3**).
2. Developed a reliable method for C₁₈ phase surface modification in a microwave system (single mode cavity). (See **chapter 4**).
3. Developed a reliable method for embedding modified gold nanoparticles within the silica monolith using microwave heating (single mode cavity). (See **chapter 5**)
4. Designed and constructed apparatus for the detection of trace amount of drugs of abuse based on a gold nanoparticles-NH₂-silica monolithic device with an integrated detection method (chemiluminescence). (See **chapter 5**)

5. Developed a reliable method for the modification of silica monolith with graphene phase using microwave heating (single mode cavity). (See **chapter 6**)

While decreasing the total analysis time is limited by the sample preparation. Therefore, the sample preparation step is considered a bottleneck in a system for chemical analysis.

This PhD project combines two advanced techniques, sol-gel processing and microwave processing of materials. In order to develop a portable, integrated drugs of abuse processing/analysis device for 'at the scene of crime' use with capability to produce qualitative and quantitative results at very short time.

For this specific application, the modified silica monolithic column must be capable of extracting selected drugs of abuse from biological samples and detection them using chemiluminescence based immunoassays or HPLC-UV.

2 Experimental

(Chapter 2)

2.1 *Fabrication of monolithic materials*

2.1.1 *Fabrication of silica monoliths using a conventional heating method*

Silica based monoliths were prepared using a method similar to that described by Nakanishi ^[67] with some modifications in the chemical composition and experimental conditions. Silica monolithic rods were fabricated using a polymer (polyethylene oxide PEO, polyethylene glycol PEG and pluronic F127) [purchased from Sigma-Aldrich, Poole, UK] present in an acid catalyst (such as nitric acid 1 M or acetic acid 0.02 M) [purchased from Fisher Scientific, Loughborough, UK]. The acidified polymer solution was placed in a 50 mL falcon tube [Scientific Laboratory Supplies, Nottingham, UK], located in an ice bath, and stirred for 60 min until the polymer fully dissolved [Stirrer purchased from VWR International, West Chester, PA, USA]. Two mL of metal alkoxide (such as TMOS-tetramethylorthosilicate 98 % or TEOS- tetraethylorthosilicate 98 %) [purchased from Sigma-Aldrich, Poole, UK] were then added to the acidified polymer mixture and stirred for a further 60 min in the ice bath until a clear solution formed (see Figure 2-1).

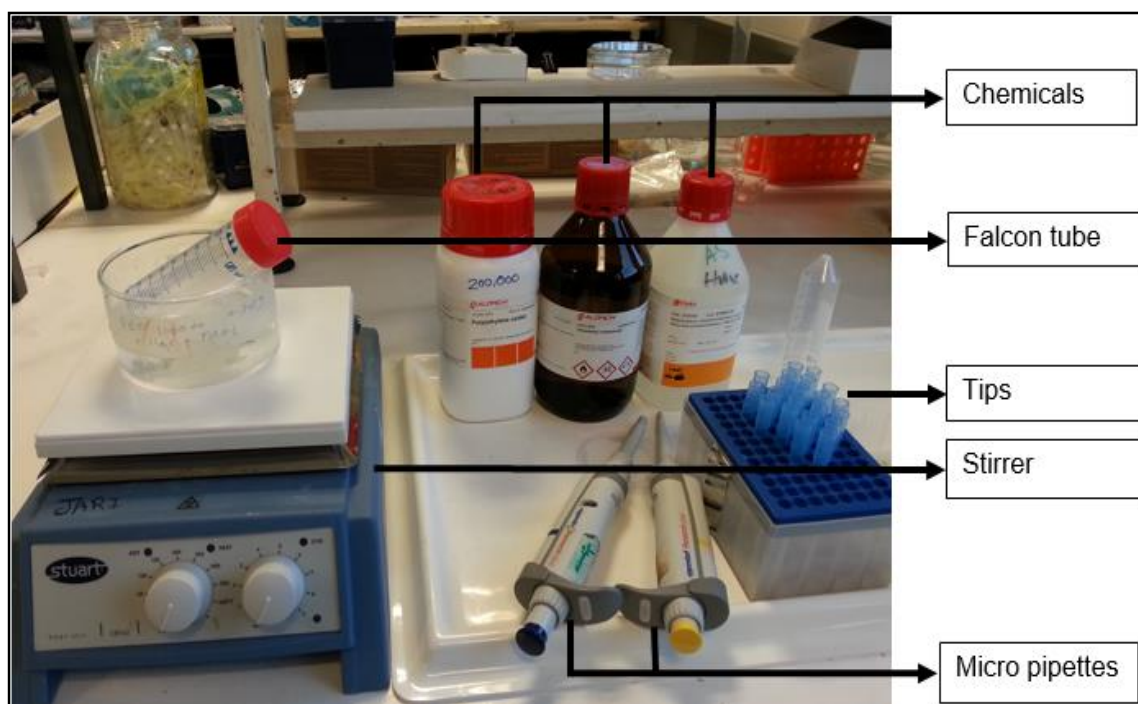


Figure 2-1 Experimental setup for silica monolith fabrication. The starter mixture contains polymer, acid catalyst and metal alkoxide. Ice bath and stirrer plate are used for dissolving starter mixture component. Micropipettes are used to measure and transfer small volumes of liquids. Falcon tube is used for mixing the chemical composition.

When the mixture was homogeneous, it was left to settle for 2 min to remove any bubbles that may have formed during mixing. A plastic syringe (B.D Plastipak 1 mL) [Scientific Laboratory Supplies, Nottingham, UK] after that sealed at the outlet end with PTFE tape [ARCO Ltd. Hull, UK] and filled with the monolith solution (0.5 mL). The syringe barrel was then placed upright into a conventional thermal oven at 40 °C for 3 days [Mega Electronics, Cambridge, UK]. The resulting wet-semi-sold gel monoliths were washed with copious amounts of water and transferred to an aqueous solution of 1 M NH_4OH (30 mL) [Fisher Scientific, Loughborough, UK] contained within a conical flask (100 mL) [Fisher Scientific, Loughborough, UK], as shown in Figure 2-2. At this time the flask was wrapped in aluminium foil and placed into an oil bath at 90 °C measured using a thermometer for 24 h.

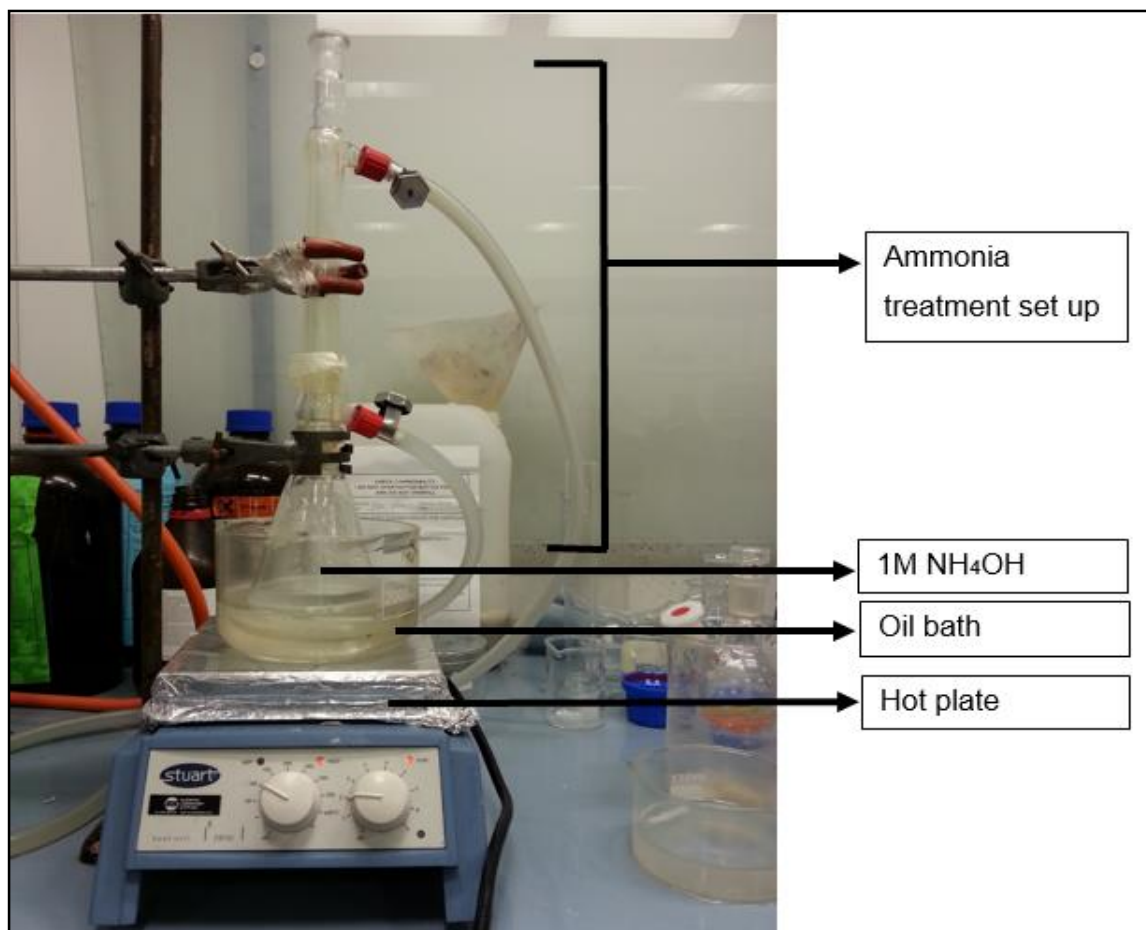


Figure 2-2 Set up for ammonia treatment process. Aqueous ammonium hydroxide was used as a porogen for forming mesoporous. The mesoporous in the wet gel skeleton was made by alternating the fluid phase with an external solution (ammonium hydroxide solution).

Next, the monolithic rods were taken out of the conical flask, washed with purified water and finally placed back into an oven at 40 °C for 6 h and at 90 °C for 3 h [Mega Electronics, Cambridge, UK]. In the last step the rods were transferred to a furnace microwave for further heat treatment at 600 °C for 3 h (heating rate: 2 °C / min) to remove the remaining PEO and form white silica-monolith rods. After preparation, the silica monolithic rods were cut to a desired length of 1 cm.

2.1.2 Fabrication of silica monolith using a microwave heating method

Silica monolithic rods were fabricated using a polymer (polyethylene oxide PEO, polyethylene glycol PEG and pluronic F127) [purchased from Sigma-Aldrich, Poole, UK] present in an acid catalyst (such as nitric acid 1 M or acetic acid 0.02 M)

[purchased from Fisher Scientific, Loughborough, UK]. The acidified polymer solution was placed in a 50 mL falcon tube [Scientific Laboratory Supplies, Nottingham, UK], located in an ice bath, and stirred for 60 min until the polymer fully dissolved [Stirrer purchased from VWR International, West Chester, PA, USA]. Two mL of metal alkoxide (such as TMOS-tetramethylorthosilicate 98 % or TEOS- tetraethylorthosilicate 98 %) [purchased from Sigma-Aldrich, Poole, UK] were then added to the acidified polymer mixture and stirred for a further 60 min in the ice bath until a clear solution formed. The resulting homogeneous solution was left to settle for 2 min to remove any bubbles that may have formed during mixing. After that, a plastic syringe (B.D Plastipak 1 mL) [Scientific Laboratory Supplies, Nottingham, UK] sealed at the outlet end with PTFE tape [ARCO Ltd. Hull, UK] and filled with the monolith solution (0.5 mL). The syringe barrel was then positioned in the cavity of a Discover microwave system [CEM Microwave Technology Ltd, Buckingham, UK] with the capability of delivering 0–300 W of microwave power at 2.45 GHz with mono-mode operation (see Figure 2-3 and 2-4). The fibre optic temperature measurement was used to monitor the temperature of the external surface of the monolith [Omega Engineering Limited, Manchester, UK] in addition to the infrared sensor fitted in the microwave cavity. This microwave system also incorporates CEM's Synergy software, offering increased functionality and makes documentation recording and automating data handling much easier.

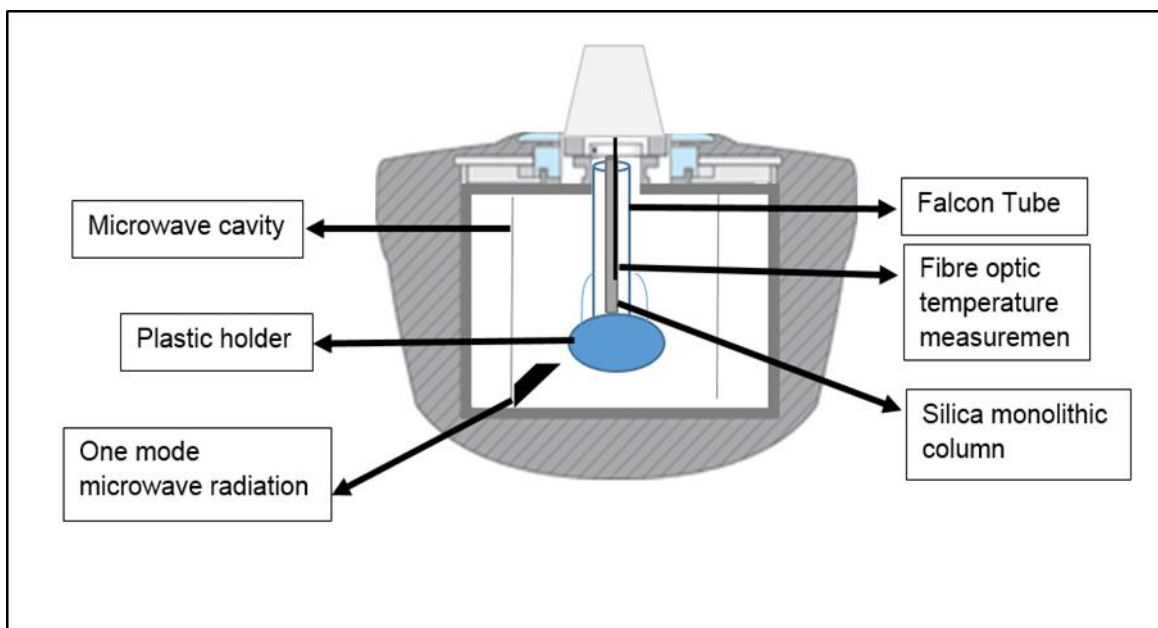


Figure 2-3 Set up for silica monolith fabrication and modification using single mode cavity microwave. The fibre optic temperature measurement was used to monitor the temperature of the external surface of the silica monolith during the fabrication and modification processes in addition to the infrared sensor fitted in the microwave cavity.

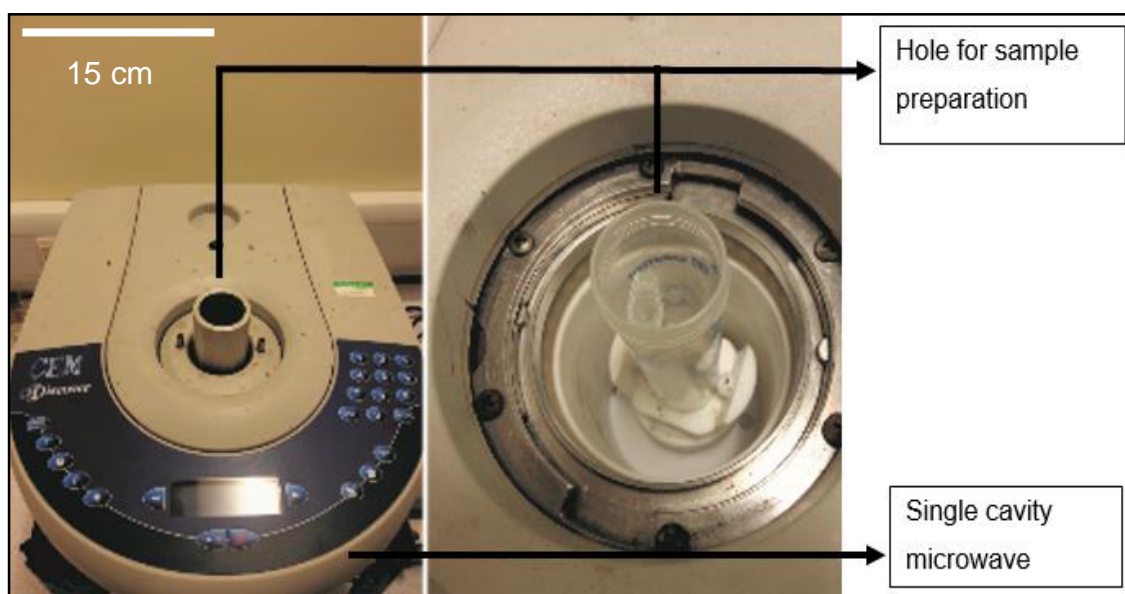


Figure 2-4 Single cavity microwave that focuses the microwaves (2.45 GHz) around the sample with maximum efficiency and offers rapid, reliable and reproducible microwave-assisted fabrication and modification of silica monoliths.

The produced wet-gel monoliths were washed with copious amounts of purified water and transferred to an aqueous solution of 1 M NH_4OH (30 mL) [Fisher Scientific, Loughborough, UK] contained within a conical flask (100 mL) [Fisher Scientific, Loughborough, UK]. The flask was wrapped in aluminium foil and placed into an oil bath

at 90 °C for 24 h. Next, the monolithic rods were taken out of the conical flask, washed with purified water and placed back into an oven at 40 °C for 6 h and at 90 °C for 3 h [Mega Electronics, Cambridge, UK]. Finally, the rods were transferred to a furnace microwave for further heat treatment at 600 °C for 3 h (heating rate: 2 °C / min) [CEM Microwave Technology Ltd, Buckingham, UK] to remove the remaining PEO and form white silica-monolith rods. After preparation, the silica monolithic rods were cut to a desired length of 1 cm (as shown in Figure 2-5).

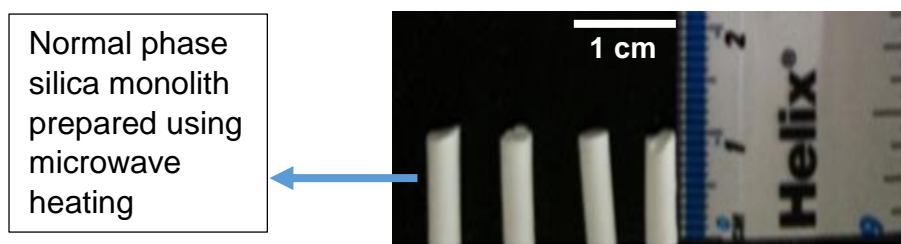


Figure 2-5 Photograph of silica monolithic rods obtained using microwave heating cut to 1 cm.

2.1.3 Connecting the silica monolith with the borosilicate tube using the heat shrinkable sleeving polytetrafluoroethylene (PTFE) tube

Before the monolithic silica rod was functionalised, it was connected to borosilicate tubes (O.D. 3.90 mm) [Glassware, University of Hull, UK] using heat shrinkable polytetrafluoroethylene (PTFE) sleeving, whose internal diameter shrinks from 4.8 mm to 2.8 mm [Adtech Polymer Engineering Ltd., Stroud, UK]. The monolithic silica rod and the borosilicate tube were placed inside the shrinkable tube, which was then placed in the furnace [CEM Microwave Technology Ltd, Buckingham, UK] at 360 °C for 30 min to seal the heat shrinkable tube around the borosilicate tube and monolithic silica rod. The resulting silica monolithic column was ready to use for surface modification and drug extraction.

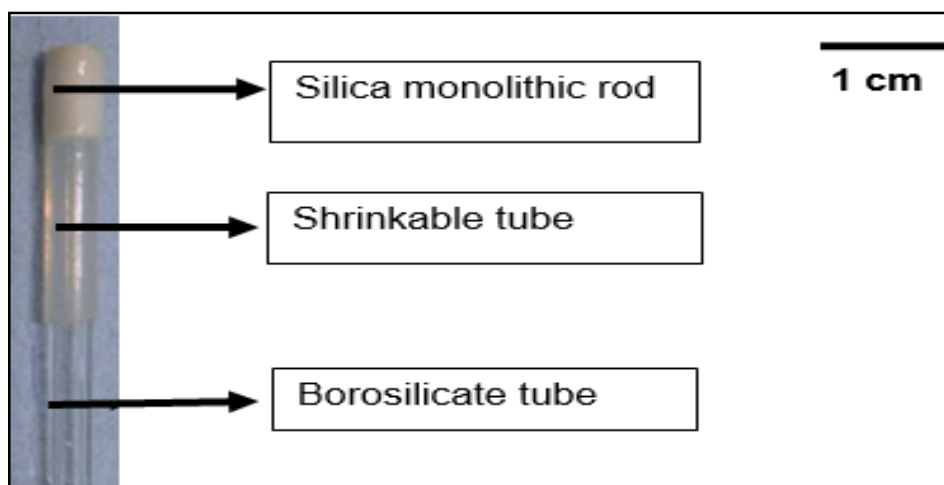


Figure 2-6 Silica-based monolith that was connected to the borosilicate tube using PTFE shrinkable tube.

2.2 Derivatisation of the silica based monoliths with C_{18} phase

The surface of the silica monolith was chemically modified with C_{18} phase (octadecyl groups) using two methods:

2.2.1 C_{18} phase modified silica monolith using conventional heating method

In the first procedure the silica monolithic column was washed with toluene [Fisher Scientific, Loughborough, UK], which was followed by continuously flowing chlorodimethyl octadecyl silane 95 % (CDMOS) [Sigma-Aldrich, Poole, UK] solution at a flow rate of 20 $\mu\text{L}/\text{min}$ for 9 hours. The surface functionalization was carried out at 80 $^{\circ}\text{C}$ for 9 h using conventional thermal heating. After C_{18} surface modification process the monolithic silica column was thoroughly washed with toluene at a flow rate of 100 $\mu\text{L}/\text{min}$ for 3 min.

2.2.2 C_{18} phase modified silica monolith using microwave heating method

The second silica monolith was first washed by toluene [Fisher Scientific, Loughborough, UK] and then filled with ODS [Sigma-Aldrich, Poole, UK] solution prepared by mixing ODS/Toluene 50% / 50% (v/v). C_{18} surface modification was achieved using single cavity microwave system [CEM Microwave Technology Ltd, Buckingham, UK] for 40 min at

80 °C and 120 W. The fibre optic temperature measurement was used to monitor the temperature of the external surface of the monolith [Omega Engineering Limited, Manchester, UK] in addition to the infrared sensor fitted in the microwave cavity. Next, the monolithic silica columns were thoroughly washed with toluene at a flow rate 100 µL/min for 3 min.

2.3 *Extraction*

2.3.1 *Materials*

Caffeine anhydrous and eserine were used for preparation of standard solutions purchased from [Sigma-Aldrich, Poole, UK]. C₁₈-bonded monolithic silica columns (monolithic diameter 3.2 mm, length 1 cm) were prepared within the Department of Chemistry, University of Hull.

2.3.2 *Preparation of standard solutions*

Stock standard solutions of caffeine and eserine were prepared separately by dissolving an accurately weighed amount of each compound in purified water to achieve a concentration of 1 mg/mL. All stock solutions were stored at 4 °C. 6 standard solutions (10, 50, 100, 20, 300 and 400 µg/mL) in purified water were prepared by serial dilution from the stock solutions (1 mg/mL). All standard solutions were freshly prepared every week and stored at 4 °C.

2.3.3 *HPLC conditions*

All analyses were performed using HPLC-UV system [785A UV/Visible Detector from PerkinElmer, California, USA] with a Symmetry C₁₈ column, 4.6 mm × 250 mm packed with silica particles 5 µm from Waters [United Kingdom, Waters Limited, Centennial Court, Centennial Park]. Samples were injected using a 20 µL internal-loop sample injector. For caffeine analysis the mobile phase was methanol / (0.01) acetic acid

(30% : 70%) (v/v) [Fisher Scientific, Loughborough, UK] run under isocratic conditions at a flow rate of 1 mL/min and the detection wavelength was adjusted to 205 nm. For eserine analysis the mobile phase was ACN /H₂O (0.01 ammonium acetate) (80% : 20%) (v/v) [Fisher Scientific, Loughborough, UK] run under isocratic conditions at a flow rate of 1 mL/min and the detection wavelength was adjusted to 248 nm.

2.4 *Fabrication of silica based monoliths with gold nanoparticles*

2.4.1 *Fabrication of silica monolith embedded by gold nanoparticles*

The initial mixture of sol-gel was prepared by adding (0.305 g) PEO [Sigma-Aldrich, Poole, UK] and 5 μ L gold nanoparticles (50 nm diameter, amine functionalized NH₂) [Sigma-Aldrich, Poole, UK] to 4 mL (0.02 M) acetic acid solution [Fisher Scientific, Loughborough, UK]. The mixture was stirred for 60 min while immersed in an ice bath. After that two mL TMOS (tetramethylorthosilicate 98 %) [Sigma-Aldrich, Poole, UK] was added to the former mixture and stirred for a further 60 min in the ice bath. A plastic syringe (B.D Plastic 1 mL) [Scientific Laboratory Supplies, Nottingham, UK] was then sealed at the outlet end with PTFE tape [ARCO Ltd. Hull, UK] and filled with the monolith solution (0.5 mL). Next, the syringe barrel was placed into the single cavity microwave [CEM Microwave Technology Ltd, Buckingham, UK] for 5 min at 120 °C and 300 W. The fibre optic temperature measurement was used to monitor the temperature of the external surface of the monolith [Omega Engineering Limited, Manchester, UK] in addition to the infrared sensor fitted in the microwave cavity. The resulted wet-semi-sold gel monolith was treated with an aqueous solution of 1M NH₄OH (30 mL) [Fisher Scientific, Loughborough, UK] contained within a conical flask (100 mL) [Fisher Scientific, Loughborough, UK]. Afterwards the flask was wrapped in aluminium foil and placed into an oil bath at 90 °C for 24 h. Finally, the monolithic rods were taken out of

the conical flask and placed back into an oven at 40 °C for 6 h and at 90 °C for 3 h. After preparation, the silica monolithic rods were cut to a desired length of 1 cm.

2.4.2 Physical modification of silica based monolith with gold nanoparticles labelled with NH₂ groups

The same sol-gel mixture and experimental setup as described in section (2.4.1) were used to fabricate silica monoliths, except 5, 10 and 50 μL of gold nanoparticles labelled by NH₂ groups was placed on the top surface of the wet gel silica monoliths using different moulds (such as 1 mL PD plastic syringe or Eppendorf tube 1 mL or UV plastic cuvette 1 cm × 1 cm) [Scientific Laboratory Supplies Limited, East Riding of Yorkshire, UK] (see Figure 2-7). In this procedure the resultant wet-semi-sold gel monoliths modified with GNP-NH₂ were treated with an aqueous solution of 1M NH₄OH using a special holder to keep GNP-NH₂ out of the basic solution.

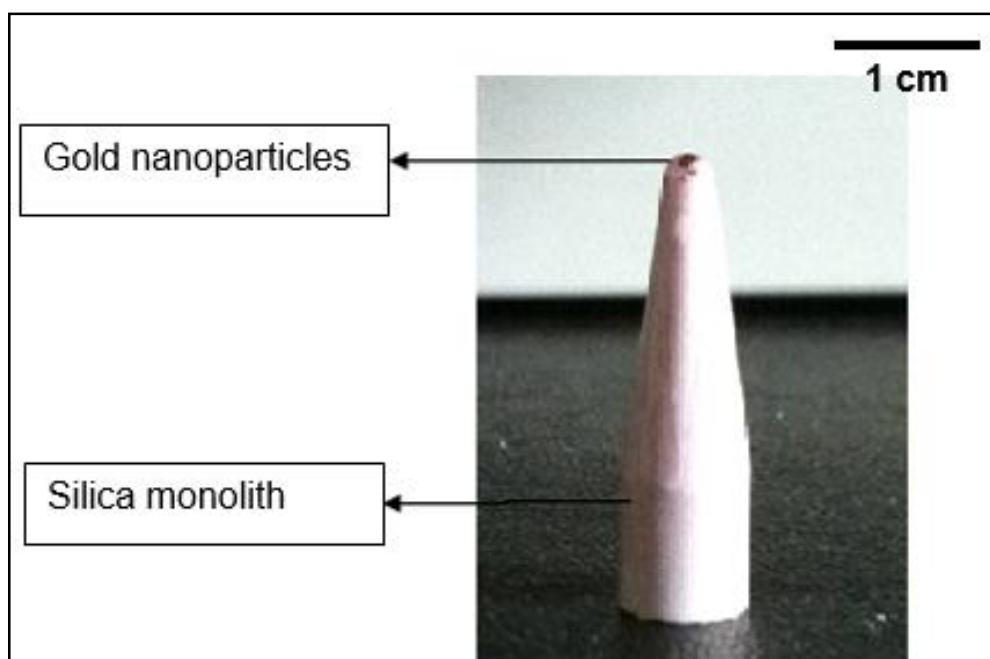


Figure 2-7 Modified silica based monoliths with gold nanoparticles.

2.4.3 Connecting silica monoliths with borosilicate tubes using heat shrinkable sleeving polytetrafluoroethylene (PTFE) tube and heat gun

The silica monolithic rods were connected to the borosilicate tubes (o.d. 3.90 mm) using the heat shrinkable sleeving polytetrafluoroethylene (PTFE) tubes. The average of shrinking of internal diameter for PTFE tube was from 4.8 mm to 2.8 mm [Adtech Polymer Engineering Ltd., Stroud, UK]. The monolithic silica rod and the borosilicate tube were placed inside the shrinkable tube and a heat gun was then used for 5 min to seal the heat shrinkable tube around the borosilicate tube and monolithic silica rod. The resulting silica monolithic column was ready to use for surface modification and drug extraction.

2.4.4 Oxazepam detection (antigen-antibody reaction)

The aim of the experiment was to immobilise the antibodies on the gold nanoparticles (GNP) coated silica monolithic rods and to investigate their efficiency as immunosensor using chemiluminescence. The procedure used to link the anti-oxazepam with amine groups on the surface of GNP coated silica monolithic rods was as follows:

- I- 2.2 mg of *N*-Hydroxysulfosuccinimide sodium salt [Sigma-Aldrich, Poole, UK] and 0.8 mg of *N*-(3-dimethylaminopropyl)-*N*-ethyl-carbodiimide hydrochloride (EDC) [Sigma-Aldrich, Poole, UK] were dissolved in 2 mL of phosphate buffer saline (PBS) [Sigma-Aldrich, Poole, UK].
- II- 5 μ L of Sulfo-NHS + EDC solution was taken and mixed with 5 μ L of anti-oxazepam to make anti-oxazepam solution.
- III- 10 μ L anti-oxazepam solution was spotted on the surface of GNP coated silica monolithic rods and left overnight in the refrigerator at 4 °C for 18 hours, and covered (see Figure 2-8).

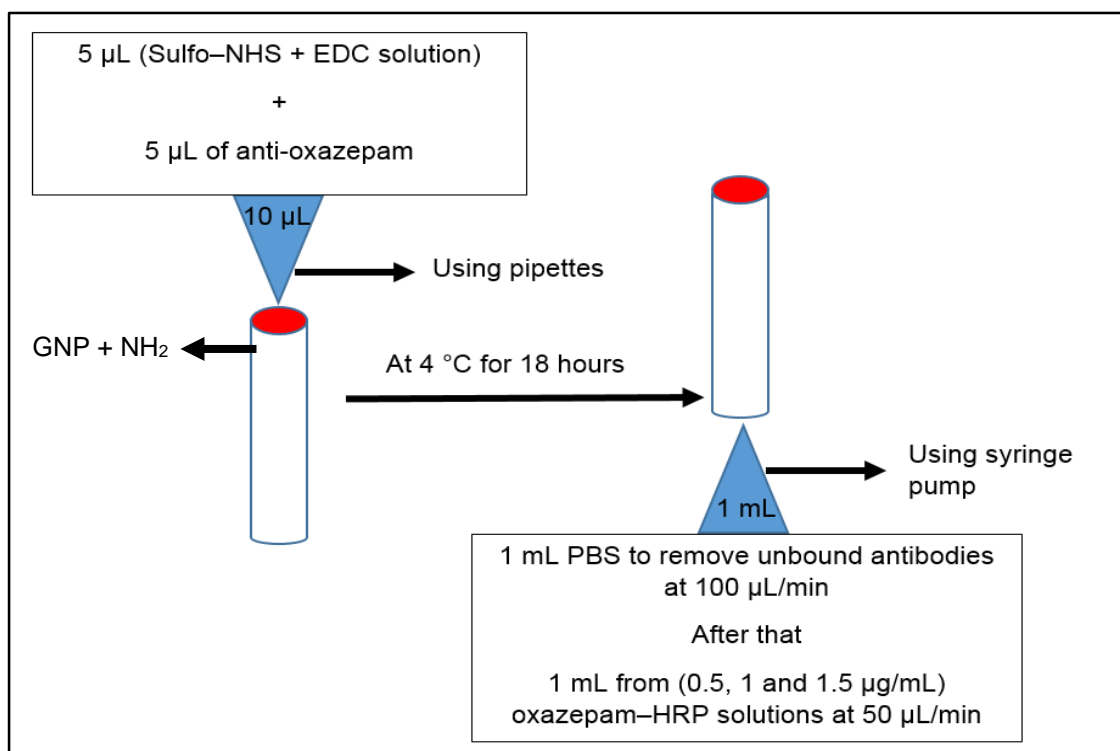


Figure 2-8 The procedure for immobilization of anti-oxazepam on the surface of GNP coated silica monolithic rods and detection of oxazepam-HRP.

The resulting silica monolithic columns were removed from the refrigerator and washed each column with 1 mL PBS to remove unbound antibodies. After that, 1 mL from 0.5, 1 and 1.5 μg/mL oxazepam-HRP solutions were injected into modified (GNP-NH₂) silica monolithic columns at 50 μL/min. The columns were left for 1 hour to allow for oxazepam-HRP to bind with their antibodies. To remove any unbound oxazepam, the silica monolithic columns were then washed with 1 mL of PBS at 100 μL/min (see Figure 2-8). A solution of luminol and hydrogen peroxide 1:1 (v/v) were added to each top surface of silica monolithic column coated with GNP and a CCD camera was used for analysis.

2.4.5 CCD camera

The light emitted from the chemiluminescent reaction that takes place is detected using a Charge Coupled Device (CCD) Camera (QHY6 CCD camera) [QHXCCD, USA] fitted with an 8 mm high resolution pixel lens [Coputar, USA]. Analysis was carried out using

a custom – made control software [Radox Laboratories Ltd, UK]. The exposure time was 2 min and concentrations of luminol and H₂O₂ were 10 mM.

2.5 Graphene monoliths

2.5.1 Fabrication of graphene monoliths using microwave heating

The graphene monoliths were fabricated following the Lianbin Zhang procedure^[203] with some modifications in the fabrication conditions. The monolithic structures of graphene were prepared by the *in situ* reduction method using a combination of sodium iodide (NaI) and oxalic acid (OA) as the reducing agents [Fisher Scientific, Loughborough, UK]. Briefly, 0.125 g of OA and 0.25 g of NaI were added to 5 mL of the GO suspension with a concentration of 1 mg/mL. The initial mixture was sonicated for 10 min in order to dissolve the OA and NaI. The resulting solution was transferred to a single cavity microwave for 1 min at 90 °C and 130 W. The fibre optic temperature measurement was used to monitor the temperature of the external surface of the monolith in addition to the infrared sensor fitted in the microwave cavity. The resulted black rod of graphene monoliths were thoroughly washed with ethanol and water to remove residual impurities.

2.5.2 Modification of silica based monolith with graphene using microwave heating

The silica monolithic column was filled with a mixture of graphene oxide (GO) suspension [Sigma-Aldrich, Poole, UK] at a concentration of 1 mg/mL, 0.125 g of oxalic acid (OA) and 0.25 g of sodium iodide (NaI) [Fisher Scientific, Loughborough, UK]. The surface functionalization of silica monolith with graphene phase was carried out using single cavity microwave system for 1 min at 90 °C and 130 W. The fibre optic temperature measurement was used to monitor the temperature of the external surface of the monolith [Omega Engineering Limited, Manchester, UK] in addition to the infrared sensor fitted in the microwave cavity. After the surface modification process the monolithic silica

column was thoroughly washed with ethanol and water to remove residual impurities (see Figure 2-9).

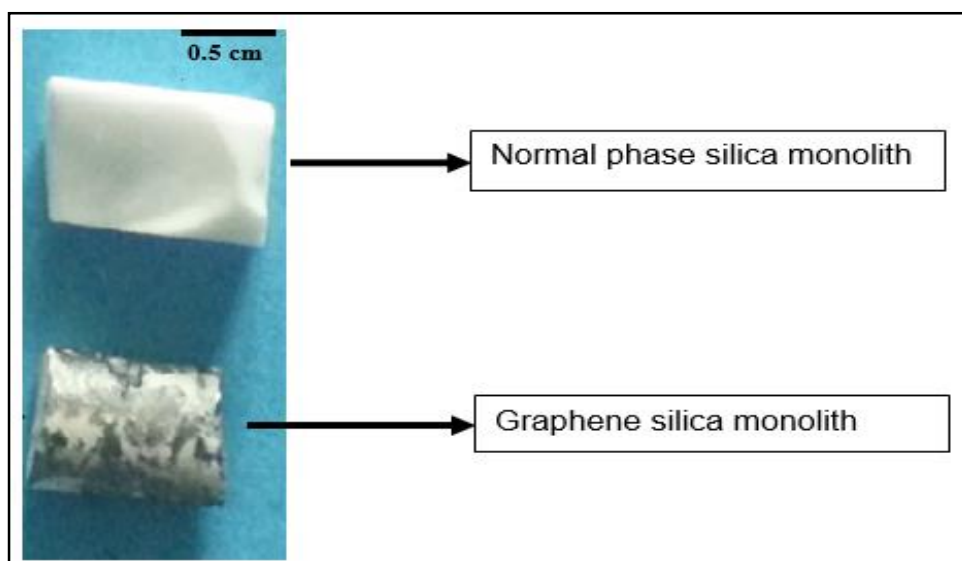


Figure 2-9 Silica based monoliths before and after graphene modification.

The resulting graphene silica monolithic column was ready to use for drugs extraction or surface modification.

2.5.3 Amphetamine extraction

Stock standard solutions of amphetamine were prepared separately by dissolving an accurately weighed amount of compound in purified water to achieve a concentration of 1 mg/mL. The stock solution was stored at 4 °C. Three standard solutions (2, 20, 40 µg/mL) in purified water were prepared by serial dilution from the stock solutions (1 mg/mL). Every week all the standard solutions were freshly prepared and stored at 4 °C. The monolith was used to extract the amphetamine drug. First, the total volume of solution required to fill the column was determined by pumping the solution through the column at constant flow rates (100 µL/min) until the first drop was observed at the exit. All solutions were injected (monolithic volume) using a syringe pump at 50 µL/min. The loading and extraction steps were as follows: first, cleaning and conditioning by methanol (twice) and water (twice) at 100 µL/min; second, loading the standard solution

(monolithic volume) at 50 $\mu\text{L}/\text{min}$; and third, washing the column with water (monolithic volume) at 100 $\mu\text{L}/\text{min}$. This step was repeated three times. Fourth, the elution step was carried out by the mobile phase (10:90 CAN: water with 1 % phosphoric acid pH 4) (monolithic volume) at 50 $\mu\text{L}/\text{min}$. After each step a fraction was collected and injected into the HPLC instrument, which used a C_{18} column and ultraviolet (UV) detection at 210 nm at a flow rate of 1 mL/min.

2.6 *Characterisation of monolithic materials*

2.6.1 SEM analysis

The morphology of silica monoliths were characterised by scanning electron microscopy (SEM) using a Cambridge S360 scanning electron microscope [Cambridge Instruments, Cambridge, UK]. The samples for SEM analysis were coated with a thin layer of gold-platinum (thickness approximately 2 nm) using a SEMPREP 2 Sputter Coater [Nanotech Ltd., Sandy, UK] in order to reduce microscope beam damage, increase thermal conduction, reduce sample charging (increase conduction), improve secondary electron emission and reduce beam penetration with improved edge resolution. The scanning electron micrographs of silica monoliths were obtained using an accelerating voltage of 20 kV and a probe current of 100 pA in high vacuum mode.

2.6.2 BET and BJH analysis

The Brunauer-Emmett-Teller (BET) was used to measure the surface area, pore size and volume within the monoliths using nitrogen adsorption and desorption isotherms at 77 K [Micromeritics Ltd., Dunstable, UK]. The pore volume and pore size distribution within the monoliths were also determined from the isotherms using the BJH (Barrett-Joyner-Halenda) model. As the micron-scale pores were too large to be determined by the

adsorption isotherms, they were estimated by averaging 10 pore diameters measured from the SEM images.

2.6.3 EDX analysis

To determine the significant difference of the chemical composition on the internal surface of the silica-based monolith, before and after modification using Energy dispersive X-ray (EDX), analysis was performed by an INCA 350 EDX system [Oxford Instruments, Abingdon, UK].

3 Fabrication of silica monoliths based on microwave heating

(Chapter 3)

3.1 Introduction

The complexity of biological matrixes are used to test drugs of abuse, make drug abuse screening very difficult without sample preparation.^[204] Despite the development of highly efficient analytical instrumentation for the endpoint determination of analytes in biological samples, sample pre-treatment is still necessary to extract, isolate, matrix modify and concentrate the analytes of interest.^[205] Most analytical instruments have difficulty in detecting sample analytes directly from biological sample when present at low levels, and different methodologies are required for different sample or matrix types.^[205] The interest in using solid phase methodology, based on monolithic structure for analytes' extraction, has grown recently in a number of areas such as environmental, food and biological analyses.^[66] This approach has also contributed to the miniaturization of sample preparation, which can reduce the cost and time required for sample preparation, in addition to improving the efficiency of the extraction. However, the fabrication of silica monoliths does come with some problems, such as cost, limited capacity and fabrication methodology, which can be time consuming and labour intensive. ^[43]

This chapter will focus on the time advantage gained by fabricating silica monoliths using microwave heating compared to conventional oven heating methodology, which takes around 3 days. The work will also investigate the effect of microwave heating on the internal structures of silica monolith including surface area, pore volume and pore size, and compares these to conventionally produce monoliths.

3.2 Experimental

In this work monolithic silica rods were prepared according to the procedures described in sections 2.1.1 and 2.1.2. Two types of heating were used during gel formation: conventional thermal heating and microwave heating. The chemical composition and reaction conditions utilized during silica monoliths' fabrication are shown in Table 3-1 .

Table 3-1 Composition and reaction conditions for the preparation of monolithic silica columns.

Column	Silica 2 mL	Polymer PEO / kDa	Catalyst 4 mL	Method of heating
1	TMOS	PEO 100 (0.282 g)	Acetic acid (0.02 M)	Microwave at 25-70 °C and 10-300 W
2	TMOS	PEO 100 (0.282 g)	Acetic acid (0.02 M)	Oven at 40 °C
3	TMOS	PEO 100 (0.305 g)	Acetic acid (0.02 M)	Microwave at 25-70 °C and 10-300 W
4	TMOS	PEO 100 (0.305 g)	Acetic acid (0.02 M)	Oven at 40 °C
5	TMOS	PEO 200 (0.282 g)	Acetic acid (0.02 M)	Microwave at 25-70 °C and 10-300 W
6	TMOS	PEO 200 (0.282 g)	Acetic acid (0.02 M)	Oven at 40 °C
7	TMOS	PEO 200 (0.305 g)	Acetic acid (0.02 M)	Microwave at 25-70 °C and 10-300 W
8	TMOS	PEO 200 (0.305 g)	Acetic acid (0.02 M)	Oven at 40 °C

After preparation, the resultant silica monolithic rods were cut to a desired length of 1 cm and characterised by SEM analysis for internal structure; energy dispersive X-ray (EDX) analysis to find the elemental composition; and BET and BJH analysis to measure the surface areas, pore volume and pore size.

3.3 Results and discussion

3.3.1 Silica monoliths fabrication using conventional thermal heating

In this work, the silica monolithic rods were prepared by a sol–gel method using conventional thermal heating during the gel formation process according to that procedure reported by Ping He.^[72] The rods produced were found to be white and crack-free, as can be seen in Figure 3-1. Shrinkage of the monolithic structure during the gelation process enabled the silica rods to be released easily from the mould. The rods were then treated with an aqueous ammonia solution (1 M) at 90 °C for 24 h to produce the mesoporous structure of the silica monoliths.

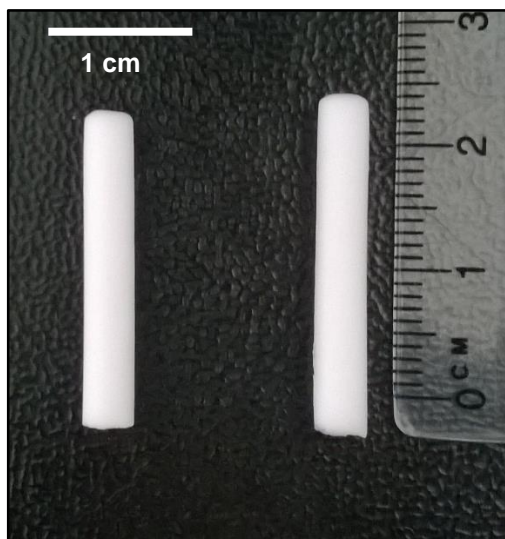


Figure 3-1 Photograph of white and crack-free silica monolithic rods using thermal heating for preparation.

In order to identify the effect of each step of the sol gel process on the internal structure of the silica monoliths, scanning electron micrographs were obtained (see Figure 3-2).

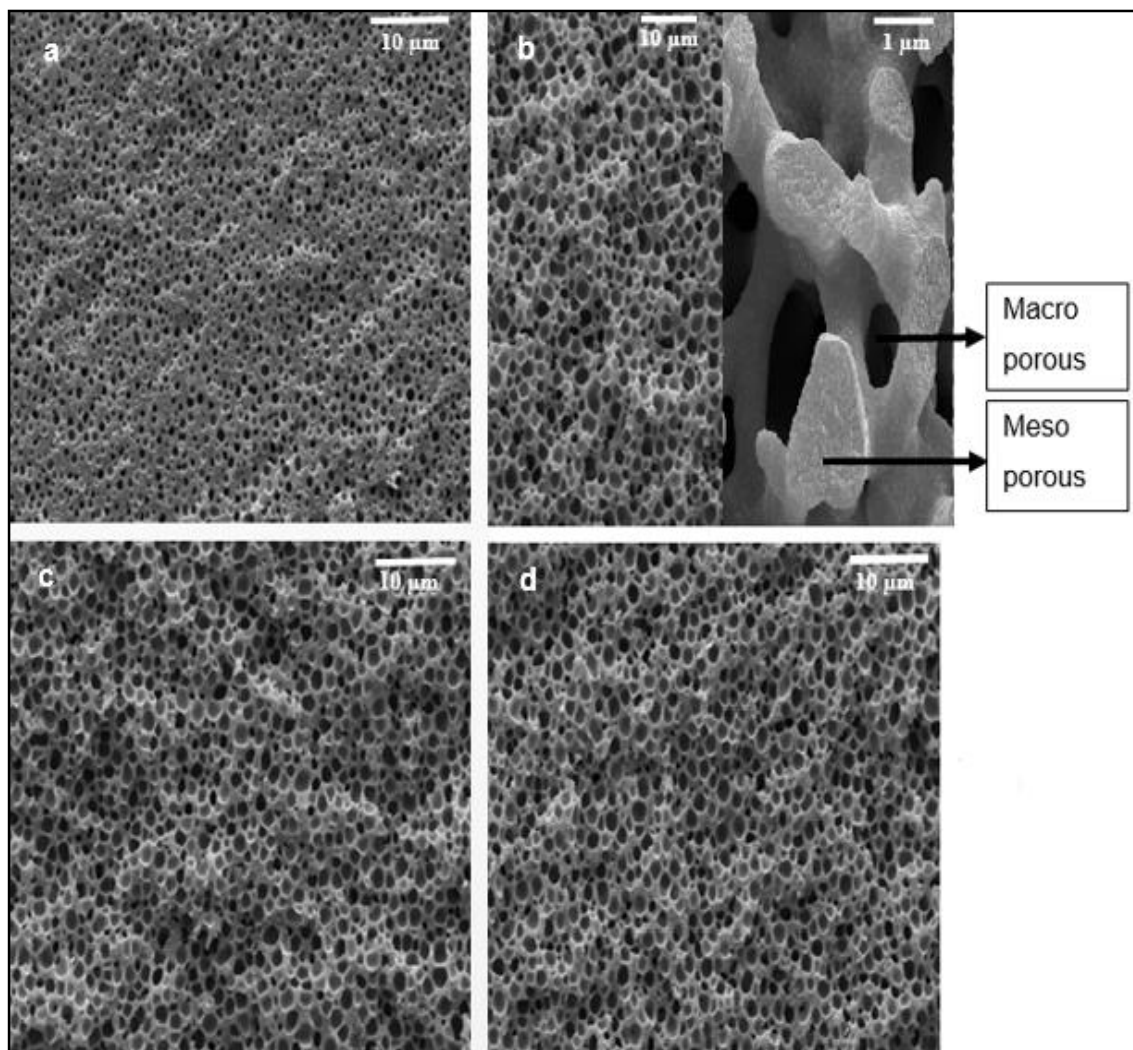


Figure 3-2 Photographs for silica monolith consist of TMOS + PEO + 1 M nitric acid (a) before 1 M NH_4OH treatment (b) after 1 M NH_4OH treatment (c) after 1 M NH_4OH treatment but before calcination (d) after 1 M NH_4OH treatment and calcination.

The images show that all silica monoliths contain co-continuous porous morphology (shown in Figure 3-2), macro-porous structure created by the presence of PEO (see Figure 3-2 a), and meso-porous structure produced after basic treatment (see Figure 3-2 b). In addition, it can be observed from Figure 3-2 (c) and (d) that there were no significant differences on the internal structure of the silica monolith before and after calcination step.

3.3.2 Silica monolith fabrication using microwave heating

The gelation process in the sol-gel method is time consuming (3 days). Therefore, to reduce the time of gel formation, microwave heating was used during gelation process and an evaluation of the monolith morphology carried out. The mode and degree of heating applied during the gel formation process plays a very important role in the formation of the silica gel, because of their influence on the evolution of the hierarchical pore size regimes. Due to flexibility of the sol-gel network, the silanol groups can react with unreacted Si-OR groups or with other adjacent silanol groups during the condensation process. Decreasing the gelation temperature in the sol-gel method resulted in a delay in the phase separation. However, at temperatures above 70 °C the phase separation and sol-gel transition are carried out together.^[90]

In the initial work the fabrication of silica monolith using microwave heating during gel formation was carried out according to the earlier procedure reported by *Neves*,^[206] where the starting mixture included silicon alkoxide (TMOS), acid catalyst and polymer. The power of the microwave was 300 W and the temperature was between 180 °C and 260 °C for 10 minutes. A typical chemical composition used for the preparation of silica based monolith is shown in Table 3-2.

Table 3-2 Chemical composition for preparation silica monolithic columns using microwave heating.

Monolith	Microwave Power	PEO 100 kDa	TMOS	1M nitric acid	Temperature	Time
	/W	/g	/mL	/mL	/°C	/min
1	300	0.305	4	2	180-260	10



Figure 3-3 Photograph of silica monolith prepared from TMOS + 1 M nitric acid + PEO using microwave heating at 180-260 °C for 10 min and 300 W.

The photograph in Figure 3-3 shows a tiny fraction of silica monolith produced from the initial experiments. The rather poor result is probably due to using microwave heating at very high temperatures (180-260 °C) and high power (300 W) during the gelation step, which created a weak cross-linked silica network resulting in a substantial deformation and shrinkage of the monolithic structure. For this reason, the next experiment was carried out at a reduced microwave power of 150 W and the heating temperature was at 100 °C for 10 min, in order to control the sol-gel formation and create a uniform macro porous network structure (see Figure 3-4).

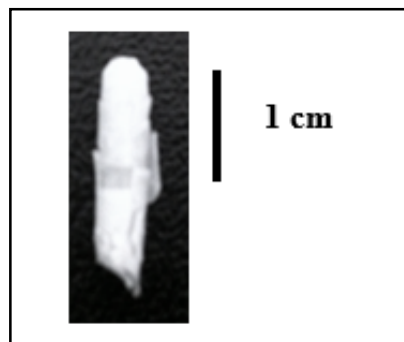


Figure 3-4 Photograph of silica monolith prepared from TMOS + 1 M nitric acid + PEO using microwave heating at 100 °C for 10 min and 150 W.

This figure indicates that decreasing the temperature and power of the single mode cavity microwave produced a rod shaped silica monolith, but to improve the morphological structure of the silica monolith it was decided to increase the time of gelation to 30 min and decrease the heating power to 50 W, to see if that would assist the formation of the silica monolith structure.

Nakanishi et al.^[91] reported that the silica monolith morphology is strongly dependent on the time interval between the on-set of phase separation and the sol-gel transition. If the gelation and phase separation of the silica monolith are in contact with each other a fine macro porous network will be produced. This phenomenon is a possible reason for the silica monoliths produced in this work.



Figure 3-5 Photograph of silica monolith prepared from TMOS + 1 M nitric acid + PEO using microwave heating at 40 °C for 30 min and 50 W.

It was found that reducing the power of the microwave resulted in a decrease in heating temperature (40 °C), which formed a transparent silica monolith due to a high water content (see Figure 3-5).

In general, the effective dielectric loss (ϵ''_{eff}) for most materials is elevated by increasing the temperature over room temperature. However, once the material reaches T_c (critical temperature), either through microwave absorption or through an external source, the heating rate increases significantly. If the microwave power applied to the material continues after T_c , then ϵ''_{eff} increases very rapidly.

To solve this problem we decided to use a gradient microwave heating profile (1 min at 10 W then 1 min at 20 W then 1 min at 40 W then 1 min at 80 W then 1 min at 160 W). The heating profile was started from very low power to gradually enhance the hydrolysis and polycondensation reactions, and reached the maximum heating temperature of 75 °C in the last min where phase separation and sol-gel transition was carried out together.



Figure 3-6 Photograph of silica monolith prepared from TMOS + 1M nitric acid + PEO using microwave heating with this condition 1 min at 10 W then 1 min at 20 W then 1 min at 40 W then 1 min at 80 W then 1 min at 160 W.

Disappointingly, this method produced an irregular monolithic rod; however, the monolithic rod was dry and white (see Figure 3-6). A possible explanation could be incompatible hydrolysis and polycondensation reactions during the process of gel formation due to the high concentration of acidic catalyst in the starter mixture. Since the interaction of microwave radiation with a molecule depends on its molecular polarizability, 0.02M acetic acid was suggested to use as the catalyst in the starter mixture which, N-O bonds is not nearly as polar as O-H bonds.



Figure 3-7 Photograph of silica monolith prepared from TMOS + 0.02 M acetic acid + PEO using microwave heating with this condition 1 min at 10 W then 1 min at 20 W then 1 min at 40 W then 1 min at 80 W then 1 min at 160 W.

It was found that a decrease in the concentration of the acid catalyst, and using gradient heating profile (microwave conditions 1 min at 10 W then 1 min at 20 W then 1 min at 40 W then 1 min at 80 W then 1 min at 160 W then 1 min at 300 W), produced a white uniform silica monolithic rod, as can be seen in Figure 3-7. Thus, by using a gradient

microwave heating process, with an appropriate starter mixture, a suitable silica monolithic structure with low content of water could be successfully produced.

SEM analysis was used to evaluate the internal structure of silica monolith obtained by microwave heating.

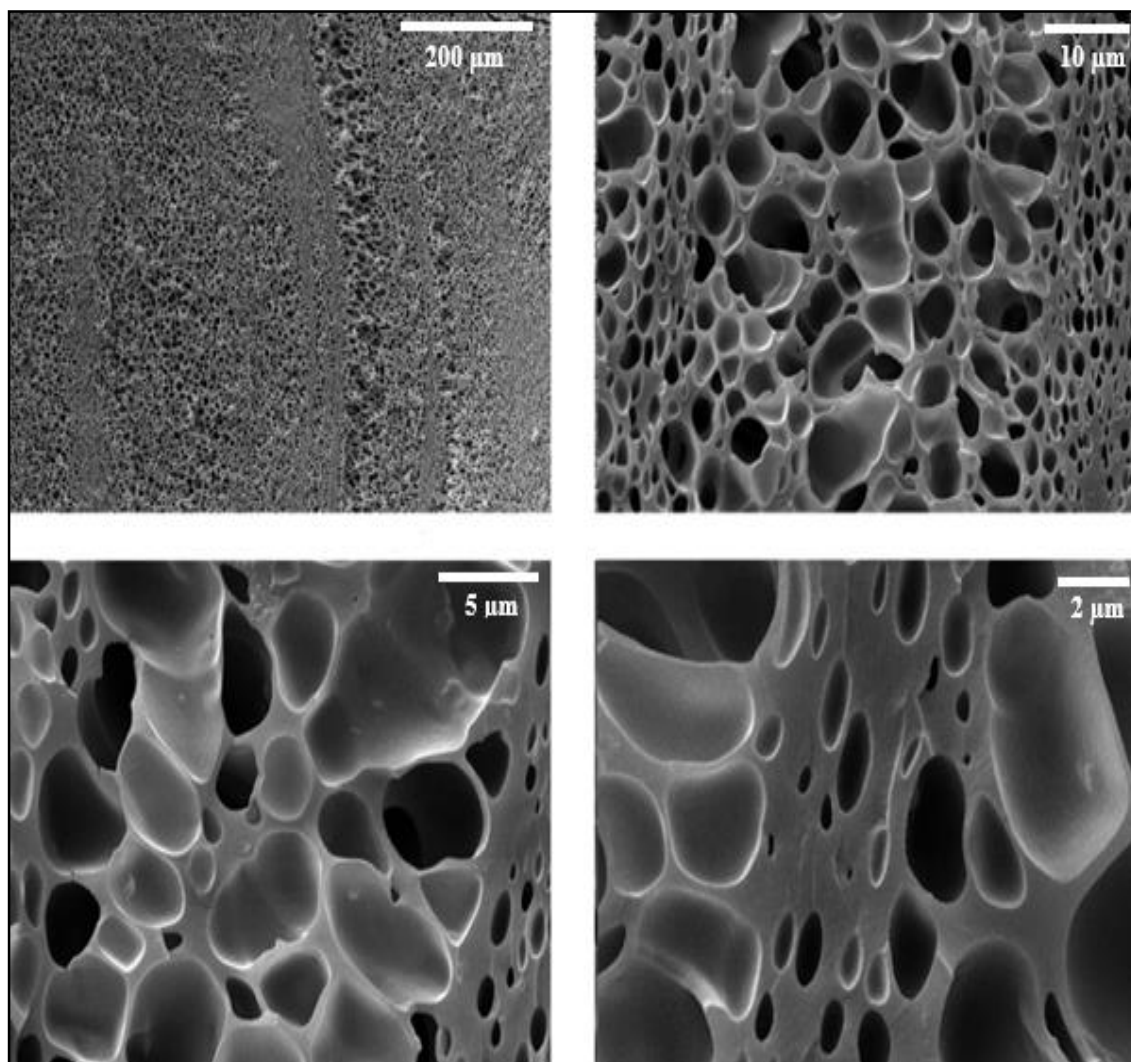


Figure 3-8 Scanning electron micrographs for silica monolith prepared from TMOS + 0.02 M acetic acid + PEO using microwave heating at this condition 1 min at 10 W then 1 min at 20 W then 1 min at 40 W then 1 min at 80 W then 1 min at 160 W.

The resulting monolithic rod contains co-continuous porous morphology. However, the sizes of the macro-porous structures varied and were randomly distributed within the silica monolith (see Figure 3-8). The most likely reason could be unequal distribution of the microwave heating within the silica monolithic rod or an inadequate time of microwave heating during gel formation process. In order to find a suitable procedure for producing silica monolithic rods with a uniform bimodal pore structure, the effect of

heating time, when using the microwave during gel formation step, was investigated. The time of gradient microwave heating during the gelation process was increased to 11 min (2 min at 10 W then 2 min at 20 W then 2 min at 40 W then 2min at 80 W then 2 min at 160 W then 1 min at 300 W).

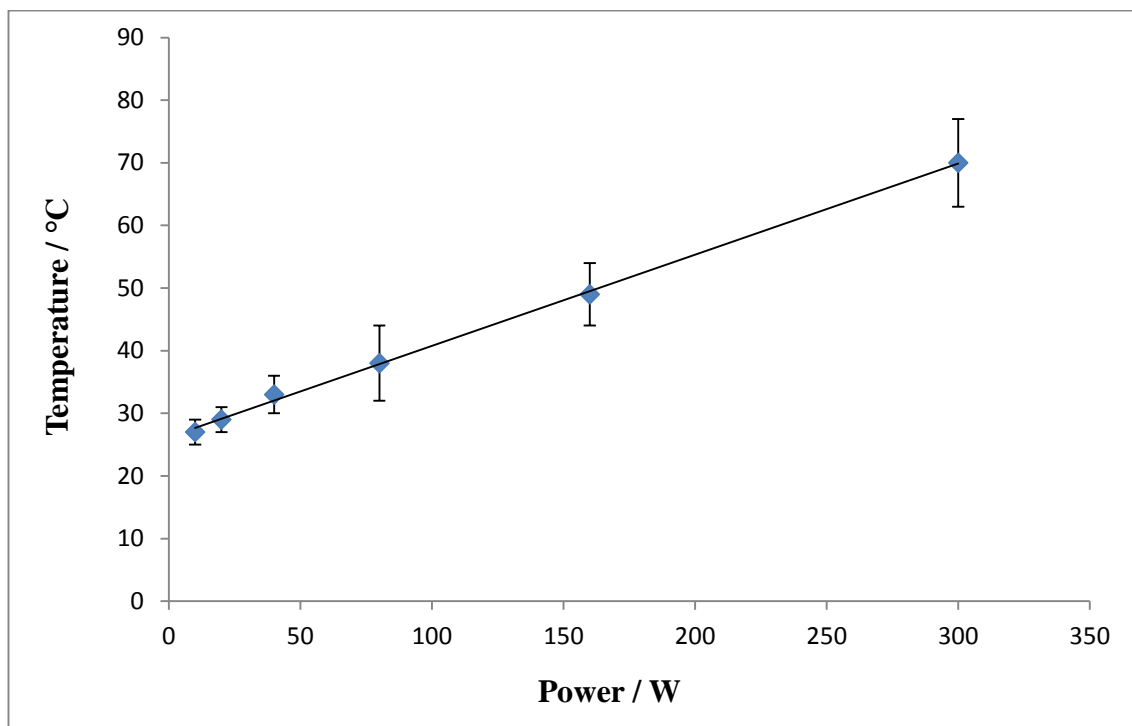


Figure 3-9 The relation between applied power (W) by single cavity microwave and temperature (°C) of the external surface of the silica monolith measured using the fibre optic temperature sensor. The error bars represent the standard deviation of 5 repeat experiments.

The Figure 3-9 indicates that the temperature of silica structure was rapidly increased by increasing the power of the microwave. The chemical composition and conditions were applied to fabricate the silica monolith are listed in Table 3-3.

Table 3-3 Chemical composition and conditions for silica monolith fabrication using microwave heating.

Heating method	PEO 100K /g	TMOS /mL	Acetic acid 0.02M /mL	Temperature ^a /°C	Time ^b /min
MW	0.282	2	4	25-70	11

MW for microwave.

^a Temperature for gel formation.

^b Time for gel formation



Figure 3-10 Photograph of (TMOS + PEO + 0.02 M acetic acid) monolith obtained using microwave heating at this condition 2 min at 10 W then 2 min at 20 W then 2 min at 40 W then 2min at 80 W then 2 min at 160 W then 1 min at 300 W.

The resultant silica monolithic rod was found to be white and crack-free as can be seen in Figure 3-10. Evaluation of the internal structure of formed silica monolith was carried out using SEM analysis (see Figure 3-11).

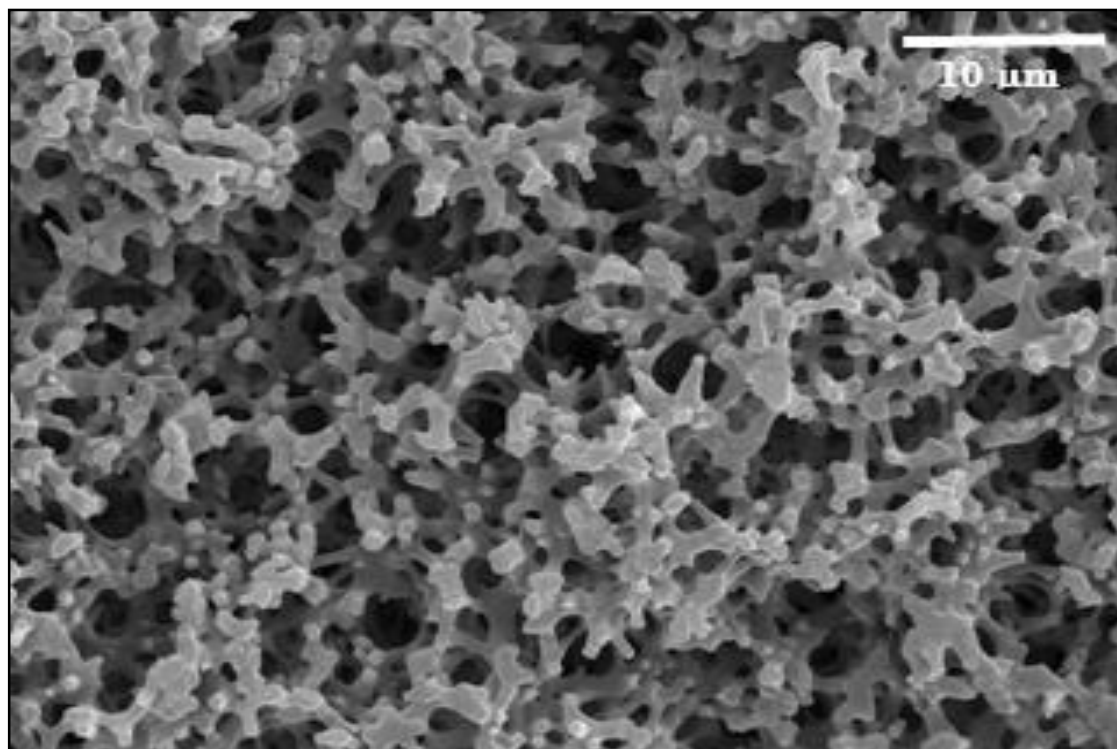


Figure 3-11 Scanning electron micrographs for silica monolith prepared from TMOS + 0.02 M acetic acid + PEO using microwave heating at this condition 2 min at 10 W then 2 min at 20 W then 2 min at 40 W then 2min at 80 W then 2 min at 160 W then 1 min at 300 W.

The result shows that increasing the time of gradient microwave heating from 5 min to 11 min produced a silica monolithic with improved bimodal pore structure distributed over the silica monolith with uniform size. A possible reason could be the increased time of gradient microwave heating offered sufficient time for two major reactions in the sol-gel method to occur in sequence: hydrolysis and polycondensation. Moreover, using the gradient mode for microwave heating enhanced the time interval between the on-set of phase separation and the sol-gel transition, and caused the skeleton growing behaviour to be more efficient.

A schematic comparing the fabrications of silica based monoliths using microwave heating and conventional heating methodology (oven) during gel formation process is shown in Figure 3-12.

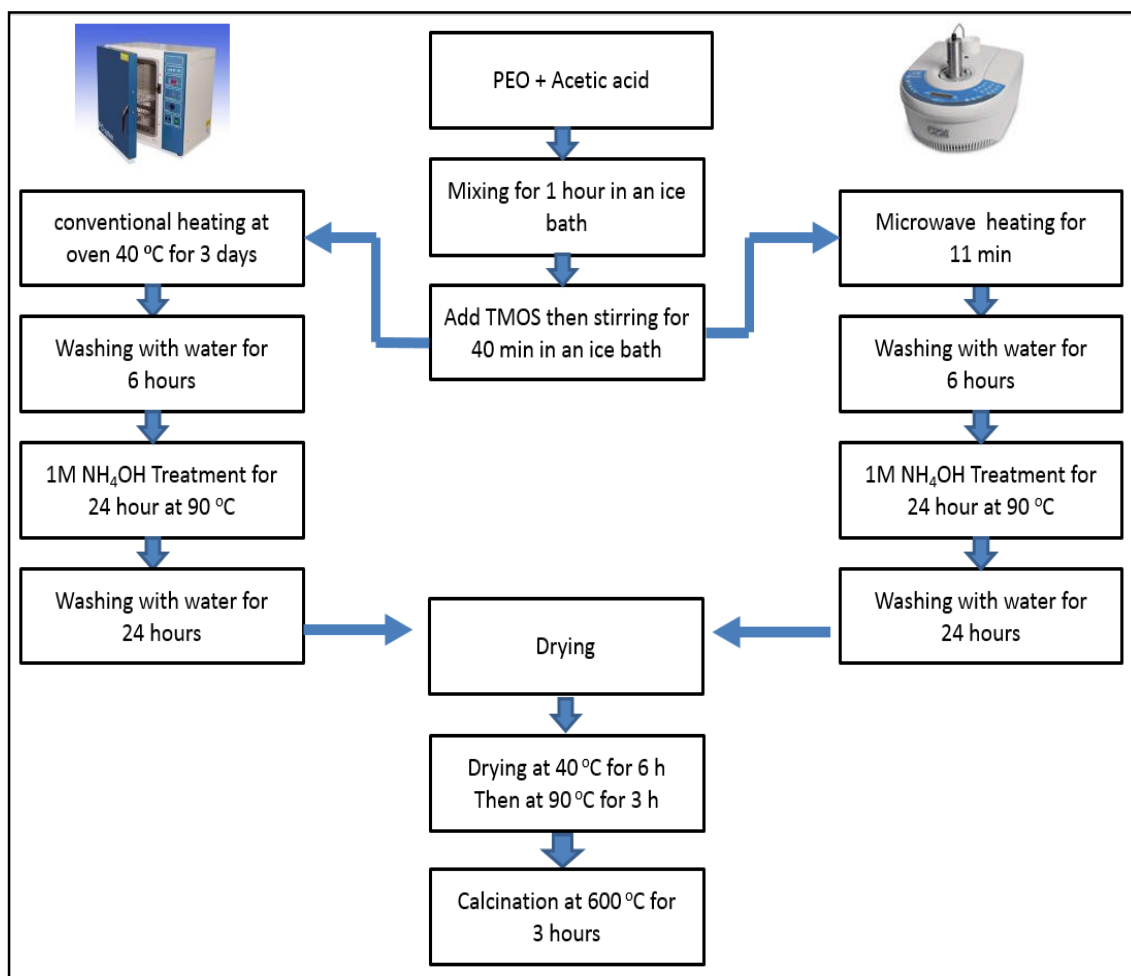


Figure 3-12 Methods for silica monolith preparation based on microwave heating and conventional thermal heating.

3.3.3 Effects of the concentration and molecular weight of polymer in the internal structure of the silica monoliths

Since the composition of the starter mixture has a great effect on the physical and chemical properties of the silica monolith (e.g. morphology, permeability and selectivity), the influence of the amount of polymer on the internal structure of the silica monolith was investigated. A number of silica monoliths were prepared in this study based on TMOS, acetic acid and PEO. The concentration and molecular weight of PEO were varied. The compositions of the initial solutions using microwave and conventional oven heating methods during gel formation processes are listed in Table 3-1.

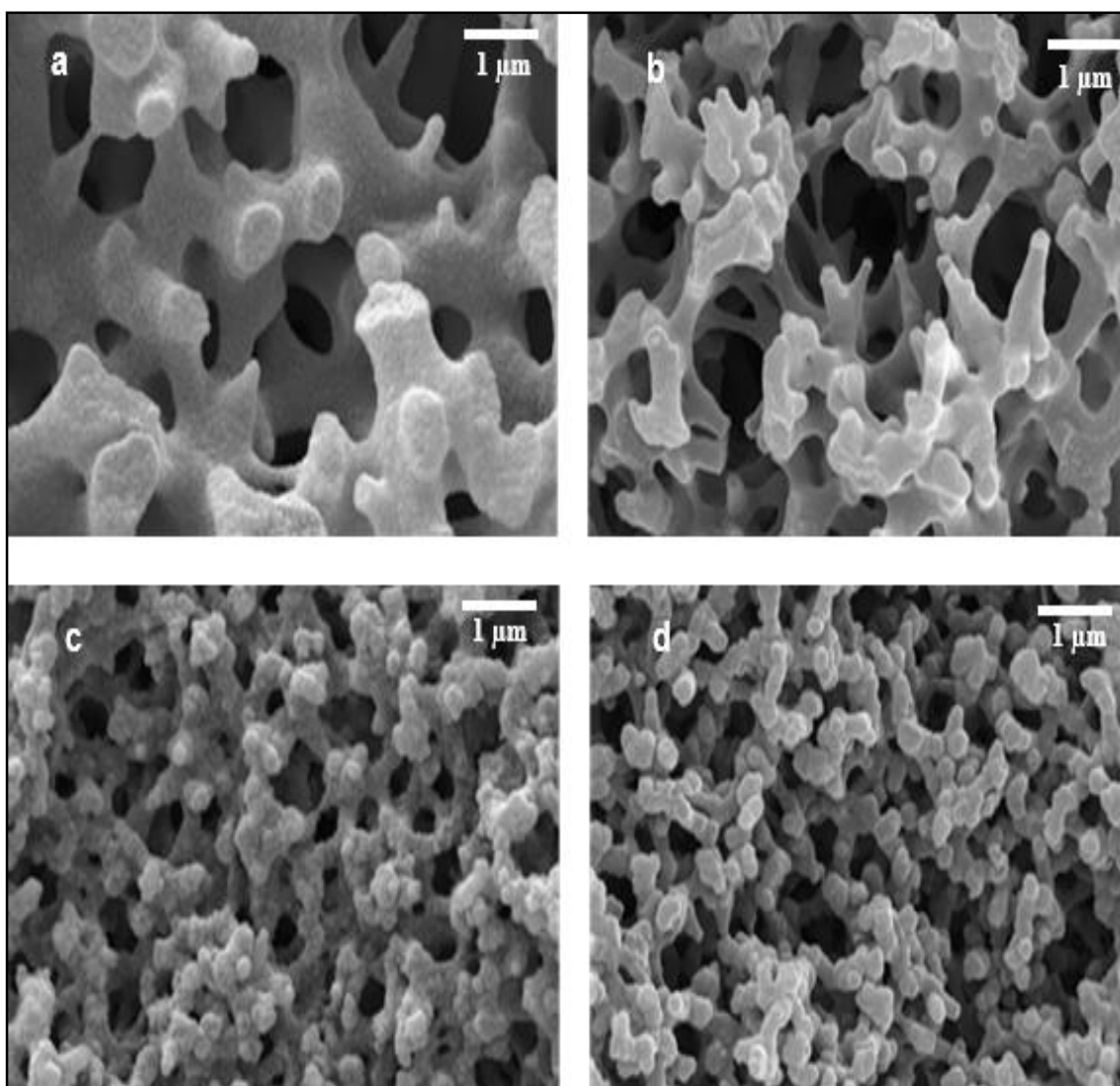


Figure 3-13 Scanning electron micrographs of silica monoliths prepared from tetramethoxysilane, (0.02 M) acetic acid and polyethylene oxide PEO 0.282 g (a) MW heated, (b) oven heated; or 0.305g PEO (c) MW heated, (d) oven heated.

Scanning electron micrographs of the silica monoliths produced using the same composition but different heating modes during gel formation, indicated that a similar uniform channel structure distributed homogeneously throughout the bulk phase (see Figure 3-13), and that bimodal pore structure was found in both of them (see Figure 3-14). However, the microwave method offered a significant reduction in the time required for gel formation (11 min), compared to the conventional oven heating methodology (3 days).

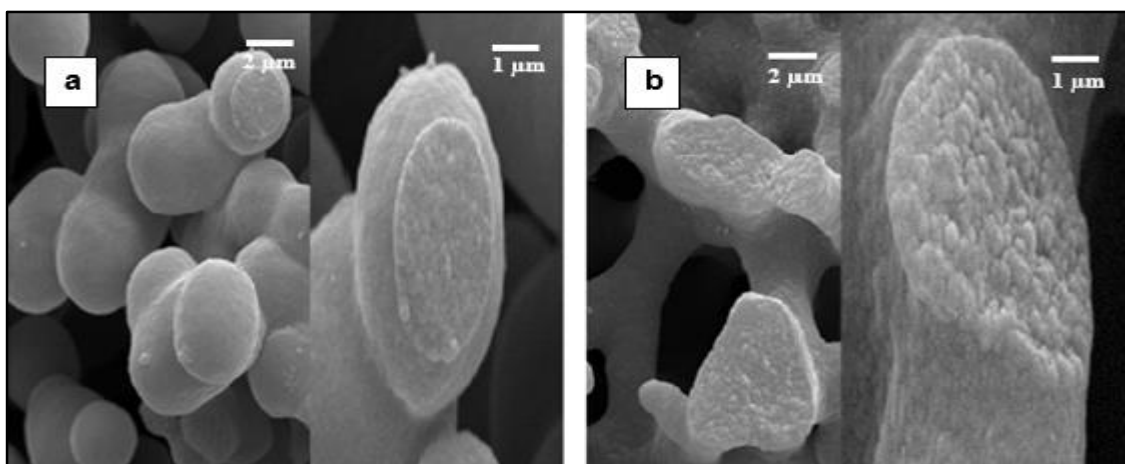


Figure 3-14 Scanning electron micrographs of silica monoliths prepared from tetramethoxysilane, 0.02 M acetic acid and polyethylene oxide PEO 0.282 g (a) MW heated and (b) oven heated.

The effect of microwave heating on the sol-gel reactions was observed from the formation of condense network structure (see Figure 3-14 a). The physical properties include surface areas, pore volume and pore size of silica monolithic rods, measured using BET and BJH analysis (see Table 3-4).

Table 3-4 Physical properties of silica monoliths 1-8 using microwave heating and oven heating methodology during gel formation process.

Column	Heating method	Surface area /m ² g ⁻¹	Diffusion pore size /nm	Diffusion pore volume /cm ³ g ⁻¹	Flow-through pore diameter /μm
1	MW	333	13.4	1	1.3
2	Oven	513	7.4	0.98	.89
3	MW	440	10.3	1.4	1
4	Oven	470	7.9	0.92	.97
5	MW	521	9.1	1.2	1.1
6	Oven	460	8.5	0.99	1.5
7	MW	574	9	1.3	0.8
8	Oven	479	7.9	0.99	0.96

MW for microwave

Table 3-4 shows the data obtained from the silica monoliths prepared using the same chemical composition but different heating methods during gel formation process. In earlier work, *Motokawa et al.*^[95] prepared silica monolithic columns with various sizes of skeletons and through-pore structures. The silica monoliths with smaller through-pore size and thinner skeleton structure offered higher surface area, lower back pressure and greater efficiency. From the results it can be observed that the monolithic column obtained from the microwave heating procedure gave an average pore volume of between 1 and 1.4 cm³/g and a surface area between 333 and 574 m²/g, compared to silica monoliths obtained using oven heating method during gel formation process, where the average pore volume was between 0.92 and 0.99 cm³/g and the surface area between 460 and 513 m²/g (see Table 3-4). The reduction of through-pore size and skeleton size was increased by increasing the amount of PEO in the starter mixture. This observation indicated that the monoliths produced using microwave heating do not appear to be significantly different from similar monoliths, with the same chemical composition, produced by conventional

oven based heating. However, the microwave method makes a significant reduction in the time required for gel formation.

3.3.4 Comparison between the weights of silica monoliths obtained by microwave heating and similar monoliths obtained by thermal heating

In this experiment the weights of silica monoliths using microwave heating and similar monoliths using thermal heating were measured by analytical balance (Ray-Ran Test Equipment Ltd. UK).

Table 3-5 Composition and weights of monolithic silica columns 1-8 using microwave heating and oven heating methodology during gel formation process.

Col.	Method of heating	PEO /g	PEO /kDa	TMOS /mL	Acetic acid 0.02M /mL	Length /cm	Weight after calcination /g
1	MW	0.282	100	2	4	1	0.0265
2	Oven	0.282	100	2	4	1	0.0275
3	MW	0.305	100	2	4	1	0.0280
4	Oven	0.305	100	2	4	1	0.0278
5	MW	0.282	200	2	4	1	0.0255
6	Oven	0.282	200	2	4	1	0.0280
7	MW	0.305	200	2	4	1	0.0275
8	Oven	0.305	200	2	4	1	0.0280

MW for microwave

Interestingly, the silica monoliths prepared with microwave heating were found to have a similar mass compared to the same monoliths obtained by conventional thermal heating (see Table 3-5). This indicates that the weights of the silica monoliths were not significantly affected when microwave heating and thermal heating was used during the gel formation process.

3.3.5 Effect of use F127 on the internal structures of silica monolith

In this experiment the effect of using F127 instead of PEO on the internal structures of the silica monoliths using microwave heating or conventional thermal heating during gel formation process was investigated.

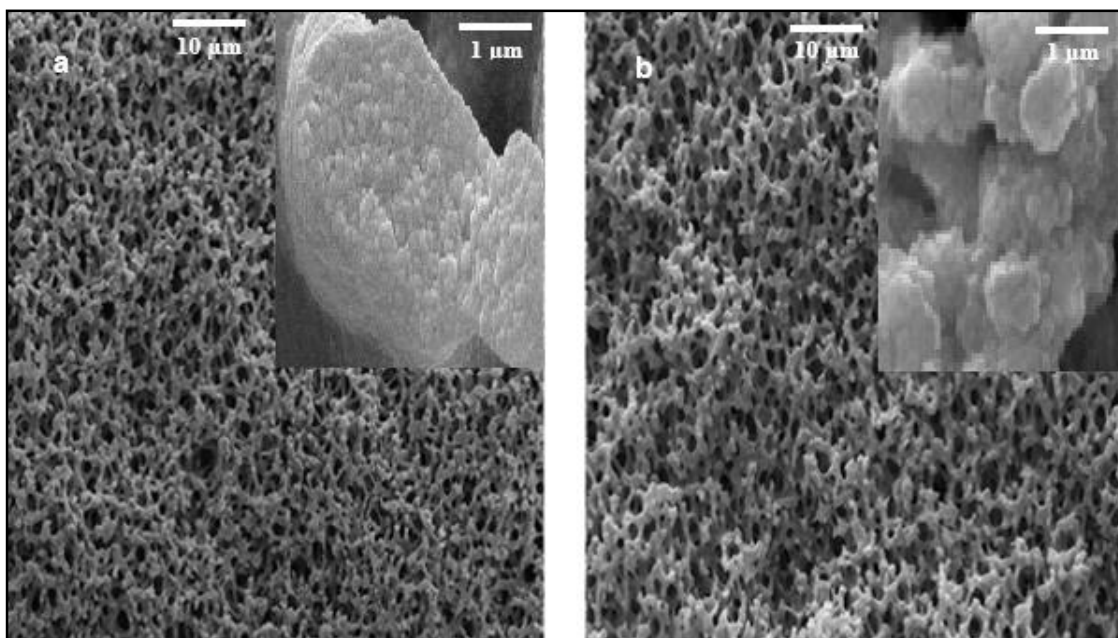


Figure 3-15 Scanning electron micrographs of silica monoliths prepared from tetramethoxysilane, (0.02 M) acetic acid and F127 (a) oven heated and (b) MW heated.

Scanning electron micrographs of the silica monoliths (see Figure 3-15) confirmed that microwave heating procedure can form a wide range of the silica monoliths including bimodal pore structure that can allow for extraction large and small molecules at same time.

Table 3-6 Physical properties of monoliths 9 and 10 using microwave heating and oven heating methodology during gel formation process.

Col.	Method of heating	Surface area / m ² g ⁻¹	Diffusion pore size /nm	Diffusion pore volume /cm ³ g ⁻¹	Flow-through pore diameter /μm
9	MW	326	10.8	0.86	1.4
10	Oven	387	10	0.96	1.3

Table 3-6 shows that using thermal heating with F127 silica monolith created a slightly larger surface area compared to the similar monolith produced using microwave heating. Furthermore, there are no significant differences in the rest of comparative physical properties.

3.4 Summary

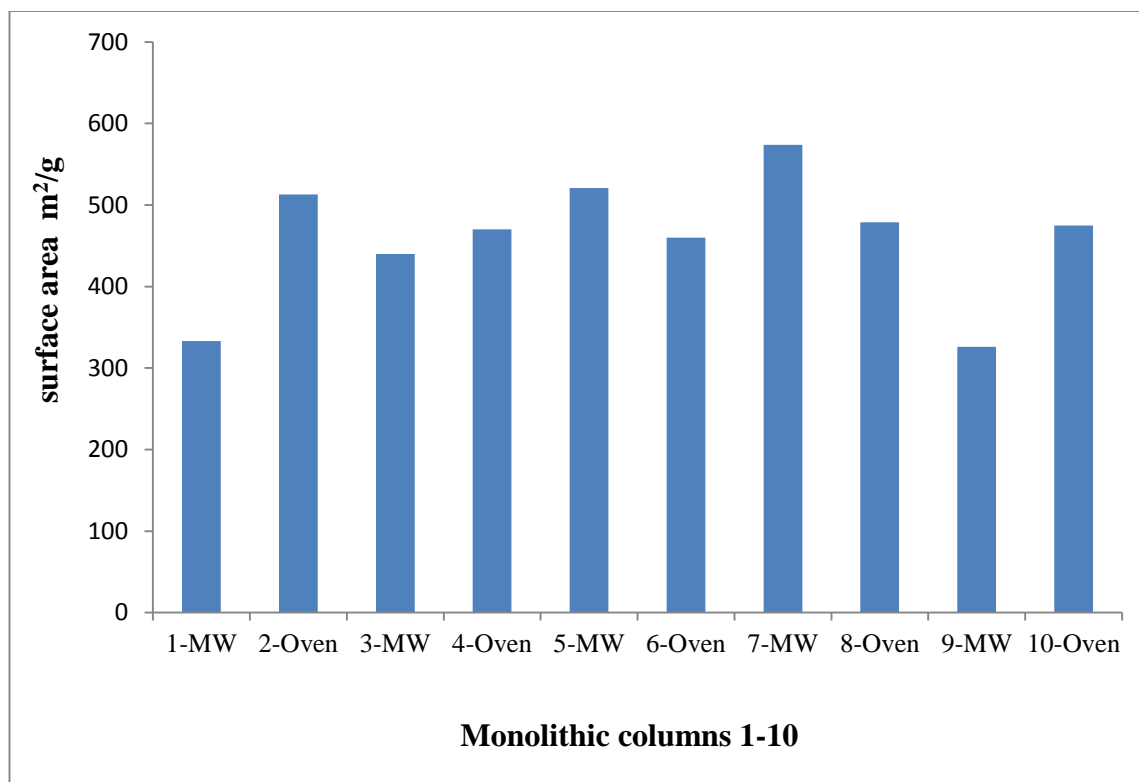


Figure 3-16 Surface areas of monolithic silica columns 1-10 using microwave heating and oven heating methodology during gel formation process.

The use of microwave heating during the gel formation process has been found to not only reduce the gelation time but also improve the physical characteristics of the silica monolith (such as surface area). A range of microwave heating methods were investigated for their potential to form silica monoliths.

The choice of chemical composition is important since it has a significant effect on the internal structure of the silica monolith. The initial successes using a gradient microwave heating during the gel formation process showed a significant variation in the size of macro-porous structure. Under optimised conditions, the use of a microwave based

method can significantly reduce the gelation time to 11 min, with ideal morphological features, compared to the gelation step using the thermal heated oven methodology 4,320 min. Monoliths produced with PEO 200K by microwave heating showed higher surface area than oven heated monoliths. The highest surface area was found on the silica monolith prepared using microwave heating and a chemical composition including TMOS (2 mL), 0.02 M acetic acid (4 mL) and 0.305 g of PEO (200K MW). Extending this approach into the surface functionalization of silica monolith will be the subject of ongoing research.

4 Modification of silica based monoliths with C₁₈ phase using microwave heating

(Chapter 4)

4.1 Introduction

The current methodology for screening drugs of abuse in biological samples involves several extraction techniques such as solid-phase extraction (SPE) and liquid–liquid extraction (LLE). The method of solid-phase extraction (SPE) can be combined with high performance liquid chromatography (HPLC) to be suitable for extracting and detecting a wide range of drugs and their metabolites.^[23]

The distinctive properties of highly porous silica monolith make it an ideal base material for drug extraction. The hydroxyl groups on the silica surface allow for different functional groups to be bonded and increase its selectivity.^[44]

C₁₈ silica monolith is the most common column used for drug extraction.^[220] To make the sorbent hydrophobic the surface of the silica based monolith can be chemically modified with a long alkyl chain. The hydrophobicity of silica monoliths can be increased by lengthening the alkyl chain and, as a result, the hydrophobic interaction will be increased between the sorbent and selected compound.^[93]

There are three different methods for C₁₈ modification. The first one is known as the brush form, which is obtained by a reaction of the silanol groups on the silica surface with monochlorodimethyloctadecylsilane and produces monomeric ligands chemically attached to the silica monolithic surface. The second form is called oligomer, which is obtained by reacting dichloromethyloctadecylsilane with each silanol site of silica surface. The last form is a bulk form where the trichlorooctadecylsilane reacts with a silica surface and produces a three dimensional polymer surface structure. Synthesis of oligomer and bulk form is difficult and expensive.^[23]

It was decided to use the brush form in this project, due to its easy fabrication and the high extraction efficiency it offers. However, the conventional method for C₁₈ surface modification using thermal heating takes a very long time: 9 h according to the

procedures described in the previous literature. ^[66] Therefore, this work attempts to enhance the modification reaction by using an appropriate heating method, such as microwave, to complete the modification process within a shorter period, and to improve the efficiency of the modified surface.

4.2 Experiment

The silica monolithic column was fabricated and modified with C₁₈ phase according to the procedures described in sections 2.1.2 and 2.2.2, respectively. The chemical composition and reaction conditions that produced the highest surface area in the previous work (chapter 3 - column 7) were initially selected for the functionalization work. Using a very high temperature 330 °C during sealing process can decompose the C₁₈ stationary phase as shown in Figure 4-1. Therefore, the modification of the silica monolith with octadecyl groups needs to be carried out after sealing.

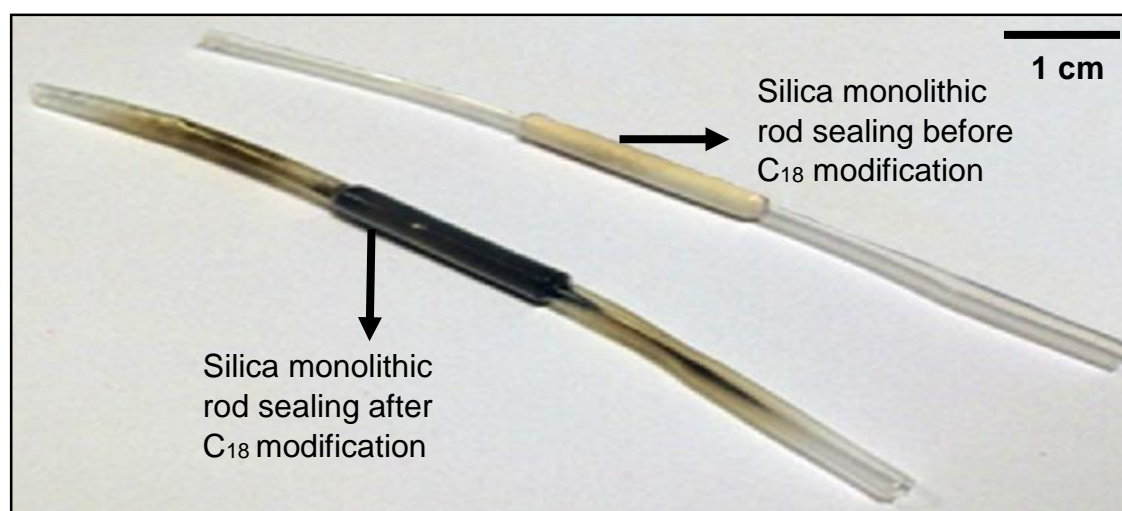


Figure 4-1 Effect of using high temperature (330 °C for 2 hours) during sealing process on the appearance of the octadecylated silica monolithic columns.

4.2.1 C₁₈ phase modification

The mechanism of modification reaction of C₁₈ phase with silica monolithic surface is shown in Figure 4-2.

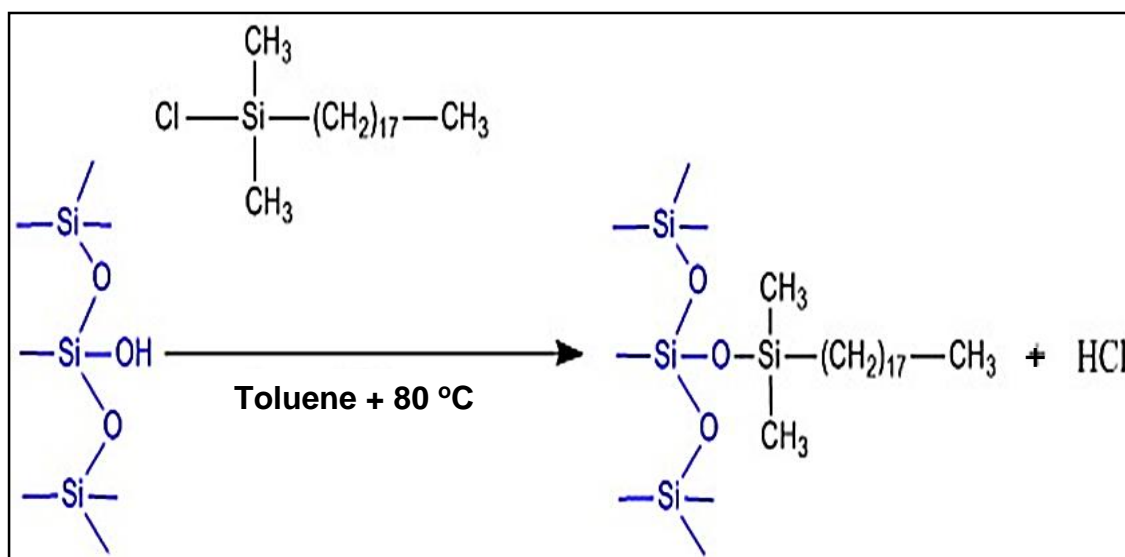


Figure 4-2 Shows the reaction of the silanol groups of the monolithic silica surface with octadecyl groups in the chlorodimethyloctadecylsilane solution. [66]

A typical weight and reaction conditions that were utilized for modification of silica surface with C₁₈ phase are shown in Table 4-1.

Table 4-1 Chemical composition and reaction conditions for C₁₈ phase modification

Method of heating	ODS /g	Toluene /mL	Flow rate / μ L/min	Temperature / $^{\circ}$ C	Time /min
Thermal	1	10	20	80	540
Microwave	1	1.2 = 1g	Just fill the column	80	40

After C₁₈ modification process the monolithic silica column was thoroughly washed with toluene, THF, MeOH / H₂O 50/50 (V/V), MeOH and H₂O in sequence at a flow rate 100 μ L/min for 15 min.

4.3 Results and discussion

Initially, the C₁₈ surface modification of silica monoliths was carried out using conventional thermal heating methodology. The elemental characterization of normal

phase silica monolith and modified silica monolith with C₁₈ phase were obtained using energy dispersive X-ray (EDX) analysis (shown in Figure 4-3 and Figure 4-4).

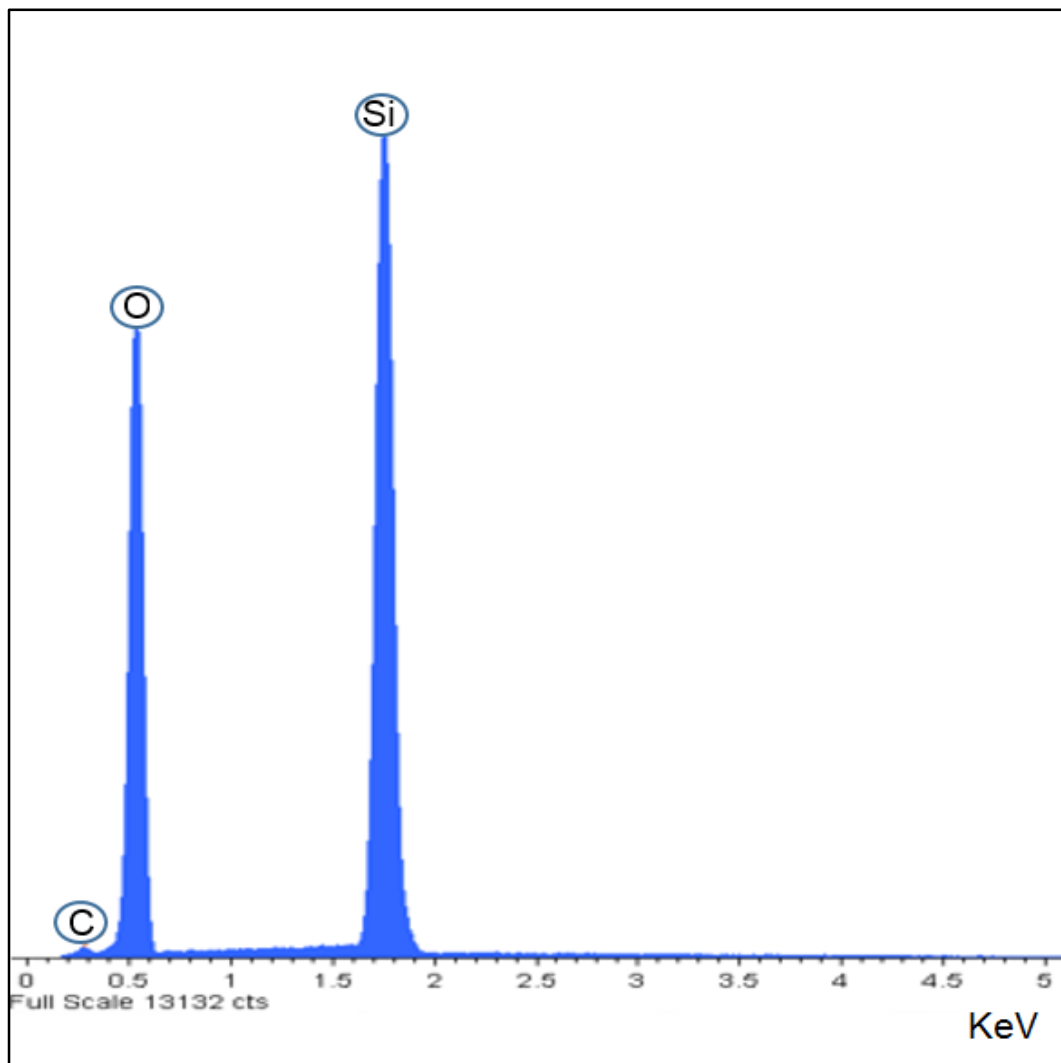


Figure 4-3 EDX spectra of non-modified silica-based monolith.

Table 4-2 Quantitative EDX analysis for all elements in non-modified silica-based monolith using quantitative EDX analysis.

Spectrum	C	O	Si	Total
sample 1	1.93	46.69	51.38	100.00

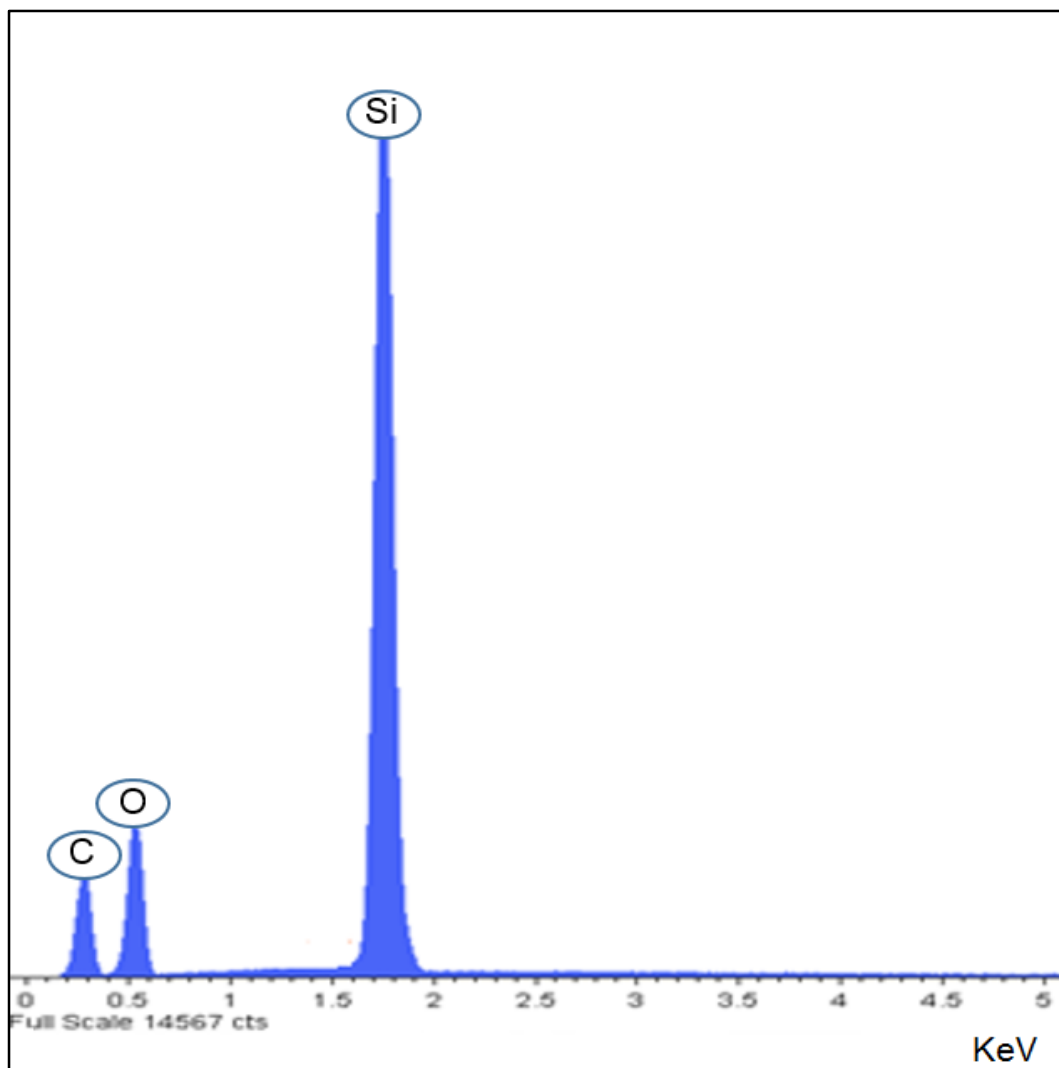


Figure 4-4 EDX spectra of silica-based monolith modified with C₁₈ phase using thermal heating method.

Table 4-3 Quantitative EDX analysis for all elements in silica-based monolith modified with C₁₈ phase using thermal heating method.

Spectrum		C	O	Al	Si	Total
sample 2		40.3	32.3	0.1	27.3	100.0

The EDX spectra indicates that the carbon (C) peak on the silica surface after C₁₈ surface modification increases significantly compared to the normal phase of silica-based monolith.

4.3.1 Optimisations of silica monoliths modification with C₁₈ phase

When developing this procedure, speed of analysis was the main issue. For this reason, a range of reaction times were carried out to see if a reduction could be achieved whilst maintaining the increased attachment of the octadecyl groups. In order to modify the surface of silica monoliths as quickly as possible, the effect of time of microwave heating on the C₁₈ surface modification process was investigated. EDX analysis of silica monolithic columns before and after C₁₈ surface modification was also obtained.

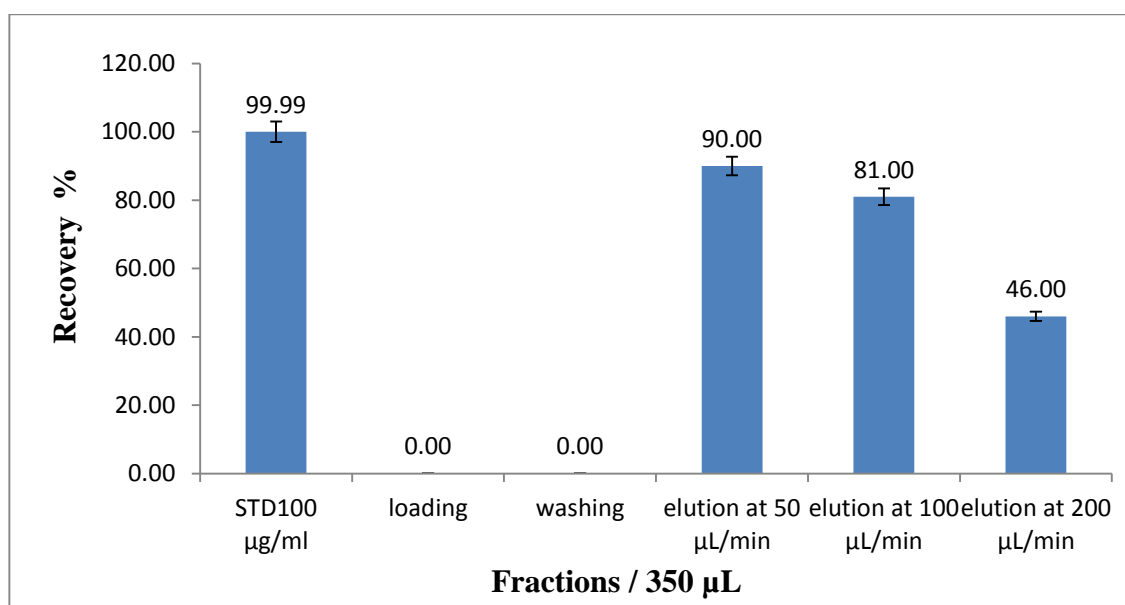


Figure 4-5 Chart of percentages of extracted caffeine (100 µg/mL) at three different flow rates 50, 100 and 200 µL/min using C₁₈ silica monolithic column prepared using conventional thermal heating. The error bars represent the standard deviation of 3 repeat experiments.

To find the best flow rates can be used during the extraction of caffeine. Three samples of caffeine standard (350 µL) 100 µg/mL were extracted at three different flow rates 50, 100 and 200 µL/min using C₁₈ silica monolithic column prepared using conventional thermal heating. From the results it was observed that increasing the flow rate during extraction from 50 µL/min up to 200 µL/min resulted in a decrease in caffeine yield. The greatest average of caffeine extracted by C₁₈ silica column prepared using the conventional heating method was found 90 % at a flow rate of 50 µL/min. The recoveries

of caffeine at flow rates 100 and 200 $\mu\text{L}/\text{min}$ decreased to approximately 81 % and 46 %, respectively (see Figure 4-5).

4.3.2 Calibration curve

The calibration curve was carried out using reference standard solutions of caffeine with a range of concentrations: 10, 50, 100, 200, 300 and 400 $\mu\text{g}/\text{mL}$. All standard solutions were analysed directly in triplicate by HPLC-UV and the peak areas were plotted against concentration. Good linearity was observed for the calibration curve, which was used to quantify the fraction during extraction experiments (see Figure 4-6).

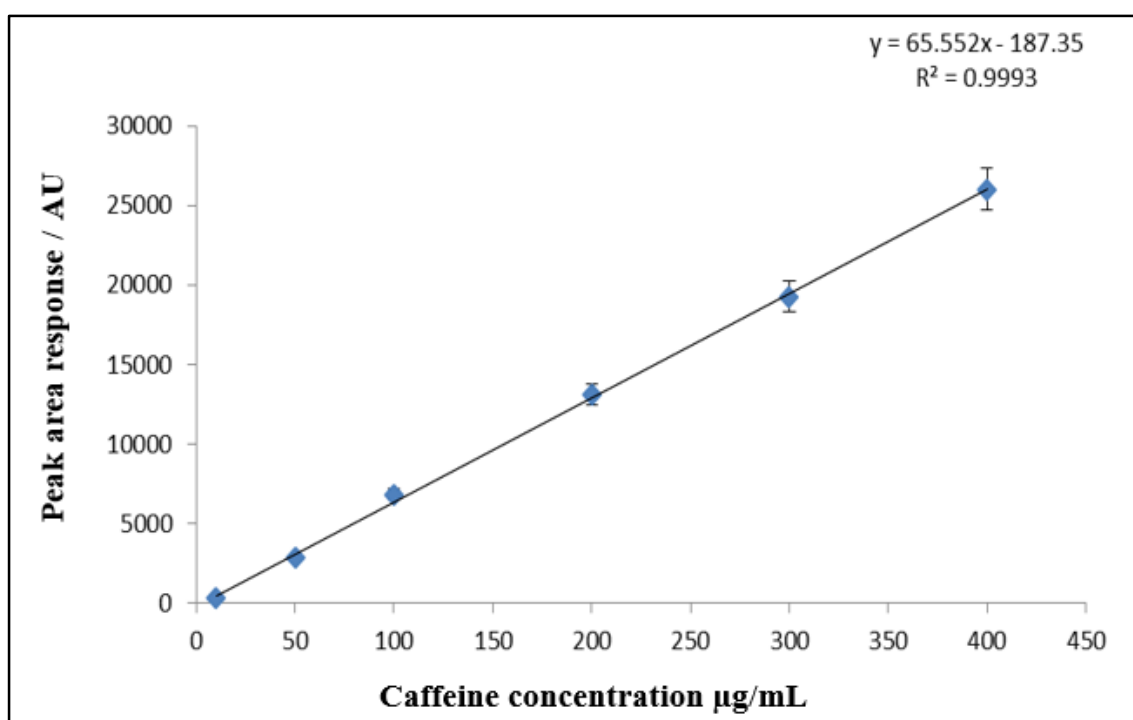


Figure 4-6 Calibration curve for caffeine was obtained using a wide range of concentrations: 10, 50, 100, 200, 300 and 400 $\mu\text{g}/\text{mL}$ in order to check the ability of column to extract low and high concentration sample. The error bars represent the standard deviation of 3 repeat experiments.

Caffeine is known to absorb UV light in the wavelength range of 205-273 nm.^[207] In this work, the signal intensities of the standard sample of caffeine (100 $\mu\text{g}/\text{mL}$) were investigated at three different wavelengths: 205, 245, and 273 nm according to the procedure in section 2.3.3. Figure 4-7 shows the absorbance of caffeine using three different UV wavelengths. The strongest maximum absorbance for caffeine was found at

205 nm, whereas the highest of the peaks significantly reduced at 273 and 245 nm.

Therefore, the detection of caffeine was done at 205 nm.

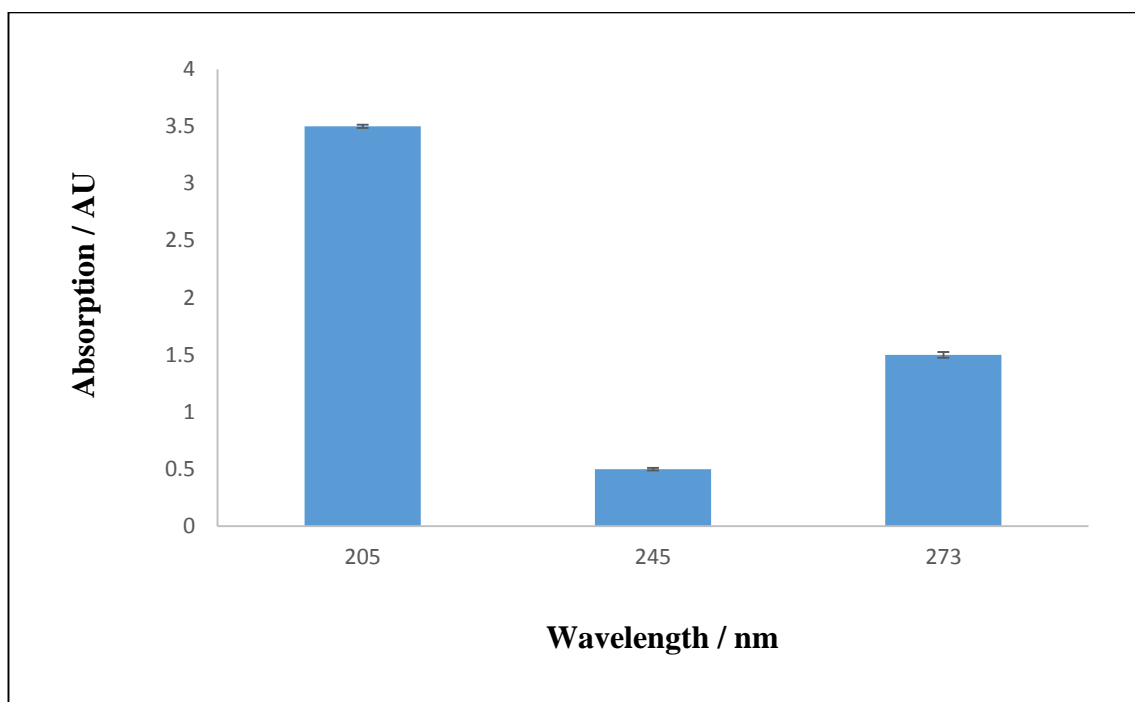


Figure 4-7 UV absorbance wavelength for caffeine standard (100 µg/mL). The error bars represent the standard deviation of 3 repeat analyses.

The retention time of caffeine standard that was injected directly into the HPLC-UV system was 2.02 min. No interfering or impurity peaks were observed around the peak of analyte (see Figure 4-8).

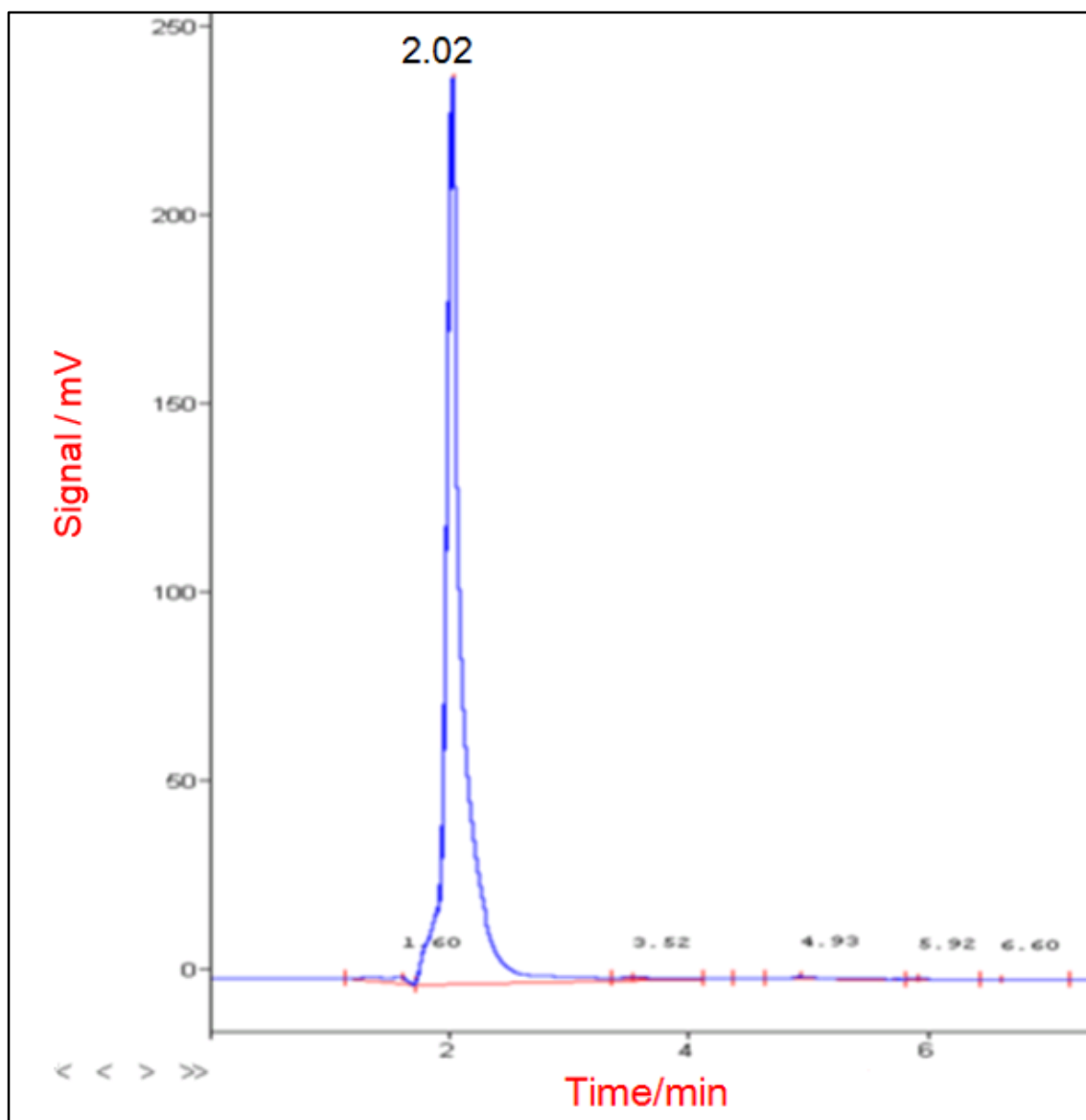


Figure 4-8 The UV chromatograms of caffeine standard (100 $\mu\text{g/mL}$). Experimental conditions: the mobile phase was methanol / 0.01 acetic acid (30:70) (V/V) run under isocratic conditions at flow rate 1 mL/min and the detection wavelength was adjusted to 205 nm, injection volume was 20 μL . The separation column was Symmetry C₁₈, 4.6 mm \times 250 mm packed with silica particles size 5 μm . All experiments were performed at ambient temperature around 25 $^{\circ}\text{C}$.

According to the literature, the most useful temperature for modifying a silica surface with a C₁₈ phase is 80 $^{\circ}\text{C}$.^[208] To find the best temperature for microwave heating during C₁₈ surface modification, three degrees of heating were used (see Table 4-4).

Table 4-4 Quantitative EDX analysis for all elements in three silica-monolithic columns modified with C₁₈ phase using microwave heating at 80 °C, 100 °C and 110 °C for 10 min.

TMOS monolith modified with C ₁₈ phase using microwave heating	C	O	Si	Cl	Total
At 80 °C for 10 min	10.5	42.1	47.3	0.1	100.0
At 100 °C for 10 min	9.6	42	48.3	0.1	100.0
At 110 °C for 10 min	8	44.1	47.8	0.1	100.0

Based on all previous results it was found that the best UV wavelength for detection of extracted caffeine was 205 nm, and the optimum temperature of microwave heating for C₁₈ surface modification was 80 °C.

The general procedure for caffeine (100 µg/mL) extraction was as follows:

Table 4-5 sequence of extraction procedure of caffeine standard using the C₁₈ silica monolithic column.

Step	Procedure	Amount /µL	Flow rate /µL/min	Time /min
Conditioning	Inject THF, MeOH/ H ₂ O 50/50 (V/V), MeOH and H ₂ O in sequence.	300 from each solution or reagent (volume of the monolithic column was 300 µL)	100	12
Load sample	Inject standard of caffeine dissolved in a purified water (100 µg/mL).	300	50	6
Washing	Inject purified water	900	100	9
Elution	Inject MeOH/ H ₂ O and collect the eluent into the Eppendorf tube (1 mL).	300	50	6

In the initial work the temperature of microwave heating during C₁₈ surface modification was adjusted to 80 °C at 120 W for 10 min, and detection of caffeine was done at 205 nm.

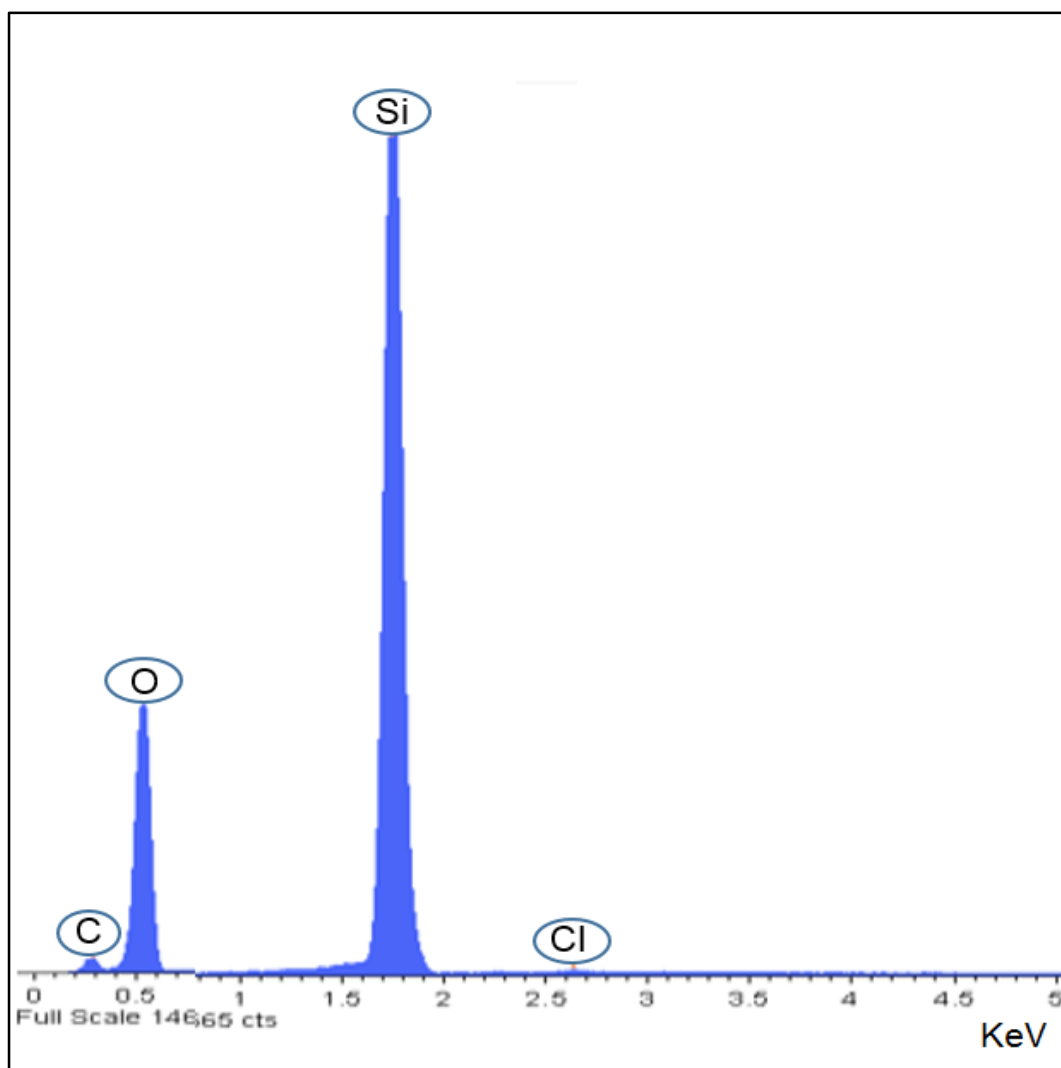


Figure 4-9 EDX spectra of silica-based monolith modified with C₁₈ phase using microwave heating for 10 min at 80 °C and 120 W.

Table 4-6 Quantitative EDX analysis for all elements in silica-based monolith modified with C₁₈ phase using microwave heating for 10 min at 80 °C and 120 W.

Spectrum		C	O	Si	Cl	Total
sample 3		10.5	42.1	47.3	0.1	100.0

The EDX result shows that new peaks for carbon (C) and chlorine (Cl) were observed on the modified silica surface due to the chemical composition of the modification reagent

(chlorodimethyl octadecyl silane) (shown in Figure 4-9 and Table 4-6). In this case the recovery of caffeine (100 µg/mL) was found to be only 55 %.

To overcome this issue of low binding, it was decided to increase the time of C₁₈ modification reaction to investigate if increasing the time of reaction would help the C₁₈ phase to cover more surface binding sites and increase the area of adsorption.

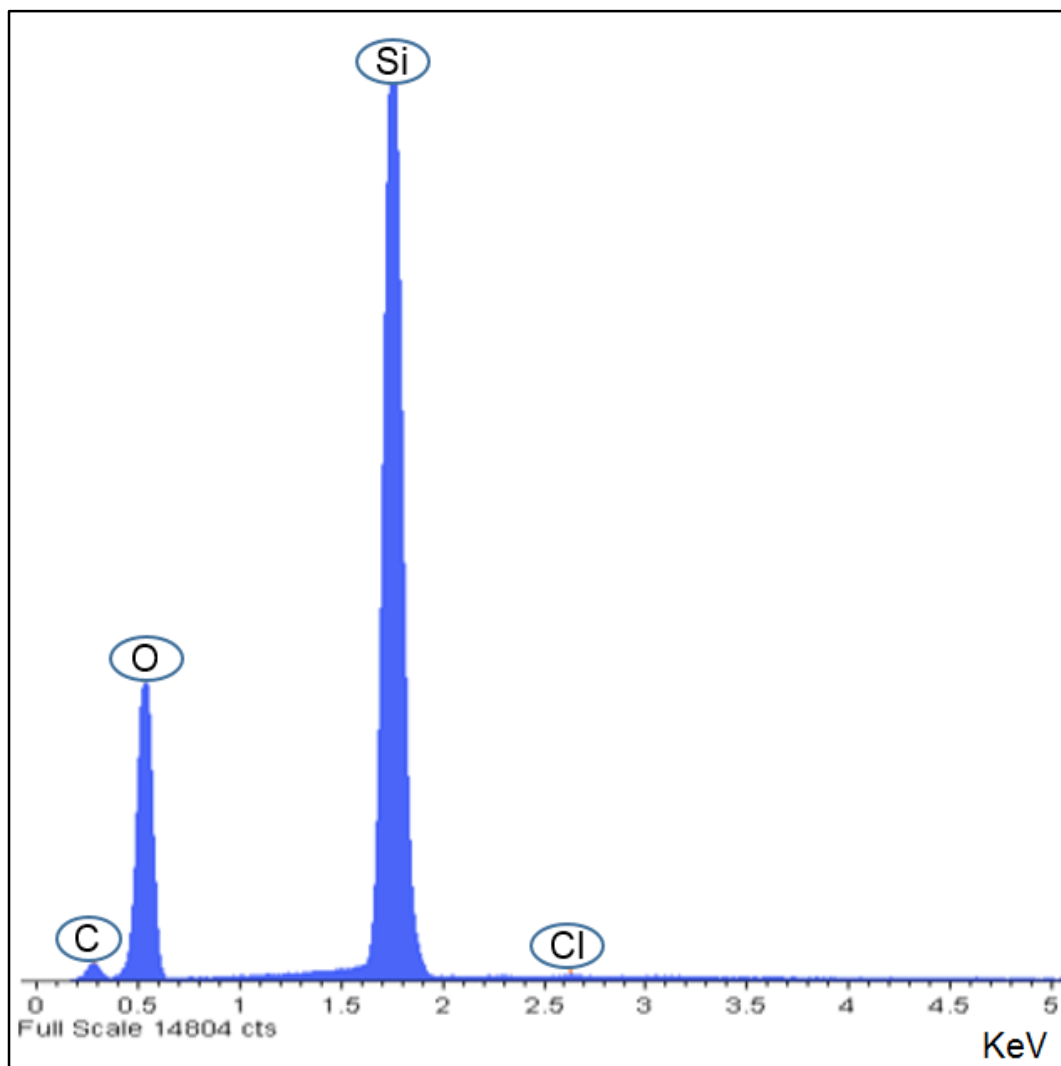


Figure 4-10 EDX spectra of silica-based monolith modified with C₁₈ phase using microwave heating for 20 min at 80 °C and 120 W.

Table 4-7 Quantitative EDX analysis for all elements in silica-based monolith modified with C₁₈ phase using microwave heating for 20 min at 80 °C and at 120 W.

Spectrum		C	O	Si	Cl	Total
sample 4		11.2	51.4	37.3	0.1	100.0

Increasing the time of microwave heating from 10 min to 20 min at 80 °C and 120 W, during the modification binding step, resulted in an increase in the recovery of caffeine from a standard sample (100 µg/mL) to 65 %. In addition, the peak of carbon (C) on the silica surface was found to be slightly larger (shown in Figure 4-10 and Table 4-7).

In order to improve the interaction further between the C₁₈ phase and internal surface of the silica monolith the time of modification was increased again to 30 min at 80 °C and at 120 W.

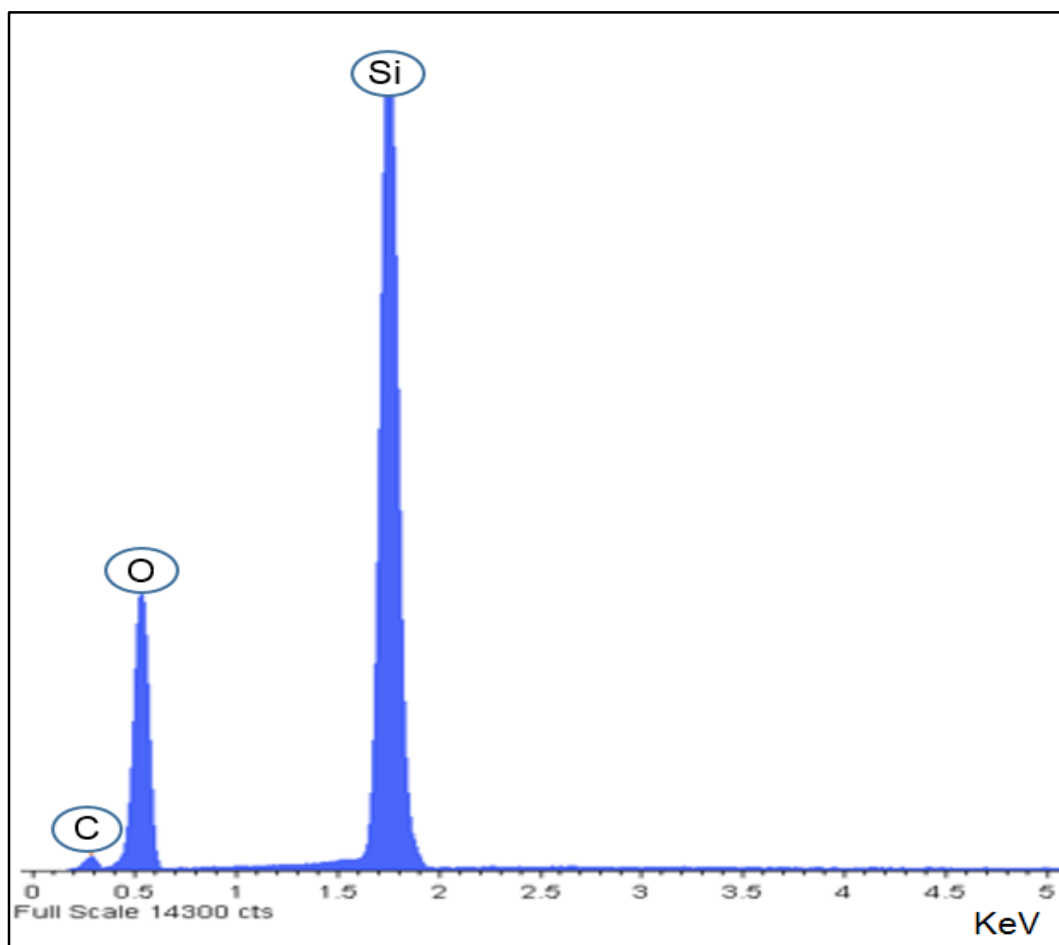


Figure 4-11 EDX spectra of silica-based monolith modified with C₁₈ phase using microwave heating at 80 °C and 120 W for 30 min.

Table 4-8 Quantitative EDX analysis for all elements in silica-based monolith modified with C₁₈ phase using microwave heating for 30 min at 80 °C and 120 W.

Spectrum		C	O	Si	Total
sample 5		11.9	50.0	38.1	100.0

The extraction efficiency of caffeine using this condition was found to be 73 % and the amount of carbon (C) on the surface of silica monolith was also slightly increased (shown in Figure 4-11 and Table 4-8).

Finally, increasing the time of C₁₈ surface modification, based on microwave heating up to 40 min at 80 °C and 120 W, hugely increased the peak associated with surface carbon (C) and enabled more binding of C₁₈ phase to the surface of the silica monolith (shown in Figure 4-12 and Table 4-9).

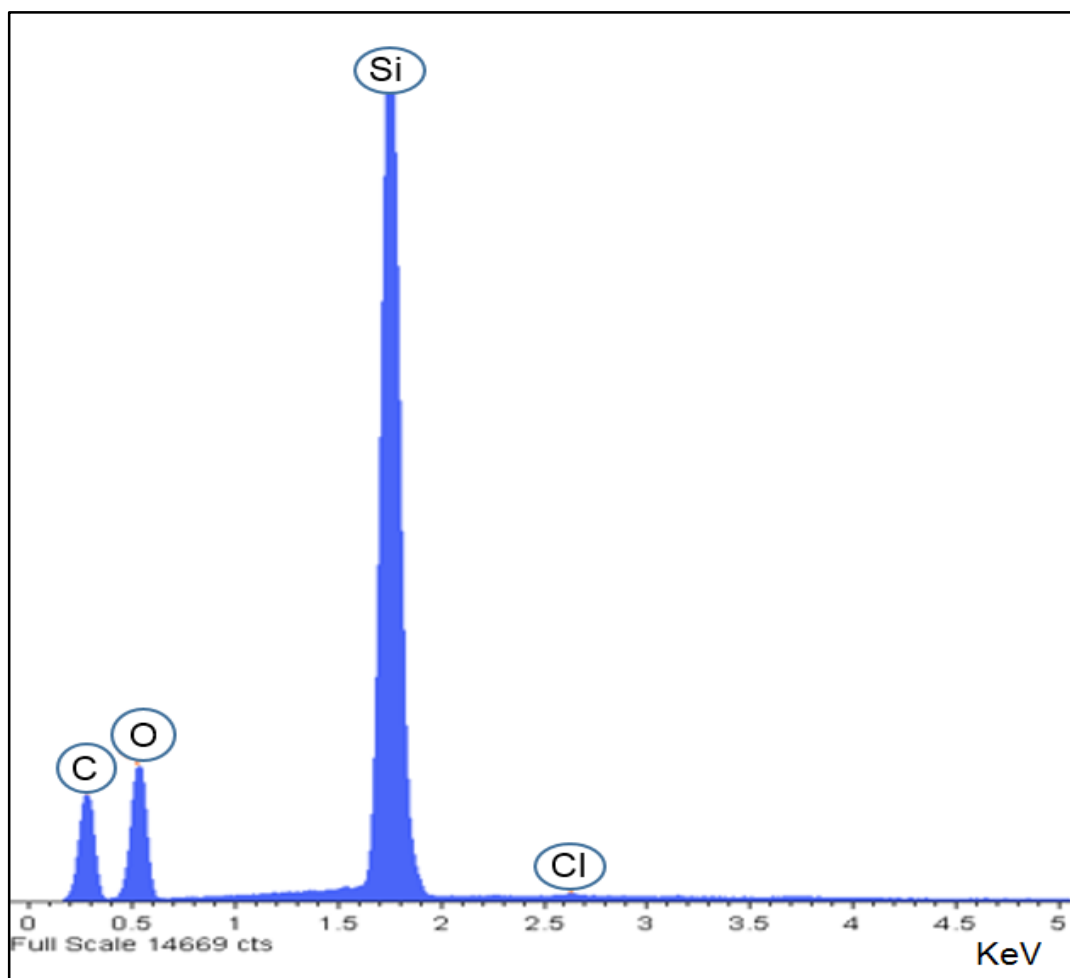


Figure 4-12 EDX spectra of silica-based monolith modified with C₁₈ phase using microwave heating at 80 °C for 40 min and 120 W.

Table 4-9 Quantitative EDX analysis for all elements in silica-based monolith modified with C₁₈ phase using microwave heating for 40 min at 80 °C and 120 W.

Spectrum		C	O	Si	Cl	Total
sample 6		42.5	30.6	26.8	0.1	100.0

The efficiency of caffeine extraction reached 102 %. However, increasing the time of microwave heating more than 40 min at 80 °C lead to burn the C₁₈ silica monolith (see Figure 4-13).



Figure 4-13 Silica monolithic column using microwave heating for 50 min at 80 °C during C₁₈ surface modification.

4.3.3 Characterisations of silica monoliths before and after silica surface modification with C₁₈ phase

Scanning electron micrographs of modified silica monoliths were obtained in order to investigate the effect of using microwave heating during C₁₈ surface modification on their morphological structure, compared to conventional thermal heating methodology.

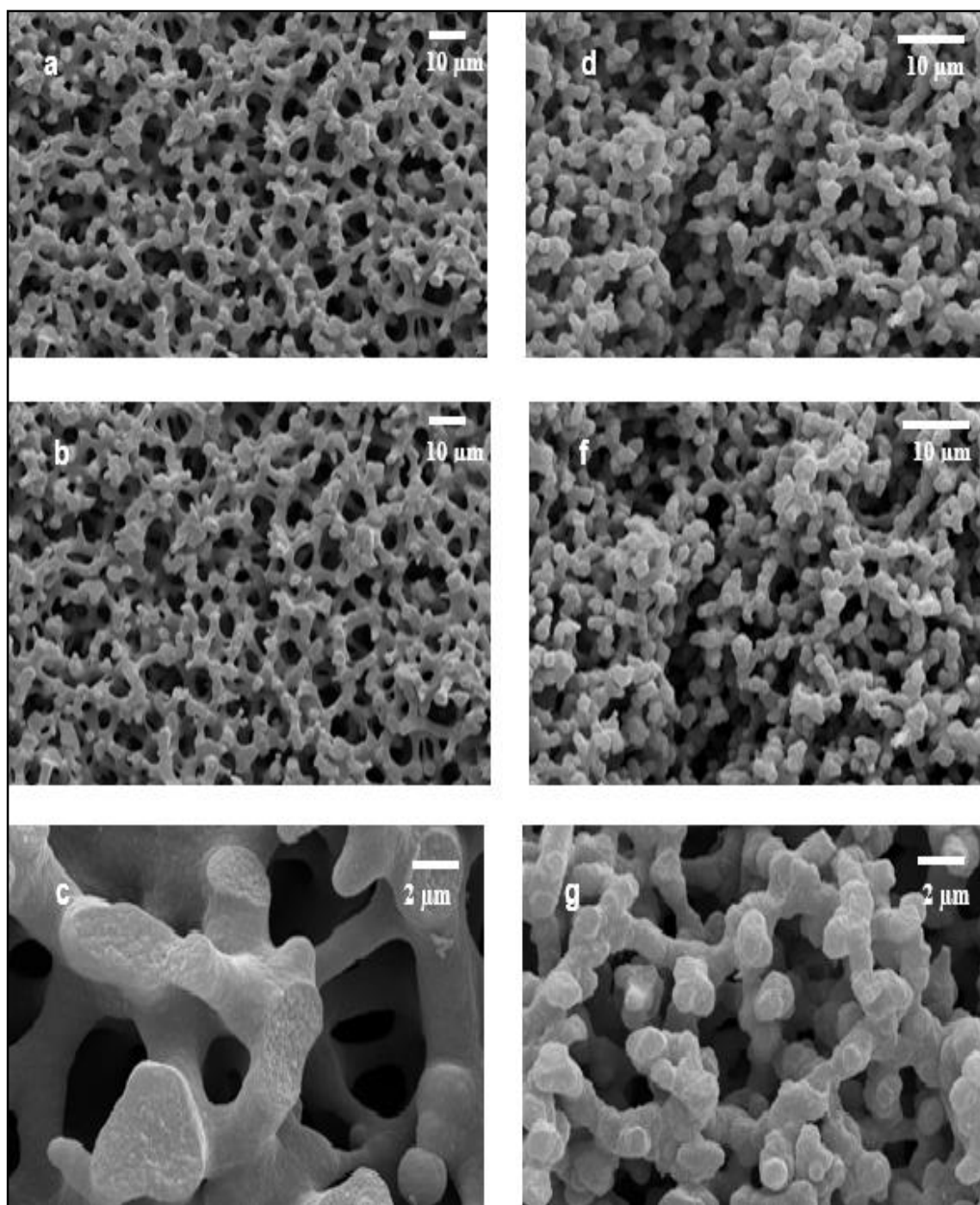


Figure 4-14 SEM images of the silica-based monolith before C₁₈ surface modification (a and d), and after surface modification with C₁₈ phase (b and c) using thermal heating, (f and g) using microwave heating.

Figure 4-14 shows images of silica monoliths before and after conventional thermal heating and microwave heating methods during the C₁₈ surface modification. It was observed that the shapes of the through-pores structures of C₁₈ silica monoliths were relatively round and smaller than those in non-modified silica-based monoliths. A possible reason could be anchoring of organic moieties on the inner surface of the pores structure. However, the structural morphology of both silica monoliths before and after C₁₈ surface modification process was found to be similar, and there was no significant difference in the size of macroporous in both of them.

4.3.4 Physical properties of C₁₈ silica monoliths

In order to compare the silica monoliths before and after using conventional thermal and microwave heating methods during C₁₈ surface modification, the physical properties of the silica monoliths were obtained using BET and BJH analysis. The effects of the C₁₈ surface modification on the total surface area, average pore size, total pore volume and macro pore diameter of silica based monoliths were investigated (see Table 4-10).

Table 4-10 Physical parameters of silica monoliths before and after C₁₈ surface modification using microwave heating and thermal heating methodology.

Column	Surface area /m ² g ⁻¹	Diffusion pore size /nm	Diffusion pore volume /cm ³ g ⁻¹	Flow-through pore diameter /μm
MW before C ₁₈ modification	570	9.1	1.2	1.1
MW after C ₁₈ modification	527	9.0	1.1	1
Oven before C ₁₈ modification	479	8.5	0.99	1.5
Oven after C ₁₈ modification	424	7.9	0.88	1.3

Table 4-10 shows that the BET surface areas of the silica-based monoliths using microwave heating and conventional thermal heating methods during C₁₈ surface

modification decreased compared to non-modified silica monoliths. The average mesoporous size of C₁₈ silica monoliths were found in the range 7.9-9 nm, which was a little smaller than the average mesoporous size in the non-modified silica-based monoliths 8.5-9.1 nm. That could be due to microwave interaction with the OH which is possibly more specific than the thermal heating which can improve the replacement of surface silanol groups on the silica monoliths by larger chemical groups. The total pore volumes of these monoliths also decreased after C₁₈ surface modification, to 1.1 cm³/g in microwave one and 0.88 cm³/g in the thermal C₁₈ silica monolith. The reduction of the surface area, pore size and volume of C₁₈ silica monoliths was expected; however, the alkyl chains attached to the surface of the silica monoliths were not visible in the SEM micrograph, probably due to the low density of the organic moieties compared to the silica monolith matrix, or the low sensitivity of the characterisation method. For this reason, it was very important to make sure that the C₁₈ phase coated not only the outer surface of the silica monolith but also the inner surface of whole monolithic column. Three cross-sections from each modified silica monolith, using microwave heating methodology during the C₁₈ surface modification process, were obtained (upper - mid and lower). The percentage of carbon in each cross-section was investigated using energy dispersive X-ray (EDX) analysis.

Table 4-11 Quantitative EDX analysis for all elements in all cross sections of silica-monoliths modified with C₁₈ phase using microwave heating for 40 min at 80 °C.

Spectrum	C	O	Si	Cl	Total
Upper-section	40.5	32.9	26.6	0.0	100.0
Mid-section	42.6	30.6	26.8	0.0	100.0
Lower-section	39.2	33.7	27.0	0.1	100.0

From the results in Table 4-11, it can be seen that the internal surface of all cross sections were modified with the C₁₈ phase. The EDX results show that the percentage of carbon (C) in all cross sections was found similar, as can be seen in Table 4-11. The previous results confirmed that the ability of microwave heating to be used in the monolithic fabrication and C₁₈ surface modification.

4.3.5 Performance of C₁₈ silica monoliths

One of the most effective methods for characterising stationary phases is a simple evaluation of extraction efficiency. Therefore, extraction of selected analytes, using microwave C₁₈ silica monoliths and thermal C₁₈ silica monolithic columns, were performed. Two types of analytes were chosen: caffeine and eserine.

4.3.5.1 Extraction procedure

All details of the extraction process, including materials, sample preparation and HPLC conditions, were described in sections 2.3.1, 2.3.2 and 2.3.3 respectively.

4.3.5.2 Breakthrough curve

One of the most important factors to determine the capacity of the extraction device is the analyte breakthrough volume. To plot the breakthrough curve, the same amount of analyte was introduced into the C₁₈ silica columns at the same flow rate. The analyte was quantitatively retained by the stationary phase from the first sample up to the point where the mass of the analyte exceeds retention capacity of the extraction phase. At the saturation point the amount of analyte entering and exiting the extracting device becomes identical. The breakthrough point is the first point on the curve where the analyte is detected at the outlet of the extracting device. In order to calculate the capacity of the extracting device the mass fractions of the analyte added during sampling time, up to the breakthrough point, are quantitatively summed to obtain the retained quantity.

4.3.5.3 Capacity of C₁₈ phase

The capacity of both types of C₁₈ TMOS columns (microwave and thermal functionalization) for caffeine were calculated. A standard solution was prepared by dissolving 100 µg of caffeine in 1 mL of purified water. After conditioning both C₁₈ monoliths (1 cm) with 2 mL of methanol, and 2 mL of purified water at flow rate 100 µL/min, 25 fractions (350 µL each) of the analyte were loaded and the eluent collected during the loading step. The amount of caffeine present in each fraction loaded was 35 µg. Each fraction was collected manually and measured by the HPLC-UV system using Symmetry C₁₈, 4.6 mm × 250 mm packed with silica particles size 5 µm and the detected wavelength was 205 nm. A standard calibration curve was used to quantify the extracted caffeine (see section 4.3.2). Breakthrough occurred on microwave C₁₈-TMOS monolith after loading 7000 µL of caffeine standard solution, compared to the thermal C₁₈-TMOS monolith where the breakthrough took place after loading 5650 µL of the same standard solution (see Figure 4-15).

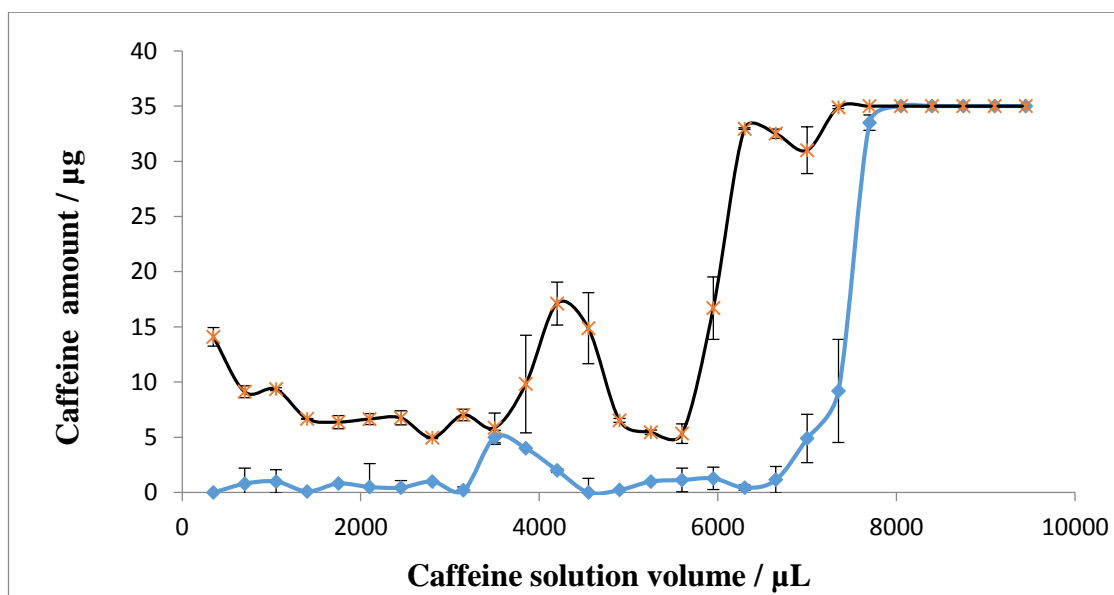


Figure 4-15 Breakthrough curves for Caffeine standard (100 µg/mL), each point represents one fraction of solution (350 µL) contain (35 µg) of caffeine adsorbed on (—◆—) microwave C₁₈ silica monolith and (—x—) on thermal C₁₈ silica monolith. The error bars represent the standard deviation of 3 repeat experiments.

The capacity of both C₁₈ TMOS monoliths was calculated, as shown in Table 4-12.

Table 4-12 Composition and capacity of microwave C₁₈ -TMOS column (C₁₈ at 80 °C for 40 min and 120 W) and thermal C₁₈-TMOS column.

Column	Heating for gelation	Modification phase	Heating for modification	Time for modification /min	weight /mg	breakthrough volume /mL	Capacity /mg
1	MW	C ₁₈	MW	40	25	7.00	0.70
2	Oven	C ₁₈	Oven	500	25	5.65	0.56

*MW for microwave

The results in Table 4-12 show that the C₁₈-TMOS columns using microwave heating for monolithic fabrication and C₁₈ surface modification offered bigger capacity for caffeine compared to C₁₈-TMOS columns using conventional thermal heating for monolithic fabrication and C₁₈ surface modification.

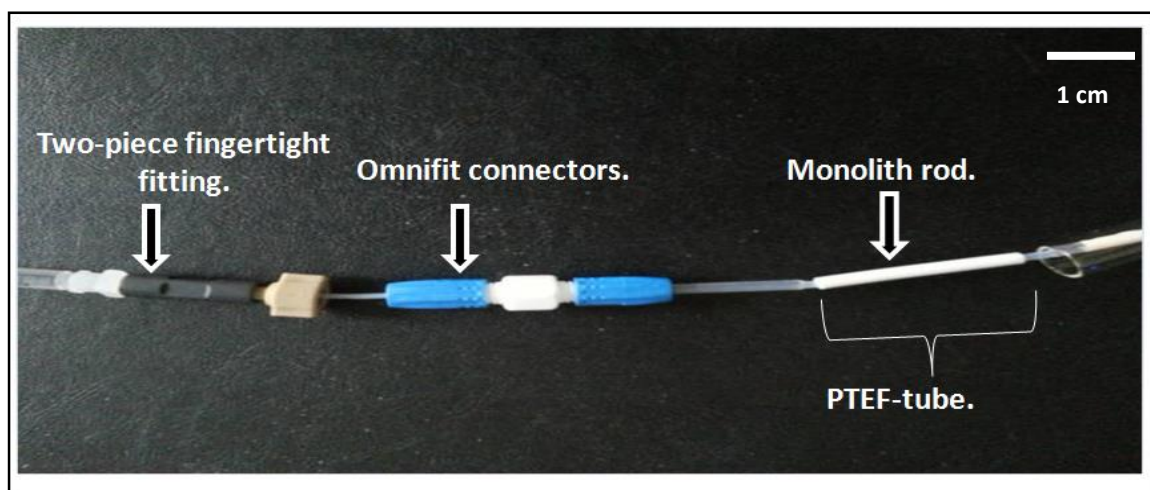


Figure 4-16 Photograph of silica monolithic rod connected to the borosilicate tube (o.d. 3.90 mm) within the poly (tetrafluoroethylene) (PTFE) shrinkable tube to be suitable for drug extraction.

4.3.5.4 Evaluation of recovery

Recovery of the target analytes was calculated by comparing chromatographic peaks areas of direct injection of standard samples with those obtained by the same samples after extraction. The concentration of each analyte (caffeine and eserine) was 100 µg/mL. Each analysis was carried out in triplicate. The precision was determined by calculating the relative standard deviation (coefficient of variation, CV) and the efficiency was expressed as a percentage of mean recovery.

Within batch CVs were obtained from the low, intermediate and high standard solution samples (caffeine 10, 50 and 100 $\mu\text{g/mL}$), which were analysed three times. The same procedure was repeated for three days to determine between batches CVs. The results were represented the average of three replicate analyses of each standard solution. All standard deviations were computed using Microsoft Excel software.

4.3.5.5 Method Validation

Distinct peaks and retention times for caffeine at 2.02 min and eserine at 2.11 min were observed with no interfering or impurity peaks around them (see Figure 4-17)

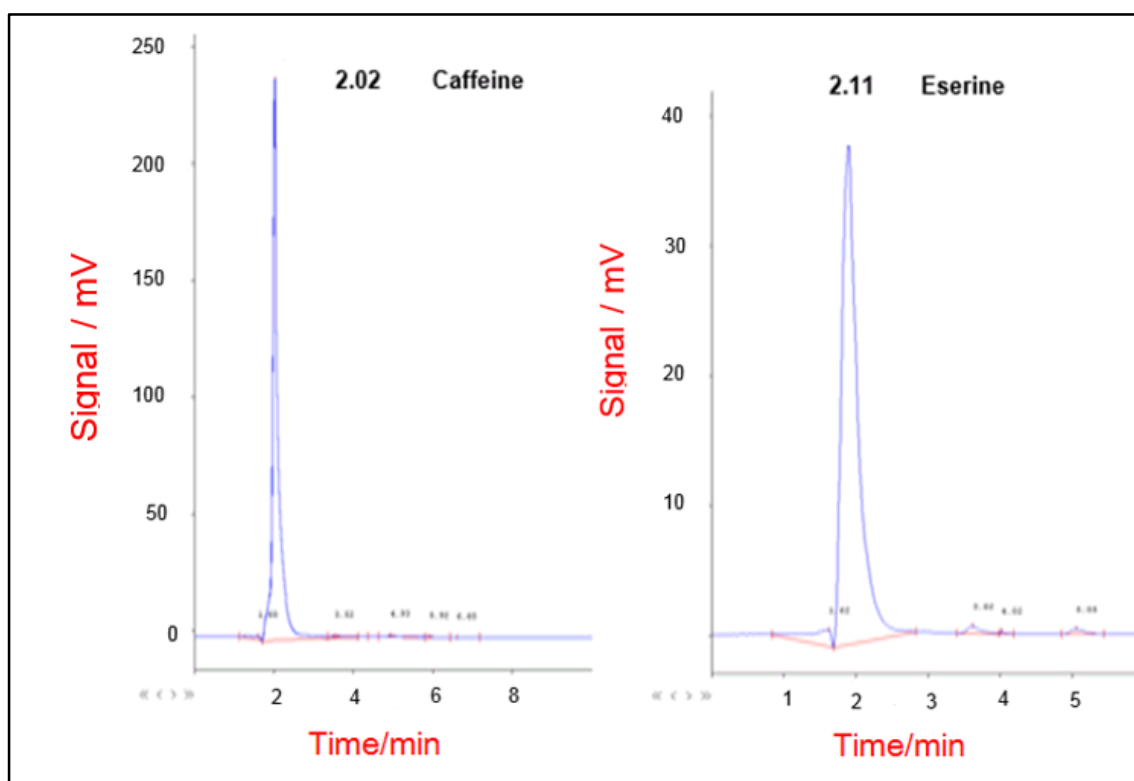


Figure 4-17 The UV chromatograms of caffeine and eserine standards (100 $\mu\text{g/mL}$). The separation column was Symmetry C_{18} , 4.6 mm \times 250 mm packed with silica particles size 5 μm . All experiments were performed at ambient temperature around 25 $^{\circ}\text{C}$ according to the HPLC conditions in section 2.3.3.

Recoveries of both analytes from standard solutions are presented in Table 4-13.

Recoveries of caffeine and eserine with C_{18} -TMOS columns using microwave heating for monolithic fabrication and C_{18} surface modification were 103 % and 97 %, respectively.

These recoveries were found to be highest compared to those obtained by thermal C₁₈-TMOS columns, which were 90 % and 97 % for caffeine and eserine, respectively.

Table 4-13 Percentages of recoveries of caffeine and eserine from standard solutions (100 µg/mL) using microwave C₁₈ -TMOS column (C₁₈ at 80 °C for 40 min and 120 W) and thermal C₁₈ -TMOS column.

Column (SPE)	Compound	Concentration µg /mL	Recovery ^m %
MW C ₁₈ - TMOS	caffeine	100	103 ± 1.7
Oven C ₁₈ - TMOS	caffeine	100	90 ± 0.29
MW C ₁₈ - TMOS	eserine	100	97 ± 2.8
Oven C ₁₈ - TMOS	eserine	100	97 ± 3.5

^mValues represent means ± SD of 3 experiments
 SPE for solid phase extraction
 MW for microwave

Within batch and between batches CVs were evaluated by assessing standard samples prepared in purified water, and are summarized in Table 4-14. Within batch CVs for the caffeine concentrations investigated by C₁₈-TMOS columns using microwave heating for monolithic fabrication and C₁₈ phase modification were between 2 % and 4.3 %. By comparison, within batch CVs for the same concentrations of caffeine examined by C₁₈-TMOS columns using thermal heating for monolithic fabrication and C₁₈ phase modification were between 3.7 % and 8.8 %.

The data obtained for between batches CVs for the caffeine concentrations investigated by MW C₁₈- TMOS columns were between 3.1 and 4.5 %, whereas the between batches CVs for the same concentrations of caffeine examined by thermal C₁₈-TMOS columns were between 6 and 10 %.

The mean recovery of caffeine standard solutions using MW C₁₈-TMOS columns were in the range 101–111 %, in contrast the mean recovery of caffeine standard solutions using thermal C₁₈-TMOS columns were in the range 42–101 %. Thus, the data indicated that the C₁₈-TMOS columns using microwave heating for monolithic fabrication and C₁₈

phase modification provided better recoveries and precision for the quantification of caffeine levels in three standard solutions compared to C₁₈-TMOS columns using conventional thermal heating for monolithic fabrication and C₁₈ surface modification. Finally, the experimental results (Table 4-14) indicate that using the microwave heating during the modification of silica monolith with C₁₈ phase is possibly leading to more specific interaction than the thermal heating method which produced more accurate and precise C₁₈ silica monolithic column.

Table 4-14 precision of extraction caffeine from standard solutions samples.

Column (SPE)	Concentration µg /mL	Within batch (n = 3)		Between batches (n = 3)	
		CV %	Mean recovery %	CV %	Mean recovery %
MW C ₁₈ -TMOS	10	4.3	102	4.5	101
	50	3.7	111	4.5	109
	100	2	104	3.1	102
Oven C ₁₈ -TMOS	10	8.8	46	10	42
	50	4.5	101	6	101
	100	3.7	95	6.5	91

*SPE for solid phase extraction

4.4 Summary

The use of microwave heating during fabrication and C₁₈ surface modification improves not only the physical structure of the silica monoliths but also extraction of caffeine and eserine from standard solutions. The choice of stationary phase is very important as it has a significant effect on the efficiency of the drug extraction method. The increased microwave heating time during C₁₈ surface modification up to 40 min at 80 °C resulted in an increase in the percentage of carbon due to the attachment of more C₁₈ chains on the silica surface.

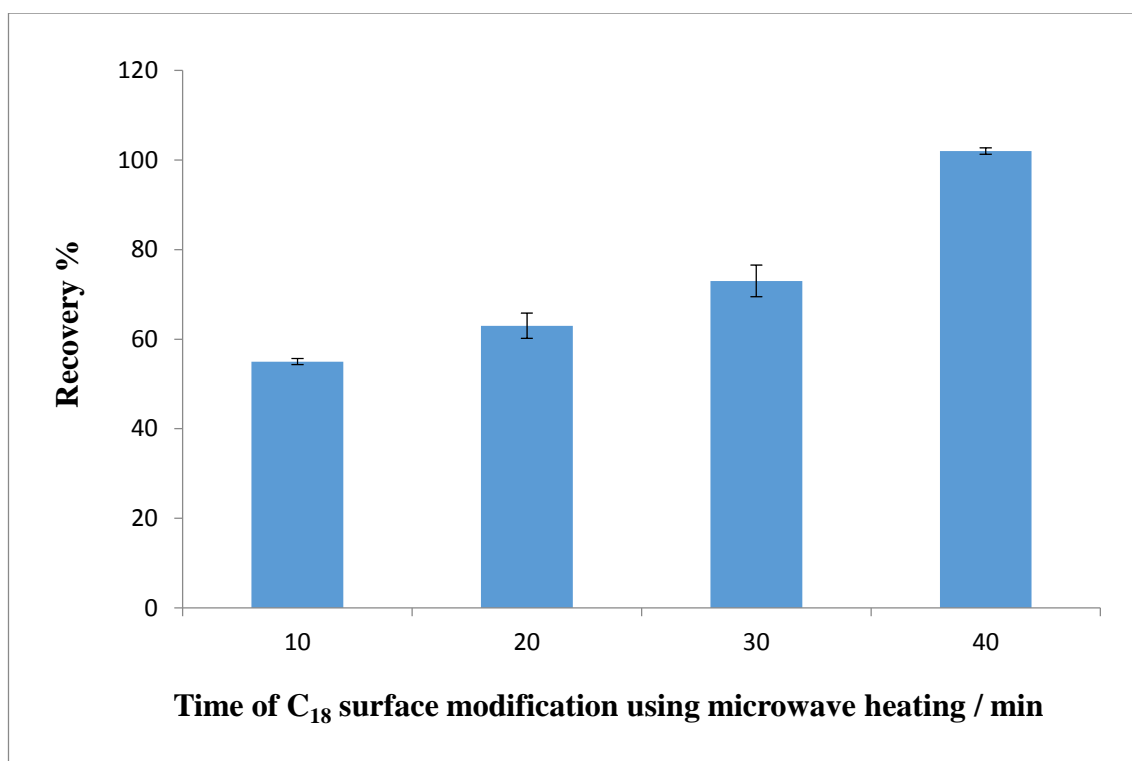


Figure 4-18 Recoveries (%) of caffeine (100 µg/mL) extracted by four C₁₈-TMOS columns using microwave heating during C₁₈ modification for 10, 20, 30 and 40 min respectively at 80 °C. The error bars represent the standard deviation of 3 repeat experiments.

The C₁₈ silica monoliths produced using microwave heating method showed higher caffeine and eserine extraction efficiency, and were produced more quickly than conventional thermal heating monoliths. The potential for the optimised method for drug extraction presented here, suitable for performing drug extraction and detection together, will be discussed in detail in chapter 5.

5 Using gold nanoparticles within silica monoliths structure and for surface modification

Chapter 5

5.1 Introduction

In recent years the use of gold nanoparticles (GNP) has expanded in forensic research. They are used in extraction due to their unique properties of large surface area to volume ratio, small size and stability over high temperatures, and the potential of gold nanoparticles to enhance the sensitivity of methods of detection, such as chemiluminescence, and their electrical conductivity.^[209]

The chemiluminescence reaction is a simple detection method that depends on the emission of light from a chemical reaction. Chemiluminescence is used in many applications because it is highly sensitive, can be detected with simple instrumentation, has a low background signal, and has a wide range of linear response. The efficiency of chemiluminescence detection can also be improved by combining enzymatic reactions, such as horseradish peroxidase and alkaline phosphatase, with chemiluminescence reagents (luminol, isoluminol etc).^[210]

Several methods of optical detection, such as those based on fluorescent or colorimetric, require complex optical systems for light excitation or illumination (light source, lenses, filters etc.). However, chemiluminescence emits light directly and so needs no special optical system, considerably simplifying detector design.^[209]

In previous work (chapter 4), C₁₈ phase was used to improve the extraction of two different analytes at low concentrations based on functionalized silica monolithic column. While the C₁₈ phase was effective for extraction the presence of gold nanoparticles have the ability to advance both the extraction and detection of drugs of abuse using immunoassays with chemiluminescence.

In this work a simple design of solid phase extraction, coupled with the potential of gold nanoparticles to enhance the sensitivity of an immunological assays, is considered.

5.2 Experimental

5.2.1 Fabrication of silica monoliths embedded by gold nanoparticles using microwave heating during gel formation process

To develop a new method that has the capability to extract and detect drugs of abuse simultaneously, the starter mixture of the sol-gel was blended with gold nanoparticles labelled by an amino group (NH₂). The GNP-NH₂-silica monolithic column was fabricated according to the procedure described in section 2.4.1. The typical chemical composition and reaction conditions used during fabrication of GNP-NH₂-silica monoliths are listed in Table 5-1.

Table 5-1 Composition and reaction conditions for preparation of silica monolithic columns embedded by gold nanoparticles.

TMOS	PEO (200K)	Acetic acid (0.02M)	Functionalized gold nanoparticles 50 nm-NH₂	Microwave heating at 300 W	Time of heating
/mL	/g	/mL	/μL	/°C	/min
2	0.305	4	5	120	5

5.3 Results and discussions

5.3.1 Characterization

The silica monolithic columns embedded by gold nanoparticles were characterised by different techniques such as digital photograph, SEM analysis, EDX analysis and BET and BJH analysis.

5.3.1.1 External morphology

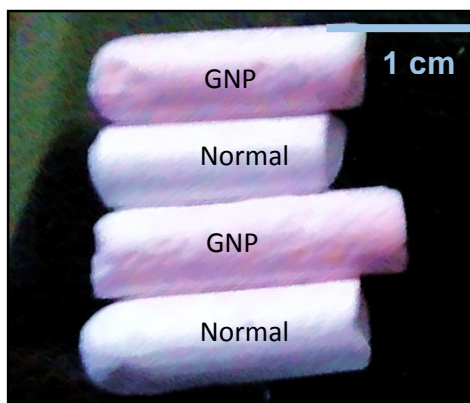


Figure 5-1 Images of TMOS silica monoliths: (GNP-monolith) embedded by gold nanoparticles 5 μL using microwave heating for 5 min at 300 W during gelation time and (Normal-monolith) fabricated without gold nanoparticles using microwave heating during gelation time for 11 min at 10-300 W.

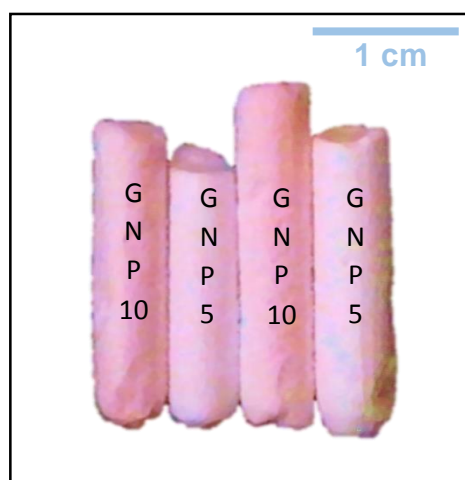


Figure 5-2 Images of TMOS silica monoliths: (GNP 5-monolith) embedded by gold nanoparticles 5 μL using microwave heating for 5 min at 300 W during gelation time and (GNP 10-monolith) embedded by gold nanoparticles 10 μL using microwave heating for 5 min at 300 W during gelation time.

From the photograph in Figure 5-1, it can be seen that the colour of the silica monolithic rods embedded by gold nanoparticles gives a pink tint compared to the white colour of normal phase silica monolithic rods. The possible reason for that could be formation of gold oxide during the sol-gel process. It was also observed that the intensity of the colour was increased by increasing the amount of gold nanoparticles within the silica matrix as shown in Figure 5-2.

5.3.1.2 SEM analysis

The scanning electron micrographs were obtained in order to confirm the existence of GNP within the silica structures. In this case, the samples for SEM analysis were coated with a thin layer of carbon (thickness approximately 2 nm) due to high charge of gold nanoparticles.

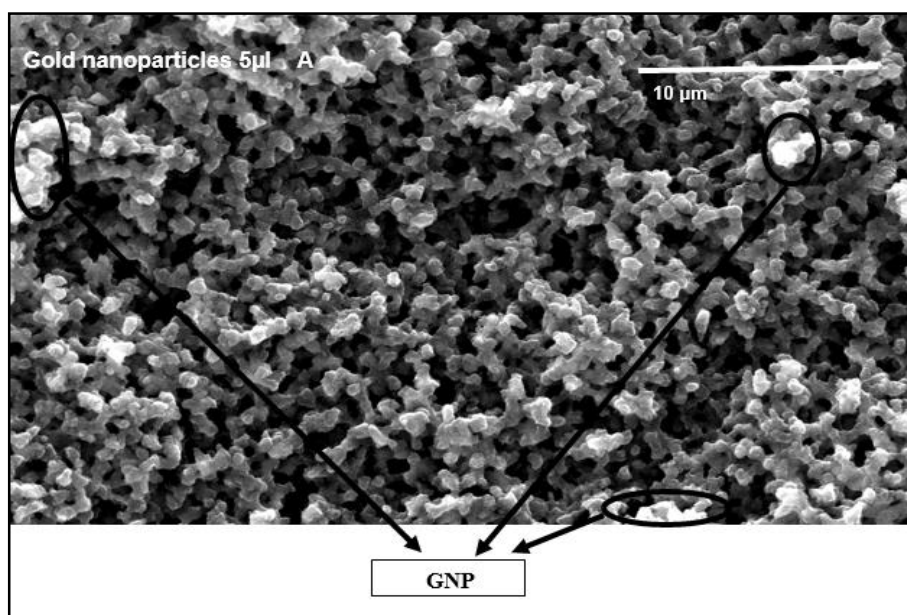


Figure 5-3 Scanning electron micrographs of TMOS silica monolith embedded by gold nanoparticles 5 µL, using microwave heating during gelation time (5 min at 300 W).

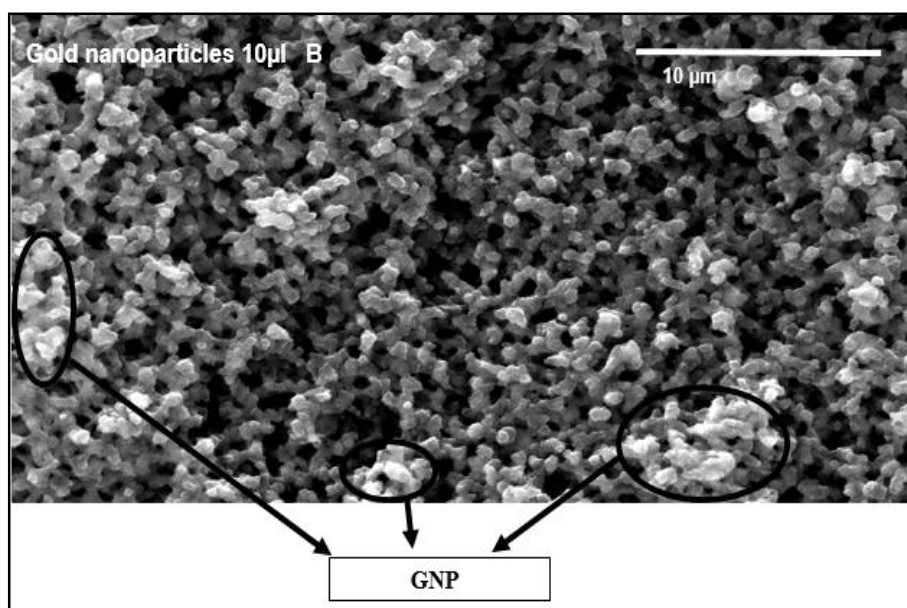


Figure 5-4 Scanning electron micrographs of TMOS silica monolith embedded by gold nanoparticles 10 µL, using microwave heating during gelation time (5 min at 300 W).

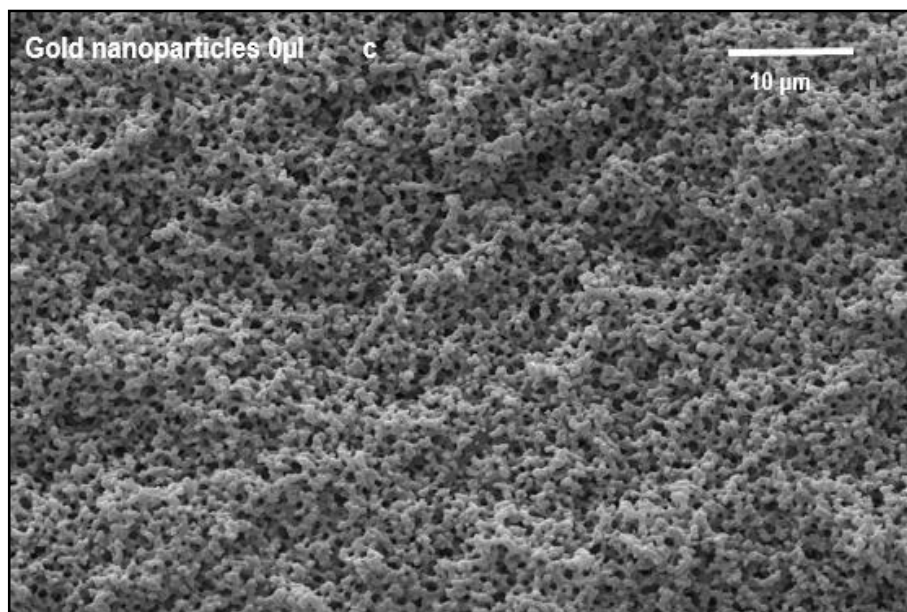


Figure 5-5 Scanning electron micrographs of TMOS silica monolith without gold nanoparticles, using microwave heating during gelation time (11 min).

From the images above it will be clear that the bright white appearance in the internal structure of the silica monoliths came from the negative charges on the gold nanoparticles, as can be seen in Figure 5-3 and Figure 5-4. Increasing the amount of gold nanoparticles embedded in the silica monoliths resulted in an increase in the brightness of gold nanoparticles within the silica structure (the brightness in Figure 5-4 more than Figure 5-3).

5.3.1.3 Physical properties of GNP silica monoliths

The physical properties of GNP-NH₂-silica monoliths were obtained using BET and BJH analysis in order to investigate the effect of embedding GNP during gel formation in the internal structure of the silica monoliths (surface area, average pore size and total pore volume).

Table 5-2 Physical properties of silica monoliths without and with GNP-NH₂.

Column	Surface area /m ² g ⁻¹	Diffusion pore size /nm	Diffusion pore volume /cm ³ g ⁻¹	Flow-through pore diameter /μm
Without GNP	569	9.1	1.2	0.8
With GNP-NH ₂ (5 μL)	404	15	1.3	1

Table 5-2 shows that the BET surface areas of the silica monoliths after embedding of GNP-NH₂ (5 μL) decreased compared to the same silica monoliths without GNP-NH₂. The average pore size distributed over the GNP-silica monolith using microwave heating during gel formation, measured by the BJH method, were found to be larger than the average pore size in the non-embedded silica-based monolith. A possible reason for the observed decrease in surface area could be a variation in the gel formation process when using microwave heating due to embedding of GNP which are presumably very microwave active (e.g. local hot spots are generated). The total pore volumes of these monoliths also slightly increased after embedding GNP to 1.3 cm³/g. Conversely, the flow-through pore diameter within the GNP-NH₂-silica monoliths were found to be a little smaller than the flow-through pore diameter in the non-embedded silica-based monoliths. Whilst a reduction of the surface area and flow-through pore diameter in the GNP-NH₂-silica monolith was expected, the increase in the average pore size in the GNP-NH₂-silica monolith was a surprise. This would be due to converting the microwave radiation to thermal heating within starter mixture of the GNP-NH₂-silica monolith much more quickly, compared to normal phase silica monoliths.

The internal structure of the silica based monolith includes siloxane (Si-O-Si) and silanol (Si-OH) groups on the surface area, which can be utilised as anchors for the organic groups. However in this study, immobilisation of the antibody on the surface of GNP-NH₂ embedded into silica-based monolith was performed. The EDC solution was

injected into the silica monolithic column embedded with GNP-NH₂ at 50 μ L/min followed by the Sulfo-NHS at 50 μ L/min in order to immobilise of anti-oxazepam on the amino group bonded to the GNP. After that 1000 μ L of anti-oxazepam 5 μ g/mL was injected through the silica monolithic column at 50 μ L/min. To remove any unbound antibody, the monolithic columns were then washed with 1000 μ L of PBS at 100 μ L/min. The washing fraction was collected to check whether the antibody immobilised on the amine-bonded GNP embedded within the silica monolithic column.

It was very important to make sure that the anti-oxazepam immobilised on the surface of GNP-NH₂ is able to bind with the antigen-HRP and determine the incubation time for antigen–antibody reaction before analysis of collected fractions. This was performed by placing 5 μ L of GNP-NH₂ in three glass tubes filled by 1 mL of purified water. Only the GNP-NH₂ in the first tube (a), 5 μ L of GNP-NH₂ with 5 μ L of antibody were present in the second tube (b) and 5 μ L of GNP-NH₂ with 5 μ L from antibody and 1000 μ L from their antigen–HRP 0.5 μ g/mL were present in the third tube (c).

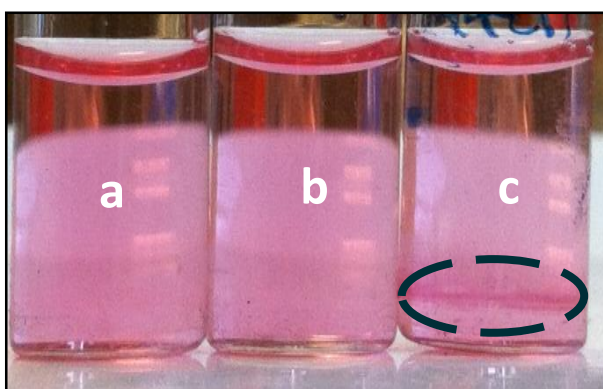


Figure 5-6 Image of antigen antibody reaction took place in three glass tubes contain 1 mL of purified water and 5 μ L of GNP-NH₂ in tube (a) plus 5 μ L anti-oxazepam in tube (b) and 5 μ L anti-oxazepam and their antigen–HRP in tube (c) (after 5 min).

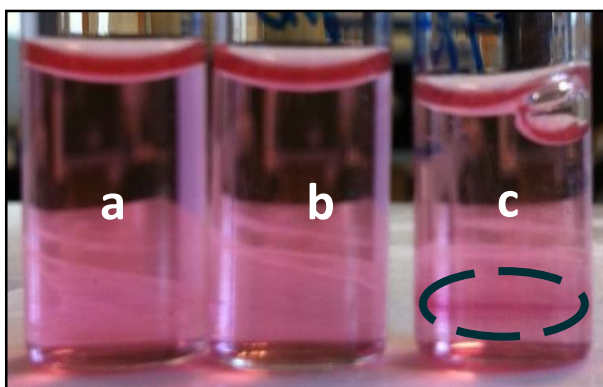


Figure 5-7 Image of antigen antibody reaction took place in three glass tubes contain 1 mL of purified water and 5 μL of GNP-NH₂ in tube (a) plus 5 μL anti-oxazepam in tube (b) and 5 μL anti-oxazepam and their antigen-HRP in tube (c) (after 10 min).

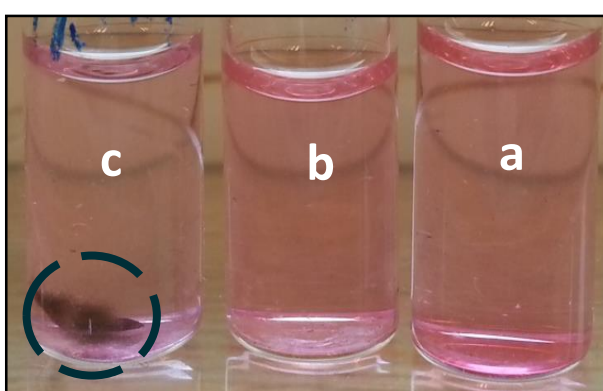


Figure 5-8 Image of antigen antibody reaction took place in three glass tubes contain 1 mL of purified water and 5 μL of GNP-NH₂ in tube (a) plus 5 μL anti-oxazepam in tube (b) and 5 μL anti-oxazepam and their antigen-HRP in tube (c) (after 3 months).

The results show the efficiency of using GNP-NH₂ to immobilise the antibody. In addition, the antigen-antibody reaction was successful and selective after a relatively short period (5 min) and was found to be stable for a long period (3 months), as can be seen in Figure 5-6 and Figure 5-8, respectively.

5.3.2 Assay condition optimization

Main parameters affecting chemiluminescence-based immunoassay were studied. All of the optimization results discussed below were based on three repeat experiments, while the error bars indicate one standard deviation. Since the analysis time is very important

in drugs of abuse testing, the effects of the exposure times and the concentration of the assay reagents on chemiluminescence signals were investigated.

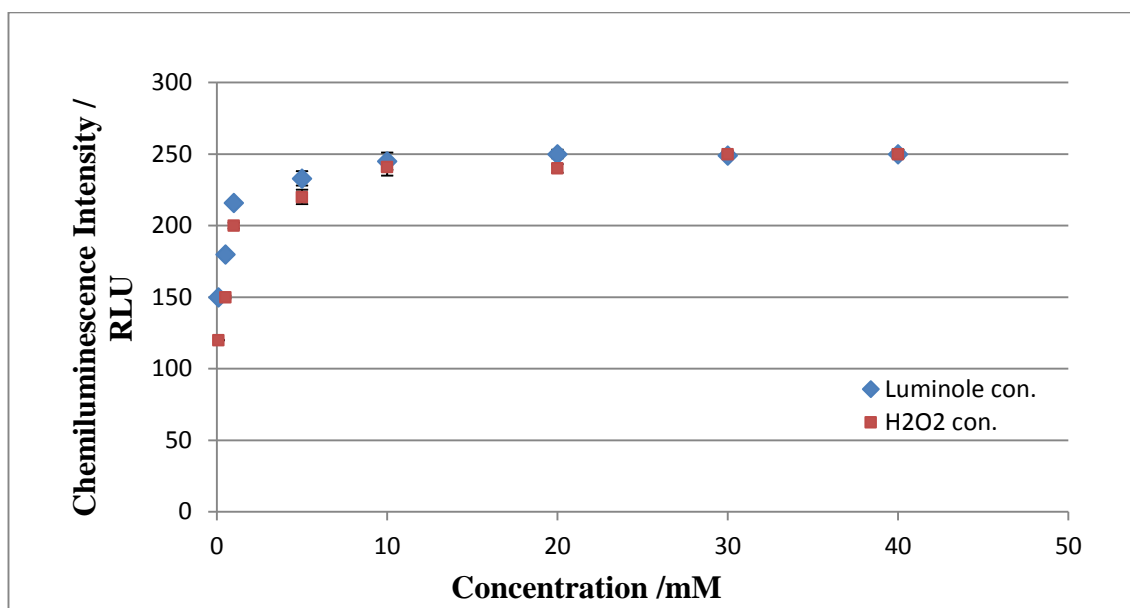


Figure 5-9 Parameter optimization for chemiluminescence-based immunoassay. Each datum represents the average of three repeat experiments, while the error bars indicate one standard deviation. (♦) Effects of the luminol concentration on the signal / noise ratio of chemiluminescence detection. (■) Effects of the hydrogen peroxide (H₂O₂) concentration on the signal / noise ratio of chemiluminescence detection.

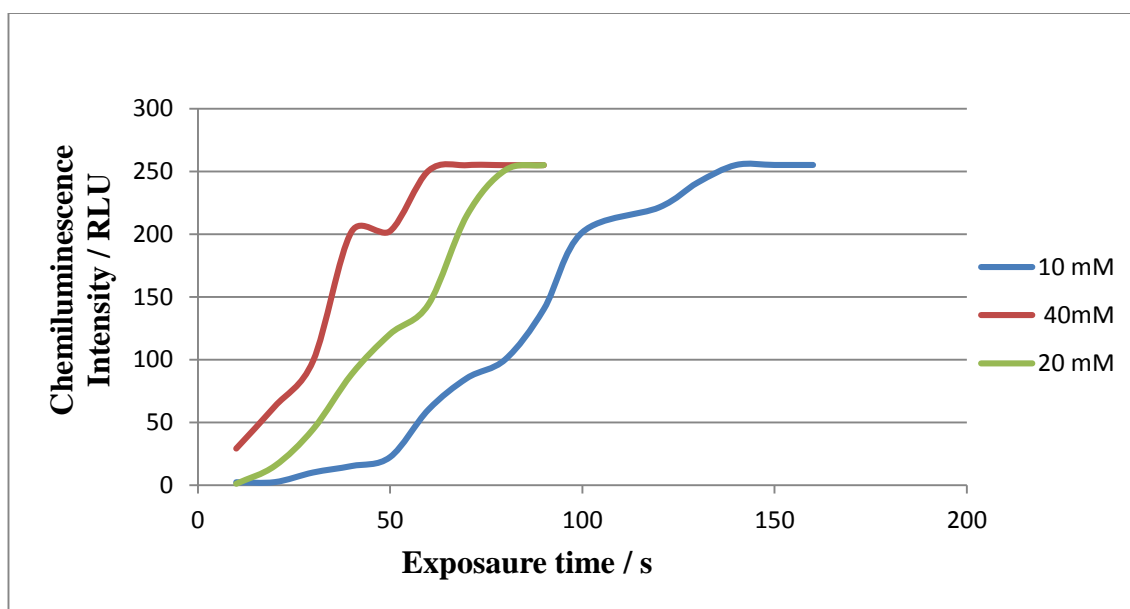


Figure 5-10 Parameter optimization for chemiluminescence-based immunoassay. Effects of the luminol and H₂O₂ concentrations on the exposure time of chemiluminescence signal.

Figure 5-9 shows the chemiluminescence intensity as a function of the luminol and H₂O₂ concentrations. As the background signal changed for different luminol and H₂O₂

concentrations used the signal to noise ratio to search for the optimum concentration. The results indicate that the optimum concentrations of luminol and H₂O₂ are 10 mM. The effects of luminol and H₂O₂ concentrations on the exposure times of chemiluminescence were also investigated and the results are shown in Figure 5-10. The exposure times of highest chemiluminescence signal (RLU = 250) decreased with increasing luminol and H₂O₂ concentrations. The results indicated that 2 min for exposure time is sufficient to obtain the highest chemiluminescence signal at the optimum concentrations of luminol and H₂O₂ (10 mM).

5.3.3 Calibration Curve

Under the optimum conditions obtained the calibration curve of oxazepam-HRP detection using chemiluminescence based immunoassays as shown in Figure 5-11. Since oxazepam-HRP attached with a fixed amount of anti-oxazepam immobilized on the surfaces of the detection zone and the chemiluminescence intensity represents the amount of oxazepam-HRP, the increase in signal from the first sample indicates increasing of oxazepam-HRP in a sample, and the degree of the decrease is proportional with the concentration of oxazepam-HRP.

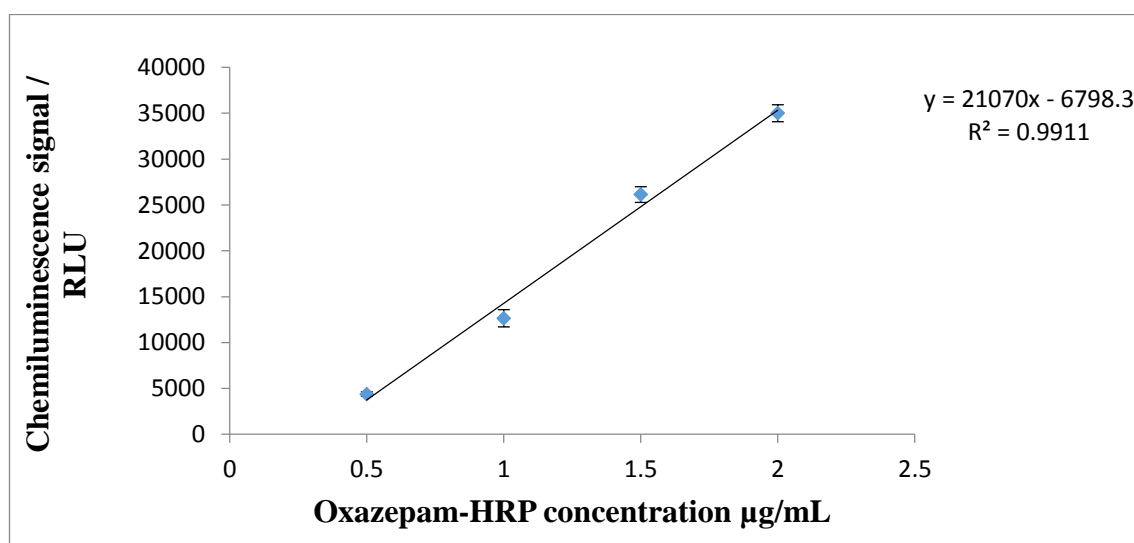


Figure 5-11 Calibration curve for oxazepam-HRP analysis based immunoassays. Each data point represents an average from three repeat experiments using chemiluminescence, and the error bars indicate one standard deviation.

Good linearity was observed that meant the calibration curve was useful in quantifying the fraction during detection experiments. The limit of detection and limit of quantitation for oxazepam-HRP were calculated from the slope and standard deviation (SD) of the linearity curve.

Detection Limit, $DL = SD \times 3/\text{slope}$

Quantitation Limit, $QL = SD \times 10/\text{slope}$

It was found the LOD 0.33 $\mu\text{g/mL}$ and the LOQ was 1.1 $\mu\text{g/mL}$.

The analysis of the collected washing fraction was carried out using chemiluminescence based immunoassay, which added 1000 μL of oxazepam-HRP solution to the washing fraction, and were left for 10 min to allow for antigen-HRP to bind with their antibodies. After that a 1:1 ratio of luminol and hydrogen peroxide were added to the mixture (100 μL) and placed under the CCD camera for analysis.

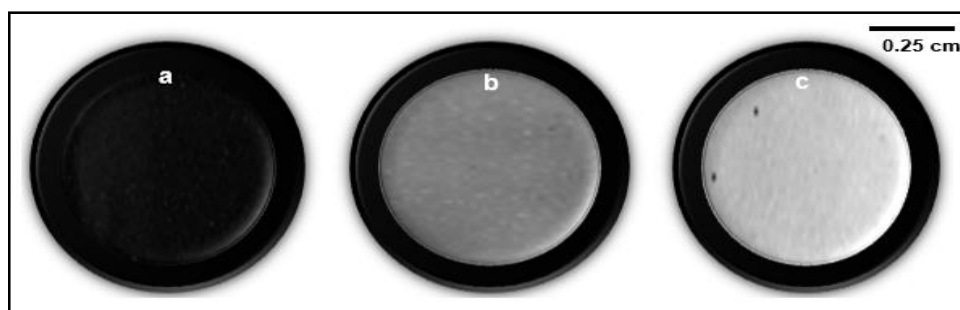


Figure 5-12 Images of the antigen-antibody reaction based on chemiluminescence response upon addition of luminol and hydrogen peroxide (a) negative sample (b) washing fraction and (c) positive sample.

From the result it is clear that embedding of gold nanoparticles inside silica-based monolith could be used to trap and detect oxazepam-HRP however, using microwave heating during gel formation lead to a loss of some antibody during immobilization process due to decompose the organic moieties (NH_2) or formation of gold oxide at very high temperature (see Figure 5-12). To overcome this issue the silica monolithic column

was fabricated according to that procedure described in section 2.1.2 and its top surface was coated physically by GNP-NH₂ in order to immobilise of anti-oxazepam.

5.3.4 Coating the surface of silica based monolith with GNP-NH₂

The top surface of the silica monolithic column was physically coated by GNP-NH₂. The resulted silica monolithic columns were characterised by different techniques such as SEM analysis and BJH and BET analysis.

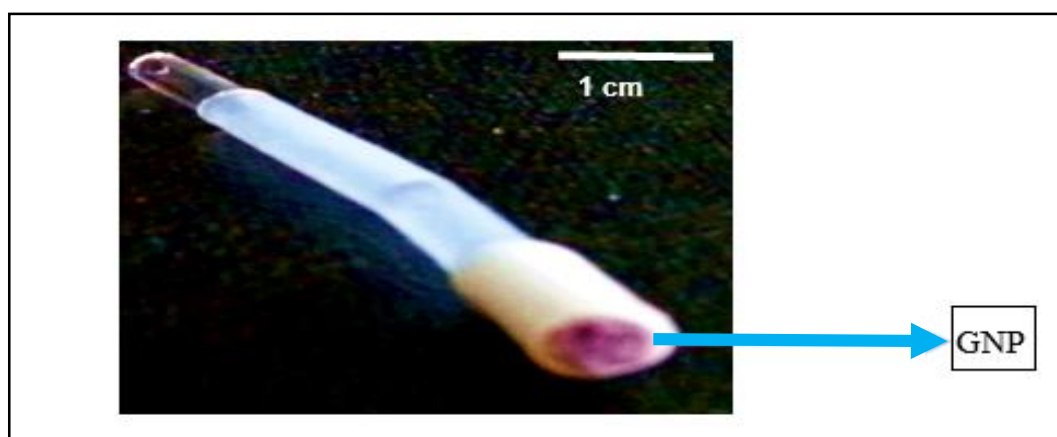


Figure 5-13 Image of silica monolithic column coated by GNP-NH₂.

Table 5-3 Physical properties of silica monoliths without and after coating by GNP-NH₂.

Column	Surface area /m ² g ⁻¹	Diffusion pore size /nm	Diffusion pore volume /cm ³ g ⁻¹	Flow-through pore diameter /μm
Without GNP	574	9	1.3	0.8
After coating by GNP-NH ₂ 10 μL	552	9.1	1.3	0.85

The table shows no significant difference in the internal structure of the silica monolith without, and after, adding GNP-NH₂ to the top surface, as can be seen in Table 5-3.

5.3.5 Immobilisation of anti-oxazepam on the top surface of silica monolithic column coated by GNP-NH₂

The amine functional groups are highly reactive to many functional groups and can offer the necessary active sites for other components for further immobilisation. The mechanism of immobilisation of the antibody on the surface of GNP-NH₂ is shown in

Figure 5-14.

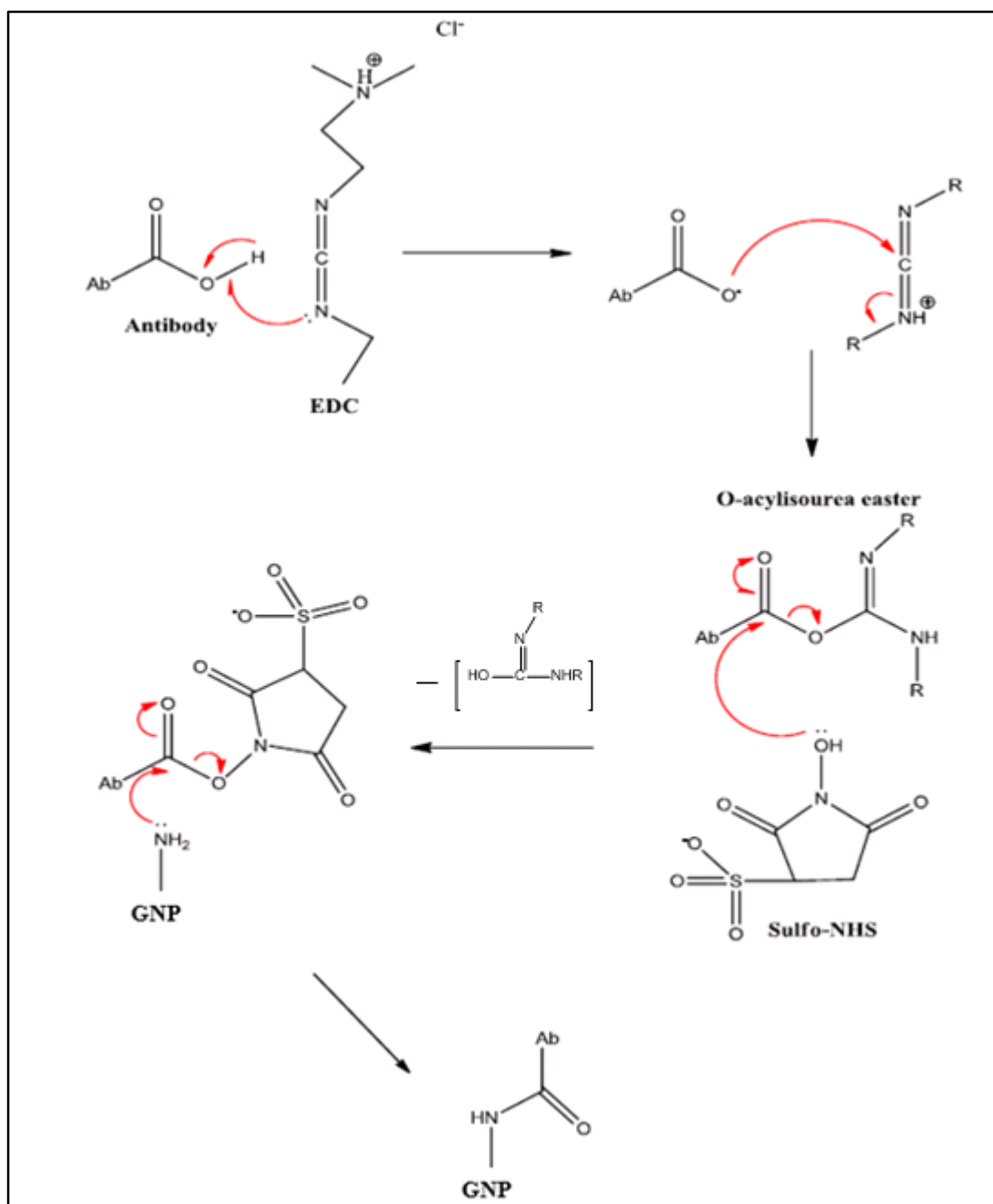


Figure 5-14 Mechanism of reaction of the antibody with the surface of GNP-NH₂.

Coating of the top surface of silica monolithic column was carried out using the acid groups on the antibody. This was activated by EDC and produced O-acylisourea ester that was then stabilised by the Sulfo-NHS on the GNP-NH₂ monolith. It is very important to make sure that the GNP-NH₂ coated silica monolithic column and the attached antibody can catch the antigen-HRP sample. As the NH₂ terminal groups on the surface of GNP coated the silica monolithic column resulted in a covalent coupling between the antibody and the top surface of the silica monolith, immobilised antibodies cannot be washed out. The monolithic column coated with GNP-NH₂ was qualitatively tested using the chemiluminescence-based immunoassay. The initial experiment was carried out to determine the efficiency of immobilisation of anti-oxazepam on the GNP-NH₂ surface. 1000 μ L Oxazepam-HRP solution (0.5 μ g/mL) was injected into three silica monolithic columns coated with GNP-NH₂ at a flow rate of 50 μ L/min to allow antigens to link with their antibodies. The HRP was used as a catalyst for the luminol and hydrogen peroxide reaction, which will generate an emission of light when the antibodies bind to their antigens. The CCD camera detected light resulting from (antigen-HRP)-antibody reactions (this experiment was repeated three times) and the images are shown in Figure 5-15 below.

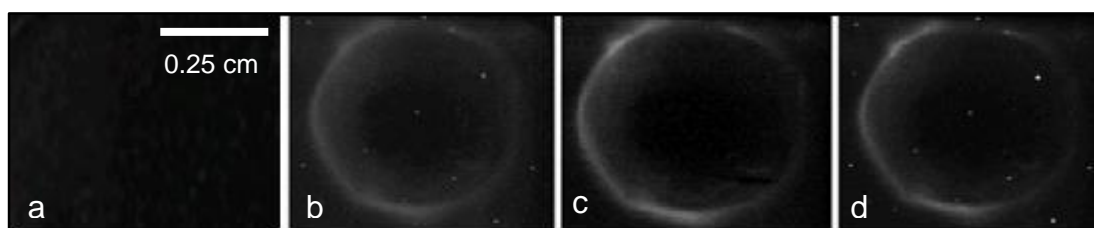


Figure 5-15 Different images for silica monoliths coated by gold nanoparticles (GNP 10 μ L + anti-oxazepam 5 μ L) reacted with a same concentrations of oxazepam-HRP (1000 μ L). (a) Negative sample (b, c and d) 0.5 μ g/mL of oxazepam-HRP.

The chemical composition and experimental conditions are listed in Table 5-4.

Table 5-4 RLU-values for three silica monolithic columns coated by GNP-NH₂-anti oxazepam reacted with same concentration of oxazepam-HRP.

Monolith	Gold nanoparticles /μL	Anti-oxazepam /μL	Antigen (oxazepam-HRP) /μg/mL	RLU
b-TMOS	10	5	0.5	4000
c-TMOS	10	5	0.5	4207
d-TMOS	10	5	0.5	4190

It will be clear from these images in Figure 5-15 that using this method for extraction and detection of oxazepam-HRP was effective, and there was no significant difference in the intensity of light in all of the samples using the same conditions, as can be seen in Table 5-4. However, the reaction of hydrogen peroxide and luminol has a short lifetime. In order to study the effect of increasing the amount of antigen-HRP on the intensity of light produced by antigen-antibody reaction using three different concentrations of antigen-HRP, the same amount of antibodies (5 μL) were immobilized on the same amount of gold nanoparticles (10 μL) coating the silica monolithic columns (this experiment was repeated three times).

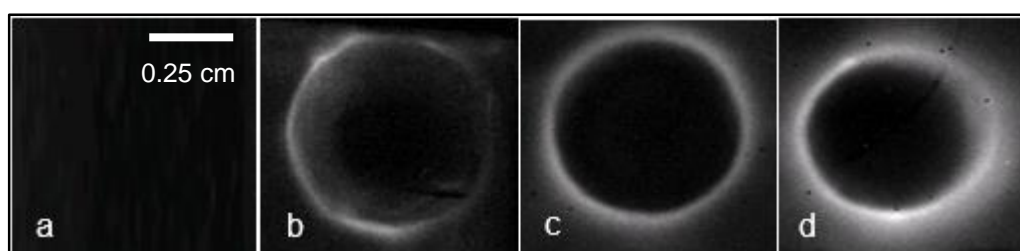


Figure 5-16 Different images for silica monoliths coated by gold nanoparticles (GNP 10 μL + anti-oxazepam 5 μL) reacted with three different concentrations of oxazepam-HRP (1000 μL). (a) Negative sample (b) 0.5 μg/mL of oxazepam-HRP (c) 1 μg/mL of oxazepam-HRP (d) 1.5 μg/mL of oxazepam-HRP.

The images in Figure 5-16 show that the intensity of light produced by antigen–antibody reaction was increased by raising the concentration of antigen–HRP sample (see Table 5-5). A possible reason could be enhancing the chemiluminescence reaction by increasing the concentration of antigen-HRP decreases the number of un-bonded antibodies on the surface of GNP-NH₂. However, the antigen-antibody reaction still occurred just on the edge of the surface of silica monolithic columns coated by GNP-NH₂ because the top surface of silica rod is possibly not even or flat well.

Table 5-5 RLU-values for three silica monolithic columns coated by GNP-NH₂-anti oxazepam reacted with three different concentrations of oxazepam-HRP

Monolith	GNP μL	Anti oxazepam μL	Antigen (oxazepam) -HRP μg/mL	RLU ^{sd}
b-TMOS	10	5	0.5	4.000 ± 0.13
c-TMOS	10	5	1	9.500 ± 0.58
d-TMOS	10	5	1.5	23.500 ± 0.53

^{sd}Values represent means ± SD of 3 experiments

In order to avoid this problem, the next procedure used a new mould for monolithic fabrication, which would be able to localize the antigen-antibody reaction just on the top point of the silica surface where the GNP-NH₂ could be coated. The shape of the top surface of silica monolithic column using microwave heating for fabrication (see section 2.1.2) was changed from cylindrical to conical. The top point on the cone shape of silica monolithic column was coated by GNP-NH₂ (5 μL).

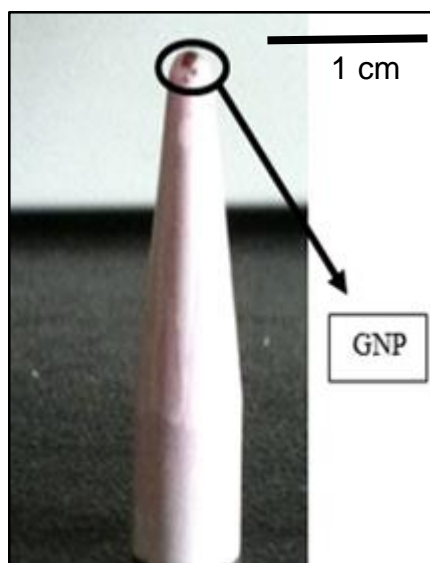


Figure 5-17 Images of cone shape TMOS silica monoliths coated by GNP-NH₂ using microwave heating during gel formation step for 11 min.

Immobilisation of the antibodies on the GNP-NH₂ coating the top surface of the cone shaped silica monoliths was carried out according to the procedure described in section (5.3.5), and the evaluation of those monoliths (see Figure 5-17) was also carried out using the chemiluminescence based immunoassay (see Figure 5-18). This experiment was repeated three times.

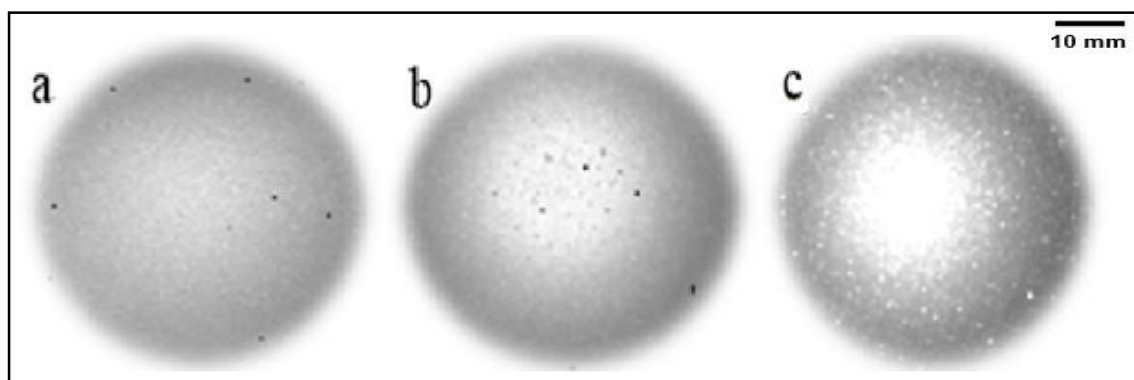


Figure 5-18 Different images for cone shaped silica monoliths coated by gold nanoparticles (GNP 5 µL + anti-oxazepam 5 µL) reacted with three different concentrations of oxazepam-HRP (1000 µL). (a) 0.5 µg/mL of oxazepam-HRP (b) 1 µg/mL of oxazepam-HRP (c) 1.5 µg/mL of oxazepam-HRP.

Table 5-6 RLU-values for three cone shaped silica monolithic columns coated by GNP-NH₂-anti oxazepam reacted with three different concentrations of oxazepam-HRP.

Monolith	GNP μL	Anti-oxazepam μL	Antigen (oxazepam-HRP) μg/mL	RLU ^{sd}
a-TMOS	5	5	0.5	5.130 ± 0.11
b-TMOS	5	5	1	9.840 ± 0.43
c-TMOS	5	5	1.5	27.325 ± 0.5

^{sd}Values represent means ± SD of 3 experiments

These images for the top surfaces of the cone shaped silica monoliths coated by GNP-NH₂ show that the efficiency of using this method for extraction and detection of drugs of abuse was improved, and the intensity of light produced by antigen-antibody reaction was also enhanced and increased in response to an increase in the concentration of antigen-HRP that attached to the antibody present (see Table 5-6). The main reason for this could be by changing the shape of the monolithic silica column to a cone made the area of antigen antibody reaction very small and more effective. However, the size of the top surface of the cone shaped silica monolithic column minimizes the ability of this column to detect more than one type of drugs of abuse at the same time. For this reason, the next procedure used another type of mould for fabrication of the silica monolith to make the top surface area for antigen-antibody reaction much bigger and more suitable for detecting more than one type of drugs of abuse at the same time.

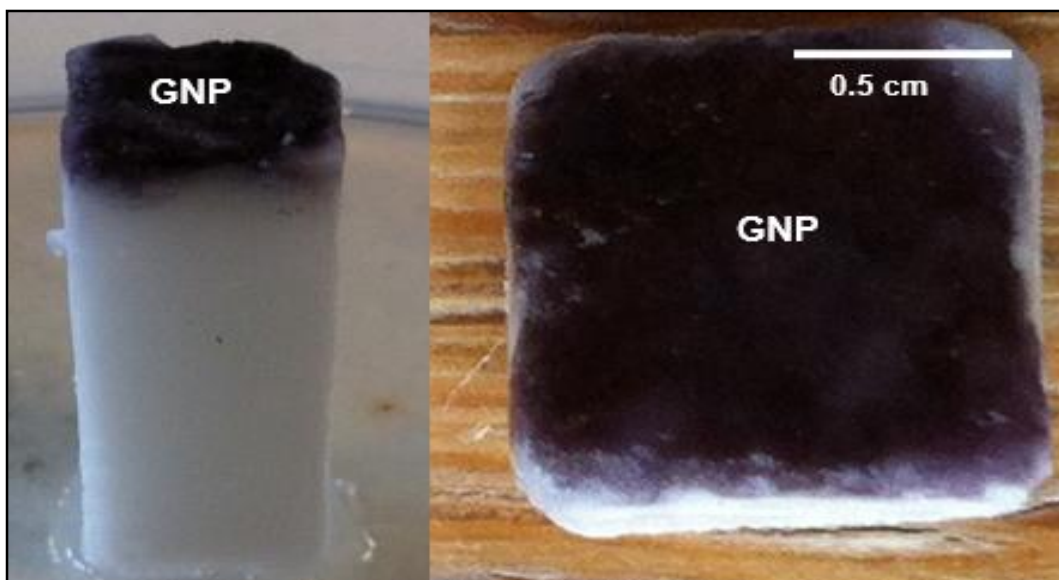


Figure 5-19 Square surface of silica monolithic column coated with gold nanoparticles.

In this work silica monolithic column was fabricated inside a plastic cuvette that was a small tube with a square cross section (see section 2.1.2). The top surface of the monolithic column was physically modified by GNP-NH₂.

In order to immobilise the anti-drug of abuse on the GNP-NH₂ coated square top surface of the silica monolithic column used the procedure explained in section 5.3.5. In addition, its efficiency was also tested by the chemiluminescence based immunoassay. This experiment was repeated three times.

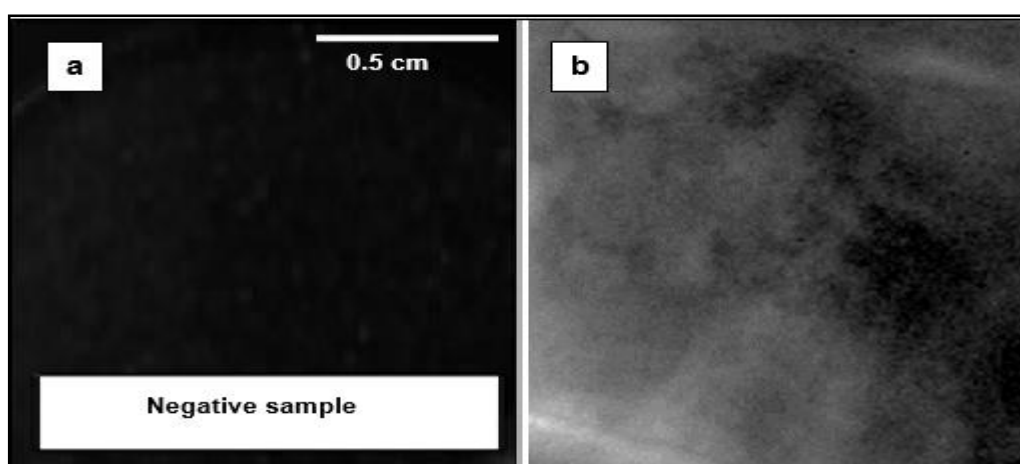


Figure 5-20 Images for the top square surface of the silica monolithic column coated by (GNP-NH₂ 50 μ L + anti-oxazepam 5 μ L) reacted with a-) negative sample b-) oxazepam-HRP 0.5 μ g/mL.

The image of the top of the square surface of the silica monolithic column coated by GNP-NH₂ proved the effectiveness of using this method for extraction and detection of drugs of abuse at the same time. The spreading of light over the top square surface of silica monolith produced by (antigen-HRP)-antibody reaction was obvious (see Figure 5-20). Changing the shape of monolithic silica column to a square enabled the area of antigen antibody reaction to be much larger and more appropriate for the detection of more than one type of drugs of abuse.

The next experiment was performed by using an artificial urine sample and two types of antibodies and antigens-HRP (amphetamine and methamphetamine). The top surface of the silica based monolith coated by 50 μ L gold nanoparticles was divided into two sides, in order to immobilise 5 μ L anti-amphetamine in side (I) and 5 μ L anti-methamphetamine in side (II). The urine sample (1000 μ L) included the same concentration of both antigens labelled with HRP (0.5 μ g/mL), which were injected into the silica monolithic column at a flow rate of 50 μ L/ min. The luminol and hydrogen peroxide reaction was took place and emitted light when the antibodies bound to their type of antigen. The resulting light from (antigens-HRP)-antibodies reactions was recognised using the CCD camera (this experiment was repeated 3 times), and the images are shown in Figure 5-21.

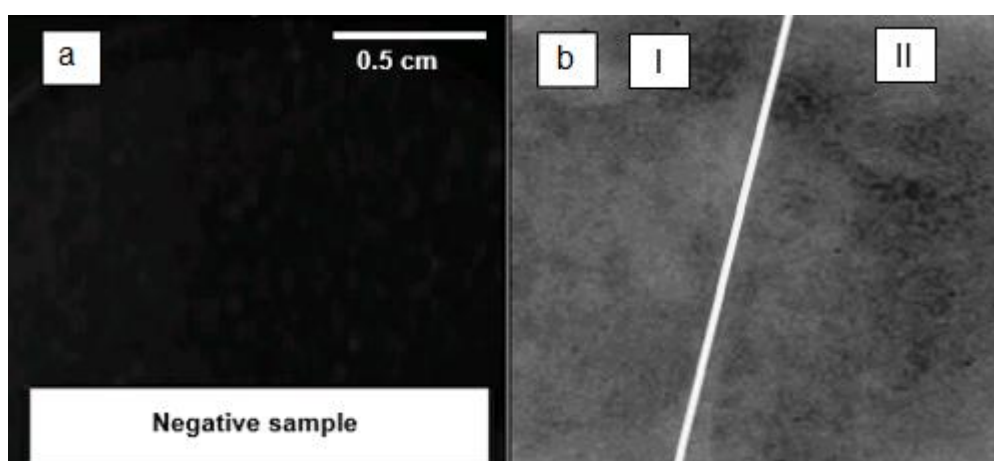


Figure 5-21 Images for the divided square surface of the silica monolithic column coated by GNP-NH₂ 50 μ L + anti-amphetamine 5 μ L in side (I) and anti-methamphetamine 5 μ L in side (II) reacted with a) negative sample b) amphetamine-HRP 0.5 μ g/mL in side (I) and methamphetamine-HRP 0.5 μ g/mL in side (II).

The image of the divided square surface of silica monolithic column coated by GNP–NH₂ showed that the intensity of light produced by antigen–antibody reaction was similar on both sides (see Table 5-7), and the spread of light on both sides was also well distributed (see Figure 5-21). The main reason for this could be the increase in the immobilisation of anti-drugs of abuse on the upper surface of the monolithic column, due to a square shape, improved the orientation of anti-drugs of abuse and the efficiency of antigen antibody reaction.

Table 5-7 RLU-values for three divided square shape silica monolithic columns coated by GNP-NH₂ + anti-amphetamine and anti-methamphetamine and detected same concentration from amphetamine-HRP and methamphetamine-HRP.

Monolith	GNP μL	Anti-amphetamine and anti-methamphetamine μL	antigen-HRP μg/mL	RLU ^{sd}
b-TMOS (I)	50	5	0.5 amphetamine	4.130 ± 0.21
b-TMOS (II)	50	5	0.5 methamphetamine	4.310 ± 0.18

In order to check the sensitivity and selectivity of the silica monolithic column, the square top surface coated by GNP–NH₂ used two types of drugs of abuse antigens (amphetamine and methamphetamine) with different concentrations in the artificial urine sample. The top surface of silica based monolith coated by gold nanoparticles was divided into two sides to immobilise 5 μL anti-amphetamine in side (I) and 5 μL anti- methamphetamine in side (II).

The urine sample (1000 μL) containing different concentrations of two antigens 0.5 μg/mL amphetamine-HRP (I) and 1 μg/mL methamphetamine-HRP (II) was then injected into the silica monolithic column at a flow rate of 50 μL/ min. Next, the luminol and hydrogen

peroxide reaction took place and produced light when the antibodies bound to their type of antigen. The resultant light from the antigen-antibody reaction was recognised by CCD camera. This experiment was repeated 3 times.

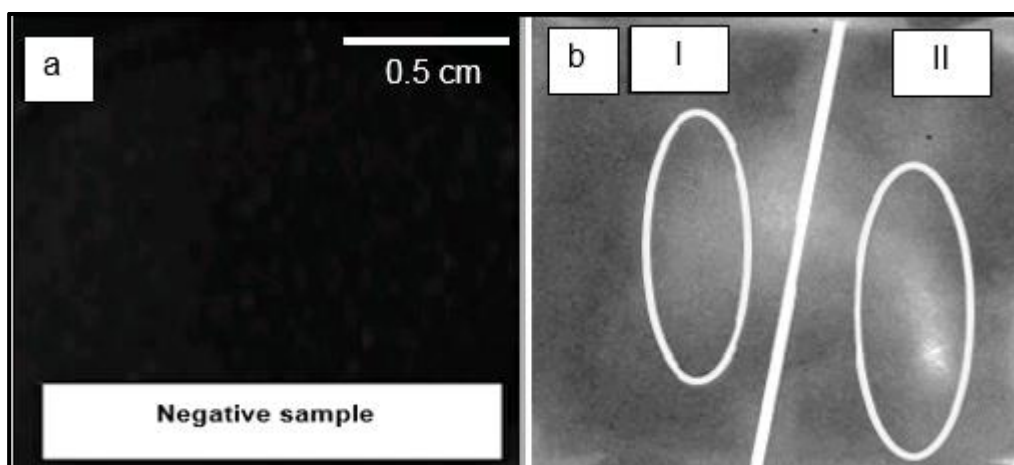


Figure 5-22 Images for the divided square surface of the silica monolithic column coated by GNP-NH₂ 50 μ L + anti-amphetamine 5 μ L in side (I) and anti-methamphetamine 5 μ L in side (II) reacted with a) negative sample b) amphetamine-HRP 0.5 μ g/mL in side (I) and methamphetamine-HRP 1 μ g/mL in side (II).

The image of the divided square surface of silica monolithic column coated by GNP-NH₂ showed the variation in the intensity of light produced by antigen-antibody reaction in side (I) (0.5 μ g/mL) and side (II) (1 μ g/mL) (see Figure 5-22).

Table 5-8 RLU-values for three divided square shape silica monolithic columns coated by GNP-NH₂ + anti-amphetamine and anti-methamphetamine and detected different concentrations from amphetamine-HRP and methamphetamine-HRP.

Monolith	GNP μ L	Anti-amphetamine and anti-methamphetamine μ L	antigen-HRP μ g/mL	RLU ^{sd}
b-TMOS (I)	50	5	0.5 amphetamine	4.260 \pm 0.42
b-TMOS (II)	50	5	1 methamphetamine	7.560 \pm 0.67

The reason for that was increased the amount of antigen-HRP in the side (II) resulted in a raise the antigen–antibody reaction , whereas decreasing the amount of antigen-HRP led to a reduction in the antigen–antibody reaction and the intensity of light in side (I) (see Table 5-8). The spreading of light on the both sides was expected; however, the antigen antibody reaction also occurred in the area between sides (I) and (II) in Figure 5-22.

5.4 Summary

The use of GNP within the silica structure enabled microwave heating to reduce the gelation time to 5 min, but the surface area of those monoliths decreased compared to the same non-embedded silica monoliths. In addition, using microwave heating during gel formation process causes a degradation for amine groups linked to the surface of GNP. Choosing to modify the top surface of silica columns with GNP did not affect the internal structure of silica monoliths. In addition, initial successes for silica monolithic column coated with GNP-NH₂ in detecting drugs of abuse showed a significant problem due to the location of antigen-antibody reaction on the edge of surfaces.

Under optimised conditions, the fabrication of silica monoliths into a cone shape did improve the efficiency of the method of detection. A square shaped monolith produced a higher surface area for antigen-antibody reaction compared to previous monoliths.

Finally, it is clear from the results that the sensitivity and selectivity of this method for extracting and detecting more than one type of drugs of abuse is possible. However, this method requires more optimisation to be more efficient, especially when attaching the antibody to the silica surface.

**6 Using microwave heating for fabrication
graphene monoliths and graphene silica
monoliths**

(Chapter 6)

6.1 Introduction

In recent years graphene has attracted the interest of scientists due to its physicochemical properties, such as superb thermal conductivities of $5000 \text{ W m}^{-1} \text{ K}^{-1}$, extraordinary electro catalytic activity, high stiffness and high-speed electron mobility of $200000 \text{ cm}^2 \text{ V}^{-1} \text{ s}^{-1}$ at room temperature, high specific surface area (SSA) of $2600 \text{ m}^2 \text{ g}^{-1}$ and optical properties.^[211]

There are different structures for graphene. A two-dimensional macrostructure can be produced by three different techniques: layer-by-layer assembly, direct chemical vapour deposition and vacuum-assisted filtration.^[212] However, the large accessible area of the graphene nanosheet is sacrificed due to the susceptibility of graphene monolayer membranes to restack and aggregate as a result of hydrophobic interactions, strong p-p interactions and van der Waals forces.^[203] To overcome this problem, three-dimensional (3D) graphene-based macrostructures have been developed, including hydrogel and aerogels. Three-dimensional graphene not only has large surface areas, but also has several micrometres porous structures.^[203] Recently, many applications have been developed for these materials, such as energy storage and conversion ^[168, 213], catalysis ^[214], water purification ^[215] and oil absorption.^[216]

The great potential of graphene hydrogel and aerogels for the separation and extraction of small molecules has also attracted increasing interest in analytical chemistry. The unique physicochemical properties of graphene makes it suitable to be used as a superior extraction material for solid phase extraction (SPE).^[217] However, the direct use of graphene as SPE material may cause irreversible binding for the target analytes; furthermore, graphene itself may escape from the SPE holder under high pressure.^[218]

This chapter explores ways of retaining the advantageous properties of graphene by reducing graphene oxide (GO) into bimodal silica porous material. This technique might offer access to novel solid phase for extraction and separation sciences.

6.2 Experiment

6.2.1 Graphene monoliths

6.2.1.1 A typical procedure for graphene oxide (GO) reduction

From the literature it was found that the optimum conditions for reducing graphene oxide (GO) by thermal heating was 12 hours at 90 °C. ^[203] Therefore, in the initial work the degree of microwave heating was adjusted to 90 °C during graphene oxide (GO) reduction. A mixture of 5 mL GO suspension (1 mg/mL), 0.125 g of oxalic acid (OA) and 0.25 g of sodium iodide (NaI) was heated by microwave at 90 °C and 130 W. A black graphene monolith was formed after 1 min as shown in Figure 6-1. The fibre optic temperature measurement was used to monitor the temperature of the external surface of the monolith in addition to the infrared sensor fitted in the microwave cavity. In contrast, the black graphene monoliths using conventional thermal heating to reduce GO usually take a very long time to be formed (12 h) according to that procedure reported by Lianbin Zhang in 2012. ^[203] The effect of microwave heating on the time of graphene oxide (GO) reduction was investigated.

6.2.1.2 Characterization of graphene monoliths

During reduction of GO the characterization of the graphene monolith produced through microwave heating was achieved through different approaches. This was based on a digital camera for external morphology, SEM analysis for internal structure, BET and BJH analyses for the physical properties and energy dispersive X-ray (EDX) analysis to find the chemical composition of 3D graphene structure.

6.2.2 Silica monoliths

6.2.3 Fabrication of silica monolith

The silica monolithic columns were fabricated according to the procedure described in section 2.1.2. (Used column number 7/ chapter 3).

6.2.4 Modification of silica monoliths with graphene phase

The modification of silica monoliths with graphene was achieved by reducing the graphene oxide (GO) solution within the silica monolith. The internal pores' structure, within the silica monolithic column, was filled with a mixture of 1 mL of GO suspension (1 mg/mL), 0.025 g of OA and 0.05 g of NaI. Subsequently, the silica monolithic column was heated in a microwave for 1 min at 90 °C and 130 W.

6.2.5 Characterization of modified silica monoliths with graphene phase

During GO reduction the characterization of graphene-silica-monoliths, produced through microwave heating, was achieved by using a digital camera for external morphology, SEM analysis for internal structure and energy dispersive X-ray (EDX) analysis for chemical composition of the graphene-silica-structure. The surface area and macro-pore size of silica monoliths, before and after graphene modification, were obtained using BET analysis. In addition, their performance was also characterized by extraction of the drug of abuse compound known as amphetamine.

6.3 *Result and discussion*

6.3.1 Graphene monoliths

The external morphology of fabricated graphene monoliths through conventional thermal and microwave heating during reduction of GO was obtained using a digital camera. Photographs of graphene monoliths indicated that a reduced time for GO reduction, based

on microwave heating, does not make any difference in the external morphology of the graphene monolith, as seen in Figure 6-1.

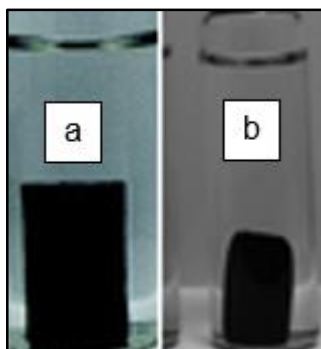


Figure 6-1 Images of graphene monoliths a) using microwave heating during reduction of GO b) using conventional thermal heating for reducing GO.^[203]

The internal structures of graphene monoliths were also investigated by SEM analysis. This was to compare the internal features of the microwave graphene monolith and the 3D graphene structure using conventional thermal heating during reduction of GO.

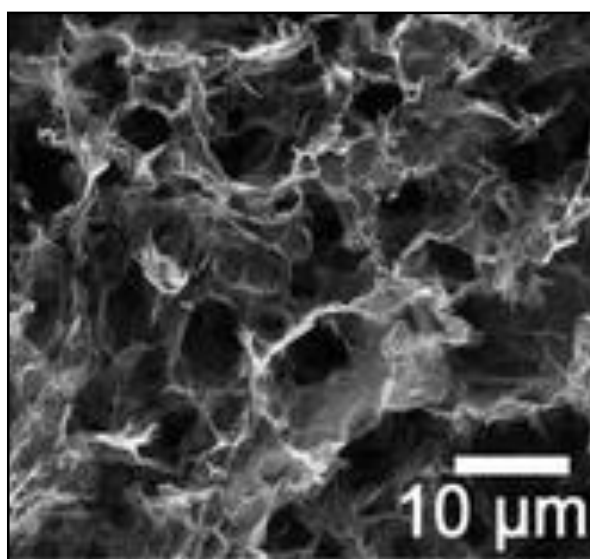


Figure 6-2 Scanning electron micrograph for internal structure of graphene monolith used conventional thermal heating for GO reduction.^[203]

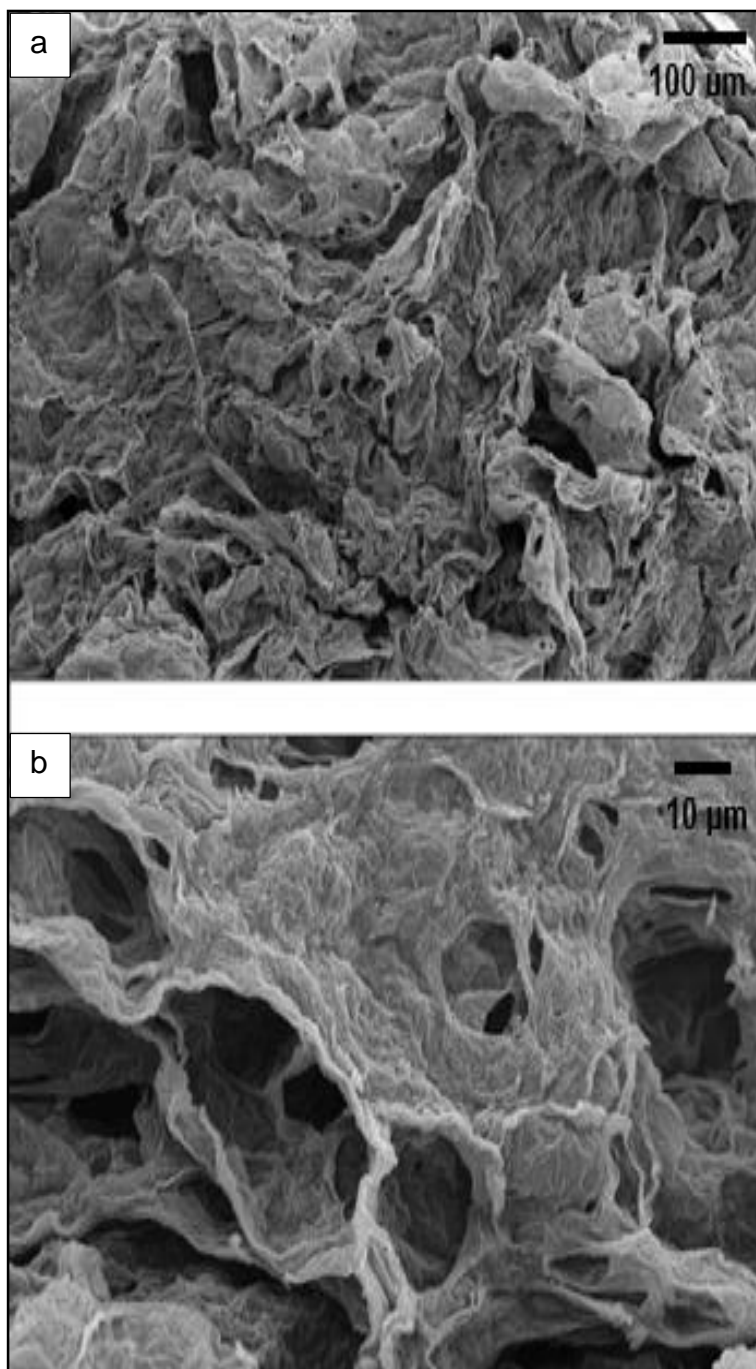


Figure 6-3 Scanning electron micrograph (a and b) for internal structure of graphene monolith used microwave heating for GO reduction.

It was observed that the internal structural of both graphene monoliths were similar (see Figure 6-2 and Figure 6-3), but there were slight differences in the size of the macroporous structure in both of them, as can be seen in Table 6-1. The results indicate the ability of microwave heating to produce graphene monolith in a very short time with an optimal structure, compared to conventional thermal heating methodology.

Table 6-1 Physical properties of the graphene monoliths using microwave and thermal heating methods for GO reduction.

Method of heating	GO concentration mg/mL	Average pore size ^a μm
Thermal	1	4.6 ± 1.3
Microwave	1	7.3 ± 3.4

^a Determined from the SEM images.

The chemical composition of microwave graphene structure was obtained using energy dispersive X-ray (EDX) analysis.

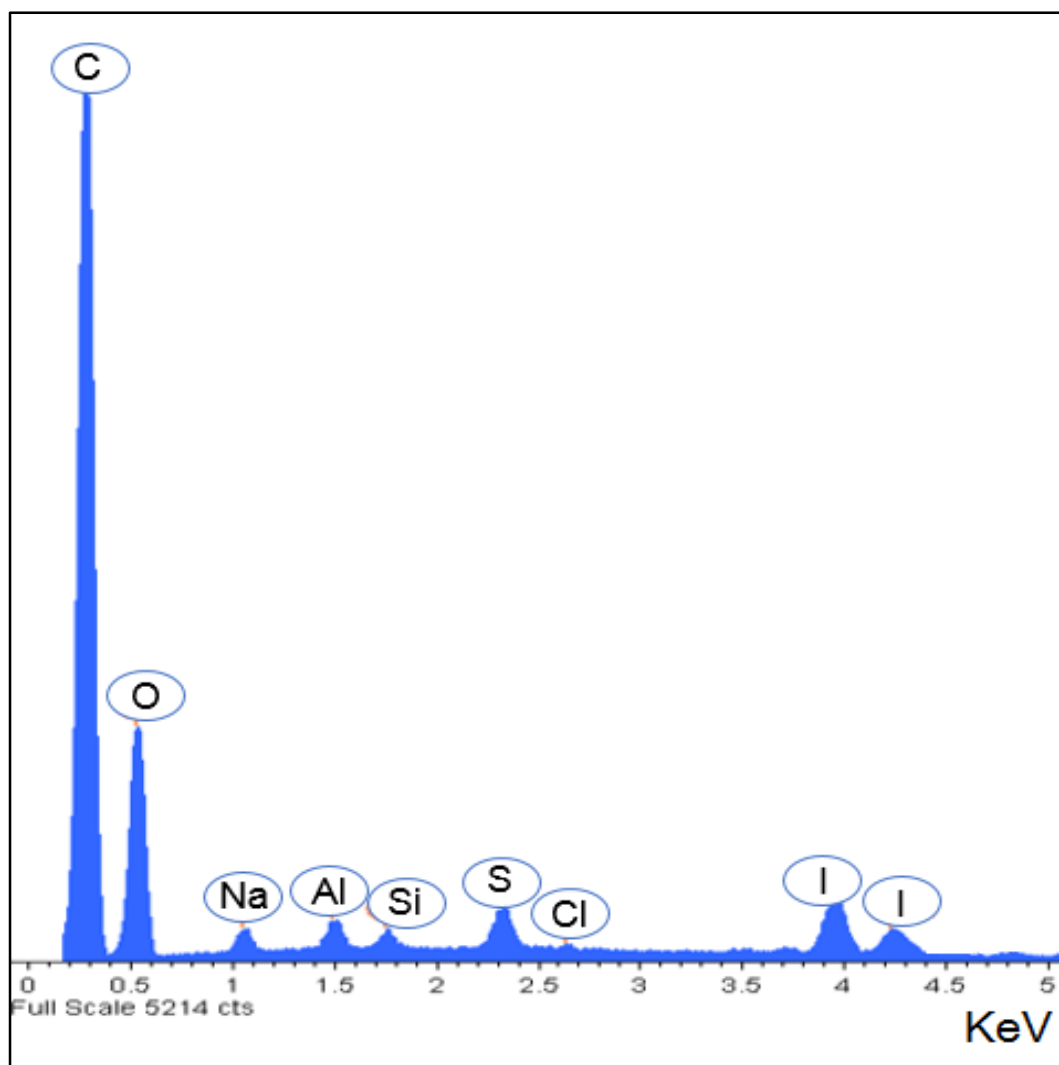


Figure 6-4 Scanning electron micrographs of the graphene monoliths using microwave heating during GO reduction.

Table 6-2 Quantitative EDX analysis for all elements in graphene monolith using microwave heating during reducing of GO.

Spectrum	C	O	Na	Al	Si	S	Cl	Ag	I	Total
sample 1	61.1	30.4	0.8	0.5	0.3	0.9	0.2	0.0	5.8	100.0

The EDX spectra of graphene monolith prepared with microwave heating shows two large peaks for carbon (C) and oxygen (O) on the 3D graphene structure. Smaller peaks for sodium (Na), aluminium (Al), silicon (Si), sulphur (S), chlorine (Cl) and iodine (I) were also observed (see Figure 6-4). The smaller peaks were found in the graphene monolith due to using reducing reagents that include sodium iodide (NaI) and oxalic acid (OA) with graphene oxide (GO) suspension. The reduction of GO by microwave heating was performed in an extremely short time. However, the direct use of graphene monolith as a solid phase extractor can lead to the irreversible binding of analytes due to its high hydrophobicity. To avoid this problem, whilst retaining the advantages of graphene, it was decided to modify the surface of silica monolithic column that possess the unique bimodal porous structure with graphene phase.

6.3.2 Graphene-silica monoliths

In this work the silica monolithic column was fabricated and modified with graphene phase according to the procedures explained in sections 2.1.2 and 2.5.2). The modified silica monolithic columns with graphene phase were characterised using digital photograph, SEM analysis, BET analysis and EDX analysis.

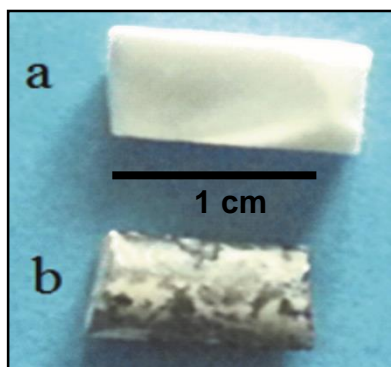


Figure 6-5 Images of silica monoliths a) non-modified silica rod b) modified silica rod with graphene phase (GO 1 mg/mL).

The external morphology of modified silica monolithic column indicated that the reduction of GO within the silica structure was achieved, which the black colour of graphene becoming visible (see Figure 6-5). The formation of a graphene structure inside the silica monolithic column was also confirmed by SEM analysis.

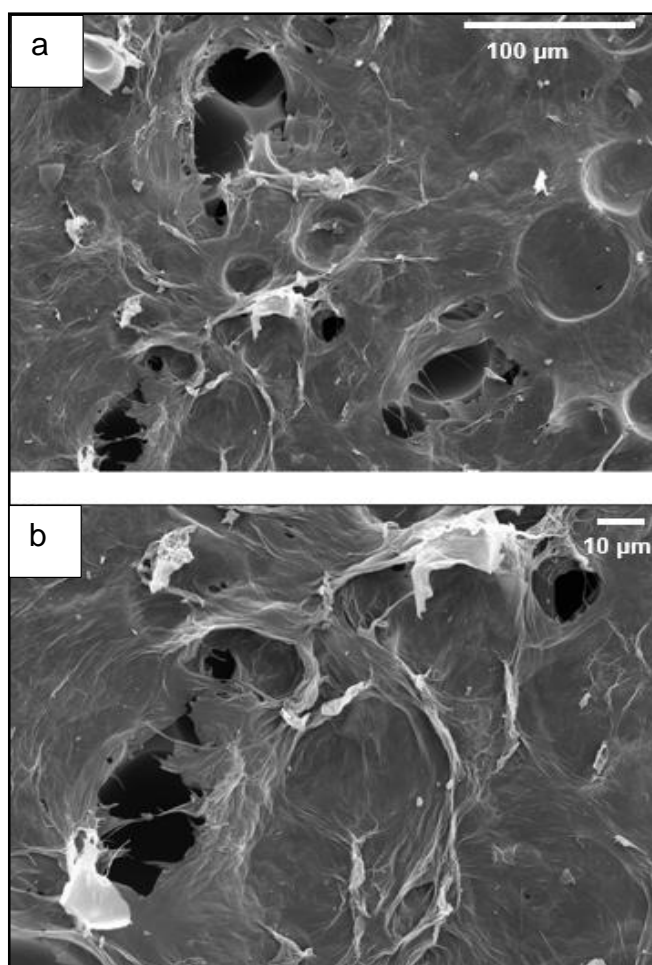


Figure 6-6 Scanning electron micrograph (a and b) for modified silica monoliths with graphene phase (GO 1 mg/mL).

From SEM images it was observed that the internal porous structures of silica monolithic column were blocked by graphene phase, as can be seen in Figure 6-6.

The efficiency of using microwave heating during modification of silica monoliths with graphene phase was investigated using EDX analysis.

The EDX result shows that tiny peaks of carbon (C), sodium (Na), aluminium (Al) and iodine (I) were detected on the internal surface of silica monolithic column after 10 seconds, when using microwave heating at 90 °C and 130 W. The peak of carbon (C) in the graphene silica surface was raised by increasing the time of microwave heating up to 60 seconds at 90 °C and 130 W, as can be seen in Figure 6-7 and Figure 6-8.

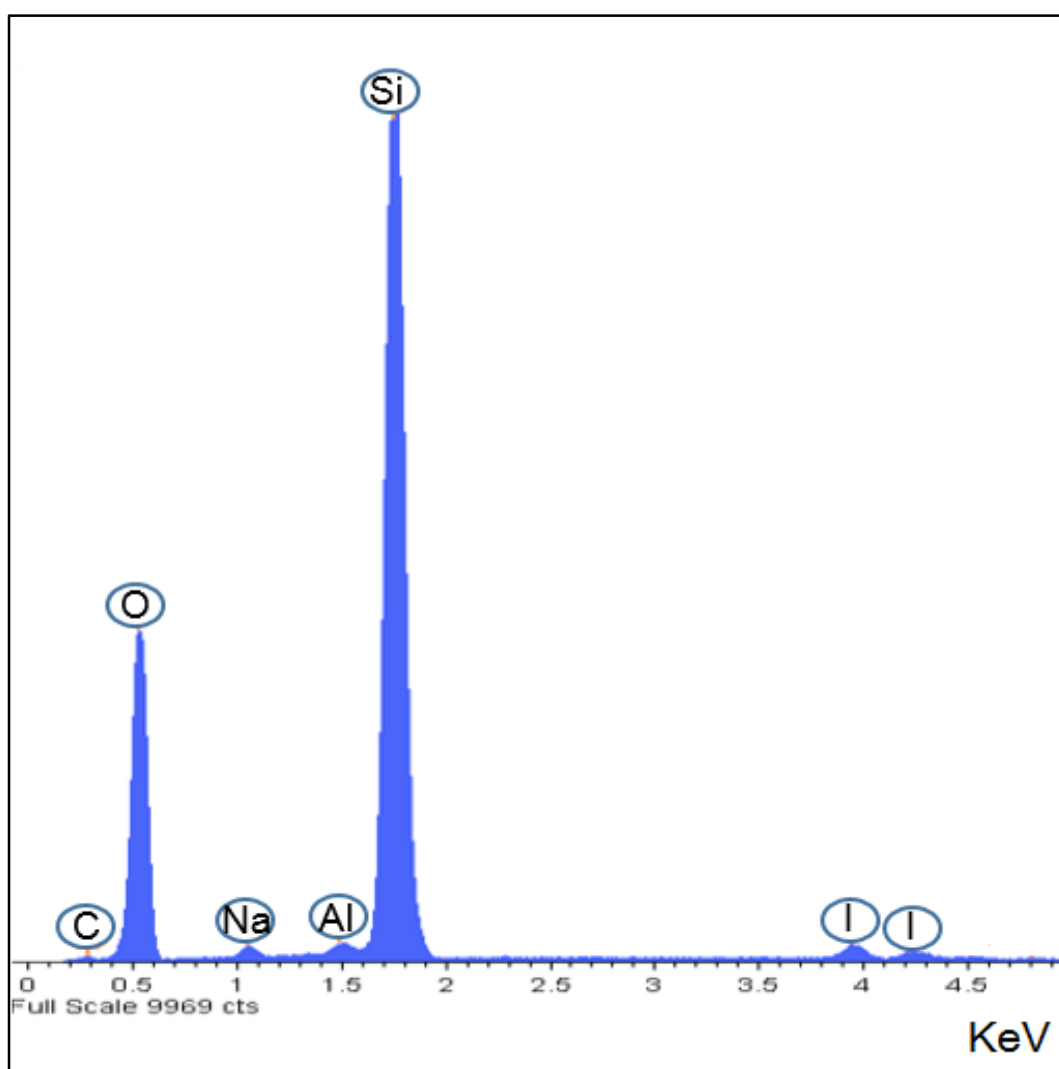


Figure 6-7 EDX spectra of silica-based monolith modified with graphene phase using microwave heating for 10 seconds at 90 °C and 130 W.

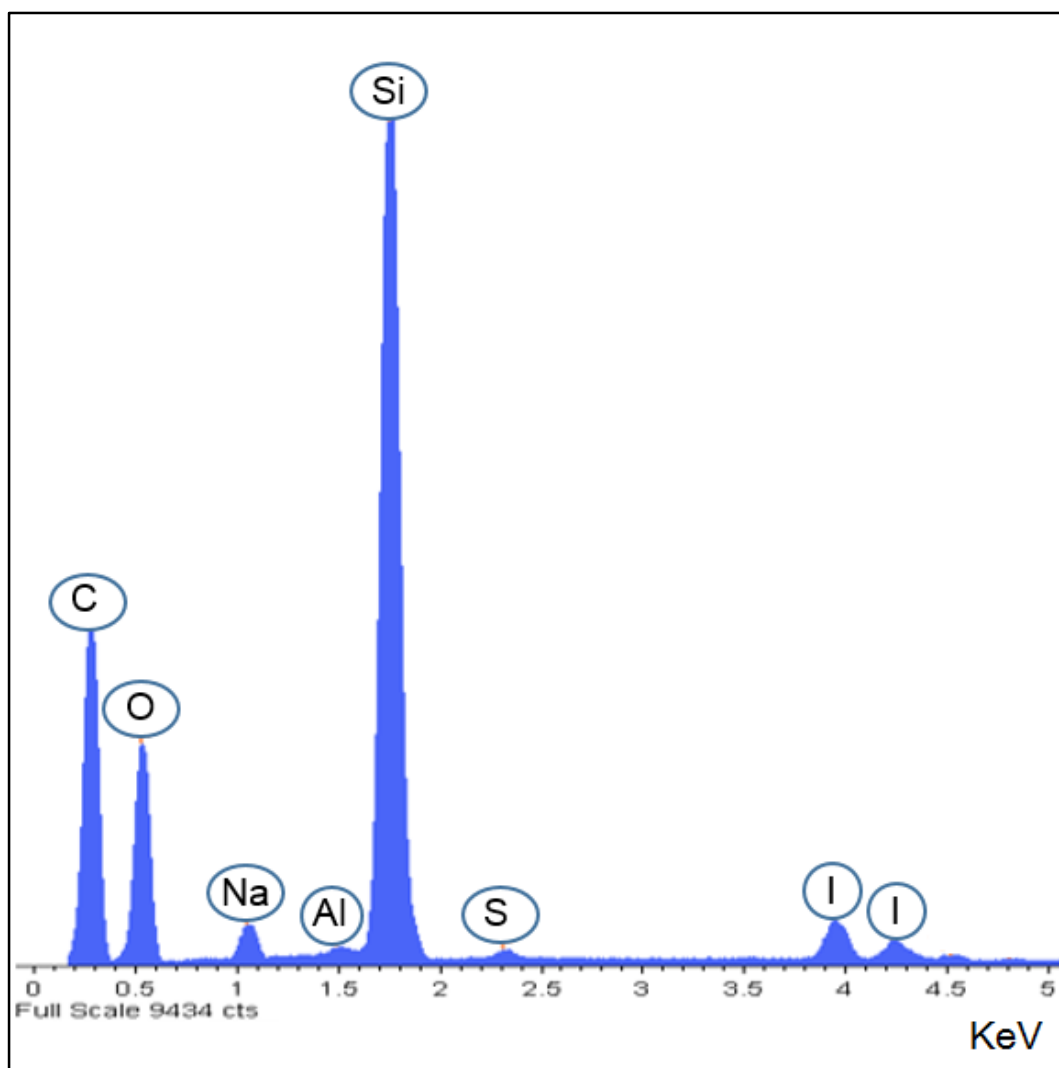


Figure 6-8 EDX spectra of silica-based monolith modified with graphene phase using microwave heating for 60 seconds at 90 °C and 130 W.

The graphene silica monolith using microwave heating was obtained in a very short time (1 min), however, formation of a graphene structure within the silica monolith blocked macro porous structure and produced very high back pressure. The main reason could be the concentration of the GO suspension, which was very high (1 mg/mL). In order to solve this problem, the next procedure reduced the concentration of GO suspension to 0.5 mg/mL. The resultant graphene silica monolithic columns were then characterised using SEM analysis, BET analysis and EDX analysis.

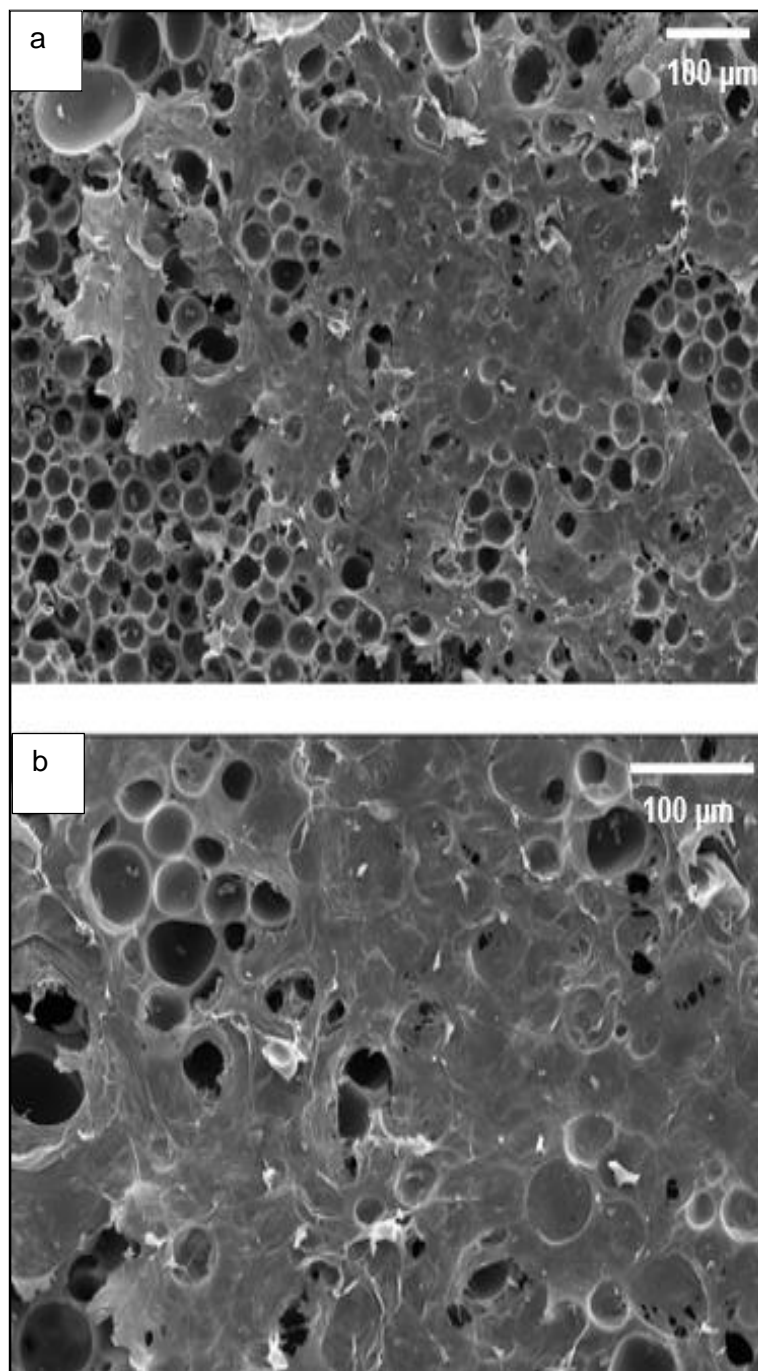


Figure 6-9 Scanning electron micrograph (a and b) for modified silica monolith with grapheme phase (GO 0.5 mg/mL).

SEM micrographs show a decreased number of blocked macro porous structures following a reduction in the concentration of GO to 0.5 mg/mL in the starter mixture, as seen in Figure 6-9. However, spreading the graphene structure over the silica surface covered some macro porous structures, and decreased the surface area of the modified silica monolith as shown in Table 6-3.

Table 6-3 Physical properties of the graphene monoliths using microwave heating methods before and after GO reduction.

Column	Surface area /m ² g ⁻¹	Flow-through pore diameter ^a /μm
7-Microwave monolith (chapter 3)	Value ± SD	Value ± SD
Normal phase TMOS-monolithic column	577 ± 8.4	0.8 ± 2.4
Graphene-TMOS-monolithic column	144 ± 4.4	0.9 ± 5.6

^a Determined from the SEM images.
SD standard deviation

The results indicate the capability of using this graphene silica monolith as stationary phase for extraction of small organic molecules.

The performance of this graphene silica monolith in the extraction of small organic molecules was investigated using amphetamine. A range of amphetamine concentrations (up to 40 μg/mL) were extracted based on grapheme-silica monolithic column (GO 0.5 mg/mL) according to the procedure described in section (2.5.3).

6.3.3 Optimization of amphetamine extraction using graphene silica monolithic column

For individual optimisation experiments the flow rate was varied. In general, the process for amphetamine extraction was as follows:

- 1) The solid-phase matrix was pre-conditioned with 5 mL methanol and purified water at 100 μL/min.
- 2) The standard sample (amphetamine dissolved in a water) was flowed over the solid-phase matrix at 50, 100, and 200 μL/min, resulting in amphetamine binding.
- 3) A purified water was used to wash the solid-phase matrix at a flow rate of 100 μL/min.
- 4) The amphetamine was eluted in 10% : 90% acetonitrile: water with 1 % phosphoric acid (pH 4) at 50 μL/min. All steps described above were performed

sequentially and, from the time of adding the amphetamine to the final step, all solutions that had flowed over the solid-phase matrix were collected. These samples were then analysed using HPLC-UV system using Symmetry C₁₈, 4.6 mm × 250 mm packed with silica particles size 5 µm, at wavelength 254 nm according to the manual of National Drug Testing Laboratories and United Nations Drug Control Programme and the Centre for International Crime Prevention (UNODC). Recoveries were calculated by comparing chromatographic peaks of collected fractions from extracted standard samples with those obtained by direct injection of the same standard solutions in HPLC-UV system. Distinct peak and retention time (6.69 min) for amphetamine standard, injected directly into HPLC-UV, were investigated. No interfering or impurity peaks were observed around the peak of the test compound (see Figure 6-10).

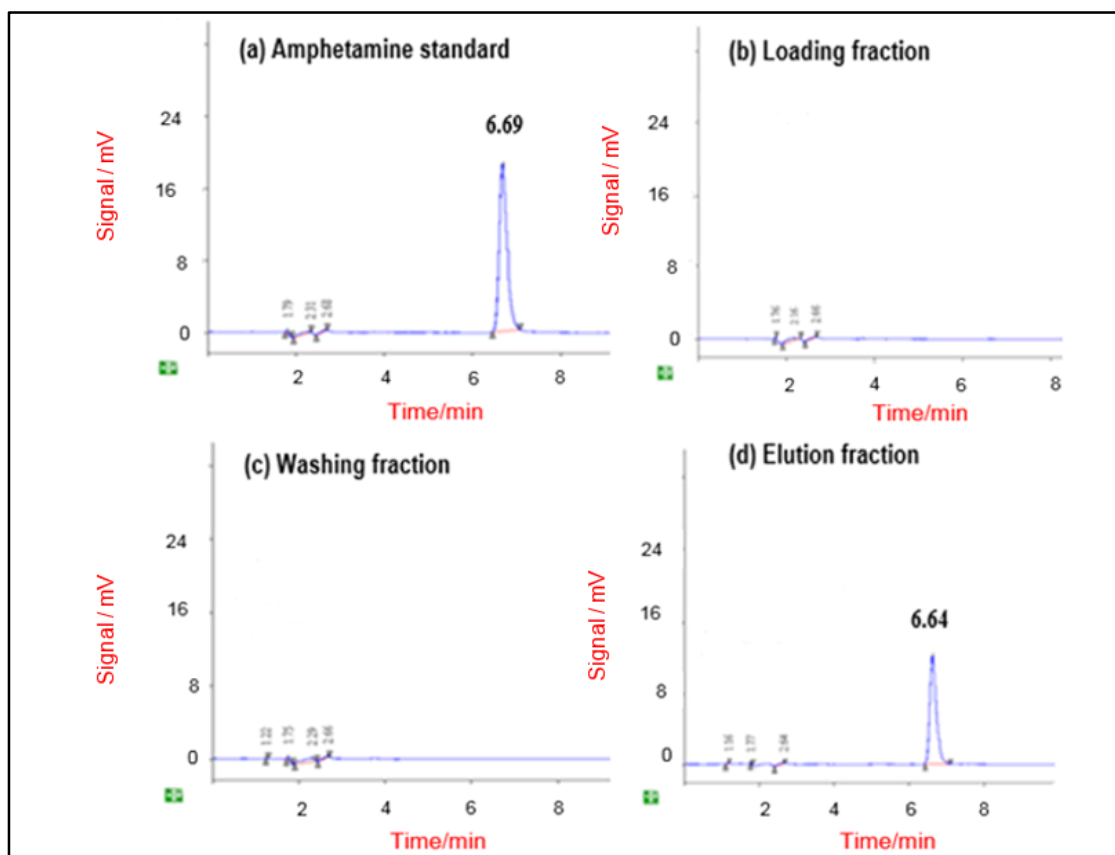


Figure 6-10 Chromatograms of amphetamine and those samples were collected during loading, washing and elution steps; the concentration of amphetamine was 20 µg/mL. All results were obtained from HPLC-UV system under that HPLC conditions described in section 2.5.3.

The results show there is no peak for amphetamine in the collected fraction from the loading and washing steps that indicates the monolith has been trapped (see Figure 6-10 b and c). In the chromatogram of elution fraction (see Figure 6-10 d) there was a high peak at the retention time of the amphetamine standard (6.64 min), but no impurity peaks were observed around it, which confirmed the validity of using this method for extraction of amphetamine.

To find the best flow rate to be used during the extraction of amphetamine by graphene-silica monoliths several flow rates were applied: 50, 100 and 200 $\mu\text{L}/\text{min}$.

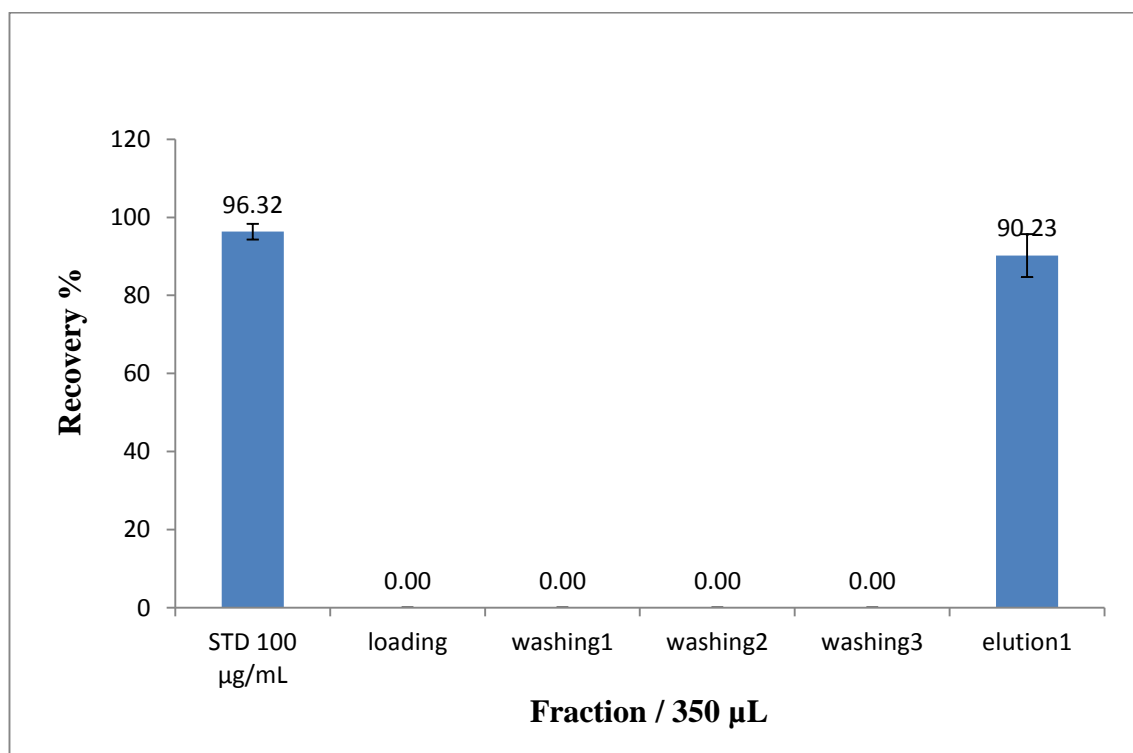


Figure 6-11 Percentage of amphetamine standard (100 $\mu\text{g}/\text{mL}$) extracted using graphene-silica monolithic column (GO 0.5 mg/mL) at flow rate 50 $\mu\text{L}/\text{min}$ compared to direct injection of the same amphetamine standard. The error bars represent the standard deviation of 3 repeat experiments.

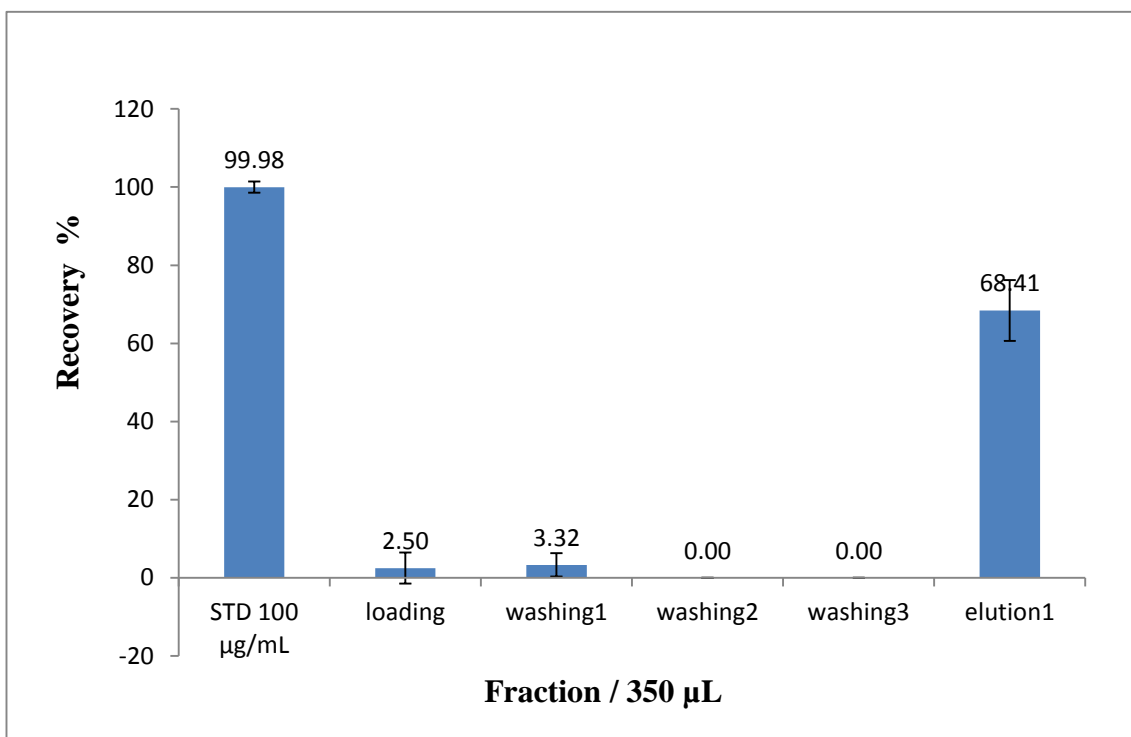


Figure 6-12 Percentage of amphetamine standard (100 µg/mL) extracted using graphene-silica monolithic column (GO 0.5 mg/mL) at flow rate 100 µL/min compared to direct injection of the same amphetamine standard. The error bars represent the standard deviation of 3 repeat experiments.

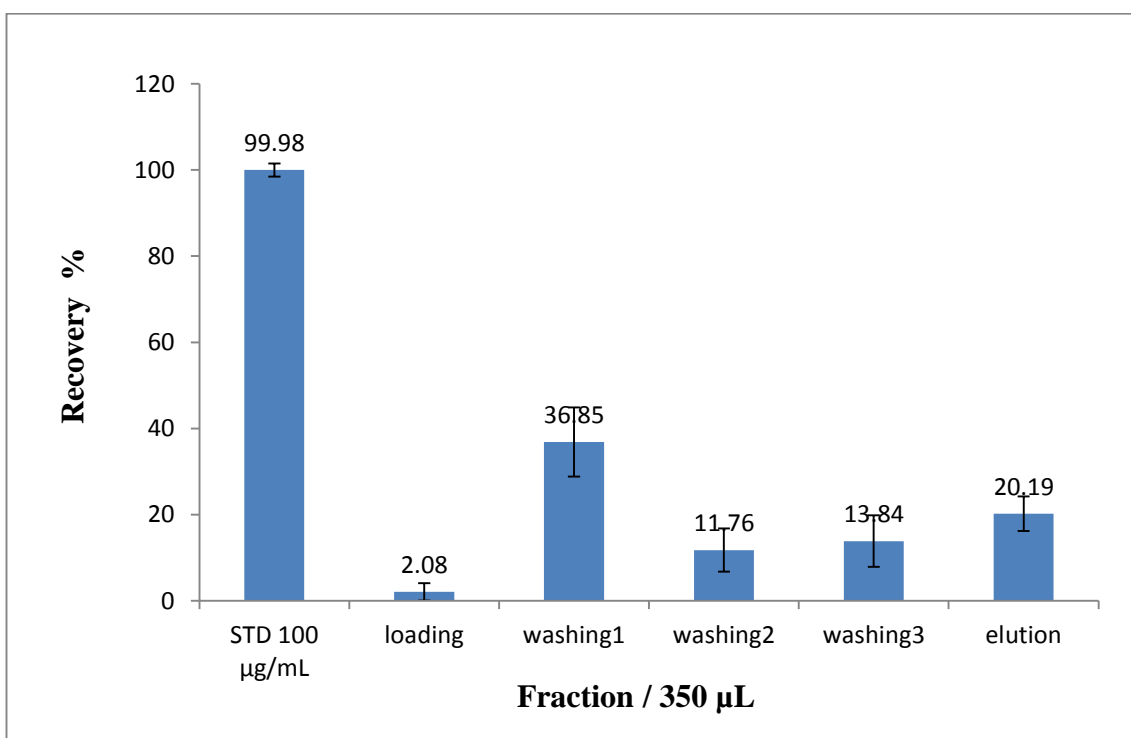


Figure 6-13 Percentage of amphetamine standard (100 µg/mL) extracted using graphene-silica monolithic column (GO 0.5 mg/mL) at flow rate 200 µL/min compared to direct injection of the same amphetamine standard. The error bars represent the standard deviation of 3 repeat experiments.

The results show that increasing the flow rate from 50 $\mu\text{L}/\text{min}$ up to 200 $\mu\text{L}/\text{min}$ resulted in a decrease in amphetamine yield during the elution phase. The best average (90 %) of amphetamine extracted by the graphene silica column was found at a flow rate of 50 $\mu\text{L}/\text{min}$. This can be compared to the amount of amphetamine extracted at flow rates 100 and 200 $\mu\text{L}/\text{min}$, where the averages decreased to approximately 62 % and 20 %, respectively (see Figure 6-11, Figure 6-12 and Figure 6-13). A possible reason could be the decreased time of interaction between the analyte and the internal surface of graphene silica monolith. Increasing the flow rate to 100 $\mu\text{L}/\text{min}$ and 200 $\mu\text{L}/\text{min}$ during extraction led to the release some of amphetamine during loading and washing steps (see Figure 6-12 and Figure 6-13). According to the previous results it was decided to use the flow rate of 50 $\mu\text{L}/\text{min}$ in all subsequent experiments. Noticeably, all percentages were obtained from an overall average of the peak areas obtained.

6.3.4 Calibration curve

A calibration curve was produced using reference standard solutions of amphetamine with a wide range of concentrations 40, 20, 10, 5, 2 and 1 $\mu\text{g}/\text{mL}$. All standard solutions were analysed in triplicate directly by the HPLC at UV wavelength 254 nm, and the mean peak areas were plotted against concentration (see Figure 6-14). Good linearity was observed that meant the calibration curve was useful in quantifying the fraction during extraction experiments.

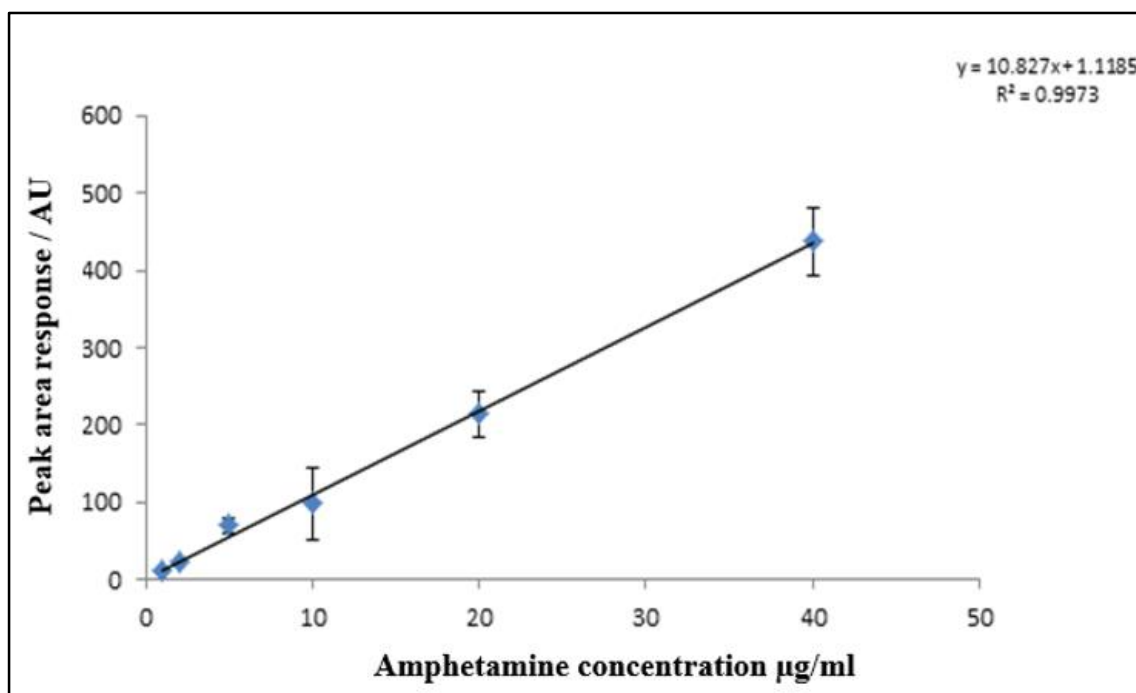


Figure 6-14 Calibration curve for wide range concentrations of amphetamine (40, 20, 10, 5, 2 and 1 $\mu\text{g/mL}$). (W.L. 254 nm). The error bars represent the standard deviation of 3 repeat experiments.

The efficiency of graphene silica monoliths in extraction of amphetamine was evaluated using three standard solutions of amphetamine with low, medium and high concentrations (2, 20 and 40 $\mu\text{g/mL}$). The extraction of all samples was carried out at a flow rate of 50 $\mu\text{L/min}$ and detected at UV wavelength 254 nm. The error bars represented the average of three replicate analyses of the standard samples. All standard deviations were computed using Microsoft Excel software.

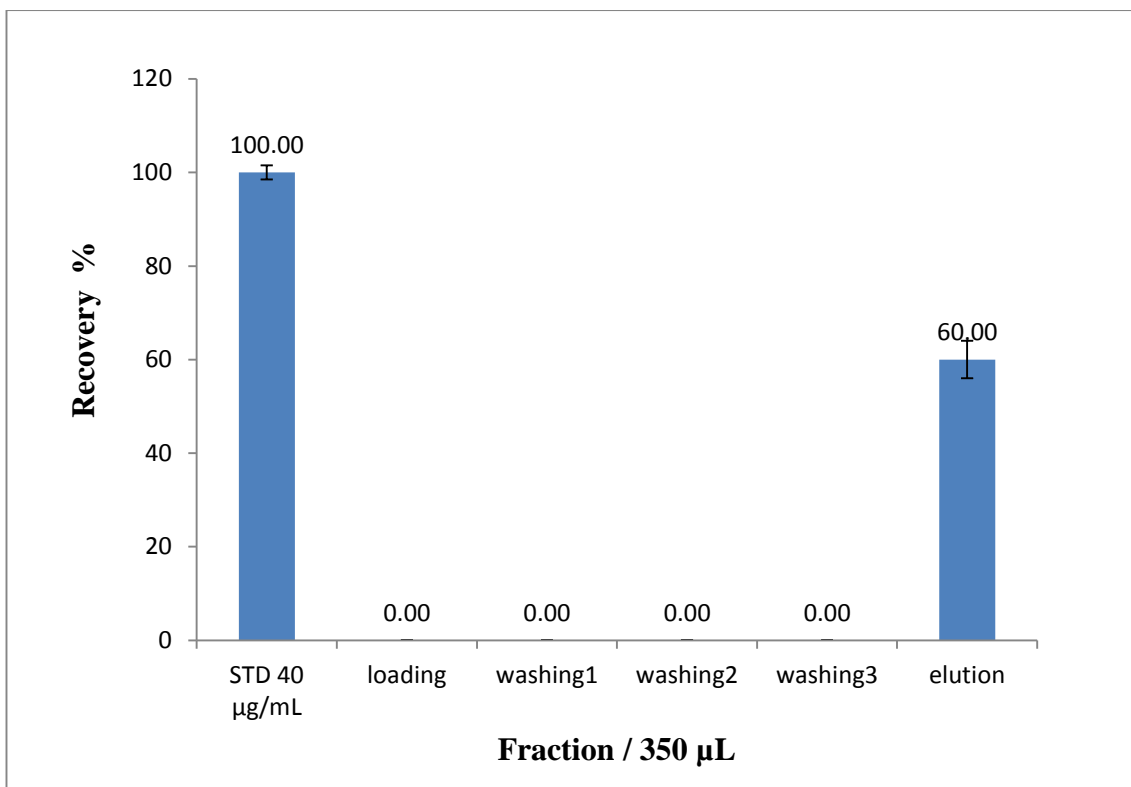


Figure 6-15 Percentage of amphetamine standard (40 µg/mL) extracted using graphene-silica monolithic column (GO 0.5 mg/mL) at flow rate 50 µL/min compared to direct injection of the same amphetamine standard. The error bars represent the standard deviation of 3 repeat experiments.

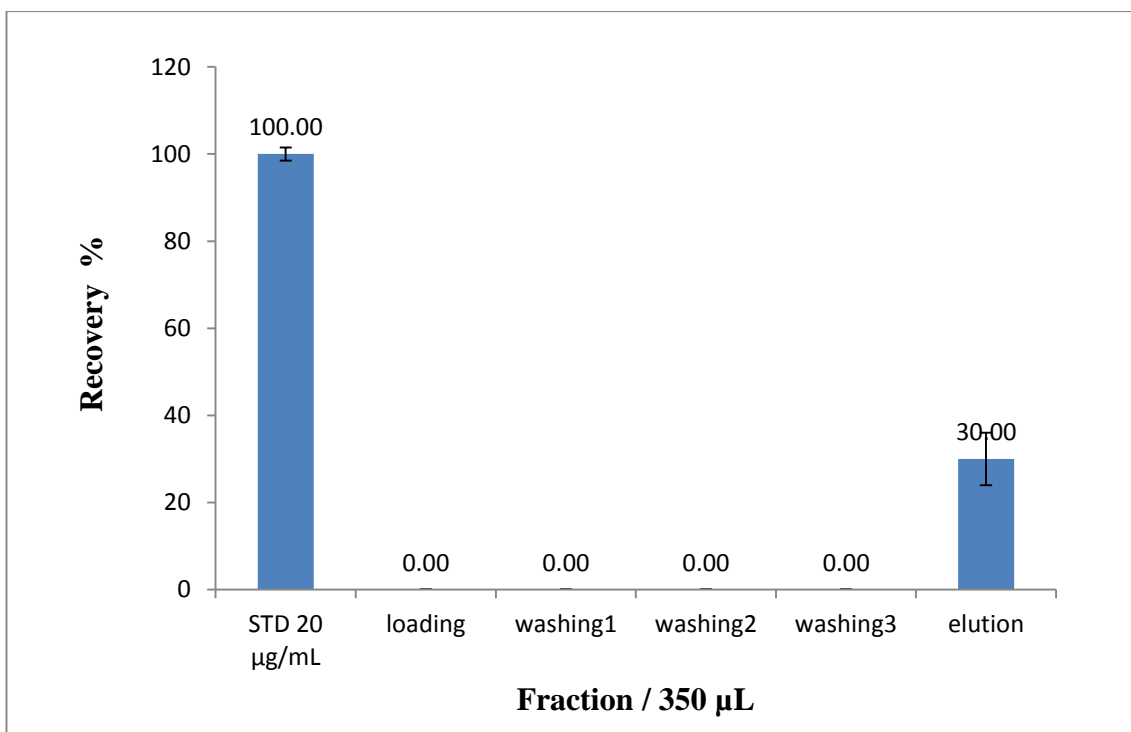


Figure 6-16 Percentage of amphetamine standard (20 µg/mL) extracted using graphene-silica monolithic column (GO 0.5 mg/mL) at flow rate 50 µL/min compared to direct injection of the same amphetamine standard. The error bars represent the standard deviation of 3 repeat experiments.

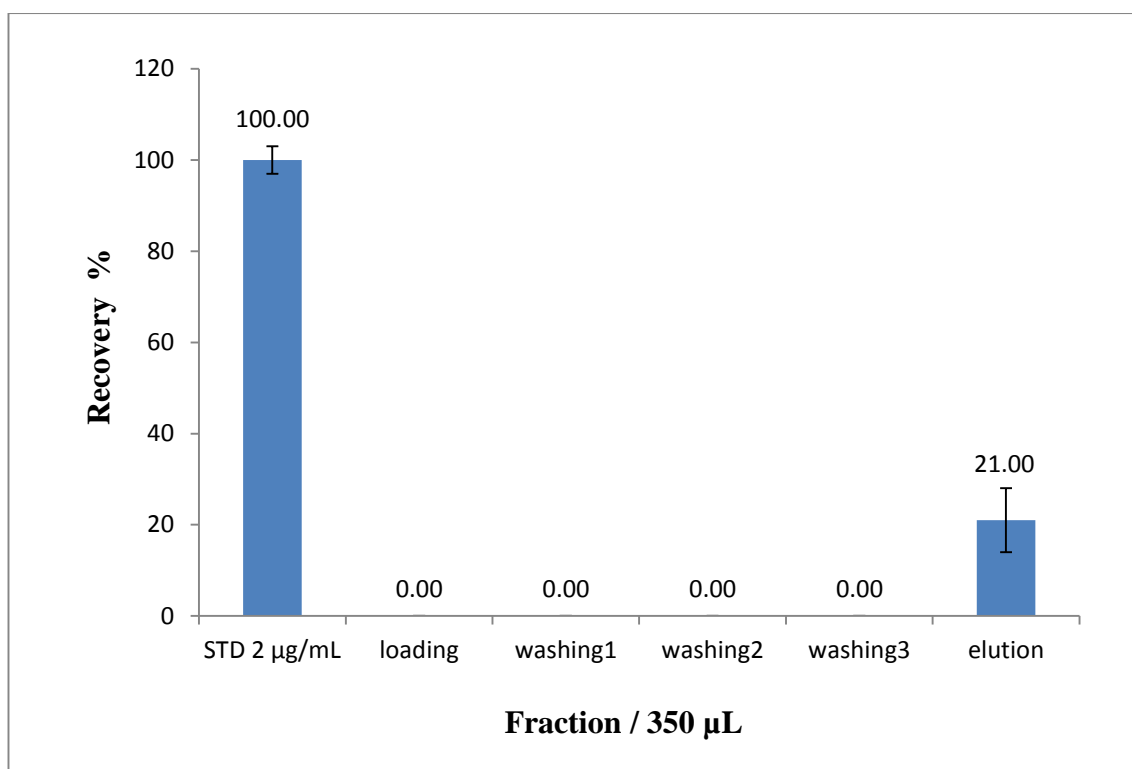


Figure 6-17 Percentage of amphetamine standard (2 µg/mL) extracted using graphene-silica monolithic column (GO 0.5 mg/mL) at flow rate 50 µL/min compared to direct injection of the same amphetamine standard. The error bars represent the standard deviation of 3 repeat experiments.

It is clear from the figures above that increasing the concentration of amphetamine resulted in an increase in amphetamine yield during the elution phase up to 40 µg/mL. In addition, using graphene in the extraction process enabled more effective binding of amphetamine to the silica. However, the amphetamine yield during the elution step was found to be low, with the average between 20 % and 60 % (see Figure 6-15, Figure 6-16 and Figure 6-17). There remains a question mark over the amount of amphetamine lost during the extraction processes using graphene silica monolithic columns. The possible reason could be the direct proportion between the concentration of graphene phase and the adsorption within the silica monolith, which caused irreversible binding of the amphetamine. To solve this problem, the next procedure decreased the concentration of GO to 0.25 mg/mL to control for the thickness of the graphene phase, improve permeability and reduce the amount of irreversible analytes.

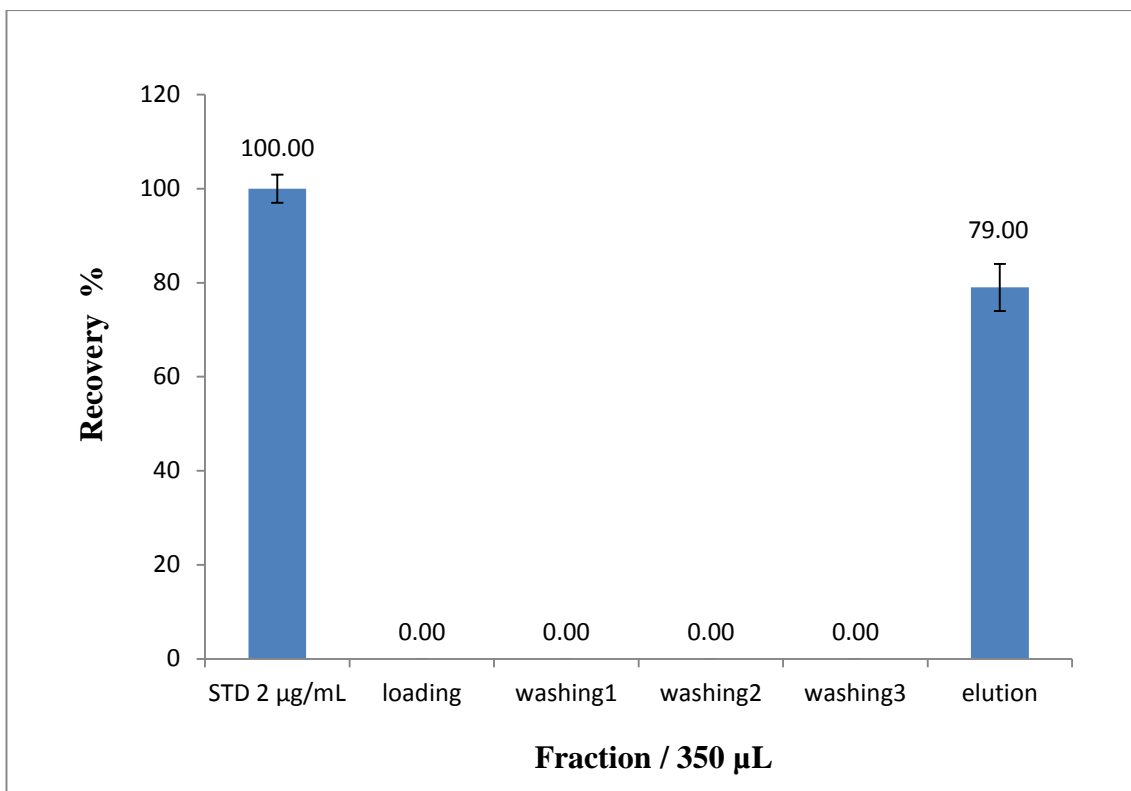


Figure 6-18 Percentage of amphetamine standard (2 µg/mL) extracted using graphene-silica monolithic column (GO 0.25 mg/mL) at flow rate 50 µL/min compared to direct injection of the same amphetamine standard. The error bars represent the standard deviation of 3 repeat experiments.

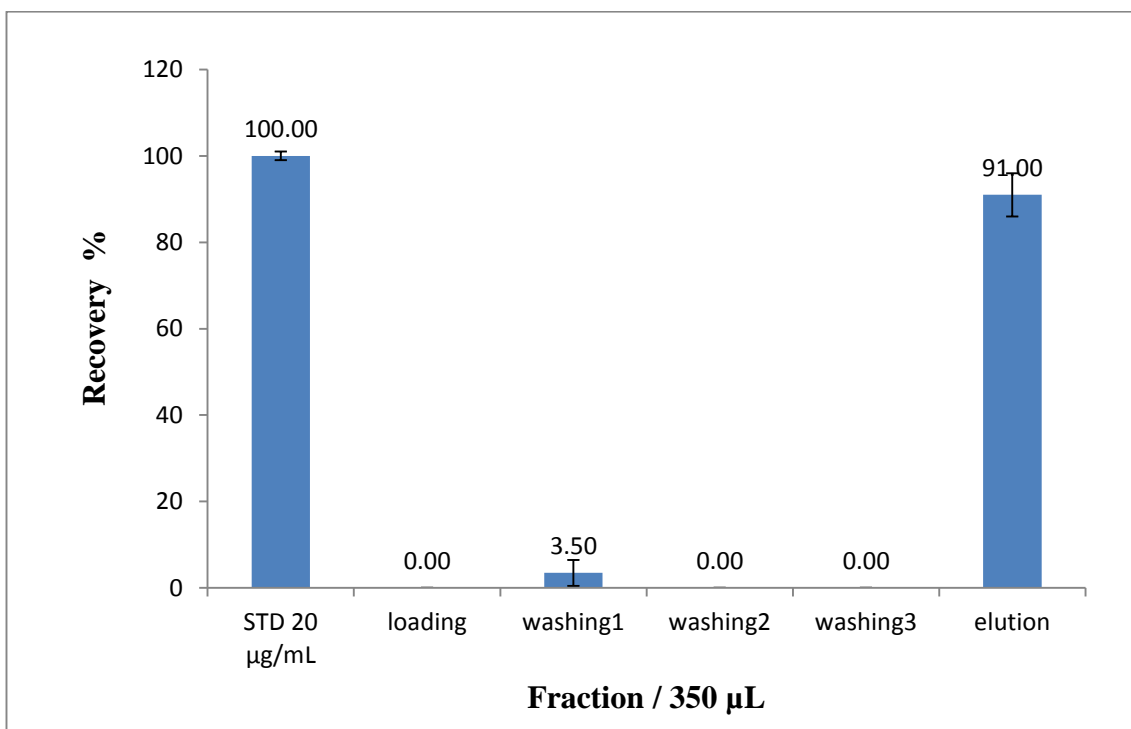


Figure 6-19 Percentage of amphetamine standard (20 µg/mL) extracted using graphene-silica monolithic column (GO 0.25 mg/mL) at flow rate 50 µL/min compared to direct injection of the same amphetamine standard. The error bars represent the standard deviation of 3 repeat experiments.

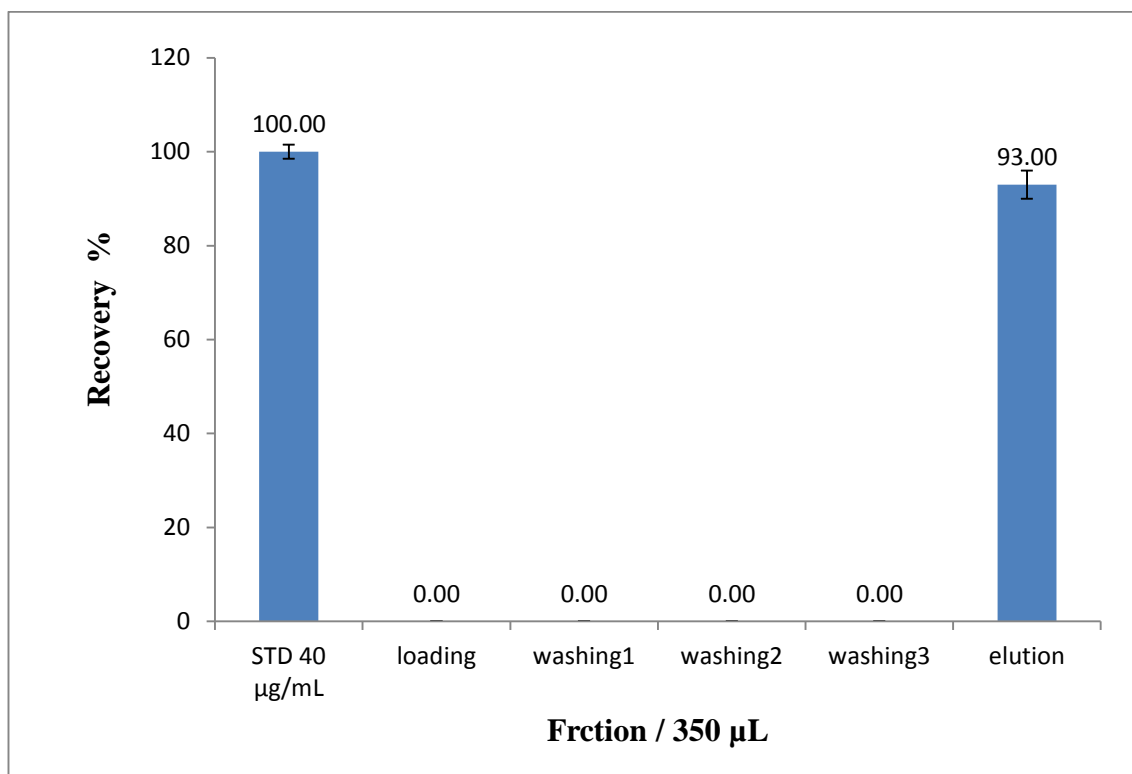


Figure 6-20 Percentage of amphetamine standard (40 µg/mL) extracted using graphene-silica monolithic column (GO 0.25 mg/mL) at flow rate 50 µL/min compared to direct injection of the same amphetamine standard. The error bars represent the standard deviation of 3 repeat experiments.

The results show that the average percentage of extracted amphetamine from the low standard 2 µg/mL sample was 79 %. Increasing the concentration of amphetamine standard to 20 µg/mL led to a slight increase in the percentage of amphetamine extracted 91 % (see Figure 6-19). Finally, the percentage of extracted amphetamine reached 93 % when the concentration of the standard increased to 40 µg/mL (see Figure 6-20). The comparison between the efficiency of extracting the same standard solutions of amphetamine using graphene silica monolith and C₁₈ silica monolithic column was concluded (see Table 6-4).

Table 6-4 Recoveries of three amphetamine standards (low, mid and high) using graphene silica monolith and C₁₈ silica monolith during extraction processes.

Column (SPE)	Compound	Concentration µg /ml	Recovery^m % ± SD
C ₁₈ - TMOS	Amphetamine	2	85 ± 2.27
TMOS-GRAPHENE	Amphetamine	2	79 ± 3.45
C ₁₈ - TMOS	Amphetamine	20	86 ± 7.13
TMOS-GRAPHENE	Amphetamine	20	91 ± 2.41
C ₁₈ - TMOS	Amphetamine	40	94± 2.80
TMOS-GRAPHENE	Amphetamine	40	93 ± 2.95

SD standard deviation

All standard deviations were computed using Microsoft Excel software.

Similar percentages for recoveries were obtained from both monoliths. However, solving the problem of irreversible binding in a graphene silica monolith can improve yield of amphetamine to be superior (100 %). In addition, these results confirm the ability of graphene phase to be used instead of C₁₈ phase during the extraction of small organic molecules.

6.4 Summary

The use of graphene monolith as the solid-phase makes the elution of small organic molecules very difficult due to the high hydrophobicity of the graphene phase. However, using microwave heating during reduction of GO speed up the reaction, which was achieved in 1 min.

The use of graphene phase for modification of silica monoliths enables not only purification but also extraction of amphetamine from a standard solution. A range of graphene silica based monoliths have been investigated for their potential in extracting small organic molecules such as amphetamine. The concentration of GO in the starter mixture, used for modification the silica-based monoliths, is very important as it has a substantial effect on the efficiency of amphetamine extraction and elution processes. The

graphene-silica-monoliths produced by microwave heating showed higher amphetamine extraction efficiency and were easier to produce than thermal heating graphene-silica-monoliths. Despite initial successes in using graphene-silica-monoliths for amphetamine extraction, efficiency studies showed a significant problem with permeability. In addition, blocking of the macro pores structure with graphene phase often led to difficulty with high back pressures during extraction process.

In comparison to C₁₈ silica monoliths, the extraction efficiency of amphetamine by graphene silica monolith provided a similar percentage of recoveries for the same standard solutions. However, the modification of silica surface with C₁₈ phase by microwave heating takes approximately 40 min, whereas the modification of silica monolith with graphene phase can be carried out in just 1 min.

The potential for the method of graphene modification to be optimized to perform drugs of abuse extraction and detection, will be discussed in future work.

7 Conclusion and future work

7.1 *Fabrication of silica monoliths using microwave heating (chapter 3)*

The number of applications of monolithic materials, such as SPE, has increased in recent years, especially for the extraction of drugs of abuse. Nevertheless, the fabrication process of silica monolith is still time-consuming and laborious. In this work, silica monolithic rods were fabricated using microwave heating during the gel formation process. Different microwave conditions were investigated for their potential in the formation of silica monoliths. It was found that the use of microwave heating enables the rapid formation of silica monolithic rods with improved physical characteristics, compared to silica monolithic rods prepared using conventional heating methods. In 2002 Gisele M. Neves^[97] also used microwave heating during the sol-gel process; the fabrication of silica monolith was achieved in 10 min, however, the surface area of the created silica structure was very low (112 m²/g). In this work a high surface area (574 m²/g) was achieved.

Under optimised conditions, microwave heating reduces the gelation time from 4,320 min, in the thermal heated oven methodology, to 11 min producing ideal morphological features.

This work not only confirmed the ability of microwave heating to enhance the gel formation process in a very short time, with no morphological differences from the same monoliths prepared using oven heating method, it also improved the surface area of the microwave produced silica monoliths.

Future work should be carried out to optimise the fabrication of the silica monoliths using microwave heating in order to increase the surface area and the permeability of the monolithic column. In addition, it would also be interesting to investigate different types

of chemical composition, as the internal structure of silica monolith can be affected by any variation on the processing parameters.

7.2 C₁₈ modification of silica monoliths using microwave heating (chapter 4)

Using microwave heating during C₁₈ surface modification produced a greater coverage of functional groups on the silica surface in a reduced time. Many researchers have reported that the performance of C₁₈ silica columns is affected by the number of C₁₈ chains on the silica surface during the modification process. For example, Martin et al. [44] reported that the C₁₈ silica columns used to extract polar and non-polar compounds from biological matrices should have intermediate carbon loading plus some residual silanols. C₁₈ silica monolith is the most common column used for drug extraction, however, the C₁₈ modification process remains time-consuming. In this work the application of microwave heating in C₁₈ surface modification was carried out in order to increase the amount of carbon loading on the silica surface. This was found to improve the extraction efficiency of caffeine and eserine from standard solutions.

The modification of silica monoliths with C₁₈ phase using microwave heating was found to offer a high carbon percentage loading, but at a slightly reduced surface area. The mean recoveries of three caffeine standards using microwave C₁₈ silica monolithic columns were found to be very high 101 % –111 %, in comparison with recoveries of the same standards using thermal C₁₈ columns, which were in the range 42 % – 101 %.

This work indicated that the potential of microwaves (single mode cavity) to control the loading of octadecyl groups on the silica surface during the modification process produces quicker (40 min) and more efficient heating.

Ongoing work should focus on the extraction of more complex samples, such as proteins from biological samples after optimisation of the pore size of the octadecylated silica monolith.

7.3 Modification of silica monolithic column with gold nanoparticles using microwave heating (chapter 5)

The combination of silica monolithic structure with gold nanoparticles was found to offer direct on-column detection of drugs of abuse based on an immunoassay. Many research groups have made this combination between the silica frameworks and gold nanoparticles. However, the reported methods for combining GNP with silica monoliths usually reduced the surface area, closed some porous structure and hydrolysed the functional surface groups during the sol gel process. In this work the potential to use gold nanoparticles for detection, coupled with a silica monolithic column for extraction, produced using microwave heating, was investigated as a sensitive immunological assay. In addition, an investigation of the efficiency in using an immunosensor based on GNP-silica monoliths in the extraction and detection drugs of abuse was carried out simultaneously.

The use of GNP-NH₂ within the silica structure based on microwave heating reduced gelation time to (5 min). Under optimised conditions, the functionalization of GNP with antibodies allowed a cone shaped silica monolith to be used for the direct detection of one type of drug of abuse. Square shape monoliths also allowed several drugs of abuse to be detected at the same time.

This procedure improves the sensitivity and selectivity of modified silica surfaces that are suitable for extracting and detecting more than one type of drugs of abuse at the same time.

Future work could further investigate the extraction of some real forensic samples and use of a reference material with drugs of abuse, in addition to the modification of gold nanoparticles with different functional groups suitable for the extraction of a huge number of analytes.

7.4 Modification of silica monolithic column with graphene phase using microwave heating (chapter 6)

The considerable potential and unique physicochemical properties of a graphene phase in offering the extraction of polar and very-polar compounds from large sample volumes is much easier compared to conventional C₁₈ silica columns. However, the direct use of graphene as SPE material may cause irreversible binding for the target analytes. Furthermore, graphene itself may escape from the SPE holder under high pressure. In 2014 Xiaojia Huang extracted strongly polar aromatic amines (AAs) from water samples using poly (ethylene glycol dimethacrylate/graphene oxide) (EDMA/GO) monolith. However, recoveries of AAs spiked in different matrices ranging from 74.2 % to 105 % and the fabrication process was time consuming.

In this work the generation of GO in a silica monolith using microwave heating was achieved in an extremely short time (1 min). The extraction efficiency of a polar analyte (amphetamine) by graphene-silica monoliths was evaluated using HPLC-UV system. The extraction of amphetamine by graphene silica column was found to be high 93 %, indicating the extraction of non-polar, polar, very polar and water-soluble analytes, based on both hydrophobic and electronic interactions, could be easy and simple using the approach developed. However, the elution of amphetamine from a graphene silica column is still difficult.

Future work would therefore need to investigate the extraction of more types of drugs of abuse from different biological samples using graphene silica monolith. In addition, the modification of graphene silica monolith with different functional groups, suitable for extracting different types of analytes, would be worth future investigation.

8 References

- [1] G. Cooper and A. Negrusz, *Clarke's analytical forensic toxicology*, London, *Pharmaceutical Press*, Second edition, 2013.
- [2] F. Smith, *Handbook of forensic drug analysis*, San Diego, *Elsevier Academic Press*, 2004.
- [3] P. N. Hoaken and S. H. Stewart, *Drugs of abuse and the elicitation of human aggressive behavior*, *Addictive Behaviors*, 2003, 28, 1533-1554.
- [4] E. Kaufman, *The abuse of multiple drugs, definition, classification, and extent of problem*, *The American Journal of Drug and Alcohol Abuse*, 1976, 3, 279-292.
- [5] N. D. Volkow, *Commonly abused drugs chart*, National Institute on Drug Abuse, *Corsini Encyclopedia of Psychology*, 2011.
- [6] A. McBay, *Legal challenges to testing hair for drugs*, *International Journal of Drug Testing*, 1998, 1, 34-42.
- [7] United Nations, *United Nations documents index, January-March 2006*, New York, *United Nations publications*, 2007.
- [8] United Nations Office on Drugs and Crime, *World drug report 2010*, Vienna, *United Nations Publications*, 2010.
- [9] D. A. Armbruster, M. D. Tillman and L. M. Hubbs, *Limit of detection (LOD)/limit of quantitation (LOQ): comparison of the empirical and the statistical methods exemplified with GC-MS assays of abused drugs*, *Clinical Chemistry*, 1994, 40, 1233-1238.
- [10] M. Wood, M. Laloup, M. D. M. R. Fernandez, K. M. Jenkins, M. S. Young, J. G. Ramaekers, G. D. Boeck and N. Samyn, *Quantitative analysis of multiple illicit drugs in preserved oral fluid by solid-phase extraction and liquid chromatography–tandem mass spectrometry*, *Forensic Science International*, 2005, 150, 227-238.

- [11] L. Nováková and H. Vlčková, *Review of current trends and advances in modern bio-analytical methods: chromatography and sample preparation*, *Analytica Chimica Acta*, 2009, 656, 8-35.
- [12] R. Kronstrand, I. Nyström, J. Strandberg and H. Druid, *Screening for drugs of abuse in hair with ion spray LC–MS–MS*, *Forensic Science International*, 2004, 145, 183-190.
- [13] F. E. Ahmed, *Sample preparation and fractionation for proteome analysis and cancer biomarker discovery by mass spectrometry*, *Journal of Separation Science*, 2009, 32, 771-798.
- [14] C. Girod and C. Staub, *Analysis of drugs of abuse in hair by automated solid-phase extraction, GC/EI/MS and GC ion trap/CI/MS*, *Forensic Science International*, 2000, 107, 261-271.
- [15] K. C. Saunders, A. Ghanem, W. Boon Hon, E. F. Hilder and P. R. Haddad, *Separation and sample pre-treatment in bioanalysis using monolithic phases: A review*, *Analytica Chimica Acta*, 2009, 652, 22-31.
- [16] J. J. Pitt, *Principles and applications of liquid chromatography-mass spectrometry in clinical biochemistry*, *The Clinical Biochemist Reviews*, 2009, 30, 19-34.
- [17] K. Saito, R. Saito, Y. Kikuchi, Y. Iwasaki, R. Ito and H. Nakazawa, *Analysis of drugs of abuse in biological specimens*, *Journal of Health Science*, 2011, 57, 472-487.
- [18] G. Vas and K. Vekey, *Solid-phase microextraction: a powerful sample preparation tool prior to mass spectrometric analysis*, *Journal of Mass Spectrometry*, 2004, 39, 233-254.
- [19] R. Dams, M. A. Huestis, W. E. Lambert and C. M. Murphy, *Matrix effect in bio-analysis of illicit drugs with LC-MS/MS: influence of ionization type, sample preparation, and biofluid*, *Journal of The American Society for Mass Spectrometry*, 2003, 14, 1290-1294.

- [20] P. L. Kole, G. Venkatesh, J. Kotecha and R. Sheshala, *Recent advances in sample preparation techniques for effective bioanalytical methods*, Biomedical Chromatography, 2011, 25, 199-217.
- [21] N. Raikos, K. Spagou, M. Vlachou, A. Pouliopoulos, E. Thessalonikeos and H. Tsoukali, *Development of a liquid-liquid extraction procedure for the analysis of amphetamine in biological specimens by GC-FID*, Open Forensic Science Journal, 2009, 2, 12-15.
- [22] E. Müller, R. Berger, E. Blass and D. Sluyts, *Liquid-liquid extraction*, Ullmann's Encyclopedia of Industrial Chemistry, 1985.
- [23] M. J. Telepchak, *Forensic and clinical applications of solid phase extraction*, New York, Humana Press, Second Edition, 2010.
- [24] J. Ledgard, *The preparatory manual of explosives*, United State, Jared Ledgard, 2007.
- [25] R. Kronstrand, J. Ahlner, N. Dizdar and G. Larson, *Quantitative analysis of desmethylselegiline, methamphetamine, and amphetamine in hair and plasma from Parkinson patients on long-term selegiline medication*, Journal of Analytical Toxicology, 2003, 27, 135-141.
- [26] L. B. Rasmussen, K. H. Olsen and S. S. Johansen, *Chiral separation and quantification of amphetamine, methamphetamine, MDA, MDMA and MDEA in whole blood by GC-EI-MS*, Journal of Chromatography B, 2006, 842, 136-141.
- [27] H. Jork, W. Funk, W. Fischer, H. Wimmer, S. MuKllner, R. Hofmann, K. Saar and B. Karbe-ThoKnges, *Bioanalytical applications: solid phase extraction*, Journal of Planar Chromatography, 2000, 3, 2142-2146.
- [28] A. Gheorghe, A. van Nuijs, B. Pecceu, L. Bervoets, P. G. Jorens, R. Blust, H. Neels and A. Covaci, *Analysis of cocaine and its principal metabolites in waste and surface*

water using solid-phase extraction and liquid chromatography–ion trap tandem mass spectrometry, *Analytical and Bioanalytical Chemistry*, 2008, 391, 1309-1319.

[29] J. Beike, *Forensic and clinical applications of solid phase extraction*, *International Journal of Legal Medicine*, 2005, 119, 115-115.

[30] M. J. Gómez, M. Petrović, A. R. Fernández-Alba and D. Barceló, *Determination of pharmaceuticals of various therapeutic classes by solid-phase extraction and liquid chromatography–tandem mass spectrometry analysis in hospital effluent wastewaters*, *Journal of Chromatography A*, 2006, 1114, 224-233.

[31] M. Tuzen, K. O. Saygi and M. Soylak, *Solid phase extraction of heavy metal ions in environmental samples on multiwalled carbon nanotubes*, *Journal of Hazardous Materials*, 2008, 152, 632-639.

[32] A. Żwir-Ferenc and M. Biziuk, *Solid phase extraction technique-trends, opportunities and applications*, *Polish Journal of Environmental Studies*, 2006, 15.

[33] E. M. Thurman and M. S. Mills, *Solid-phase extraction: principles and practice*, New York, Wiley, 1998.

[34] J. Knaack, *Solid phase extraction for hplc-ms/ms clinical analysis: finding a needle in a haystack*, *Pharmaceutica Analytica Acta*, 2012, 3, 3-10.

[35] W. Weinmann and M. Svoboda, *Fast screening for drugs of abuse by solid-phase extraction combined with flow-injection ionspray-tandem mass spectrometry*, *Journal of Analytical Toxicology*, 1998, 22, 319-328.

[36] C. Girod and C. Staub, *Analysis of drugs of abuse in hair by automated solid-phase extraction, GC/EI/MS and GC ion trap/CI/MS*, *Forensic Science International*, 2000, 107, 261-271.

[37] N. J. K. Simpson, *Solid-phase extraction: principles, techniques, and applications*, Abingdon, Taylor & Francis, 2000.

- [38] S. Rodriguez-Mozaz, M. J. Lopez de Alda and D. Barceló, *Advantages and limitations of on-line solid phase extraction coupled to liquid chromatography-mass spectrometry technologies versus biosensors for monitoring of emerging contaminants in water*, Journal of Chromatography A, 2007, 1152, 97-115.
- [39] J. Pawliszyn, *Sampling and sample preparation for field and laboratory: fundamentals and new directions in sample preparation*, Amsterdam, Elsevier Science, 2002.
- [40] Y. Alnouti, K. Srinivasan, D. Waddell, H. Bi, O. Kavetskaia and A. I. Gusev, *Development and application of a new on-line SPE system combined with LC-MS/MS detection for high throughput direct analysis of pharmaceutical compounds in plasma*, Journal of Chromatography A, 2005, 1080, 99-106.
- [41] C. Schäfer and D. Lubda, *Alkyl diol silica: restricted access pre-column packings for fast liquid chromatography-integrated sample preparation of biological fluids*, Journal of Chromatography A, 2001, 909, 73-78.
- [42] M. De Fatima Alpendurada, *Solid-phase microextraction: a promising technique for sample preparation in environmental analysis*, Journal of Chromatography A, 2000, 889, 3-14.
- [43] N. J. Simpson, *Solid-phase extraction: principles, techniques, and applications*, Boca Raton, CRC Press, 2000.
- [44] M. C. Hennion, *Solid-phase extraction: method development, sorbents, and coupling with liquid chromatography*, Journal of Chromatography A, 1999, 856, 3-54.
- [45] N. Masqué, M. Galià, R. M. Marcé and F. Borrull, *Functionalized polymeric sorbents for solid-phase extraction of polar pollutants*, Journal of High Resolution Chromatography, 1999, 22, 547-552.
- [46] M. Gonzalez and L. Arribas, *Chemically modified polymeric sorbents for sample preconcentration*, Journal of Chromatography A, 2000, 902, 3-16.

- [47] J. L. Gurav, I. K. Jung, H. H. Park, E. S. Kang and D. Y. Nadargi, *Silica aerogel: synthesis and applications*, Journal of Nanomaterials, 2010, 2010, 23.
- [48] S. Yun, H. Luo and Y. Gao, *Superhydrophobic silica aerogel microspheres from methyltrimethoxysilane: rapid synthesis via ambient pressure drying and excellent absorption properties*, RSC Advances, 2014, 4, 4535-4542.
- [49] P. Lucci, D. Pacetti, O. Núñez and N. G. Frega, *Current trends in sample treatment techniques for environmental and food analysis*, Chromatography, 2012, 5, 127-164.
- [50] D. T. T. Nguyen, D. Guillarme, S. Rudaz and J. L. Veuthey, *Fast analysis in liquid chromatography using small particle size and high pressure*, Journal of Separation Science, 2006, 29, 1836-1848.
- [51] H. Small, *Ion Chromatography*, New York, Plenum Press, 1989.
- [52] Y. Hsieh, C. J. Duncan and J. M. Brisson, *Fused-core silica column high-performance liquid chromatography/tandem mass spectrometric determination of rimonabant in mouse plasma*, Analytical Chemistry, 2007, 79, 5668-5673.
- [53] H. Minakuchi, K. Nakanishi, N. Soga, N. Ishizuka and N. Tanaka, *Effect of domain size on the performance of octadecylsilylated continuous porous silica columns in reversed-phase liquid chromatography*, Journal of Chromatography A, 1998, 797, 121-131.
- [54] T. Nema, E. Chan and P. Ho, *Application of silica-based monolith as solid phase extraction cartridge for extracting polar compounds from urine*, Talanta, 2010, 82, 488-494.
- [55] M. Keane, *Ceramics for catalysis*, Journal of Materials Science, 2003, 38, 4661-4675.
- [56] Ş. Moldoveanu and V. David, *Essentials in modern HPLC separations*, Waltham, Elsevier, 2013.

- [57] G. Guiochon, *Monolithic columns in high-performance liquid chromatography*, Journal of Chromatography A, 2007, 1168, 101-168.
- [58] I. Nischang, I. Teasdale and O. Brüggemann, *Porous polymer monoliths for small molecule separations: advancements and limitations*, Analytical and Bioanalytical Chemistry, 2011, 400, 2289-2304.
- [59] J. N. Kondo and K. Domen, *Crystallization of mesoporous metal oxides*, Chemistry of Materials, 2007, 20, 835-847.
- [60] K. Nakanishi and N. Tanaka, *Sol-gel with phase separation. Hierarchically porous materials optimized for high-performance liquid chromatography separations*, Accounts of Chemical Research, 2007, 40, 863-873.
- [61] A. Galarneau, J. Iapichella, K. Bonhomme, F. Di Renzo, P. Kooyman, O. Terasaki and F. Fajula, *Controlling the morphology of mesostructured silicas by pseudomorphic transformation: a route towards applications*, Advanced Functional Materials, 2006, 16, 1657-1667.
- [62] R. J. Hodgson, Y. Chen, Z. Zhang, D. Tleugabulova, H. Long, X. Zhao, M. Organ, M. A. Brook and J. D. Brennan, *Protein-doped monolithic silica columns for capillary liquid chromatography prepared by the sol-gel method: applications to frontal affinity chromatography*, Analytical Chemistry, 2004, 76, 2780-2790.
- [63] E. C. Peters, F. Svec, J. M. Fréchet, C. Viklund and K. Irgum, *Control of porous properties and surface chemistry in "molded" porous polymer monoliths prepared by polymerization in the presence of TEMPO*, Macromolecules, 1999, 32, 6377-6379.
- [64] N. Rupcich, R. Nutiu, Y. Li and J. D. Brennan, *Solid-phase enzyme activity assay utilizing an entrapped fluorescence-signaling DNA aptamer*, Angewandte Chemie, 2006, 118, 3373-3377.
- [65] Y. Chen, Y. Yi, J. D. Brennan and M. A. Brook, *Development of macroporous titania monoliths using a biocompatible method*, Chemistry of Materials, 2006, 18, 5326-5335.

- [66] E. Alzahrani and K. Welham, *Design and evaluation of synthetic silica-based monolithic materials in shrinkable tube for efficient protein extraction*, *Analyst*, 2011, *136*, 4321-4327.
- [67] K. Nakanishi and N. Soga, *Phase separation in silica sol-gel system containing polyacrylic acid*, *Journal of Non-Crystalline Solids*, 1992, *139*, 1-13.
- [68] L. L. Hench and J. K. West, *The sol-gel process*, *Chemical Reviews* 1990, *90*, 33-72.
- [69] D. Allen and Z. El Rassi, *Capillary electrochromatography with monolithic silica columns*, *Journal of Chromatography A*, 2004, *1029*, 239-247.
- [70] K. Cabrera, *Applications of silica-based monolithic HPLC columns*, *Journal of Separation Science*, 2004, *27*, 843-852.
- [71] L. C. Klein, *Sol-gel optics: processing and applications*, Boston, *Kluwer Acad. Publ.*, 1994.
- [72] P. D. Fletcher, S. J. Haswell, P. He, S. M. Kelly and A. Mansfield, *Permeability of silica monoliths containing micro-and nano-pores*, *Journal of Porous Materials*, 2011, *18*, 501-508.
- [73] A. Storm, *Diamond: glittering prize for materials science*, *Science*, 1990, *1640*, 1643.
- [74] C. Mulder and J. Van Lierop, *Aerogels, Preparation, densification and characterization of autoclave dried SiO₂ gels*, New York, *Springer*, 1986.
- [75] G. Pajonk, *Transparent silica aerogels*, *Journal of Non-Crystalline Solids*, 1998, *225*, 307-314.
- [76] L. Kocon, F. Despetis and J. Phalippou, *Ultralow density silica aerogels by alcohol supercritical drying*, *Journal of Non-Crystalline Solids*, 1998, *225*, 96-100.
- [77] M. Schneider and A. Baiker, *Aerogels in catalysis*, *Catalysis Reviews*, 1995, *37*, 515-556.

- [78] F. Schwertfeger, D. Frank and M. Schmidt, *Hydrophobic waterglass based aerogels without solvent exchange or supercritical drying*, Journal of Non-Crystalline Solids, 1998, 225, 24-29.
- [79] Y. K. Akimov, *Fields of application of aerogels*, Instruments and Experimental Techniques, 2003, 46, 287-299.
- [80] J. Randon, J. F. Guerrin and J. L. Rocca, *Synthesis of titania monoliths for chromatographic separations*, Journal of Chromatography A, 2008, 1214, 183-186.
- [81] J. Randon, S. Huguet, A. Piram, G. Puy, C. Demesmay and J. L. Rocca, *Synthesis of zirconia monoliths for chromatographic separations*, Journal of Chromatography A, 2006, 1109, 19-25.
- [82] I. U. Arachchige and S. L. Brock, *Highly luminescent quantum-dot monoliths*, Journal of The American Chemical Society, 2007, 129, 1840-1841.
- [83] M. Shafaei-Fallah, J. He, A. Rothenberger and M. G. Kanatzidis, *Ion-exchangeable cobalt polysulfide chalcogel*, Journal of The American Chemical Society, 2011, 133, 1200-1202.
- [84] B. Gawel, K. Gawel and G. Oye, *Sol-gel synthesis of non-silica monolithic materials*, Materials, 2010, 3, 2815-2833.
- [85] K. Fujita, J. Konishi, K. Nakanishi and K. Hirao, *Strong light scattering in macroporous TiO₂ monoliths induced by phase separation*, Applied Physics Letters, 2004, 85, 5595-5597.
- [86] S. M. Fields, *Silica xerogel as a continuous column support for high-performance liquid chromatography*, Analytical Chemistry, 1996, 68, 2709-2712.
- [87] N. Ishizuka, H. Minakuchi, K. Nakanishi, N. Soga, H. Nagayama, K. Hosoya and N. Tanaka, *Performance of a monolithic silica column in a capillary under pressure-driven and electrodriven conditions*, Analytical Chemistry, 2000, 72, 1275-1280.

- [88] J. Fricke and T. Tillotson, *Aerogels: production, characterization, and applications*, Thin Solid Films, 1997, 297, 212-223.
- [89] U. Schubert and N. Hüsing, *Synthesis of inorganic materials*, Weinheim, Bergstr Wiley-VCH, Third Edition, 2012.
- [90] C. E. Folgar, *Structural evolution of silica aerogel under a microwave field*, Blacksburg, *Materials Science and Engineering*, 2010.
- [91] O. Núñez, K. Nakanishi and N. Tanaka, *Preparation of monolithic silica columns for high-performance liquid chromatography*, Journal of Chromatography A, 2008, 1191, 231-252.
- [92] L. L. Hench, *Sol-gel silica: properties, processing and technology transfer*, New York, William Andrew, 1998.
- [93] C. J. Brinker and G. W. Scherer, *Sol-gel science: the physics and chemistry of sol-gel processing*, Boston, Acad. Press, 1990.
- [94] K. Sinkó, *Influence of chemical conditions on the nanoporous structure of silicate aerogels*, Materials, 2010, 3, 704-740.
- [95] M. Motokawa, H. Kobayashi, N. Ishizuka, H. Minakuchi, K. Nakanishi, H. Jinnai, K. Hosoya, T. Ikegami and N. Tanaka, *Monolithic silica columns with various skeleton sizes and through-pore sizes for capillary liquid chromatography*, Journal of Chromatography A, 2002, 961, 53-63.
- [96] W. Gao, G. Yang, J. Yang and H. Liu, *Formation of the monolithic silica gel column with bimodal pore structure*, Turkish Journal of Chemistry, 2004, 28, 379-385.
- [97] G. M. Neves, R. F. Lenza and W. L. Vasconcelos, *Evaluation of the influence of microwaves in the structure of silica gels*, Materials Research, 2002, 5, 447-451.
- [98] D. M. Smith, G.W. Scherer, and J.M. Anderson, *Shrinkage during drying of silica gel*, Journal of Non-Crystalline Solids, 1995, 188, 191-206.

- [99] G. W. Scherer and D. M. Smith, *Cavitation during drying of a gel*, Journal of Non-Crystalline Solids, 1995, 189, 197-211.
- [100] D. J. Griffiths, *Introduction to electrodynamics*, Essex, Pearson, 2014.
- [101] E. G. Vlakh and T. B. Tennikova, *Preparation of methacrylate monoliths*, Journal of Separation Science, 2007, 30, 2801-2813.
- [102] S. Xie, F. Svec and J. M. Fréchet, *Porous polymer monoliths: preparation of sorbent materials with high-surface areas and controlled surface chemistry for high-throughput, online, solid-phase extraction of polar organic compounds*, Chemistry of Materials, 1998, 10, 4072-4078.
- [103] J. M. Armenta, B. Gu, P. H. Humble, C. D. Thulin and M. L. Lee, *Design and evaluation of a coupled monolithic preconcentrator-capillary zone electrophoresis system for the extraction of immunoglobulin G from human serum*, Journal of Chromatography A, 2005, 1097, 171-178.
- [104] C. Schley, R. Swart and C. G. Huber, *Capillary scale monolithic trap column for desalting and preconcentration of peptides and proteins in one-and two-dimensional separations*, Journal of Chromatography A, 2006, 1136, 210-220.
- [105] L. Rieux, H. Niederländer, E. Verpoorte and R. Bischoff, *Silica monolithic columns: synthesis, characterisation and applications to the analysis of biological molecules*, Journal of Separation Science, 2005, 28, 1628-1641.
- [106] H. Kobayashi, D. Tokuda, J. Ichimaru, T. Ikegami, K. Miyabe and N. Tanaka, *Faster axial band dispersion in a monolithic silica column than in a particle-packed column*, Journal of Chromatography A, 2006, 1109, 2-9.
- [107] H. Zou, X. Huang, M. Ye and Q. Luo, *Monolithic stationary phases for liquid chromatography and capillary electrochromatography*, Journal of Chromatography A, 2002, 954, 5-32.

- [108] C. Viklund, F. Svec, J. M. Fréchet and K. Irgum, *Monolithic, "molded", porous materials with high flow characteristics for separations, catalysis, or solid-phase chemistry: control of porous properties during polymerization*, Chemistry of Materials, 1996, 8, 744-750.
- [109] S. Fanali, P. R. Haddad, C. Poole, P. Schoenmakers and D. K. Lloyd, *Liquid chromatography: fundamentals and instrumentation*, Waltham, Elsevier Science, 2013.
- [110] J. Urban and P. Jandera, *Polymethacrylate monolithic columns for capillary liquid chromatography*, Journal of Separation Science, 2008, 31, 2521-2540.
- [111] D. Luo, F. Chen, K. Xiao and Y. Q. Feng, *Rapid determination of Tetrahydrocannabinol in saliva by polymer monolith microextraction combined with gas chromatography-mass spectrometry*, Talanta, 2009, 77, 1701-1706.
- [112] G. Guiochon, *Monolithic columns in high-performance liquid chromatography*, Journal of Chromatography A, 2007, 1168, 101-168.
- [113] S. Xie, R. W. Allington, J. M. Fréchet and F. Svec, *Modern advances in chromatography, Porous polymer monoliths: an alternative to classical beads*, Berlin, Springer, 2002.
- [114] I. M. Lazar, L. Li, Y. Yang and B. L. Karger, *Microfluidic device for capillary electrochromatography-mass spectrometry*, Electrophoresis, 2003, 24, 3655-3662.
- [115] M. Kele and G. Guiochon, *Repeatability and reproducibility of retention data and band profiles on six batches of monolithic columns*, Journal of Chromatography A, 2002, 960, 19-49.
- [116] S. L. Cohen and B. T. Chait, *Influence of matrix solution conditions on the MALDI-MS analysis of peptides and proteins*, Analytical Chemistry, 1996, 68, 31-37.

- [117] V. Samanidou, A. Ioannou and I. Papadoyannis, *The use of a monolithic column to improve the simultaneous determination of four cephalosporin antibiotics in pharmaceuticals and body fluids by HPLC after solid phase extraction - a comparison with a conventional reversed-phase silica-based column*, Journal of Chromatography B, 2004, 809, 175-182.
- [118] K. Cabrera, G. Wieland, D. Lubda, K. Nakanishi, N. Soga, H. Minakuchi and K. K. Unger, *SilicaROD™ a new challenge in fast high-performance liquid chromatography separations*, TrAC Trends in Analytical Chemistry, 1998, 17, 50-53.
- [119] C. F. Poole, *New trends in solid-phase extraction*, TrAC Trends in Analytical Chemistry, 2003, 22, 362-373.
- [120] Y. Ueki, T. Umemura, J. Li, T. Otake and K. I. Tsunoda, *Preparation and application of methacrylate-based cation-exchange monolithic columns for capillary ion chromatography*, Analytical Chemistry, 2004, 76, 7007-7012.
- [121] M. Bedair and Z. El Rassi, *Recent advances in polymeric monolithic stationary phases for electrochromatography in capillaries and chips*, Electrophoresis, 2004, 25, 4110-4119.
- [122] P. Jal, S. Patel and B. Mishra, *Chemical modification of silica surface by immobilization of functional groups for extractive concentration of metal ions*, Talanta, 2004, 62, 1005-1028.
- [123] N. Ishizuka, H. Kobayashi, H. Minakuchi, K. Nakanishi, K. Hirao, K. Hosoya, T. Ikegami and N. Tanaka, *Monolithic silica columns for high-efficiency separations by high-performance liquid chromatography*, Journal of Chromatography A, 2002, 960, 85-96.
- [124] E. Alzahrani and K. Welham, *Fabrication of an octadecylated silica monolith inside a glass microchip for protein enrichment*, Analyst, 2012, 137, 4751-4759.

- [125] C. Viklund, E. Pontén, B. Glad, K. Irgum, P. Hörstedt and F. Svec, “*Molded*” *macroporous poly (glycidyl methacrylate-co-trimethylolpropane trimethacrylate) materials with fine controlled porous properties: preparation of monoliths using photoinitiated polymerization*, *Chemistry of Materials*, 1997, 9, 463-471.
- [126] F. Svec, *Porous polymer monoliths: amazingly wide variety of techniques enabling their preparation*, *Journal of Chromatography A*, 2010, 1217, 902-924.
- [127] A. Namera, A. Nakamoto, M. Nishida, T. Saito, I. Kishiyama, S. Miyazaki, M. Yahata, M. Yashiki and M. Nagao, *Extraction of amphetamines and methylenedioxyamphetamines from urine using a monolithic silica disk-packed spin column and high-performance liquid chromatography–diode array detection*, *Journal of Chromatography A*, 2008, 1208, 71-75.
- [128] F. Svec, *Less common applications of monoliths: preconcentration and solid-phase extraction*, *Journal of Chromatography B*, 2006, 841, 52-64.
- [129] A. Namera, S. Miyazaki, T. Saito and A. Nakamoto, *Monolithic silica with HPLC separation and solid phase extraction materials for determination of drugs in biological materials*, *Analytical Methods*, 2011, 3, 2189-2200.
- [130] D. Lubda, K. Cabrera, W. Kraas, C. Schaefer, D. Cunningham and R. E. Majors, *New developments in the application of monolithic HPLC columns*, *LC-GC Europe*, 2001, 14, 730-735.
- [131] K. Chandrul and B. Srivastava, *A process of method development: a chromatographic approach*, *J Chem Pharm Res*, 2010, 2, 519-545.
- [132] K. Robards, P. E. Jackson and P. R. Haddad, *Principles and practice of modern chromatographic methods*, Boston, *Elsevier Academic Press*, 1994.
- [133] S. Pelletier and C. A. Lucy, *Fast and high-resolution ion chromatography at high pH on short columns packed with 1.8 μm surfactant coated silica reverse-phase particles*, *Journal of Chromatography A*, 2006, 1125, 189-194.

- [134] D. Connolly, D. Victory and B. Paull, *Rapid, low pressure, and simultaneous ion chromatography of common inorganic anions and cations on short permanently coated monolithic columns*, Journal of Separation Science, 2004, 27, 912-920.
- [135] Q. Xu, K. Tanaka, M. Mori, M. Helaleh, W. Hu and K. Hasebe, *Monolithic ODS-silica gel column for determination of hydrogen, sodium, ammonium and potassium in acid rain by ion chromatography*, Chromatographia, 2003, 57, 19-22.
- [136] P. Hatsis and C. A. Lucy, *Improved sensitivity and characterization of high-speed ion chromatography of inorganic anions*, Analytical Chemistry, 2003, 75, 995-1001.
- [137] B. Paull, C. Ó. Ríordáin and P. N. Nesterenko, *Double gradient ion chromatography on a short carboxybetaine coated monolithic anion exchanger*, Chemical Communications, 2005, 215-217.
- [138] C. Ó Ríordáin, E. Gillespie, D. Connolly, P. N. Nesterenko and B. Paull, *Capillary ion chromatography of inorganic anions on octadecyl silica monolith modified with an amphoteric surfactant*, Journal of Chromatography A, 2007, 1142, 185-193.
- [139] M. M. Sanagi, A. A. Naim, A. Hussain and N. Dzakaria, *Preparation and application of octadecylsilyl-silica adsorbents for chemical analysis*, Malaysian Journal of Analytical Sciences, 2001, 7, 337-343.
- [140] M. L. Larrivee and C. F. Poole, *Solvation parameter model for the prediction of breakthrough volumes in solid-phase extraction with particle-loaded membranes*, Analytical Chemistry, 1994, 66, 139-146.
- [141] J. H. Knox, B. Kaur and G. Millward, *Structure and performance of porous graphitic carbon in liquid chromatography*, Journal of Chromatography A, 1986, 352, 3-25.

- [142] F. O. Boyer, J. F. Romero, M. L. de Castro and J. Quesada, *Determination of vitamins D2, D3, K1 and K3 and some hydroxy metabolites of vitamin D3 in plasma using a continuous clean-up-preconcentration procedure coupled on-line with liquid chromatography-UV detection*, *Analyst*, 1999, 124, 401-406.
- [143] A. Di Corcia, S. Marchese and R. Samperi, *Evaluation of graphitized carbon black as a selective adsorbent for extracting acidic organic compounds from water*, *Journal of Chromatography A*, 1993, 642, 163-174.
- [144] C. Crescenzi, A. Di Corcia, R. Samperi and A. Marcomini, *Determination of nonionic polyethoxylate surfactants in environmental waters by liquid chromatography/electrospray mass spectrometry*, *Analytical Chemistry*, 1995, 67, 1797-1804.
- [145] A. Di Corcia and M. Marchetti, *Multiresidue method for pesticides in drinking water using a graphitized carbon black cartridge extraction and liquid chromatographic analysis*, *Analytical Chemistry*, 1991, 63, 580-585.
- [146] E. Y. Ting and M. D. Porter, *Separations of corticosteroids using electrochemically modulated liquid chromatography: selectivity enhancements at a porous graphitic carbon stationary phase*, *Analytical Chemistry*, 1997, 69, 675-678.
- [147] G. D'Ascenzo, A. Gentili, S. Marchese, A. Marino and D. Perret, *Multiresidue method for determination of post-emergence herbicides in water by HPLC/ESI/MS in positive ionization mode*, *Environmental Science & Technology*, 1998, 32, 1340-1347.
- [148] B. Altenbach and W. Giger, *Determination of benzene-and naphthalenesulfonates in wastewater by solid-phase extraction with graphitized carbon black and ion-pair liquid chromatography with UV detection*, *Analytical Chemistry*, 1995, 67, 2325-2333.

- [149] A. Di Corcia, A. Costantino, C. Crescenzi, E. Marinoni and R. Samperi, *Characterization of recalcitrant intermediates from biotransformation of the branched alkyl side chain of nonylphenol ethoxylate surfactants*, *Environmental Science & Technology*, 1998, 32, 2401-2409.
- [150] H. Lipson and A. Stokes, *The structure of graphite*, *Proceedings A*, 1942, 181, 101-105.
- [151] C. Lin and J. Ritter, *Effect of synthesis pH on the structure of carbon xerogels*, *Carbon*, 1997, 35, 1271-1278.
- [152] C. Li and T. W. Chou, *Elastic moduli of multi-walled carbon nanotubes and the effect of van der Waals forces*, *Composites Science and Technology*, 2003, 63, 1517-1524.
- [153] I. Frank, D. M. Tanenbaum, A. Van der Zande and P. L. McEuen, *Mechanical properties of suspended graphene sheets*, *Journal of Vacuum Science & Technology B*, 2007, 25, 2558-2561.
- [154] M. C. Hennion, V. Coquart, S. Guenu and C. Sella, *Retention behaviour of polar compounds using porous graphitic carbon with water-rich mobile phases*, *Journal of Chromatography A*, 1995, 712, 287-301.
- [155] V. Coquart and M. C. Hennion, *Trace-level determination of polar phenolic compounds in aqueous samples by high-performance liquid chromatography and on-line preconcentration on porous graphitic carbon*, *Journal of Chromatography A*, 1992, 600, 195-201.
- [156] D. Barrett, M. Pawula, R. Knaggs and P. Shaw, *Retention behavior of morphine and its metabolites on a porous graphitic carbon column*, *Chromatographia*, 1998, 47, 667-672.
- [157] K. Gaudin, P. Chaminade, D. Ferrier and A. Baillet, *Use of principal component analysis for investigation of factors affecting retention behaviour of ceramides on porous graphitized carbon column*, *Chromatographia*, 1999, 50, 470-478.

- [158] J. H. Knox and P. Ross, *Carbon-based packing materials for liquid chromatography*, *Advances in Chromatography*, 1997, 37, 73-119.
- [159] C. I. De Matteis, D. A. Simpson, S. W. Doughty, M. R. Euerby, P. N. Shaw and D. A. Barrett, *Chromatographic retention behaviour of alkylbenzenes and pentylbenzene structural isomers on porous graphitic carbon and octadecyl-bonded silica studied using molecular modelling and QSRR*, *Journal of Chromatography A*, 2010, 1217, 6987-6993.
- [160] P. Ross, J. Knox and P. Brown, *Advances in chromatography*, New York, *Marcel Dekker Inc.*, 1997.
- [161] J. Knox and Q. H. Wan, *Surface modification of porous graphite for ion exchange chromatography*, *Chromatographia*, 1996, 42, 83-88.
- [162] C. West, C. Elfakir and M. Lafosse, *Porous graphitic carbon: a versatile stationary phase for liquid chromatography*, *Journal of Chromatography A*, 2010, 1217, 3201-3216.
- [163] R. Kaliszan, *Quantitative structure-retention relationships applied to reversed-phase high-performance liquid chromatography*, *Journal of Chromatography A*, 1993, 656, 417-435.
- [164] M. C. Hennion, *Graphitized carbons for solid-phase extraction*, *Journal of Chromatography A*, 2000, 885, 73-95.
- [165] M. J. Madou, *From MEMS to Bio-MEMS and Bio-NEMS: manufacturing techniques and applications*, Boca Raton, *Taylor & Francis*, 2011.
- [166] P. V. Kamat, *Graphene-based nanoassemblies for energy conversion*, *The Journal of Physical Chemistry Letters*, 2011, 2, 242-251.
- [167] S. Yin, Y. Zhang, J. Kong, C. Zou, C. M. Li, X. Lu, J. Ma, F. Y. C. Boey and X. Chen, *Assembly of graphene sheets into hierarchical structures for high-performance energy storage*, *ACS Nano*, 2011, 5, 3831-3838.

- [168] J. Hou, Y. Shao, M. W. Ellis, R. B. Moore and B. Yi, *Graphene-based electrochemical energy conversion and storage: fuel cells, supercapacitors and lithium ion batteries*, *Physical Chemistry Chemical Physics*, 2011, *13*, 15384-15402.
- [169] I. V. Lightcap, T. H. Kosel and P. V. Kamat, *Anchoring semiconductor and metal nanoparticles on a two-dimensional catalyst mat. storing and shuttling electrons with reduced graphene oxide*, *Nano Letters*, 2010, *10*, 577-583.
- [170] Z. Sui, Q. Meng, X. Zhang, R. Ma and B. Cao, *Green synthesis of carbon nanotube-graphene hybrid aerogels and their use as versatile agents for water purification*, *Journal of Materials Chemistry*, 2012, *22*, 8767-8771.
- [171] W. Gao, M. Majumder, L. B. Alemany, T. N. Narayanan, M. A. Ibarra, B. K. Pradhan and P. M. Ajayan, *Engineered graphite oxide materials for application in water purification*, *ACS Applied Materials & Interfaces*, 2011, *3*, 1821-1826.
- [172] M. J. McAllister, J. L. Li, D. H. Adamson, H. C. Schniepp, A. A. Abdala, J. Liu, M. Herrera-Alonso, D. L. Milius, R. Car and R. K. Prud'homme, *Single sheet functionalized graphene by oxidation and thermal expansion of graphite*, *Chemistry of Materials*, 2007, *19*, 4396-4404.
- [173] Q. Liu, J. Shi and G. Jiang, *Application of graphene in analytical sample preparation*, *TrAC Trends in Analytical Chemistry*, 2012, *37*, 1-11.
- [174] H. Zhang and H. K. Lee, *Plunger-in-needle solid-phase microextraction with graphene-based sol-gel coating as sorbent for determination of polybrominated diphenyl ethers*, *Journal of Chromatography A*, 2011, *1218*, 4509-4516.
- [175] X. Huang, Y. Zhang and D. Yuan, *Preparation of sorbent based on porous monolith incorporated with graphene oxide nanosheets for stir cake sorptive extraction of strongly polar aromatic amines*, *Analytical Methods*, 2014, *6*, 1510-1516.
- [176] C. Fowler, D. Khushalani, B. Lebeau and S. Mann, *Nanoscale materials with mesostructured interiors*, *Advanced Materials*, 2001, *13*, 649-652.

- [177] D. Khushalani, S. Hasenzahl and S. Manna, *Synthesis of mesoporous silica monoliths with embedded nanoparticles*, Journal of Nanoscience and Nanotechnology, 2001, *1*, 129-132.
- [178] M. Laranjo, T. Kist, E. Benvenuti, M. Gallas and T. Costa, *Gold nanoparticles enclosed in silica xerogels by high-pressure processing*, Journal of Nanoparticle Research, 2011, *13*, 4987-4995.
- [179] M. Guerrouache, S. Mahouche-Chergui, M. M. Chehimi and B. Carbonnier, *Site-specific immobilisation of gold nanoparticles on a porous monolith surface by using a thiol-yne click photopatterning approach*, Chemical Communications, 2012, *48*, 7486-7488.
- [180] Y. Vasquez, M. Kolle, L. Mishchenko, B. D. Hatton and J. Aizenberg, *Three-phase co-assembly: in situ incorporation of nanoparticles into tunable, highly ordered, porous silica films*, ACS Photonics, 2014, *1*, 53-60.
- [181] H. Shintani, *Strategies for the use of SPE*, International Journal of Clinical Pharmacology & Toxicology, 2013, *11*, 2-602.
- [182] S. H. Chuag, G.-H. Chen, H. H. Chou, S. W. Shen and C. F. Chen, *Accelerated colorimetric immunosensing using surface-modified porous monoliths and gold nanoparticles*, Science and Technology of Advanced Materials, 2013, *14*, 44-403.
- [183] Q. Wei, *Surface modification of textiles*, Cambridge, Elsevier Science, 2009.
- [184] F. Hoffmann and M. Froba, *Silica-based mesoporous organic-inorganic hybrid materials*, The supramolecular Chemistry of Organic-Inorganic Hybrid Materials, 2010, *10*, 37-111.
- [185] B. Zhao, S. M. Moochhala, C. S. Chaw and Y. Y. Yang, *Simple liquid chromatographic method for the determination of physostigmine and its metabolite eseroline in rat plasma: application to a pharmacokinetic study*, Journal of Chromatography B, 2003, *784*, 323-329.

- [186] T. Kumazawa, C. Hasegawa, X.-P. Lee, K. Hara, H. Seno, O. Suzuki and K. Sato, *Simultaneous determination of methamphetamine and amphetamine in human urine using pipette tip solid-phase extraction and gas chromatography–mass spectrometry*, *Journal of Pharmaceutical and Biomedical Analysis*, 2007, *44*, 602-607.
- [187] M. E. Salinas-Vargas and M. P. Cañizares-Macías, *On-line solid–phase extraction using a C₁₈ minicolumn coupled to a flow injection system for determination of caffeine in green and roasted coffee beans*, *Food Chemistry*, 2014, *147*, 182-188.
- [188] E. F. Vansant, P. Van Der Voort and K. C. Vrancken, *Characterization and chemical modification of the silica surface*, Amsterdam, *Elsevier Science*, 1995.
- [189] N. Kanellopoulos, *Nanoporous materials: advanced techniques for characterization, modeling, and processing*, Boca Raton, Taylor & Francis, 2011.
- [190] D. Clark, D. Folz, C. Folgar, and M. Mahmoud, *Microwave solutions for ceramic engineers*, Ohio, *The American Ceramic Society*, 2005.
- [191] L H Becker, J H Cloete, H C Reader, *Understanding microwave heating systems*, *IEEE Trans. on Electromagnetic Compatibility*, 2001, *43*, 85-88.
- [192] W. H. Sutton, *Microwave firing of high alumina ceramics*, Warrendale, *Material Research Society*, 1988.
- [193] A. P. Tomsia, *Ceramic microstructures : control at the atomic level*, New York, *Plenum Press*, 1998.
- [194] H. M. Kingston and S. J. Haswell, *Microwave-enhanced chemistry*, Washington, *American Chemical Society*, 1997.
- [195] D. E. Clark and W. H. Sutton, *Microwave processing of materials*, *Annual Review of Materials Science*, 1996, *26*, 299-331.
- [196] D. Bogdal and A. Prociak, *Microwave-enhanced polymer chemistry and technology*, Oxford, *John Wiley & Sons*, 2008.
- .

- [197] D. Atong, *Microwave-induced combustion synthesis of aluminum oxide-titanium carbide powder*, University of Florida, Ann Arbor, 2000.
- [198] A. A. Metaxas and R. J. Meredith, *Industrial microwave heating*, London, Peter Peregrinus, 1993.
- [199] M. M. Mahmoud, D. C. Folz, C. T. Suchicital and D. E. Clark, *Crystallization of lithium disilicate glass using microwave processing*, Journal of The American Ceramic Society, 2012, 95, 579-585.
- [200] M. A. Janney and H. D. Kimrey, *Diffusion-controlled processes in microwave-fired oxide ceramics*, Cambridge, Cambridge University Press, 1990.
- [201] D. E. Clark, D. C. Folz and J. K. West, *Processing materials with microwave energy*, Materials Science and Engineering A, 2000, 287, 153-158.
- [202] G. Roussy and J. A. Pearce, *Foundations and industrial applications of microwave and radio frequency fields: physical and chemical processes*, New York, John Wiley and Sons, 1995.
- [203] L. Zhang, G. Chen, M. N. Hedhili, H. Zhang and P. Wang, *Three-dimensional assemblies of graphene prepared by a novel chemical reduction-induced self-assembly method*, Nanoscale, 2012, 4, 7038-7045.
- [204] K. Dolan, D. Rouen and J. Kimber, *An overview of the use of urine, hair, sweat and saliva to detect drug use*, Drug and Alcohol Review, 2004, 23, 213-217.
- [205] S. Mitra, *Sample preparation techniques in analytical chemistry*, New Jersey, John Wiley & Sons, 2004.
- [206] G. M. Neves, R. F. Lenza, W. L. Vasconcelos, *Evaluation of the influence of microwaves in the structure of silica gels*, Materials Research, 2002, 5, 447-451.
- [207] S. Ahuja and M. Dong, *Handbook of pharmaceutical analysis by HPLC*, London, Elsevier Press, 2005.

- [208] K. K. Unger, N. Tanaka and E. Machtejevas, *Monolithic silicas in separation science: concepts, syntheses, characterization, modeling and applications*, New York, Wiley, 2010.
- [209] M. Yang, Y. Kostov, H. A. Bruck and A. Rasooly, *Gold nanoparticle-based enhanced chemiluminescence immunosensor for detection of Staphylococcal Enterotoxin B (SEB) in food*, *International Journal of Food Microbiology*, 2009, *133*, 265-271.
- [210] C. F. Duan, Y. Q. Yu and H. Cui, *Gold nanoparticle-based immunoassay by using non-stripping chemiluminescence detection*, *Analyst*, 2008, *133*, 1250-1255.
- [211] N. Li, Y. Cheng, Q. Song, Z. Jiang, M. Tang and G. Cheng, *Graphene meets biology*, *Chinese Science Bulletin*, 2014, *59*, 1341-1354.
- [212] J. C. Yoon, J. S. Lee, S. I. Kim, K. H. Kim and J. H. Jang, *Three-dimensional graphene nano-networks with high quality and mass production capability via precursor-assisted chemical vapor deposition*, *Scientific Report*, 2013, *3*, 1-8.
- [213] M. Pumera, *Graphene-based nanomaterials for energy storage*, *Energy & Environmental Science*, 2011, *4*, 668-674.
- [214] R. Kou, Y. Shao, D. Wang, M. H. Engelhard, J. H. Kwak, J. Wang, V. V. Viswanathan, C. Wang, Y. Lin and Y. Wang, *Enhanced activity and stability of Pt catalysts on functionalized graphene sheets for electrocatalytic oxygen reduction*, *Electrochemistry Communications*, 2009, *11*, 954-957.
- [215] T. Sreeprasad, S. M. Maliyekkal, K. Lisha and T. Pradeep, *Reduced graphene oxide-metal/metal oxide composites: facile synthesis and application in water purification*, *Journal of Hazardous Materials*, 2011, *186*, 921-931.
- [216] X. Dong, J. Chen, Y. Ma, J. Wang, M. B. Chan-Park, X. Liu, L. Wang, W. Huang and P. Chen, *Superhydrophobic and superoleophilic hybrid foam of graphene and carbon nanotube for selective removal of oils or organic solvents from the surface of water*, *Chemical Communications*, 2012, *48*, 10660-10662.

- [217] M. Lü, J. Li, X. Yang, C. Zhang, J. Yang, H. Hu and X. Wang, *Applications of graphene-based materials in environmental protection and detection*, Chinese Science Bulletin, 2013, 58, 2698-2710.
- [218] Q. Liu, Q. Zhou and G. Jiang, *Nanomaterials for analysis and monitoring of emerging chemical pollutants*, TrAC Trends in Analytical Chemistry, 2014.
- [219] E. Barnhardt, *Microwave ring expansion reactions performed at sub-ambient temperatures*, CEM Corporation, Life Science Division, 2004.
- [220] E. Villanueva, F. Benavente, E. Gimenez, F. Yilmaz and V. Sanz-Nebot, *Preparation and evaluation of open tubular C18-silica monolithic microcartridges for preconcentration of peptides by on-line solid phase extraction capillary electrophoresis*, Analytica Chimica Acta, 2014.
- [221] Minghuo Wu¹, Ren'an Wu, Zhenbin Zhang and Hanfa Zou¹, *Preparation and application of organic-silica hybrid monolithic capillary columns*, Electrophoresis, 2011, 32, 105–115.
- [222] P. Jal, S. Patel, B. Mishra, *Chemical modification of silica surface by immobilization of functional groups for extractive concentration of metal ions*, Talanta, 2004, 62, 1005–1028.
- [223] G. Kratz, *Novel bonding chemistry imparts enhanced polar selectivity to TSK-GEL ODS-100V reversed-phase columns*, LCGC, 2008.

9 Presentations

9.1 Poster presentations

A. Khattab and S. Haswell, “Comparison of silica monoliths fabrication using microwave and conventional heating methods”, *Analytical Research Forum 2012*, University of Durham, Durham, UK (2012).

A. Khattab and S. Haswell, “Comparison of silica monoliths fabrication and C₁₈ phase surface modification using microwave and conventional heating methods”, *6th Black sea basin conference on analytical chemistry 2013*, Karadeniz Technical University, Trabzon, Turkey (2013).

A. Khattab and S. Haswell, “Comparison of silica monoliths fabrication and C₁₈ phase surface modification using microwave and conventional heating methods for efficient extraction of small organic molecules”, *7th Saudi International Conference 2014*, University of Edinburgh, Edinburgh, UK (2014).

A. Khattab and S. Haswell, “Modification of silica monolithic column with gold nanoparticles using microwave heating”, *Analytical Research Forum 2014*, The Chemistry Centre, Burlington House, London, UK (2014).

9.2 Oral presentations

A. Khattab, “Using HPLC-UV for drugs of abuse detection”, *Toxicology and Forensic Chemistry Conference 2012*, King Fahd Hospital, Ministry of Health Madinah, KSA (2012).

A. Khattab, “Using SPE for drugs of abuse extraction”, *Toxicology and Forensic Chemistry Conference 2012*, King Fahd Hospital, Ministry of Health Madinah, KSA (2012).